This is to certify that the
dissertation entitled

THE DESIGN, SYNTHESIS AND EVALUATION OF NEW CHEMICAL ENTITIES FOR THE DEVELOPMENT OF DRUGS AGAINST CANCER, DIABETES, AUTOIMMUNE DISORDERS AND INFECTIOUS DISEASES

presented by

Li Gao

has been accepted towards fulfillment
of the requirements for the

Doctoral degree in Chemistry

Major Professor's Signature

12/05/04

Date

DATE DUE	DATE DUE	DATE DUE
MAR 0 5 2007		

THE DESIGN, SYNTHESIS AND EVALUATION OF NEW CHEMICAL ENTITIES FOR THE DEVELOPMENT OF DRUGS AGAINST CANCER, DIABETES, AUTOIMMUNE DISORDERS AND INFECTIOUS DISEASES

By

Li Gao

A DISSERTATION

Submitted to
Michigan State University
in partial fulfillment of the requirements
for the degree of

DOCTOR OF PHILOSOPHY

Department of Chemistry

2004

ABSTRACT

THE DESIGN, SYNTHESIS AND EVALUATION OF NEW CHEMICAL ENTITIES FOR THE DEVELOPMENT OF DRUGS AGAINST CANCER, DIABETES, AUTOIMMUNE DISORDERS AND INFECTIOUS DISEASES

By

Li Gao

The main objective of the work described in this dissertation was to develop strategies for the design and synthesis of nitrogen heterocyclic systems for use as glycosidase and glycosyltransferase inhibitors and as protein synthesis inhibitors. Potential applications include use as antibacterial, antiviral, cancer, diabetes and autoimmune drugs. The heterocyclic ring systems include bicyclic trihydroxy-2-thiaquinolizidine ring systems, bicyclic iminopentitols, 2,5-bis(hydroxymethyl)-3,4-dihydroxypyrrolidines, and arylsubstituted 5-phenyl-thiomorpholine-3-carboxylic acids. The biological testing showed the specificity of bicyclic trihydroxy-2-thiaquinolizidine ring systems against glycosidases, and they have some antibacterial activity. The bicyclic iminopentitols containing the structural essence of a ribosyl cation in the form of a 1,4-dideoxy-1,4-iminopentitol can be used as scaffolds for the preparation of riboside hydrolase, phosphorylase and transferase inhibitors. The arylsubstituted 5-phenyl-thiomorpholine-3-carboxylic acid derivatives showed promising antibacterial activity. The ease of synthesis

of these heterocyclic ring systems provides access to the development of completely new classes of glycosidase and glycosyltransferase inhibitors as well as new antibiotics.

ACKNOWLEDGEMENT

I would like to express my sincere gratitude to my academic advisor Dr. Rawle I. Hollingsworth, for introducing me a whole new world of scientific frontiers including carbohydrate chemistry and organic synthesis. His guidance and support are important reasons for my progress. I am also grateful to my committee members, Dr. Babak Borhan, Dr. James Jackson and Dr. Katharine Hunt for their inspiration, valued advice and help in my research. I would like to thank Dr. Carol Mindock for the DHF-riboside assay, MIC testing and Dr. Don Ward for x-ray crystallography analysis as well as group members in Prof. Hollingsworth lab.

Finally, I would like to thank my family and my friends for their support and understanding.

TABLE OF CONTENTS

LIST OF TABLES

LIST OF FIGURES

Chapter 1

Chapter 2

Chapter 3

Chapter 4

Chapter 5

Chapter

Chapter 1

Glycosidase and Glycosyltransferase Inhibitors:

A Discussion of Mechanism, Mimics and Modes of Inhibition

ABSTRACT

Carbohydrate processing is a central feature of the chemistry of life. Glycosidases and glycosyltransferases are the critical enzymes that control the breakdown, processing and synthesis of carbohydrates in biological systems. According to the stereochemistry outcomes of the enzyme catalyzed reactions, two possible mechanisms have been proposed as inversion and retention of anomeric configuration. Mechanism studies including x-ray structures of the enzyme-substrate complex, glycosyl-enzyme intermediate, and enzyme-product complex, have provided us insight into the different stages of the enzymatic reaction pathway. This insight is being used in the design of new chemical entities that can inhibit or regulate the biochemical activity of specific enzymes in a strategy for producing new drugs. Such drugs will find applications across the entire spectrum of therapeutics. In this chapter we review the progress made to date on the identification, design, and evaluation of natural and synthetic glycosidase and glycosyltransferase inhibitors that mimic the possible transition states and intermediates purported to be in the reaction pathway for these enzymes.

1.1. Introduction

Glycosidases (or glycosyl hydrolases) and glycosyltransferases are important enzymes that catalyze the cleavage and formation of glycosidic linkages in biological systems. They play crucial roles in the biosynthesis and degradation of a large number of biological structures. These include polysacchrides, oligosaccharides, antibiotics, glycolipids, glycoproteins, proteoglycans and peptidoglycans. They are also involved in a number of other processes including the remodeling of cell wall, the damage and repair of DNA by base excision or transfer, and other toxin mechanisms. Understanding their roles in the formation of oligosaccharides and glycoconjugates is essential to modulate the cellular interaction and to develop therapeutic agents.

Oligosaccharides are synthesized in step-wise fashion primarily in the endoplasmic reticulum and Golgi apparatus (**Figure 1.1**)[1], a process that affords significant product diversity[2]. Exogenously supplied monosaccharides are taken up by cells and converted to monosaccharide "building blocks" (typically nucleoside sugars) inside the cell. Several steps of metabolic transformation might take place en route from an exogenous sugar to a building block. The building blocks are imported into the secretory compartments where they are assembled by glycosyltransferases into oligosaccharides bound to a protein (or lipid) scaffold. Further trimming and elongation by glycosidases and transferases will give the fully matured form of glycoconjugates. Upon reaching the cell surface, they can serve as ligands for receptors on other cells or pathogens.

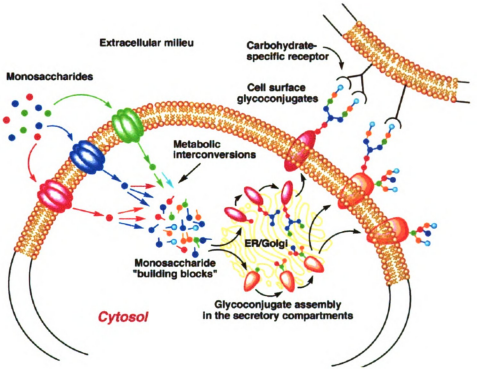

Figure 1.1. Glycoconjugate biosynthesis and cell surface recognition. (Images in this thesis are presented in color)

The N-linked glycoproteins are belived to be involved in cell-cell adhesion, differentiation, recognition, regulation, modulation of protein receptors, and so on. They present a great diversity in their structures, but all the different structures come from a common precursor, the N-linked core oligosaccharide (**Figure 1.2**)[3]. During the synthesis of N-linked glycans in mammalian cells, this core unit is assembled as a membrane-bound dolichylpyrophosphate precursor in the endoplasmic reticulum (ER)[4-6], and then transferred to a growing, nascent polypeptide chain (**Figure 1.3**). After it is coupled to an asparagine residue through an N-glycosidic bond catalyzed by an oligosaccharyltransferase complex[7], three terminal glucoses and one mannose are trimmed away by glucosidase I, II and mannosidases[4,8]. When the glycoprotein moves to

the Golgi, further mannose trimming occurs, and new sugars are added during terminal glycosidation by transferases to produce complex N-linked glycans. In one pathway shown in **figure 1.3**, GlcNAc, galactose, sialic acid, and fucose are added to the glycoprotein and only five original sugars left. The final oligosaccharide structures depend on the polypeptides and on which processing glycosidases and transferases are expressed in the cells.

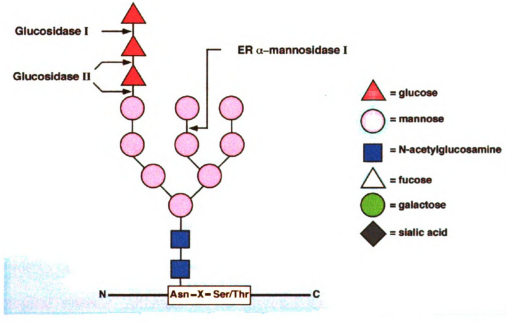

Figure 1.2. The N-linked core oligosaccharide. The symbols for the different sugars are used in the following figures.

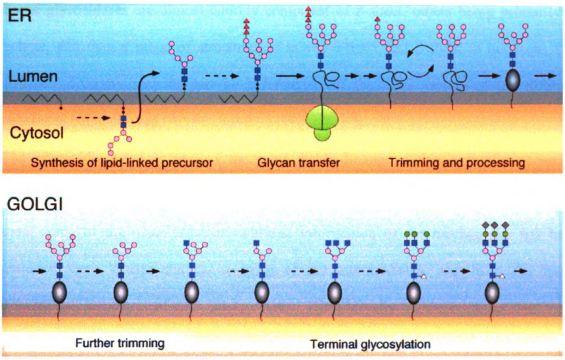

Figure 1.3. Biosynthesis of the N-linked core oligosaccharide.

1.2. Glysosidase Structure and Mechanism

Glycosidases catalyze the hydrolysis of the glycosidic bond, which exists in a wide range of biological systems. Although all the glycosidases catalyze the same reaction, the hydrolysis of an acetal, the enzymes present an incredible structural diversity. Over 2000 glycosidases have been identified, and they are grouped to over 90 families according to the amino acid sequence similarity. The number is growing steadily and updated regularly and is available on the website http://afmb.cnrs-mrs.fr/~cazy/CAZY/index.html[9]. Since the first glycosidase three-dimensional structure of hen egg-white lysozyme (HEWL) was solved, there have been over 50 structure representatives for these families available, revealing a large number of different folds.

Some glycosidases are almost entirely composed of β-sheet, others being primarily α-helical, and then a range of structures of mixed α-helix and β-sheet in between. This structure diversity may in part be a reflection of the large variety of the different substrates being cleaved.

The glycosidic bond is one of the most stable linkage within naturally occurring biopolymers[10], and the great acceleration of the hydrolysis by glycosidases has made them some of the most efficient catalysts. Information of the mechanisms has been obtained from kinetic studies, trapping of the intermediates, and from the three-dimensional structures of such intermediates. The generally believed mechanism[11,12] of glycosidic bond cleavage involves acid catalysis with protonation of the exocyclic oxygen atom at the anomeric center to give a protonated glycoside (**figure 1.4**). Subsequent cleavage of the C(1) – O(1) bond leads to an oxocarbenium ion-like transition state, in which the positive charge is delocalized over the ring oxygen and the anomeric carbon. The oxocarbenium intermediate species then reacts with a molecule of water to form the product. The oxocarbenium ion-like transition state has been confirmed by the α secondary deuterium kinetic isotope effects[13,14], with K_H/K_D value greater than 1 (K_H and K_D are rate constants for reactions of protium- and deuterium-labeled substrates). Two possible mechanisms have been proposed according to the stereochemistry outcomes of the enzyme catalyzed hydrolysis. Glycosidases that catalyze hydrolysis of glycosides with inversion of anomeric configuration are called inverting enzymes and glycosidases that catalyze the hydrolysis with retention of configuration are retaining glycosidases.

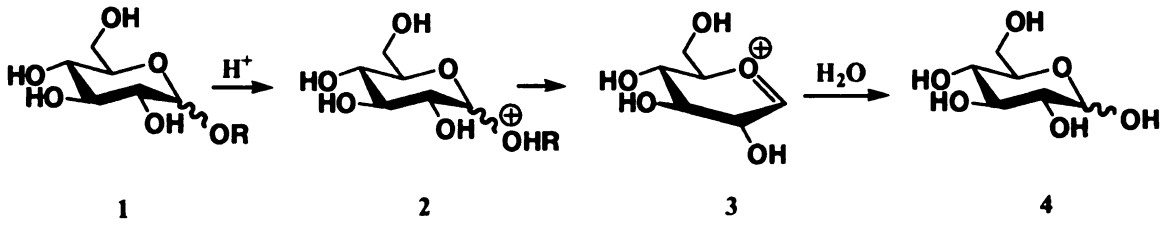

Figure 1.4. General believed mechanism of glycosidase hydrolysis

The inverting glycosidases catalyze the reaction via a singe-displacement mechanism involving an oxocarbenium ion-like transition state (**figure 1.5**). In the active site, the substrate and a water molecule are bound between two carboxyl groups. One carboxyl group acts as general acid to protonate the leaving group, while the other one deprotonates the water molecule to facilitate the nucleophilic attack.

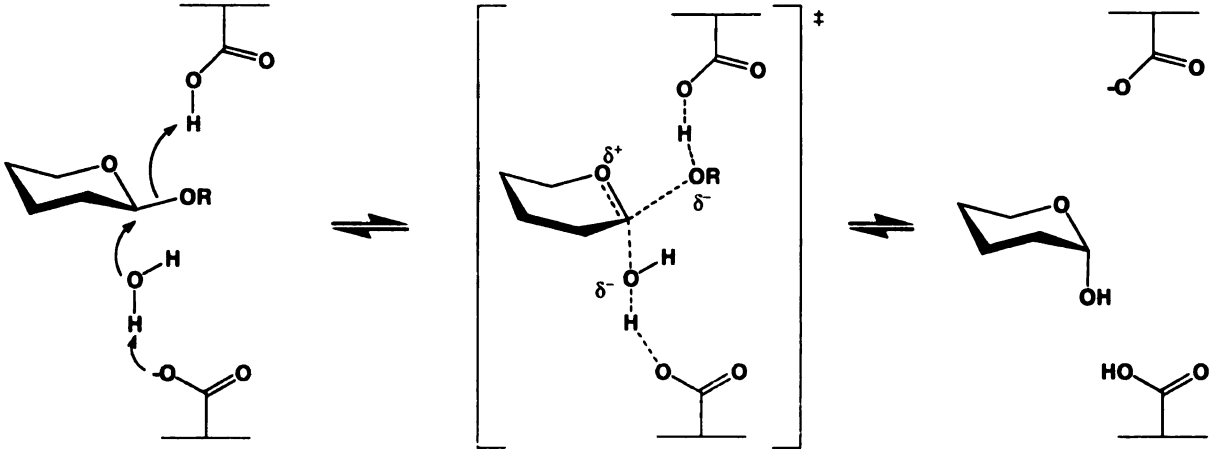

Figure 1.5. General mechanism for inverting glycosidases[15]

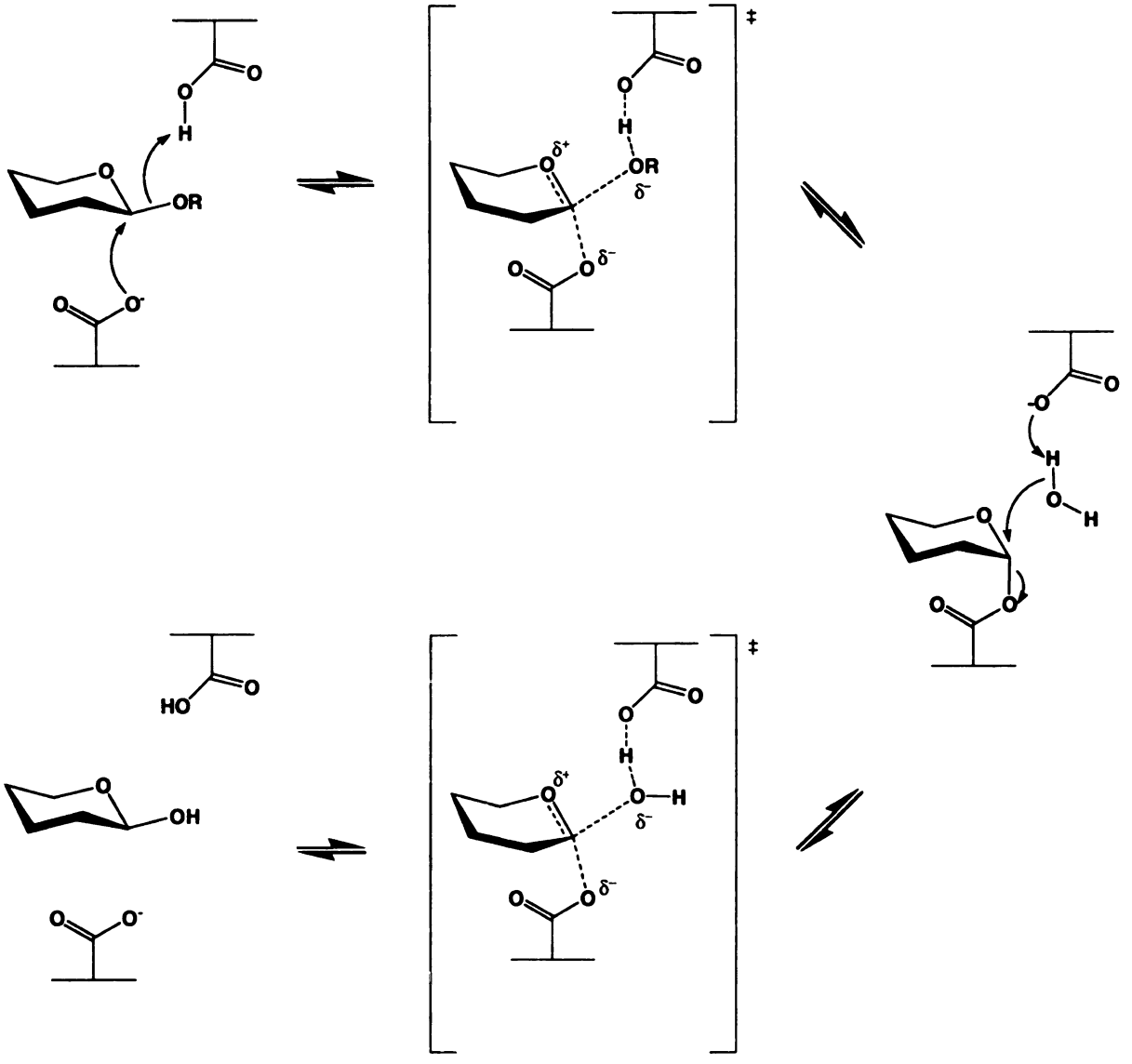

Figure 1.6. General mechanism for retaining glycosidases.

For retaining glycosidases, Koshland[16] first pointed out a double-displacement mechanism[16,17-19] (**figure 1.6**) which involves an enzyme nucleophile. In the first step, one of the carboxyl group protonates the glycosidic oxygen, and the other one acts as a nucleophile to displace the aglycon through an oxocarbenium ion-like transition state to

form a covalent glycosyl-enzyme intermediate. In the second step the carboxylate group deprotonates the incoming water molecule to generate a hydroxyl ion which attacks the anomeric center of the intermediate. The net result is the retention of the anomeric configuration. In the mechanism, there are two transition states with substantial oxocarbenium ion character and one glycosyl-enzyme intermediate. Kinetic studies, trapping technology and the corresponding three-dimensional structures have provided invaluable information about the nature of the transition state. The x-ray structures of the enzyme-substrate complex (Michaelis complex), glycosyl-enzyme intermediate, and enzyme-product complex, which are stable forms along the reaction coordinate, have been solved for some enzymes. These give us insight into the different stages of the enzymatic reaction pathway. Different structures such as natural substrates[20-22], nonhydrolyzable thiooligosaccharide substrate analogs[23-29], and 2-fluoro-2-deoxy oligosaccharides[27,30-33] have been used to obtain the enzyme-unhydrolyzed substrate complexes and the corresponding crystal structures. The introduction of the 2-fluoro group is a common strategy for trapping the enzyme complexes[34,35]. The rationale behind is that the electron-withdrawing 2-fluoro group destabilizes the positive charge that develops at the transition state. It has also been proposed that replacement by flurine also removes an important interaction between the 2-hydroxyl group of the substrate and the enzyme which is involved in the transition state stabilization[36-38]. The 2-OH is said to contribute about 20 kJ/mol and 3, 4, 6 positions provide ~10 kJ/mol each for the binding affinity[39]. This is unlikely to be the real reason because the effect of fluorine substitution is very general for all classes of sugars regardless of ring size and the configuration at the 2-position. The δ-2 effect should also be remembered. It is also possible that the 2-

oxygen stabilizes the positive charge at the anomeric position. In the absence of any nucleophile, 1,2-anhydrides (epoxides) are formed by displacing good anomeric leaving groups such as halides. From the structures of 3-D substrate-enzyme complexes, substrate distortion is a common feature. **Figure 1.7**[30] is the unhydrolyzed substrate complex of a β-glycosidase Cel5A with 2,4-dinitrophenyl 2-deoxy-2-fluoro-β-D-cellobioside. The -1 subsite sugar conformation is a $^{1}S_{3}$ skew-boat conformation, away from the preferred $^{4}C_{1}$ chair conformation. This conformation puts the leaving group in the pseudo-axial orientation, and presents the anomeric carbon to the nucleophile in an appropriate position for the in-line attack[40]. Other distortion of substrate in its ground state $^{4}C_{1}$ conformation to ^{4}E envelope or $^{1}S_{5}$ skew boat conformers has been confirmed by crystal structure analysis of Michaelis complexes. These conformational changes direct the scissile bond to an axial orientation, as required by the principle of stereoelectronic control. However, this distortion is not universal. A number of glycoside complexes have been reported without distortion[21,25,27,28]. Even with the same ligand (thiopentasaccharide), different glycosidases (Cel7B[41] and Cel5A[26]) present different binding modes (chair and skew-boat), but it is also possible these binding modes represent different steps of the reaction pathway: from an initial binding with the -1 subsite sugar in the chair conformation to the distorted complex to facilitate the nucleophilic attack. Nevertheless, there is not a 'requirement' for substrate distortion to achieve the transition state with C5, O5, C1 and C2 coplanar and pseudo-axial orientation for the leaving group. It should be pointed out that the 2,4-dinitrophenyl substituent on the anomeric oxygen is a very powerful electron withdrawing group and the $^{1}S_{3}$ skew-boat conformation places the anomeric oxygen in the same relative orientation to the lone

pair in the ring oxygen as is found in α-glycosides. This orientation is stabilized by the "anomeric effect".

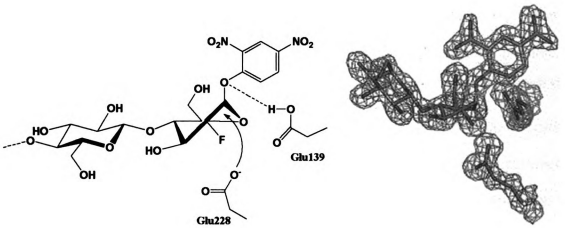

Figure 1.7. Stereographic "end-on" section through the electron density for the unhydrolyzed substrate complex of Cel5A. The enzymatic nucleophile, Glu 228, is shown, as are the -1 subsite pyranoside ring atoms and the dinitrophenyl leaving group. Substrate distortion to a skew-boat conformation permits nucleophilic attack "in-line" with leaving group departure.

The existence of the covalent glycosyl-enzyme intermediate was first illustrated by α secondary deuterium kinetic isotope effects with substrate for which the second step is rate determining. The K_H/K_D values are all greater than 1[13,42] (ranging from K_H/K_D = 1.25 for *E. coli* β-galactosidase[42] to K_H/K_D = 1.11 for both an *Agrobacterium* sp. β-glucosidase[14] and for Cex[43]), indicating the anomeric center undergoes rehybridization from sp^3 in the tetrahedral covalent intermediate to sp^2 in the oxocabenium ion-like transition state. Now, the covalent intermediate has been confirmed by trapping the intermediates and the corresponding x-ray crystal structures. The most commmon strategy for trapping is to introduce an activated leaving group to the substrate and incorporate fluorine in the 2- or 5-position[35,44-46]. Good leaving groups can lead to the

rapid formation of the glycosyl-enzyme intermediate. The electron-withdrawing 2-fluoro group can slow down reactions for both steps of glycosylation and deglycosylation. The net result is the breakdown of the intermediate is slowed to a greater extent than its formation. Therefore, the intermediate accumulates, making the trapping possible. A number of three-dimensional structures of such intermediate have been solved[30,38,47-53], and they have unambiguously revealed the covalent linkage between the anomeric carbon and the oxygen of the nucleophile. **Figure 1.8** is the schematic figure of the covalent 2-fluoro-2-deoxy-cellotriosyl-enzyme intermediate of Cel5A[31]. The sugar rings are in the relaxed chair conformation without distortion, which is observed in most of the glycosyl-enzyme intermediate. The nucleophile is Glu 228 and the acid/base catalyst is Glu139, which is hydrogen bonding to a water molecule. This water molecule is 3.1 Å away from the anomeric carbon, and is well positioned for the nucleophilic attack. All the hydroxyl groups are involved in the hydrogen bonding to the enzyme residues. The 6-OH is relatively flexible, and it has two possible conformations, with OH pointing out or backwards. Comparing the two Cel5A complexes with unhydrolyzed 2,4-dinitrophenyl 2-deoxy-2-fluoro-β-D-cellobioside and the covalent intermediate, we can see there is very little change of the atomic movement except the 'migration' of the anomeric carbon (from skew-boat to chair). A feature of these complexes is the static nature of the protein. The protein enzyme residues remain almost the same position and conformation with the exception of the nucleophile which rotate to avoid a steric clash with 2-F substituent in the trapped intermediate.

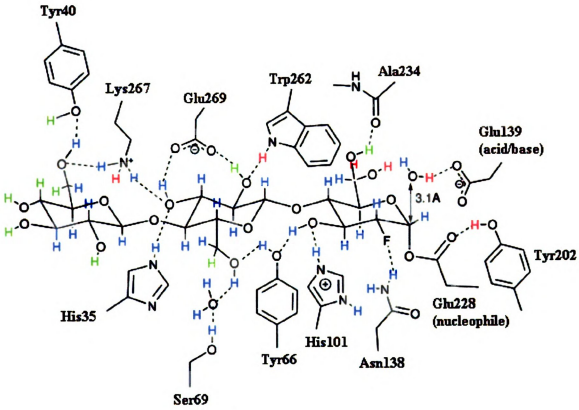

Figure 1.8. Schematic figure of the covalent 2-fluoro-2-deoxy-cellotriosyl-enzyme intermediate of Cel5A active site. Experimentally determined H atoms are indicated in blue, those with weak density in green and those for which no electron density was observed in red.

The covalent glycosyl-enzyme intermediate was also obtained for hen egg-white lysozyme (HEWL)[50], the first glycosidase with 3D structure solved. The intermediate between the HEWL (E35Q) mutant enzyme and substrate 2-acetamido-2-deoxy-β-D-glucopyranosyl-(1→4)-2-deoxy-2-fluoro-β-D-glucopyranosyl fluoride (NAG2FGlcF) was characterized by x-ray crystallography. The mutant enzyme in which the catalytic acid/base carboxylate residue had been replaced by the corresponding amide is used to reduce the rate of the reaction since no acid/base catalysts are available. **Figure 1.9** is the structure of the HEWL (E35Q) covalent glycosyl-enzyme formed by reaction with NAG2FGlcF. It is clear that the covalent linkage (~1.4 Å) is between C1 and $O^{\delta 2}$ of

nucleophile Asp 52, and the -1 pyranose ring adopts an undistorted $^4C_1$ chair conformation, as seen earlier and in the structures of most hexopyranose covalent intermediates observed. This covalent glycosyl-enzyme intermediate puts an end to a long-lived controversy and discards the ion-pair intermediate hypothesis found in all textbooks.

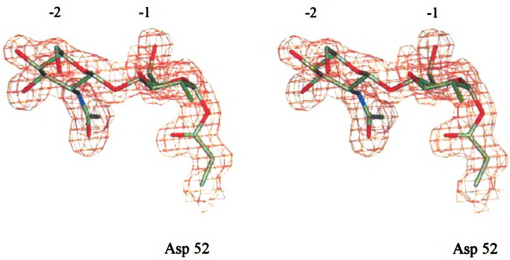

Figure 1.9. Structure of the covalent intermediate in the HEWL reaction. Maximum likelihood / $_{\sigma A}$-weighted $2F_O - F_C$ electron density for the covalent glycosyl-enzyme intermediate of HEWL, contoured at 0.4 electrons per Å.

In most trapped intermediate structures, the undistorted chair conformation is observed[27,38,41,48,50,52,53], but in the x-ray structure of 2-deoxy-2-fluoroxylobiosyl-Bcx (BCX-2FXb) intermediate[51], a distortion of the sugar ring was observed[51,54,55]. One xylose moiety remains the normal chair confirmation, while the other one, through which the sugar is linked to the enzyme via an ester bond, is distorted into a $^{2,5}B$ boat conformation (**Figure 1.10a**). This conformation of the ring allows its C5, O5, C1, and C2 atoms to achieve a nearly planar geometry. It is reasonable to assume that the enzyme may distort the substrate to a transition state conformation with C5, O5, C1, C2 coplanar,

and shorten the distance between the nuclophile and anomeric carbon to the length of a glycosidic bond. Since the formed intermediate has this feature of coplanarity, the formation and hydrolysis of this species should be considerably facilitated **(Figure 1.10b)**. It should also be noted, however, that if the original $^4C_1$ conformation were retained, there would be two unfavorable trans-annular (1,3) interactions between the acyl group and the axial H-3 and H-5 protons. One of these is relieved in the $^{2,5}B$ conformation. Note also that this would not occur with a glucoside because the bulky hydroxymethyl group would be forced to take the unfavorable "flagpole" position. Such distortion is not common in the covalent glycosyl-enzyme intermediate, but it was also observed in the covalent 2-fluoromannotriosyl-mannanase intermediate, which adopts a conformation close to the $^oS_2$ skew boat[33]. The same steric argument holds here again except that the hydroxymethyl group on carbon 5 will clash with the fluoro group. To lessen this interaction, twist boat conformation is preferred. This is normally less stable than the chair conformation and implies that the attack of the carboxylate group cannot proceed if the ring is locked in a $^4C_1$ conformation. Together with structures of Michaelis complexes, those glycosyl-enzyme intermediates provided important information about transition state structures and reaction mechanism.

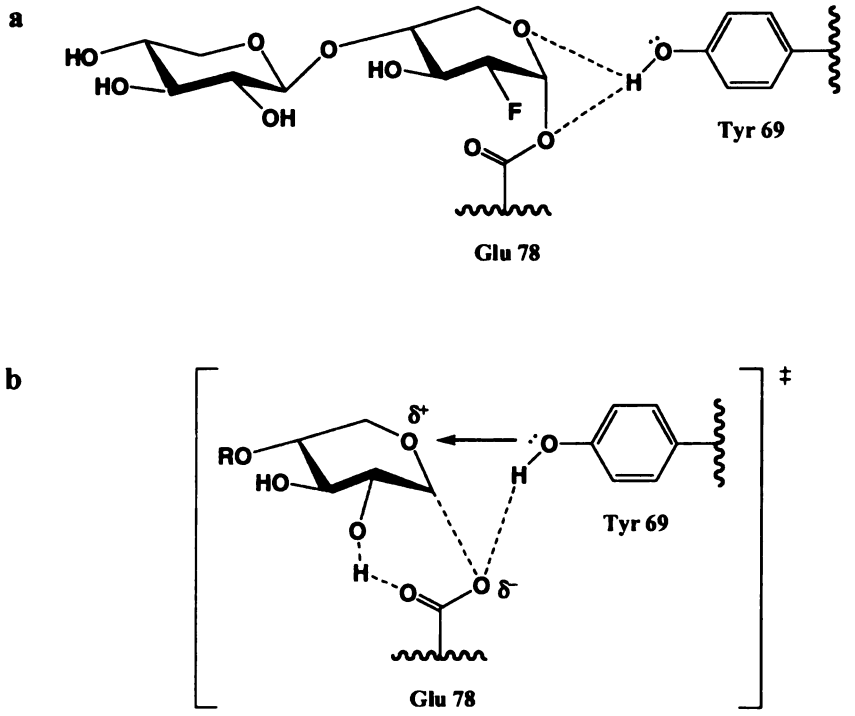

Figure 1.10 Active-site structure of *Bacillus circulans* xylanase trapped as a covalent 2-fluoroxylobiosyl intermediate (a) and implications for the transition state (b).

For enzyme complexes with product, no significant density could be observed[27,30]. This presumably results from the absence of specific stabilizing interactions at that end of the molecule. However, there is no evidence for any distortion of the reducing end ring away from a chair conformation.

1.3. Glycosyltransferases Structure and Mechanism

Glycosyltransferases catalyze the transfer of sugars from activated sugar donors to other molecules. The substrates for glycosyltransferases are relatively structurally complex. The molecules to which these enzymes transfer sugars, the glycosyl acceptors, include all

categories of biopolymers-oligosaccharides, proteins, nucleic acids, and lipids-as well as numerous natural products such as vancomycin, erythromycin, and daunomycin[56]. Although the acceptor substrates of glycosyltransferases vary widely and include many classes of oxygen and nitrogen nucleophiles, the donor substrates usually share common features with sugars attached to a nucleoside diphosphate or monophosphate which is the leaving group. **Figure 1.11** is some examples of common glycosyl donors.

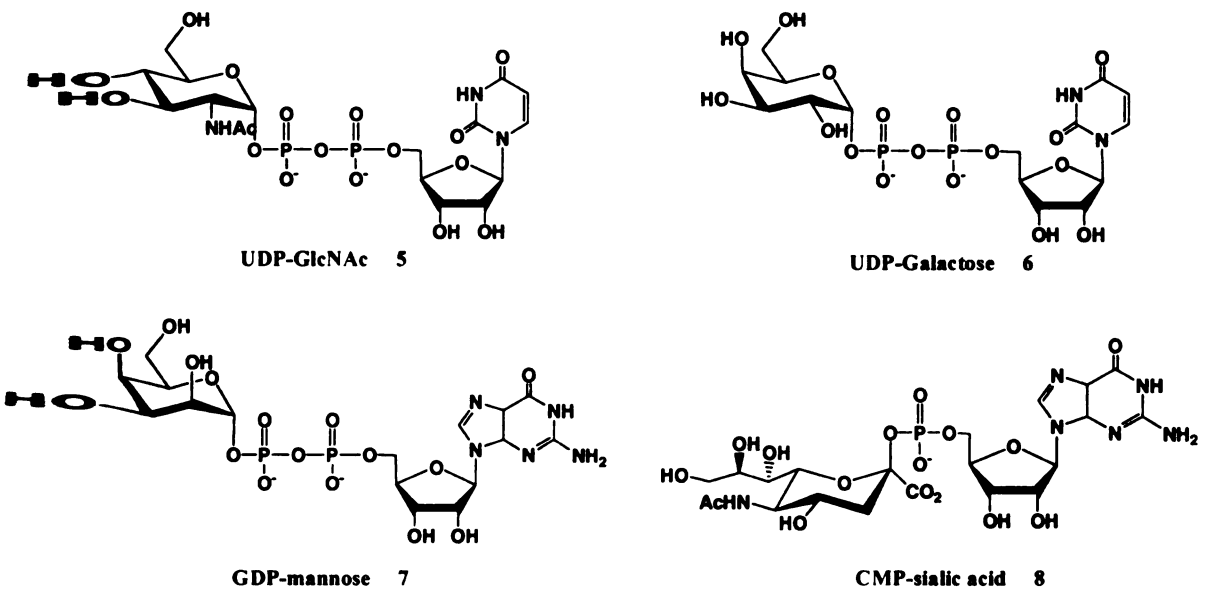

Figure 1.11. Structures of common glycosyl donors.

There is a myriad of glycosyltransferases all using similar activated sugars. Therefore, the specificity of these enzymes lies in the structures of the acceptors. Because of their function and product structure diversity, glycosyltransferases display a high level of diversity in terms of their primary sequences. There are currently >7000 known glycosyltransferase sequences in the databank and they have been classified into dozens of different families. Although there are a large number of different sequences, only two

fundamental folds[57,58] have been uncovered according to the available crystal structures of glycosyltransferases, and sequence analysis has suggested that this situation will hold true for a large number of the structurally uncharacterized families[59]. Until now, 21 glycosyltransferase structures from 14 different families have been reported, with 9 belonging to one superfamily, GT-A superfamily, and 8 to the other GT-B superfamily. The GT-A superfamily includes most of the Glycosyltransferases found in Golgi apparatus and endoplasmic reticulum. This superfamily, best represented by family GT-2 SpsA from *Bacillus subtilis* **(Figure 1.12)**[60,61], is characterized by a single Rossman fold domain, strong dependence of metal ions (most commonly Mn^{2+}) and sidechain residues from the protein. The metal ion is essential to catalysis, and it helps anchor the pyrophosphoryl group of the sugar donor in the enzyme active site. The sidechain residues are often called 'DXD motif'. The GT-B superfamily does not have such a motif and no metal ion has been identified clearly in the 3D structures. A typical example for GT-B superfamily is family 28 MurG from *E. Coli*. The crystal structure of MurG shows two similar Rossman domains, and each of the Rossman fold α/β open sheet structure is separated by a deep cleft in which the substrates bind[62,63] **(Figure 1.12)**.

SpsA **MurG**

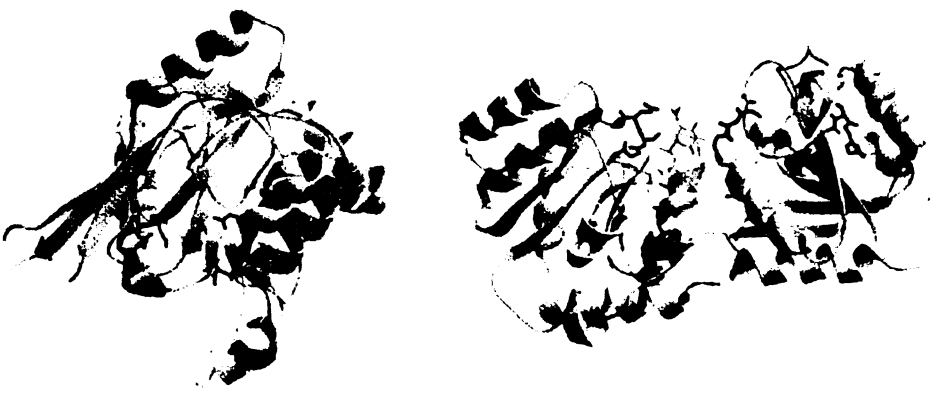

Figure 1.12. Ribbon diagrams of SpsA (PDB code 1QG8) from *B. subtilis* representing GT-A superfamily and MurG from *E. coli* complexed to UDP-GlcNAc (PDB code 1NLM) representing the GT-B superfamily. Residues important for substrate binding, specificity, ion binding, and catalysis are shown in black. In SpsA the manganese ion is shown as a dark gray sphere and in MurG substrate is shown in light gray.

Glycosyltransferase-mediated reactions are thought to proceed through an oxocarbenium-ion-like transition state, similar to that proposed for glycosidase reactions[64-66]. The α-secondary deuterium isotope effects on sucrose synthetase[67], rabbit glycogen synthetase[68], β4Gal-T1[69], and α-1,3-fucosyltransferase V[65] supported a mechanism in which the anomeric carbon of the donor sugar possesses considerable sp^2 character. An *ab initio* computational study[70] of the binding site has been performed supporting the formation of an oxocarbenium species and characterizing the transition state structure. Like the glycosidases, there are two basic mechanisms, an inverting and a retaining pathway. The inverting glycosyltransferases catalyze reactions through a single displacement with base activation of the acceptor. The retaining glycosyltransferases are suggested a double-displacement mechanism via a covalent glycosylenzyme intermediate, but no evidence has been found for the covalent intermediate on retaining transferases. The existence of this intermediate in transferases has been challenged by Withers et. al[71], and led to the revisit of the earlier suggestion of an 'internal return' (S_Ni) mechanisms[72,73] (**Figure 1.13**), in which the departure of the leaving group and attack of the nucleophile occur on the same (α) face of the glycoside, leading to a late oxocarbenium ion-like transition state.

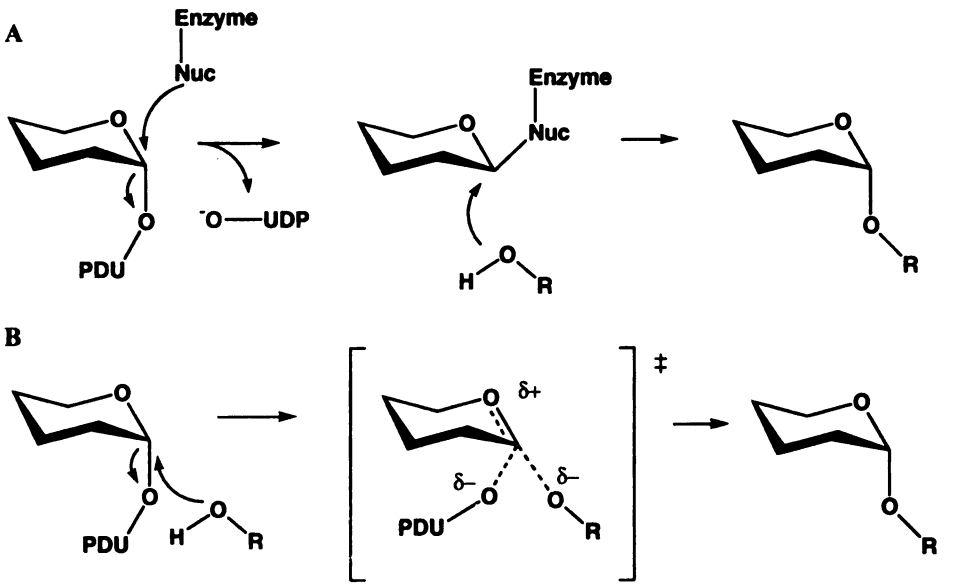

Figure 1.13 Two possible reaction schemes for retaining glycosyltransfereases. (A) A base-catalyzed double-displacement mechanism via a covalent intermediate with the enzyme. (B) An S_Ni-like mechanism involving a late oxocarbenium ion-like transition state.

1.4. Inhibitors of Glycosidic Bond

1.4.1. Glycosidase Inhibitors

Glycosidase inhibitors are invaluable tools for mechanistic studies. We have seen 2-fluoro compounds as probes for the elucidation of intermediate and transition state structures. Glycosidase inhibitors are also important targets for drug discovery. Several extremely debilitating and eventually fatal diseases such as diabetes, arthritis and several organ disorders are caused or mediated by carbohydrate processing. Inhibition of intestinal α-glucosidases can be used against diabetes by lowering the blood glucose levels. Inhibitors of glycoconjugate processing glycosidases can disrupt the biosynthesis of glycoproteins and glycolipids and hence cell-cell or cell-virus recognition. Therefore,

means of inhibiting or regulating glycosidases and glycosyl transferases, especially by small organic molecules, are much sought after in drug development.

A number of natural products which show glycosidase inhibition have been isolated from plants and microorganisms. Most of them resemble the natural carbohydrate, but an imino group replaces the endocyclic oxygen atom. They are believed to be able to mimic the ground state conformation and the positive charge character of the transition state upon protonation of the basic nitrogen atom. These natural occurring sugar mimics are classified into five structural classes[74]: polyhydroxylated piperidines, pyrrolidines, indolizidines, pyrrolizidines, and nortropanes. These natural occurring glycosidase inhibitors have provided important information for potent inhibitor design and have presented new challenges for the organic synthesis. A large number of newly designed glycosidase inhibitors have been based on the mimicry of the charge and shape of the proposed transition state. We will discuss some of the natural glycosidase inhibitors and the designed transition state analogues. Analogs that mimic the positive charge build-up in transition states as well as analogues which do not mimic the charge of the proposed transition states will be discussed. The position for the positive charge build-up includes endocyclic oxygen (**9**), anomeric center (**10**), and exocyclic oxygen (**11**).

9

10

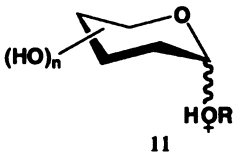

11

1.4.1.1. Inhibitors that mimic a positively charged endocyclic oxygen

The glycosyl oxocarbenium ion **9** is believed to be an important character of the transition state of glycosidases, so mimics of the cation **9** are thus potentially transition state analogs. The natural occurring nojirimycin family is an important class of this kind of inhibitors.

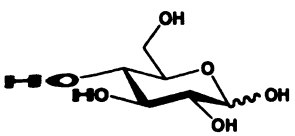

Glucose 1

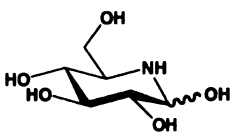

Nojirimycin 12

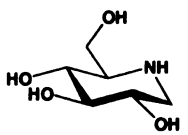

Deoxynojirimycin 13

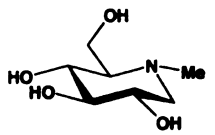

Me-Deoxynojirimycin 14

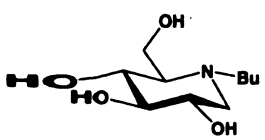

Bu-Deoxynojirimycin 15

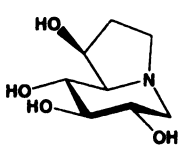

Castanospermine 16

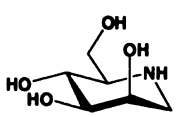

Deoxymannonojirimycin 17

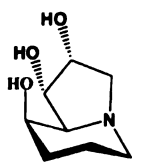

Swainsonine 18

Nojirimycin **12** was discovered as the first natural glucose mimics, with a nitrogen atom in the place of the ring oxygen[75], and it is a potent inhibitor of α- and β-glucosidases from a variety of sources[76]. The more stable form 1-deoxynojirimycin (DNJ)[77] **13** and 1-deoxymannojirimycin (DMJ)[78-80] **17** were also isolated and showed potent inhibitory activities against glycosidases. DNJ is a potent inhibitor of all kinds of glycosidases (**Table 1.1**)[12], but it is more selective to α-glucosidases and its inhibitory effect on mammalian α-glucosidases opened the possibility of a therapeutic application for DNJ. However, despite the excellent α-glucosidase inhibitory activity of DNJ in vitro, its efficacy in vivo was only moderate[81]. Therefore, a large number of DNJ derivatives were prepared in the hope of increasing the in vivo activity. Much of the work on chemical

modification has been focused on N-substitution[82,83]. N-methyl-DNJ and N-butyl-DNJ show better inhibition than DNJ, but longer alkyl chains do not show further increase in activity[84,85]. Some natural bicyclic polyhydroxyheterocycles were also discovered and isolated. The indolizidine castanospermine[86,87] **16** and swainsonine[88,89] **18** are typical examples. These compounds have less obvious structure relationship to monosaccharide but in each case the configuration of hydroxyl groups on the ring can be compared to those of sugars. Castanospermine can be considered a bicyclic derivative of DNJ, with an ethylene brige between the hydroxyl group and the ring nitrogen. Castanospermine is an excellent α-glucosidase inhibitor. Swainsonine is believed to be associated with DMJ, and showed inhibition against α-mannosidases (**Table 1.1**). The inhibition spectra of castanospermine, swainsonine and N-alkylation derivatives of DNJ showed they are more potent or more specific glycosidase inhibitors than the corresponding deoxynojirimycins and they have been targeted as anti-HIV, anticancer, antimicrobial etc. agents.

Table 1.1 Inhibition constant K_i (μM) of some natural inhibitors

Enzyme and source	**12**	**13**	**16**	**18**
α-glucosidases				
Yeast	6.3	12.6	>1500	
Rice	0.01	0.01	0.015	
Sucrase (Rabbit intestine)	0.13	0.032		
Sucrase (Rat intestine)			0.00055	
β-glucosidases				
Aspergillus wentii	0.36	2.7	0.9	

Sweet almonds	0.89	47	1.5	
Calf liver (cytosol)	-	210		
Calf spleen (lysosomes)	4.5	180		
Human placenta (lysosomes)			7	
α-mannosidases				
Jack beans				0.001
Almonds				>1000
Rat liver (lysosomes)				0.07
mannosidase I A/B				
Rat liver (Golgi ves.)				>1000
β-mannosidases				
Aspergillus wentii				>2000

Castanospermine has been found to inhibit lysosomal α- and β-glucosidases and disturb the lysosomal catabolism of glycogen[90] and glycolipids[91]. These syndromes resemble the genetic disorders Pompe's and Gaucher's disease, respectively. Both castanospermine and DNJ inhibit processing α-glucosidases I and II[92,93], but castanospermine is more effective against α-glucosidases I than DNJ[94]. Castanospermine and the N-alkylation derivatives Me-DNJ have also been shown to exhibit antimetastatic activity by inhibiting platelet aggregation of metastatic cells as well as reducing adhesion of tumor cells to the vascular endothelium[95,96]. Furthermore, these compounds have been shown to inhibit cellular transformation by altering oncogene glycosylation[97]. For the inhibition of HIV, castanospermine, DNJ, and synthetic *N*-butyl-DNJ (Bu-DNJ) are potent inhibitors of HIV

replication and HIV-mediated syncytium formation in vitro[98-100]. Bu-DNJ has been developed as an anti-HIV agent. It has been reported that a major mechanism of action of Bu-DNJ as an inhibitor of HIV replication is the impairment of viral entry at the level of post-CD4 binding, due to an effect on viral envelope components[100]. Bu-DNJ is also a specific inhibitor of the glucosyltransferase-catalyzed biosynthesis of GlcCer, the first step in the biosynthetic pathway of GlcCer-based GSLs[99]. This discovery constitutes great progress toward the treatment of this group of severe diseases. DMJ and swainsonine, which act on the later stages of *N*-linked oligosaccharide processing, have no effect on the secretion of infectious virus[100,101]. Swainsonine has no effect on Golgi α-mannosidase I[102], but it is a potent inhibitor (IC_{50}=0.2 μM) of rat liver Golgi α-mannosidase II, and swainsonine is the first compound that was found to inhibit glycoprotein processing. Swainsonine is also a potent inhibitor of lysosomal α-mannosidase[103]. The inhibition spectra of these azasugars revealed broad inhibition to all kinds of glycosidases, and poor in vivo activity. In the therapeutic applications, potent and specific inhibitor for one of the glycosidases could be more desirable. This requires more understanding of the enzyme properties and the action of the known inhibitors.

The three-dimensional structures of glycosidase complexes with DNJ and Castanospermine have been solved and have revealed different binding modes. The structure for the complex[104] of DNJ with glucoamylase (*Aspergillus awamori*) has provided information about the structural arrangement of functional groups and interactions of the inhibitor in the active site. Glucoamylase catalyzes the removal of β-D-glucose from the nonreducing ends of starch and other oligosaccharides, and it is an inverting glycosidase[105,106]. Upon binding, the overall conformation of the protein in the

complex is essentially the same as the native structure at pH 6.0. The important residues in the active site remain the same conformation and position, as seen earlier. There are two molecules of DNJ bound in the active site with one associated with strong electron density and representing the principal site of interaction. In the primary site, DNJ retains the chair conformation (**Figure 1.14**) instead of half-chair which is the assumed transition state conformation. In the active site of complex, 2-, 3-, 4- and 6- hydroxyl groups occupy the approximate positions of water molecules in the free enzyme. Only one water molecule (water 500) is present in the active site of the complex. This water molecule forms hydrogen bonding to the oxygen of Glu400, 6-OH and ring nitrogen of DNJ, and it is well oriented towards the C1 atom of the inhibitor (**Figure 1.14**). Therefore, it is reasonable to assume that this water molecule is the nucleophile of the general base catalyzed mechanism and that Glu400 is an important catalytic residue of the enzyme. In the structure of 2-fluoro-2-deoxy-cellotriosyl-enzyme intermediate of Cel5A, the 6-OH presents two possible conformations, but here the 6-OH is locked to only one conformation: upwards relative to the base of the active site to hydrogen bond Asp 55 and water 500. Mutation of Asp 55 to Asn or Tyr, and of Arg 54 to Lys or Thr leads to a complete loss of activity, indicating the essential role of these hydroxyl groups.

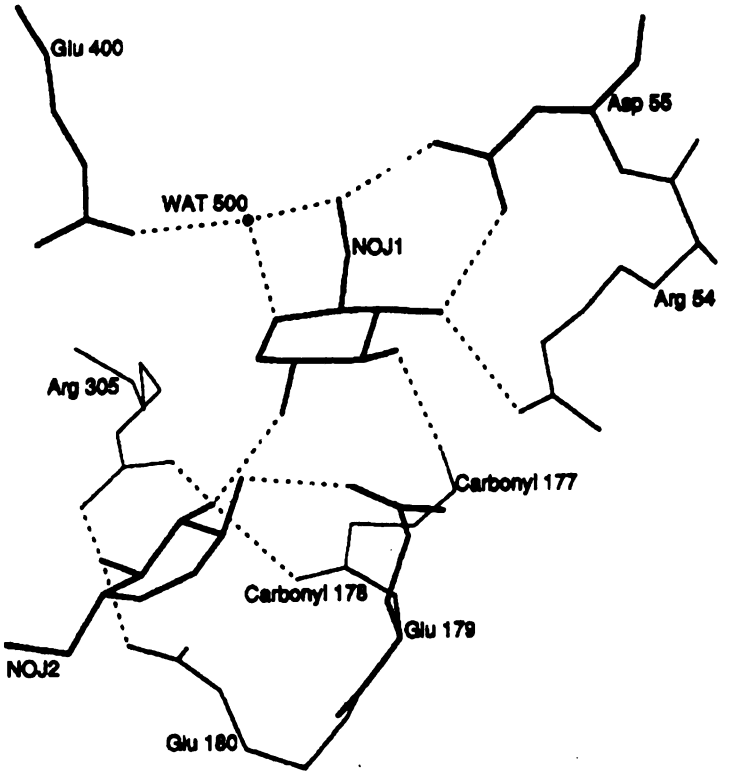

Figure 1.14. Schematic of the active site of glucoamylase II. NOJl and NOJ2 are 1-deoxynojirimycin at the primary and secondary site, respectively.

The structure of the Exo-β-(1,3)-gluconase (Exg from *Candida albicans*)[107] bound with castanospermine showed a different binding mode[108]. Castanospermine is larger and less flexible than DNJ due to the fused 5-membered ring bridged by ethylene between the nitrogen and C6. The crystal structure of the unbounded castanospermine[86,109] shows a chair conformation of the pyranose ring and an approximate envelope conformation of the 5-membered ring. However, in the complex with Exg, it presents a twisted boat conformation in which the positions of C3, C4, C5, C6 and N are almost superimposable on the equivalent atoms in the chair form, but C2 and C1 are displaced upwards relative

to the base of the active site pocket (**Figure 1.15**). This conformation would facilitate the departure of the leaving group and it can be considered a precursor to the transition state, which is assumed to be a half-chair. The ring nitrogen forms close contact to the oxygen of the nucleophile Glu229, consistent with an ionic interaction. The imino group also shows good tetrahedron geometry, indicating protonation which would be expected at the crystal pH of 6.0. Series of tight H-bonding contacts to the 2-, 3-, 4- hydroxyl groups lock the castanospermine into place. Those hydroxyl groups also occupy the positions of water molecules in the free enzyme. An important residue Glu 227 points centrally at the C3-C4 bond so that each of its carboxylate oxygen atoms interacts with a hydroxy group. The 6-OH lies axially, and interacts with two water molecules. The protein again undergoes very little change upon binding, except residue Asn 146 and Tyr 255, which are not involved in the binding. Asn rotates away for the ligand in order to avoid a clash with C2 which has moved upwards to a twisted boat conformation. Because of the rigidity caused by the 5-membered ring in castanospermine, Tyr 255 hydroxyl group moves 0.7 Å away to avoid the steric clash with C7. Again, conformations of protein, especially those of important functional groups remain unchanged to achieve tight binding.

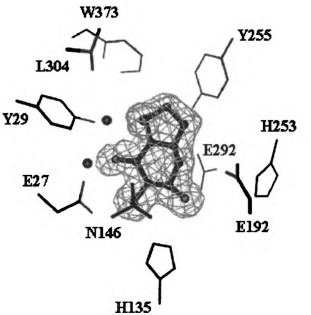

Figure 1.15. Stereoscopic images of the difference (F_o-F_c) electron density contoured at the 3σ level, and corresponding to castanospermine bound in the active site. Surrounding Exg residues are included with water molecules shown as bold circles.

Casternospermine and derivatives of deoxynojirimycin are considered selective inhibitors for α-glucosidases, because they mimic the positive charge character of the ring oxygen at transition state, which is believed to be an important feature of the α-glucosidase transition state. However, it is questionable whether they are real transition state analogues because they do not have the expected half-chair confirmation. Therefore, inhibitors that mimic both the positively charged ring oxygen and the half-chair confirmation have been developed.

The five-membered azasugars which is expected to be more flexible than six-membered rings were synthesized by C-H Wong et al[110]. The five-membered ring has more flattened chair confirmation and the positive charge can be mimicked by the positive charged imino group, so compound **19** showed better inhibition against α-glucosidase (K_i= 2.8

μM[111] for α-glucosidase) than DNJ and compound **20** showed strong inhibition to α-galactosidase from coffee bean at pH 5.5 (K_i = 0.05 μM). The x-ray crystal structure[110] of compound **19** indicated an envelop conformation of the five member ring. **Figure 1.16** shows the proposed transition state for α-glucosidase and the positive charged compound 20. Therefore, five-membered azasugars are better transition state analogs than six-membered ring azasugars. However, it is noted that compound **20** is a less potent inhibitor to α-galactosidase compared to 1-deoxy-D-galactonojirimycin **21** (K_i = 1.6 nM)[112], which has a chair conformation.

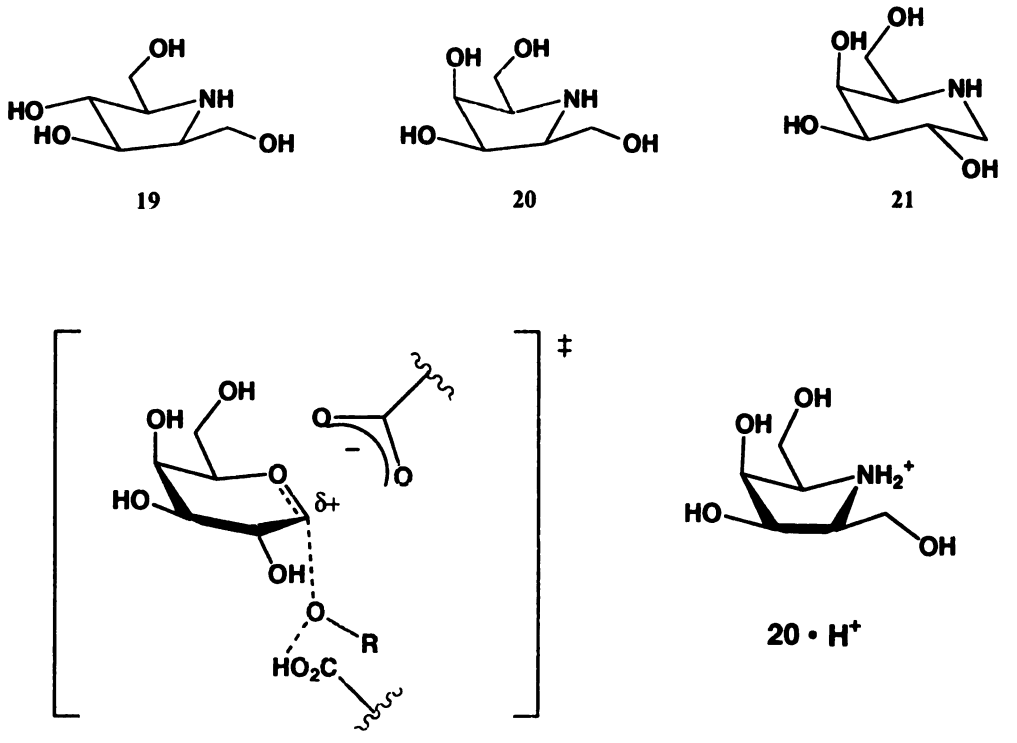

Figure 1.16. Proposed transition state structure for the α-galactosidase reaction. Compound **20** is a mimic of the galactosyl cation.

Glycosidase inhibitors with sp^2-hybridized anomeric carbon and ring nitrogen have been designed to meet the flattened chair confirmation requirement. Series of glucoimidazole-[113-117], glycopyrrole[118-120], glycotriazole[121]-type inhibitors have been synthesized. However, most of them only showed weak or modest inhibition. The stronger inhibition observed for compounds **28-32 (Table 1.3)** was suggested to come from the interaction of 2-NH_3^+ or ester function and the nucleophilic carboxylate of the enzyme[119].

Table 1.2. K_i values in μM for compound **22-27.**

		R_1	R_2	β-glu'ase[a]	β-glu'ase[b]
22	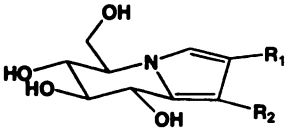	$COOCH_3$	H	6000	1150 (pH6.8)
23		H	$COOCH_3$	300	410 (pH6.8)
24		$COOCH_3$	$COOCH_3$	25000	-
25		CH_2OH	CH_2OH	14000	-
26	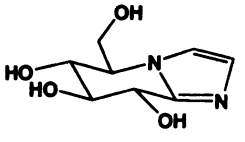			0.7 (IC_{50})	
27	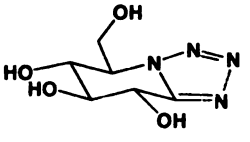			200	5

[a] Almond β-glucosidase. [b] *Caldocellum saccharolyticum* β-glucosidase.

Table 1.3. K_i values in μM for compound **28-34.**

		R	β-glucosaminidase[a]	β-glu'ase[b]
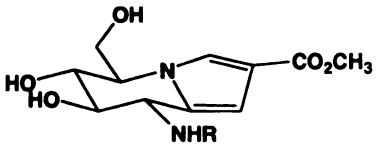	28	Ac	19	-
	29	H	-	12 (pH6.8)
	30	CF_3CO	10	-
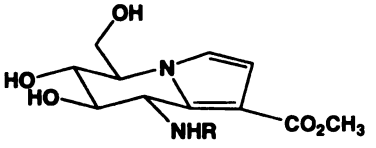	31	Ac	20	-
	32	H	-	21(pH6.8)
	33	CF_3CO	13	-
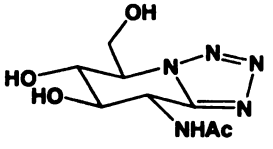	34		0.2	

[a] Bovine kidney β-glucosaminidase. [b] *Caldocellum saccharolyticum* β-glucosidase.

Compared to the imidazole analogue **26**[122] and tetrazole analogs **27** & **34**[123], compounds **22-25** & **28-33** are relatively poor inhibitors, and they lack a basic nitrogen atom at the glycosidic position. This might be essential to the strong inhibition and we will talk about this kind of inhibitors later.

A class of five-membered imidazole compounds is also synthesized and tested (**35-37**)[121,124]. Compound **36**[124] showed strong inhibition against α-mannosidase with IC_{50} = 10 μM, K_i= 5 μM), while other compounds are poor inhibitors. This is probably due to the correct configuration of hydroxyl groups in **35**.

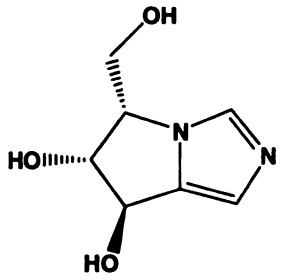

35

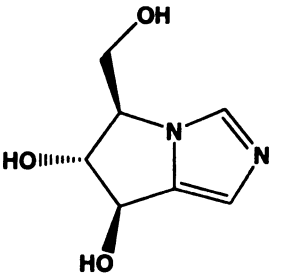

36

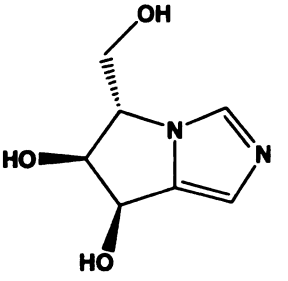

37

A new class of glycosidase inhibitors which contain cyclic sulfonium ions is worth mentioning. The natural products salacinol **38**[125,126] and kotalanol **39**[127], the herbs used in India transitional medicine for diabetes, are among the most potent glycosidase inhibitors. The permanent positive charged sulfonium ion may contribute to the high affinity to the enzyme. The x-ray crystal structure[128] of salacinol showed a unique spiro-like configuration of the inner salt comprised of 1-deoxy-4-thioarabinofuranosyl sulfonium cation and 1'-deoxyerythrosyl 3'-sulfate anion. This characteristic structure may account for the strong inhibitory effect of salacinol.

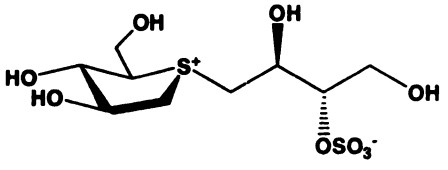

Salacinol 38

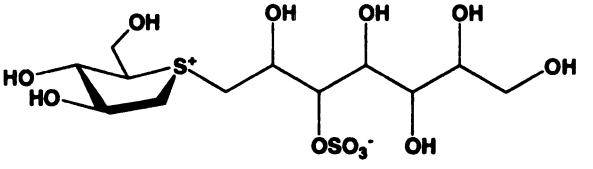

Kotalanol 39

1.4.1.2. Inhibitors mimicking the charge build-up at the anomeric center

The positively charged anomeric carbocation **10** has not been paid much attention until the mid-90s because its resonance form oxocarbenium ion **9** is believed to be a more important feature of the transition state. In 1994, Bols et al.[129,130] proposed that mimics of

the cation **10** could be transition state analogues. One way of incorporating a positive charge at the anomeric center is to introduce a basic nitrogen to the anomeric position, and replace the ring oxygen with methylene group in the corresponding sugar. Isofagomine **41** (1-aza suagr), named after the natural product fagomine **40**, was synthesized. It has nitrogen at the anomeric position and glucose configuration, while the 2-OH was removed because of the possible instability of the hemiaminals[131].

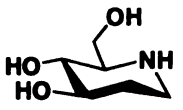

40

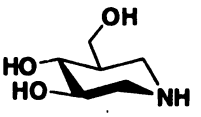

41

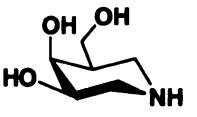

42

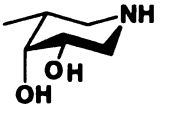

43

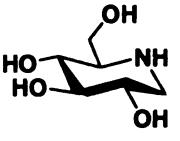

13

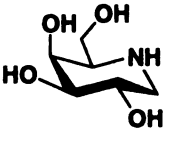

21

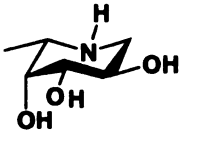

44

The inhibition studies showed that isofagomine **41** is a powerful glucosidase inhibitor[132] **(Table 1.4)**, especially for β-glucosidase, with K_i value 440 times lower than that obtained for DNJ **13**. Other 1-aza sugars with different configurations were also synthesized and tested by Ichikawa et al.[133] They were found to be very potent and specific against the corresponding β-glycosidases, with K_i values in the nanomolar range **(Table 1.4)**.

Table 1.4. Inhibition constant K_i in μM for isofagomines.

enzyme	41	13	42	21	43	44
α-glucosidase[a]	86	12.6				
Isomaltase[a]	7.2	11				
β-glucosidase[b]	0.11	47				
α-galactosidase[c]			50	0.0016		
β-galactosidase[d]			0.328	81		
β-galactosidase[e]			0.004			
β-galactosidase[f]			0.2	125		
α-fucosidase[g]					4	0.029
α-fucosidase[h]					6.4	0.0013

[a] From yeast. [b] From almonds. [c] From Green Coffee Bean. [d] From *Saccharomyces Fragilis*. [e] From *Aspargillus Oryzae*. [f] From *E. Coli*.. [g] From bovine kidney. [h] From human placenta.

The galactose type 1-aza sugar **42** is an extremely potent inhibitor of β-galactosidase, with a K_i value of 4.1 nM. The inhibition spectra of isofagomines are complementary to those of DNJs, which show selective inhibition against corresponding α-glycosidases (**Table 1.4**) by mimicking the positive charge developed at the ring oxygen. This complementary inhibition profile of DNJ and isofagomines is explained by the different positions of the positive charge build-up of the transition state and the interaction of inhibitors with the carboxylate groups of the enzymes[134-136]. For α-glucosidase, the oxocarbenium ion **9** is believed to be an important state, and the catalytic nucleophile carboxylate is located close to the β face of the pyranoside ring (**Figure 1.17a**), thus the protonated nitrogen atom is well positioned to form a hydrogen bond or a salt bridge with the anionic catalytic nucleophile. For β-glyosidases, a C-1 cation **10** is more important for

equatorial glycoside cleavage, with greater share of positive charge at anomeric carbon, which is better suited to interact with the catalytic nucelophile of a β-glyosidase (**Figure 1.17b**).

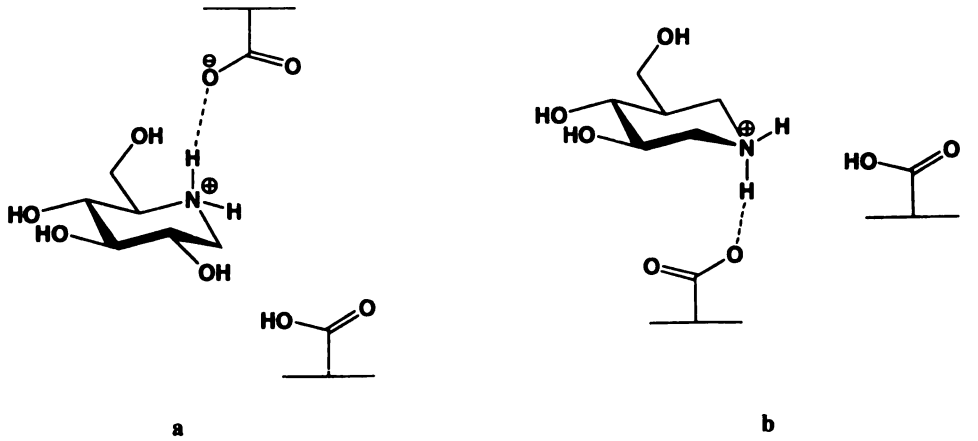

Figure 1.17. Proposed favored binding interaction of DNJ in α-glucosidase (a) and isofagomine in a β-glucosidase (b).

The thermodynamic studies[137] of binding of isofagomine **41** and DNJ **13** to β-glucosidase indicated very different binding modes for these two inhibitors (**Table 1.5**). The ΔH and ΔS values were obtained by measuring K_i at different temperatures and plotting $-\ln K_i$ vs 1/T in a Van't Hoff plot. The data show a negative enthalpy and small entropy for DNJ, which indicates that the binding of DNJ to β-glucosidase is favorable in terms of bond energies, while the entropy is relatively unimportant. This energy could be obtained from forming a hydrogen bond between 2-OH and the enzyme as well as a strong hydrogen bond or a salt bridge between the catalytic carboxylic acid group of the enzyme and ring

nitrogen. For isofagomine, the enthalpy is positive and the large entropy indicating the binding of **41** is driven by the large increase of disorder, which can compensate for the positive enthalpy.

Table 1.5. Thermodynamic parameters for the binding of the two inhibitors to almond β-glucosidase at pH 6.8

	K_i (μM, 25°C)	ΔH (kJ/mol)	ΔS (J/mol K)
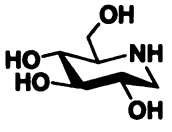	26.3	-25.7	1.3
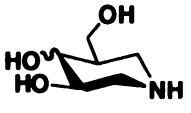	0.27	58.6	323.8

A recent study of a new inhibitor noeuromycin[138] **49**, an analogue of isofagomine with the 2-OH present, showed that the anomeric nitrogen can interact effectively with α-glycosidases as well. This is contrary to the belief that anomeric positive charge is only important to β-glycosidases. Noeuromycin (**49**) was tested for inhibition of glycosidases (**Table 1.6**) and was found to be a remarkably strong glucosidase inhibitor. The K_i values were all in the nanomolar range and between 2 and 4000 times smaller than those of **41**. Evidently the incorporation of the 2-hydroxyl group increases inhibition profoundly. The inhibitor **49** was also considerably more potent against glucosidases than the inhibitors **13**, **21** and **19** resembling oxocarbenium ion intermediate **9** (**Table 1.6**). It is remarkable that in contrast to **41** the inhibitor **49** inhibits both β- and α-glucosidase strongly. The D-galacto- (**50**) and L-fuco- (**51**) isomers of **49** were also glycosidase inhibitors in the

nanomolar range. The galactose analogue **50** is much more potent against α-galactosidase than isogalactofagomine **42**, while its inhibition of three β-galactosidases varied from 4 times more potent to 9 times less potent than **42**. The L-fucose analogue **51** was 1000 times more powerful than isofucofagomine **43** against α-fucosidase. It is clear that the incorporation of the 2-hydroxyl group contributes very tight binding to both α- and β-glycosidases. It was suggested that similar to the interaction between the anomeric nitrogen and the nucleophilic carboxylate of β-glycosidases[136,139], a salt bridge also exists between this nitrogen in **49**, **50**, **51** and the carboxylate of α-glycosidases (**Figure 1.18**).

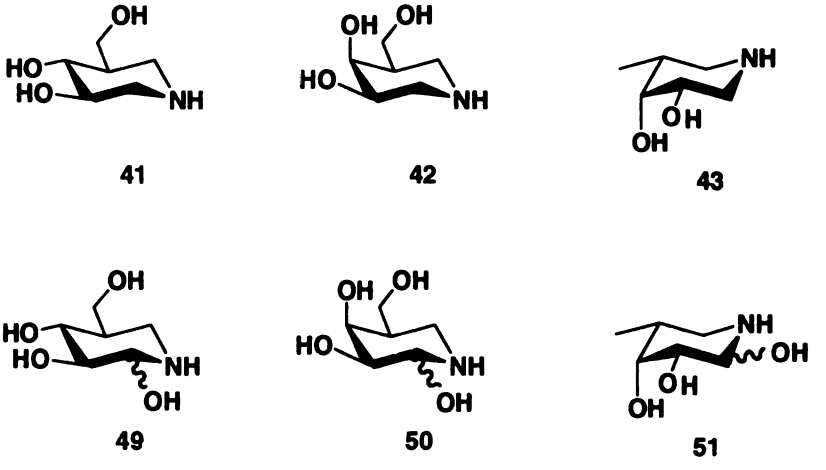

Table 1.6. Inhibition constant K_i in nM[a]

enzymes	41	49	42	50	43	51
α-glucosidase[b]	86000	22	-	-	-	-
isomaltase[b]	7200	25	-	-	-	-
β-glucosidase[c]	110	69	-	-	-	-
α-galactosidase[d]	-	-	50000	742	-	-
β-galactosidase[e]	-	-	328	91	-	-
β-galactosidase[f]	-	-	4	35	-	-

β-galactosidase[g]	-	-	200	397	-	-
α-fucosidase[h]	-	-	-	-	4000	4.7
α-fucosidase[i]	-	-	-	-	6400	3.2

[a] -: inhibition not measured. [b] From yeast. [c] From almonds. [d] From Green Coffee Bean. [e] From *Saccharomyces Fragilis*. [f] From *Aspargillus Oryzae*. [g] From *E. Coli*.. [h] From bovine kidney. [i] From human placenta.

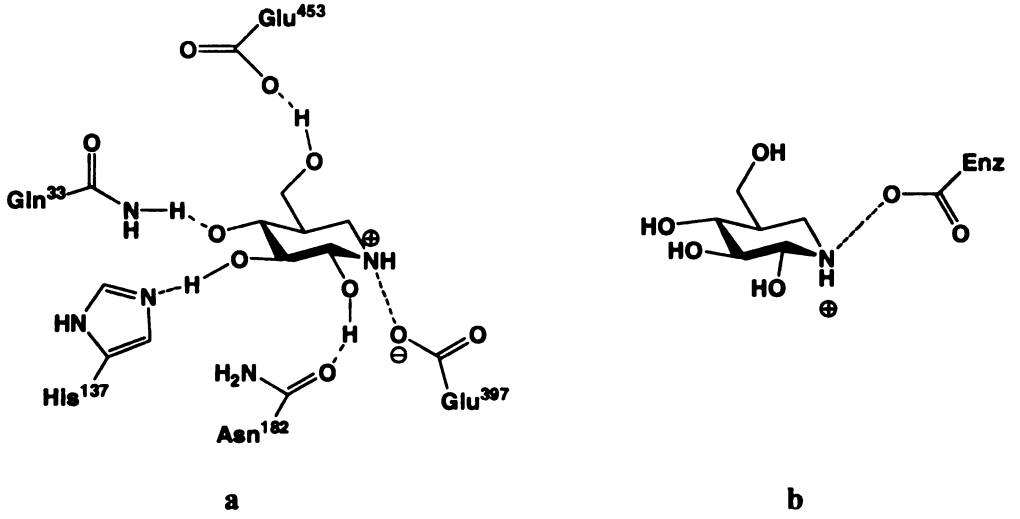

Figure 1.18. Proposed binding of **49** in the active site of a β-glucosidase (a), in this case from white clover and a retaining α-glucosidase (b).

The importance of the charge-mimicry of transition state has been demonstrated by azasugar analogs. Although it is assumed that protonated azasugars bind to the enzymes, no direct evidence of the protonation state of azasugars has been obtained until recently. The 1.0 Å resolution three-dimensional structure of Cel5A from *Bacillus agaradhaerens* in complex with compound **52** was solved by Davies al et [140].

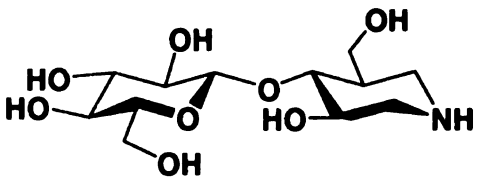

52

Figure 1.19 is the schematic representation of the interactions. It reveals that the imino sugar is protonated within the active site. The carboxylate oxygen of Glu 228 is 2.6 Å form N1 of **52**, indicating a close Coulombic interactions between the protonated isofagomine and the negatively charged nucleophile. It is also noted that glucose and isofagomine moieties are in undistorted $^4C_1$ (chair) confirmations. This is the first direct observation of the protonation state of an azasugar glycosidase inhibitor upon binding.

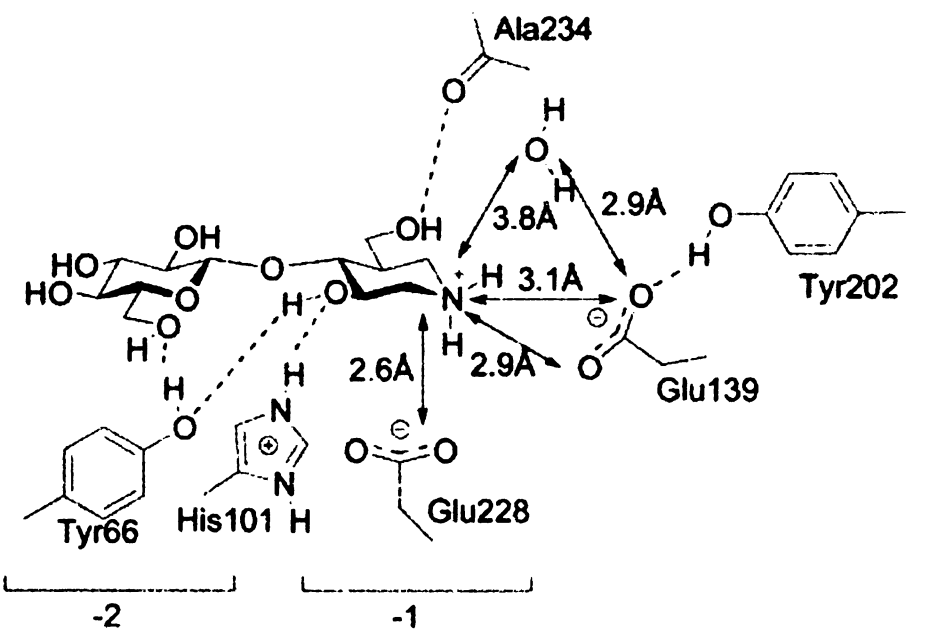

Figure 1.19. Schematic representation of the interactions observed between Cel5A and the cellobio-derived isofagomine (**52**). All hydrogen atoms shown have been observed experimentally. Only the -1 subsite interactions are shown in detail. Distances around N1 are indicated.

1.4.1.3. Inhibitors which mimic the positively charged exocyclic oxygen

Since glycoside cleavage of an ordinary *O*-glycoside involves protonation of the exocyclic oxygen of the glycosidic bond, an early transition state may have a considerable charge at this atom. Thus, stable compounds that resemble the positively charged ion **11**, may be regarded as transition-state analogues. Compounds that have an amine in place of the exocyclic oxygen are the most common transition-state analogs of this kind.

Some natural inhibitors which contain an exocyclic nitrogen have been isolated. The main classes of this type of compounds are the trehazolins **53**, the allosamidines **54**, acarbose **55**. The trehazolins exhibit powerful specific inhibition of various trehalases; the allosamidines inhibit various chitinases, and acarbose is a very potent α-glucosidase inhibitor[141].

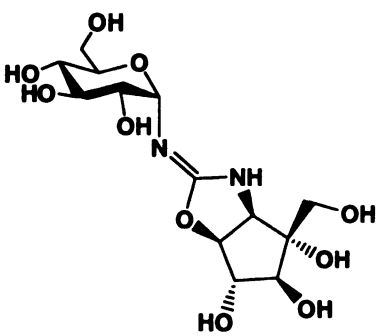

Trehazoline 53

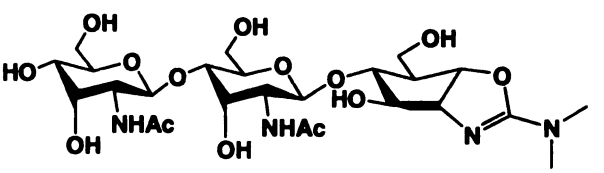

Allosamidin 54

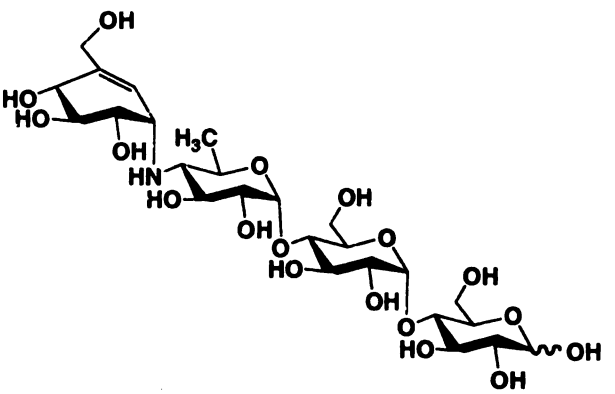

Acarbose 55

Glycosylamine are classical mimics of the protonated substrate. However, these compounds are not stable and hydrolyze very quickly under assay conditions[142]. Nevertheless, a fucosylamine was synthesized and found to be a potent inhibitor (K_i = 0.75 μM) against α-L-fucosidase from bovine kidney[143]. More stable forms have been investigated, including glycosylamidines[144], C-(glycopyranosyl)methylamines[145-148], amino-substituted (R/S)-phenylglucosides[146,149,150]. No powerful inhibition has been observed except for compounds **56-60**. Glycosylamidines **56-58**[144] showed selective inhibition against glucosidases, especially β-glucosidases. Compounds **59**[147] and **60**[149] are quite potent and selective inhibitors against β-galactosidases and α-glucosidases.

Table 1.7. K_i values in μM

Compounds 56-58	α-glu[a]	α-glu[b]	β-glu[c]	β-glu[d]	α-gal[e]	β-gal[f]
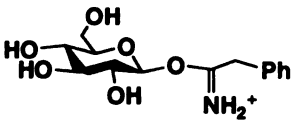	21	>2500[g]	73	0.094	-	-
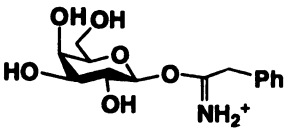	-	-	41	390	47	7.8
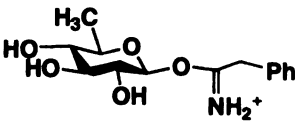	-	-	1100	11	-	-

- No inhibition at 2500 μM.[a] Yeast α-glucosidase.[b] *Aspergillus niger* α-glucosidase.[c] Almond β-glucosidase.[d] *Aspergillus niger* β-glucosidase.[e] *Aspergillus niger* α-galactosidase.[f] *E. coli* β-galactosidase.[g] Less than 50 % inhibition at 2500 μM.

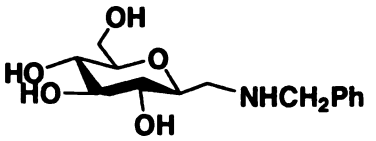

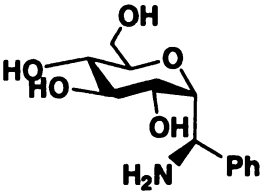

59 $K_i = 2.3\ \mu M$ **60** $K_i = 38\ \mu M$

(*E. coli* lacZ β-galactosidase) **(yeast α-glucosidase)**

Another important class of compounds is aminocyclopentanes. They have a stereochemistry similar to the stereochemistry of either gluco-, manno-, galacto-, fuco-, or xylopyranose. Great progress has been made and some strong and specific inhibitors have been synthesized. The amino(hydroxymethyl)cyclopentanetriols **61-63** with different substituents R have shown powerful inhibition against mannosidases, glucosidases, and galactosidases, with inhibition constants in the milimolar or micromolar range. There is a review by Siriwardena et. al[151] about this class of inhibitors.

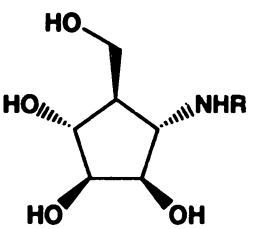

61

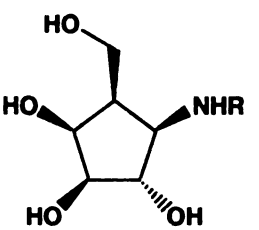

62

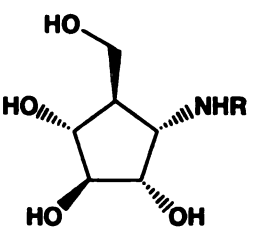

63

1.4.1.4. Inhibitors that mimic positive charge in several places (Mimics of **9** & **11**)

Both the endocyclic oxygen positive charge and the exocyclic positive charge have been shown to be important features of glycosidase transition states. It is reasonable to assume that stable compounds which mimic both the positively charged ion **9** and **11** are better transition state analogs.

9

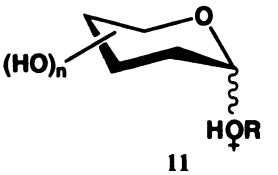

11

Ganem Group first synthesized amidine derivatives (**64** and **65**) of D-glucose[152,153], which combine the charge distribution at endo- & exocyclic oxygen and the desired conformation of glucosyl cation **9**. The amidine derivatives **64** and **65** have nitrogen in place of both endo-and exocyclic oxygens, so the positive charge can be delocalized among these two positions and anomeric center (**66**). The sp^2-hybridized anomeric carbon provides the flattened chair conformation of the assumed transition state. Inhibition testing found that amidine **64** and **65** are potent, broad-spectrum inhibitors of glycosidases (**Table 1.8**). It showed similar inhibition against β-glucosidase, β-galactosidase and α-mannosidase, and the N, N-dimethyl derivative **65** is less potent than **64**.

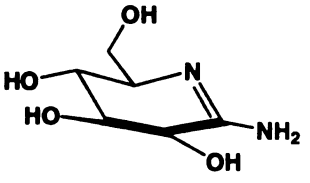

64

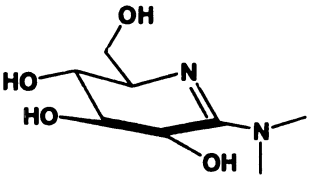

65

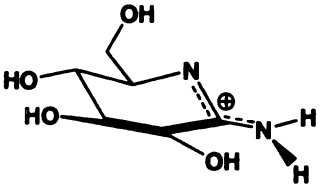

66

Table 1.8. K_i values in μM for compound **64-68.**

Enzymes	β-glucosidase[a]	β-galactosidase[b]	α-mannosidase[c]
64	8	8	9
65	83	83	40
67	8.4	19	3.1

68	13.8	19	12

[a] Sweet almond β-glucosidase. [b] Bovine liver β-galactosidase [c] Jack bean α-mannosidase

More stable forms amidrazone **67** and amidoxime **68** have been synthesized and tested[154,155]. They all showed broad spectra inhibition of glycosidases. Despite the large difference in the pK_a values of amidine **64** (pK_a = 10.4), amidrazone **67** (pK_a = 8.7), and amidoxime **68** (pK_a = 5.6), their inhibition against β-glucosidase (sweet almond) is at the same scale. This let Ganem et. al propose that it is the shape, not the charge of transition state more important for binding to β-glucosidase.

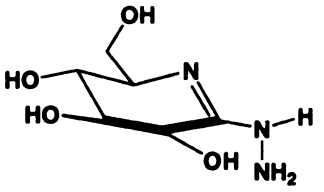

67

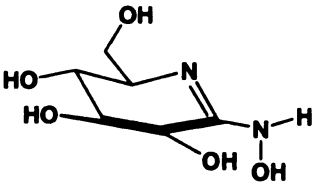

68

Another important class of inhibitors which mimic the flattened chair conformation and the positive charge at both positions consist of an azasugar fused with heterocyles such as triazoles or imidazoles[136,156]. A series of compounds can be obtained by introducing different substituents at the heterocyles, and they are more stable than amidines and their derivatives. The natural product nagstatin[157,158] **(69)** was shown to be an N-acetylgalactosamine fused with a substituted imidazole, and it is a strong N-acetyl-β-glucosaminidase inhibitor **(Table 1.9)**. Other compounds which have different

configurations and different substituents have been synthesized by Vasella's[136,156,159] and Tatsutas's groups[122,160-164] respectively. As can be seen in **Table 1.9**, the imidazoles are potent inhibitors of various glycosidases and more selective than the amidines and their derivatives. Also, the 1,2,4-triazoles are potent and selective inhibitors though they are not as strong as the imidazoles.

Table 1.9. K_i values in μM for compound **69-75.**

Enzymes		α-glu[a]	β-glu[b]	β-glu[c]	β-gal[d]	α-man[e]	β-man[f]	NAc-β-glu[g]	NAc-α--gal[h]
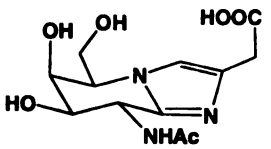	**69**		>334		>334			0.013	63
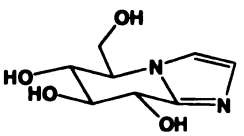	**70**	59	0.1	0.02					
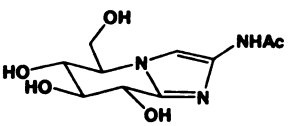	**71**	71*	3*	1.5*					
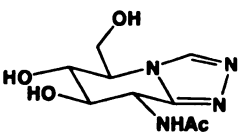	**72**							0.034	
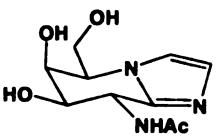	**73**		319		11			0.006	10
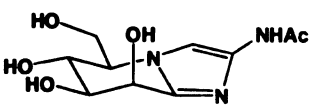	**74**					85	14		
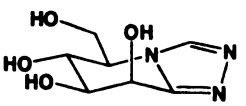									

	75	285		65	0.4		
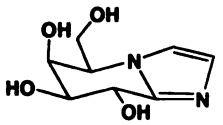	**76**	0.5	0.008	>500	370	60	125

*IC_{50} value. [a]Yeast α-glucosidase. [b]Almond β-glucosidase. [c]*Caldocellum saccharolyticum* β-glucosidase. [d]E.coli β-galactosidase. [e]Jack bean α-mannosidase. [f]Snail β-mannosidase. [g]Bovine kidney N-acetyl-β-glucosaminidase. [h]Chicken liver N-acetyl-α-glucosaminidase

The selectivity and strength of inhibitors may be enhanced by introducing substituents mimicking the aglycon. Introduction of the hydrophobic and flexible phenethyl substituent to the imidazole derivative **70** increased the inhibition of *C. saccharolyticum* β-glucosidase, leading to the strongest known inhibitor of a β-glucosidase (K_i = 0.11 nM)[165].

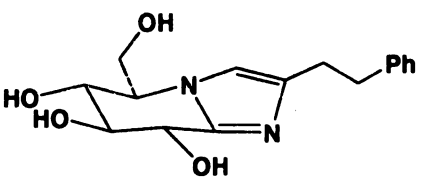

77

1.4.1.5. Inhibitors which do not mimic charge

Because the proposed transition state has considerable sp^2 hybridization with half-chair conformation, a number of nonbasic analogs have been developed to mimic this feature. δ-Aldonolactones and lactams have been found long time ago to be able to inhibit glycosidases because they resemble the transition state geometrically. Recently Nishimura's group synthesized and studied all possible D-stereoisomers of hexono-1,5-lactam and found D-manno isomer **78** was a good inhibitor of both α-mannosidase (jack bean K_i = 68 μM) and β-mannosidase (snail K_i = 9 μM) as well as β-glucosidase, and β-

galactosidase. The gluco, manno, galacto, talo and ido isomers were able to inhibit almond β-glucosidase[166]. The D-glucosaminolactam **79** is also a good inhibitor of β-glucosidase (*C. saccharomyces* $K_i = 0.7\ \mu M$)[167].

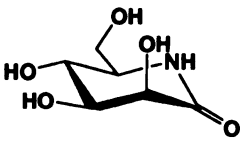

78

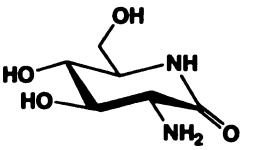

79

A new type of lactams were introduced by Wither's group in which the nitrogen is in the anomeic position similar to the isofagomines and the carbonyl group in the 2-position[168]. The rationale of this design is to incorporate the important 2-OH group to the 1-N-iminosugars and provide planarity for this molecule, if these lactams bind as the protonated iminol tautomers. The D-galacto analog[169] **(80)** showed strong inhibition against β-galactosidase from *Aspergillus oryzae*, and xylobiose analog inhibits Cex-xylanase with $K_i = 0.34\ \mu M$. However, the atomic-resolution structure of lactam with xylanase Xyn10A from *Streptomyces lividans* revealed that the lactam is bound to the enzyme as the amide tautomer, which is consistent with the free energy cost of amide-iminol isomerization (~45 kJ/mol) **(Figure 1.20)**.

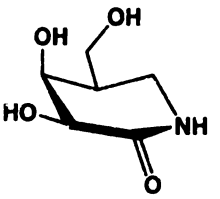

80

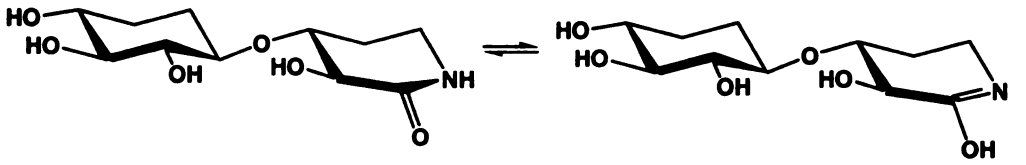

Figure 1.20. Amide-iminol isomerization

Other neutral compounds indcluding phosphonates, phosphonamides[170] and thioalditols[171] have been studied, but they were found to be poor inhibitors of glycosidases.

1.4.2. Glycosyltransferase Inhibitors

Glycosyltransferases are essential in the oligosaccharide synthesis. Abnormal cell surface glycosylation characterizes several cancers such as ovarian cancers[172], breast cancer[173-175], prostate cancer[176], and colon cancer[177,178] among a host of others such as oropharyngeal cancer, leukemias and Hodgkin's disease[179-188]. Many infectious diseases are also mediated by glycosylation. Therefore, different strategies have been explored to identify potent inhibitors of glycosyltransferases in order to modulate the formation of oligosaccharides and glycoconjugates, study functions of these biopolymers, and develop pharmaceutical agents. These strategies include design of analogs of donor molecules[189-195], acceptor molecules[196-200] transition state mimics[66,201-204] and glycosyl-enzyme intermediates[205]. A few successful examples have been reported, but rational design of transferase inhibitors still remain a difficult task because of the intrinsic features of glycosyltransferases: complex transition state with sugar donor, acceptor oligosaccharide where the sequence and linkage are extremely critical; weak binding of the enzyme with their natural substrates (usual K_m values are in the mM range); and few structural data.

A remarkable donor analog of sialyltransferase has been reported by Schmidt et. al[195]. The donor substrate for sialyltransferase, independent of their source and their acceptor specificity, is cytidine monophosphate *N*-acetylneuraminic acid (CMP-Neu5Ac). By incorporating a flattened neuraminyl residue, phosphonate, and a cytidine monophosphate (CMP) residue, a powerful sialyltransferase inhibitor (**81**) can be obtained. The inhibition constant is in nanomolar range (40 nM). Other analogs with a simple aryl or hetaryl moiety instead of the neuraminyl residue can also give potent inhibitors[206]. Therefore, a flat pyranosyl ring mimic, phosphonate and CMP residue are important for a potent sialyltransferase inhibitor.

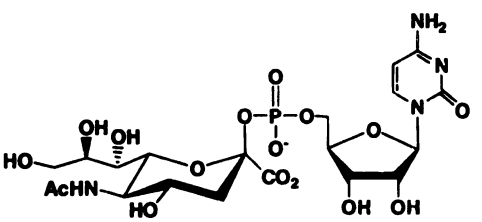

CMP-Neu5Ac

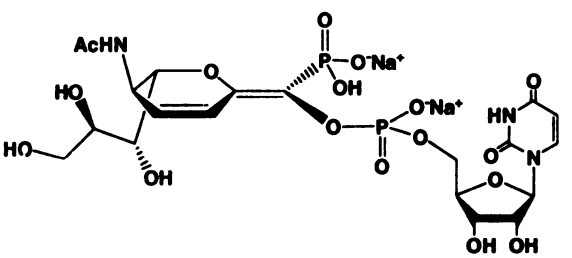

81

Because donor sugars are common substrates for glycosyltransferases, as mentioned earlier, the specificity of transferases largely resides on the recognition of the acceptor structures. One approach to specific glycosyltransferase inhibitors is to design the acceptor analogs. A simple strategy is to remove the reactive hydroxyl group of a glycosyltransferase oligosaccharide acceptor since presumably this hydroxyl group is not essential to the binding of the acceptor. Palcic et al prepared eight acceptor analogs for different glycosyltarnsferases[196] where the reactive hydroxyl groups were replaced by hydrogen. Four analogs showed competitive inhibition against the corresponding

glycosyltransferases, and the inhibition constants were in the range of the K_m values, with greater values. The other four analogs showed no inhibition, which is suggested to be lack of the critical hydrogen bonding between this acceptor hydroxyl group and the enzyme.

A peptide acceptor analog has been reported by Imperiali et. al[200]. The compound **82** is a nanomolar inhibitor of the oligosaccharyl transferase (OT), which is acting on the Asparagine-linked glycosylation. This class of cyclic peptide provided the first example of a readily available and adaptable family of potent protein glycosylation inhibitors.

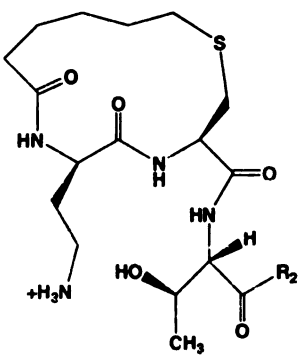

82

In 1999, Ichikawa et. al[205] reported a rationally designed α-1,3-galactosyltransferase (α 1,3-GalT) inhibitor **83**. They proposed since α 1,3-GalT is a retaining tarnsferase, a double displacement with formation of a glycosyl-enzyme intermediate is the possible mechanism (**Figure 1.21**). Molecules with nitrogen at the anomeric position should be able to mimic the glycosyl-enzyme intermediate by forming an inhibitor-enzyme complex via a favorable electrostatic interaction. The pyrophosphate moiety and the uridine residue are replaced with a vicinal diol and a 5'-thio-uridine respectively, to avoid an unnecessary negative charge on the molecule and to increase the stability of the designed inhibitor. Compound was found to be a potent and selective α 1,3-GalT

inhibitor with K_i value 4.4 μM, but not of β 1,4-GalT which is an inverting tarnsferase and does not involve a glycosyl-enzyme intermediate with a nearby carboxylate. It is noted that 1-deoxygalactonojirimycin has no inhibition against α 1,3-GalT, nor β 1,4-GalT, indicating the importance of the position of the imino group.

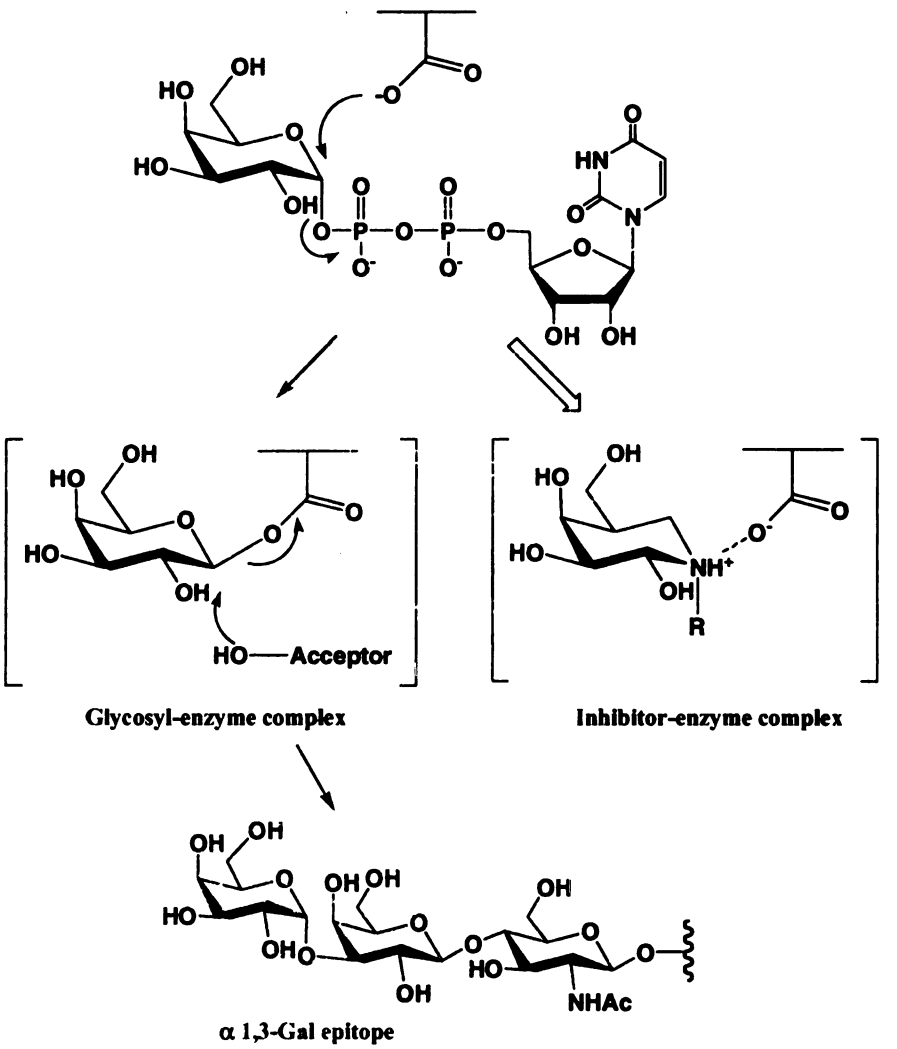

Figure 1.21. Proposed reaction mechanism of α 1,3-GalT and possible interaction between the 1-N-iminosugar-based inhibitor and the enzyme.

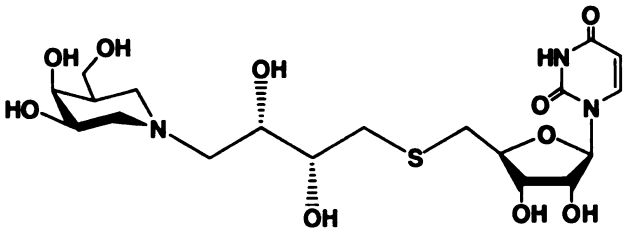

83

Fucosyltransferases are critical[4,207-209] in the biosynthesis of cell surface oligosaccharide since many of them are fucosylated and these fucose-containing structures accumulate in a large variety of human canceres[210,211]. Inhibition of these enzymes is important to study the oligosaccharide and to develop anti-inflammatory and anti-tumor agents. C-H Wong et al.[66] reported a synergistic inhibition of human α-1,3-fucosyltransferase V (**Figure 1.22**). The azatrisaccharide **85** which incorporate a fuconojirimycin moiety to the acceptor substrate was synthesized to mimic the proposed transition state with substantial oxocarbenium ion character. This azatrisaccharide alone cause moderate inhibition against fucosyltransferase with 5.7 mM. However, in the presence of 0.03 mM GDP, it showed dramatically increased inhibition with IC_{50} 0.031 mM. It was suggested that the azatrisaccharide form a complex with GDP via electrostatic interactions between the positively charged amino group and the negatively charged phosphate oxygen. This can mimic the transition state of the enzymatic reaction (**Figure 1.23**).

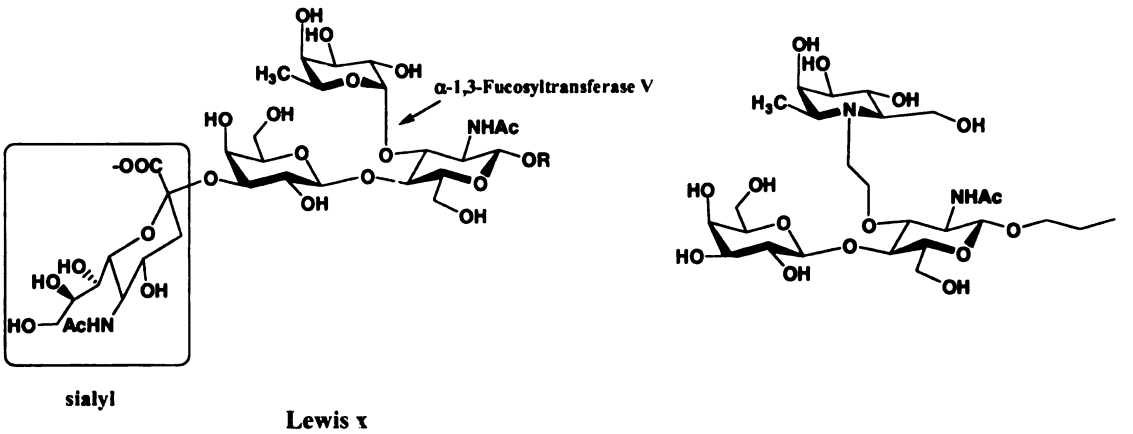

Figure 1.22. Structure of sialyl Lewis x. and the azatrisaccharide. α-1,3-fucosyltransferase V catalyze the addition of fucose to LacNAc or sialyl LacNAc.

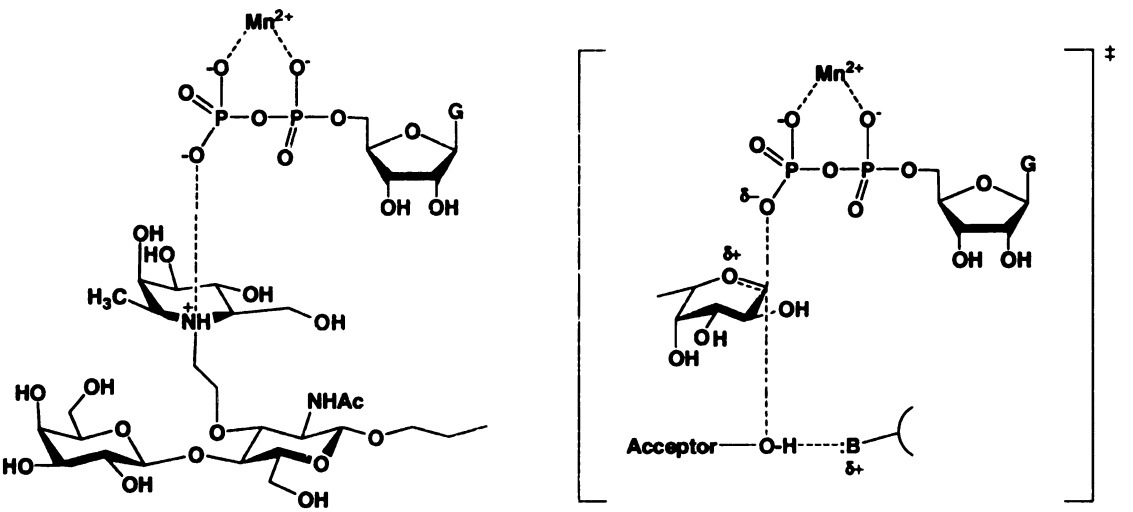

Figure 1.23. Proposed model for the synergistic inhibition of α-1,3-fucosyltransferase V by the combination of an aza sugar and GDP and the proposed mechanisms of hydrolysis fucosylation by α-1,3-fucosyltransferase V.

1.5. References

(1) Bertozzi, C. R.; Kiessling, L. L. Chemical glycobiology *Science* **2001**, *291*, 2357-2364.

(2) Jenkins, N.; Parekh, R. B.; James, D. C. Getting the glycosylation right: Implications for the biotechnology industry *Nature Biotechnology* **1996**, *14*, 975-981.

(3) Helenius, A.; Aebi, M. Intracellular functions of N-linked glycans *Science* **2001**, *291*, 2364-2369.

(4) Kornfeld, R.; Kornfeld, S. Assembly of Asparagine-Linked Oligosaccharides *Annual Review of Biochemistry* **1985**, *54*, 631-664.

(5) Gahmberg, C. G.; Tolvanen, M. Why mammalian cell surface proteins are glycoproteins *Trends in Biochemical Sciences* **1996**, *21*, 308-311.

(6) Burda, P.; Aebi, M. The dolichol pathway of N-linked glycosylation *Biochimica Et Biophysica Acta-General Subjects* **1999**, *1426*, 239-257.

(7) Silberstein, S.; Gilmore, R. Biochemistry, molecular biology, and genetics of the oligosaccharyltransferase *Faseb J.* **1996**, *10*, 849-858.

(8) Moremen, K. W.; Trimble, R. B.; Herscovics, A. Glycosidases of the Asparagine-Linked Oligosaccharide Processing Pathway *Glycobiology* **1994**, *4*, 113-125.

(9) Henrissat, B. B., A. *Biochem. J.* **1996**, *316*, 695-696.

(10) Wolfenden, R. L., X.; Young, G. Spontaneous hydrolysis of glycosides *J. Am. Chem. Soc.* **1998**, *120*, 6814-6815.

(11) Sinnott, M. L. Catalytic Mechanisms of Enzymatic Glycosyl Transfer *Chem. Rev.* **1990**, *90*, 1171-1202.

(12) Legler, G. Glycoside hydrolases: Mechanistic information from studies with reversible and irreversible inhibitors *Adv. Carbohydr. Chem. Biochem.* **1990**, *48*, 319-385.

(13) Davies, G. S., M. L.; Withers, S. G. *Glycosyl transfer. In Comprehensive Biological Catalysis*; Academic Press, 1998; Vol. 1, 119-208.

(14) Kempton, J. B.; Withers, S. G. Mechanism of Agrobacterium Beta-Glucosidase - Kinetic-Studies *Biochemistry* **1992**, *31*, 9961-9969.

(15) Zechel, D. L.; Withers, S. G. Glycosidase mechanisms: Anatomy of a finely tuned catalyst *Acc. Chem. Res.* **2000**, *33*, 11-18.

(16) Koshland, D. E. *Biol. Rev.* **1953**, *28*, 416-436.

(17) McCarter, J. D.; Withers, S. G. Mechanisms of Enzymatic Glycoside Hydrolysis *Current Opinion in Structural Biology* **1994**, *4*, 885-892.

(18) Wang, Q. P.; Graham, R. W.; Trimbur, D.; Warren, R. A. J.; Withers, S. G. Changing Enzymatic-Reaction Mechanisms by Mutagenesis - Conversion of a Retaining Glucosidase to an Inverting Enzyme *J. Am. Chem. Soc.* **1994**, *116*, 11594-11595.

(19) Davies, G.; Henrissat, B. Structures and Mechanisms of Glycosyl Hydrolases *Structure* **1995**, *3*, 853-859.

(20) Tews, I., Perrakis, A., Oppenheim, A., Dauter, Z., Wilson, K. S. & Vorgias, C. E. Bacterial chitobiase structure provides insight into catalytic mechanism and the basis of Tay-Sachs disease *Nature Struct. Biol.* **1996**, *3*, 638-648.

(21) Varrot, A.; Schulein, M.; Davies, G. J. Insights into ligand-induced conformational change in Cel5A from Bacillus agaradhaerens revealed by a catalytically active crystal form *J. Mol. Biol.* **2000**, *297*, 819-828.

(22) D. M. A. Guerin, M. B. L., M. Costabel, H. Souchon, V. Lamzin, P. Beguin and P. M. Alzari Atomic (0.94 Å) resolution structure of an inverting glycosidase in complex with substrate *J. Mol. Biol.* **2002**, *316*, 1061-1069.

(23) Sulzenbacher, G.; Driguez, H.; Henrissat, B.; Schulein, M.; Davies, G. J. Structure of the Fusarium oxysporum endoglucanase I with a nonhydrolyzable substrate analogue: Substrate distortion gives rise to the preferred axial orientation for the leaving group *Biochemistry* **1996**, *35*, 15280-15287.

(24) Sulzenbacher, G.; Schulein, M.; Davies, G. J. Structure of the endoglucanase I from Fusarium oxysporum: Native, cellobiose, and 3,4-epoxybutyl beta-D-cellobioside-inhibited forms, at 2.3 angstrom resolution *Biochemistry* **1997**, *36*, 5902-5911.

(25) J.-Y. Zou, G. J. K., J. Ståhlberg, H. Driguez, W. Nerinckx, M. Claeyssens, A. Koivula, T. T. Teeri and T. A. Jones Crystallographic evidence for substrate ring distortion and protein conformational changes during catalysis in cellobiohydrolase Cel6A from Trichoderma reesei *Structure* **1999**, *7*, 1035-1045.

(26) Varrot, A.; Schulein, M.; Fruchard, S.; Driguez, H.; Davies, G. J. Atomic resolution structure of endoglucanase Cel5A in complex with methyl 4,4(II),4(III),4(IV) tetrathio-alpha-cellopentoside highlights the alternative binding modes targeted by substrate mimics *Acta Crystallographica Section D-Biological Crystallography* **2001**, *57*, 1739-1742.

(27) Juers, D. H.; Heightman, T. D.; Vasella, A.; McCarter, J. D.; Mackenzie, L.; Withers, S. G.; Matthews, B. W. A structural view of the action of Escherichia coli (lacZ) beta-galactosidase *Biochemistry* **2001**, *40*, 14781-14794.

(28) Hrmova, M., Varghese, J. N., De Gori, R., Smith, B. J., Driguez, H. & Fincher, G. B. Catalytic mechanisms and reaction intermediates along the hydrolytic pathway of a plant beta-D-glucan glucohydrolase *Structure* **2001**, *9*, 1005-1016.

(29) Varrot, A.; Frandsen, T. P.; Driguez, H.; Davies, G. J. Structure of the Humicola insolens cellobiohydrolase Cel6A D416A mutant in complex with a non-hydrolysable substrate analogue, methyl cellobiosyl-4-thio-beta-cellobioside, at 1.9 angstrom *Acta Crystallographica Section D-Biological Crystallography* **2002**, *58*, 2201-2204.

(30) Davies, G. J.; Mackenzie, L.; Varrot, A.; Dauter, M.; Brzozowski, A. M.; Schulein, M.; Withers, S. G. Snapshots along an enzymatic reaction coordinate: Analysis of a retaining beta-glycoside hydrolase *Biochemistry* **1998**, *37*, 11707-11713.

(31) Varrot, A.; Davies, G. J. Direct experimental observation of the hydrogen-bonding network of a glycosidase along its reaction coordinate revealed by atomic resolution analyses of endoglucanase Cel5A *Acta Crystallographica Section D-Biological Crystallography* **2003**, *59*, 447-452.

(32) Nashiru, O.; Zechel, D. L.; Stoll, D.; Mohammadzadeh, T.; Warren, R. A. J.; Withers, S. G. beta-Mannosynthase: Synthesis of beta-mannosides with a mutant beta-mannosidase *Angew. Chem., Int. Ed. Engl.* **2001**, *40*, 417-420.

(33) Ducros, V. M. A.; Zechel, D. L.; Murshudov, G. N.; Gilbert, H. J.; Szabo, L.; Stoll, D.; Withers, S. G.; Davies, G. J. Substrate distortion by a beta-mannanase: Snapshots of the Michaelis and covalent-intermediate complexes suggest a B-2,B-5 conformation for the transition state *Angew. Chem., Int. Ed. Engl.* **2002**, *41*, 2824-+.

(34) Withers, S. G.; Street, I. P.; Bird, P.; Dolphin, D. H. 2-Deoxy-2-Fluoroglucosides - a Novel Class of Mechanism-Based Glucosidase Inhibitors *J. Am. Chem. Soc.* **1987**, *109*, 7530-7531.

(35) Withers, S. G.; Aebersold, R. Approaches to Labeling and Identification of Active-Site Residues in Glycosidases *Protein Science* **1995**, *4*, 361-372.

(36) Cleland, W. W. K., M.M. Low-barrier hydrogen bonds and enzymic catalysis. *Science* **1994**, *264*, 1887-1890.

(37) Gerlt, J. A., Kreevoy, M.M., Cleland, W. & Frey, P.A. Understanding enzymic catalysis: the importance of short, strong hydrogen bonds *Chemistry & Biology* **1997**, *4*, 259-267.

(38) Notenboom, V.; Birsan, C.; Nitz, M.; Rose, D. R.; Warren, R. A. J.; Withers, S. G. Insights into transition state stabilization of the beta-1,4-glycosidase Cex by covalent intermediate accumulation in active site mutants *Nature Struct. Biol.* **1998**, *5*, 812-818.

(39) Namchuk, M. N.; Withers, S. G. Mechanism of Agrobacterium beta-glucosidase: Kinetic analysis of the role of noncovalent enzyme/substrate interactions *Biochemistry* **1995**, *34*, 16194-16202.

(40) Vasella, A.; Davies, G. J.; Bohm, M. Glycosidase mechanisms *Current Opinion in Chemical Biology* **2002**, *6*, 619-629.

(41) Mackenzie, L. F.; Sulzenbacher, G.; Divne, C.; Jones, T. A.; Woldike, H. F.; Schulein, M.; Withers, S. G.; Davies, G. J. Crystal structure of the family 7 endoglucanase I (Cel7B) from Humicola insolens at 2.2 angstrom resolution and identification of the catalytic nucleophile by trapping of the covalent glycosyl-enzyme intermediate *Biochem. J.* **1998**, *335*, 409-416.

(42) Sinnott, M. L.; Souchard, I. J. Mechanism of Action of Beta-Galactosidase - Effect of Aglycone Nature and Alpha-Deuterium Substitution on Hydrolysis of Aryl Galactosides *Biochem. J.* **1973**, *133*, 89-98.

(43) Tull, D.; Withers, S. G. Mechanisms of Cellulases and Xylanases - a Detailed Kinetic-Study of the Exo-Beta-1,4-Glycanase from Cellulomonas-Fimi *Biochemistry* **1994**, *33*, 6363-6370.

(44) McCarter, J. D.; Yeung, W.; Chow, J.; Dolphin, D.; Withers, S. G. Design and synthesis of 2'-deoxy-2'-fluorodisaccharides as mechanism-based glycosidase inhibitors that exploit aglycon specificity *J. Am. Chem. Soc.* **1997**, *119*, 5792-5797.

(45) McCarter, J. D.; Withers, S. G. 5-fluoro glycosides: A new class of mechanism-based inhibitors of both alpha- and beta-glucosidases *J. Am. Chem. Soc.* **1996**, *118*, 241-242.

(46) Withers, S. G.; Rupitz, K.; Street, I. P. 2-Deoxy-2-Fluoro-D-Glycosyl Fluorides - a New Class of Specific Mechanism-Based Glycosidase Inhibitors *J. Biol. Chem.* **1988**, *263*, 7929-7932.

(47) Burmeister, W. P.; Cottaz, S.; Driguez, H.; Iori, R.; Palmieri, S.; Henrissat, B. The crystal structures of Sinapis alba myrosinase and a covalent glycosyl-enzyme intermediate provide insights into the substrate recognition and active-site machinery of an S-glycosidase *Structure* **1997**, *5*, 663-675.

(48) Notenboom, V.; Birsan, C.; Warren, R. A. J.; Withers, S. G.; Rose, D. R. Exploring the cellulose/xylan specificity of the beta-1,4-glycanase Cex from Cellulomonas fimi through crystallography and mutation *Biochemistry* **1998**, *37*, 4751-4758.

(49) White, A.; Tull, D.; Johns, K.; Withers, S. G.; Rose, D. R. Crystallographic observation of a covalent catalytic intermediate in a beta-glycosidase *Nature Struct. Biol.* **1996**, *3*, 149-154.

(50) Vocadlo, D. J.; Davies, G. J.; Laine, R.; Withers, S. G. Catalysis by hen egg-white lysozyme proceeds via a covalent intermediate *Nature* **2001**, *412*, 835-838.

(51) Sidhu, G.; Withers, S. G.; Nguyen, N. T.; McIntosh, L. P.; Ziser, L.; Brayer, G. D. Sugar ring distortion in the glycosyl-enzyme intermediate of a family G/11 xylanase *Biochemistry* **1999**, *38*, 5346-5354.

(52) Burmeister, W. P.; Cottaz, S.; Rollin, P.; Vasella, A.; Henrissat, B. High resolution x-ray crystallography shows that ascorbate is a cofactor for myrosinase and substitutes for the function of the catalytic base *J. Biol. Chem.* **2000**, *275*, 39385-39393.

(53) Sulzenbacher, G.; Mackenzie, L. F.; Wilson, K. S.; Withers, S. G.; Dupont, C.; Davies, G. J. The crystal structure of a 2-fluorocellotriosyl complex of the Streptomyces lividans endoglucanase CelB2 at 1.2 angstrom resolution *Biochemistry* **1999**, *38*, 4826-4833.

(54) Sabini, E.; Wilson, K. S.; Danielsen, S.; Schulein, M.; Davies, G. J. Oligosaccharide binding to family 11 xylanases: both covalent intermediate and mutant product complexes display B-2,B-5 conformations at the active centre *Acta Crystallographica Section D-Biological Crystallography* **2001**, *57*, 1344-1347.

(55) Sabini, E.; Sulzenbacher, G.; Dauter, M.; Dauter, Z.; Jorgensen, P. L.; Schulein, M.; Dupont, C.; Davies, G. J.; Wilson, K. S. Catalysis and specificity in enzymatic glycoside hydrolysis: a B-2,B-5 conformation for the glycosyl-enzyme intermediate revealed by the structure of the Bacillus agaradhaerens family 11 xylanase *Chemistry & Biology* **1999**, *6*, 483-492.

(56) Weymouth-Wilson, A. C. *Nat. Prod. Rep.* **1997**, *14*, 99-110.

(57) Unligil, U. M.; Rini, J. M. Glycosyltransferase structure and mechanism *Current Opinion in Structural Biology* **2000**, *10*, 510-517.

(58) Bourne, Y.; Henrissat, B. Glycoside hydrolases and glycosyltransferases: families and functional modules *Current Opinion in Structural Biology* **2001**, *11*, 593-600.

(59) Wrabl, J. O.; Grishin, N. V. Homology between O-linked GlcNAc transferases and proteins of the glycogen phosphorylase superfamily *J. Mol. Biol.* **2001**, *314*, 365-374.

(60) Charnock, S. J.; Davies, G. J. Structure of the nucleotide-diphospho-sugar transferase, SpsA from Bacillus subtilis, in native and nucleotide-complexed forms *Biochemistry* **1999**, *38*, 6380-6385.

(61) Tarbouriech, N.; Charnock, S. J.; Davies, G. J. Three-dimensional structures of the Mn and Mg dTDP complexes of the family GT-2 glycosyltransferase SpsA: A comparison with related NDP-sugar glycosyltransferases *J. Mol. Biol.* **2001**, *314*, 655-661.

(62) Ha, S.; Walker, D.; Shi, Y. G.; Walker, S. The 1.9 angstrom crystal structure of Escherichia coli MurG, a membrane-associated glycosyltransferase involved in peptidoglycan biosynthesis *Protein Science* **2000**, *9*, 1045-1052.

(63) Hu, Y. N.; Chen, L.; Ha, S.; Gross, B.; Falcone, B.; Walker, D.; Mokhtarzadeh, M.; Walker, S. Crystal structure of the MurG : UDP-GlcNAc complex reveals common structural principles of a superfamily of glycosyltransferases *Proc. Natl. Acad. Sci. U. S. A.* **2003**, *100*, 845-849.

(64) Davies G, S. M. L. a. W. S. G. *Glycosyl transfer. In: Sinnott ML (Ed) Comprehensive Biological Catalysis: A Mechanistic Reference.*; San Diego: Academic Press, 1998; Vol. 1, 119-209.

(65) Murray, B. W.; Wittmann, V.; Burkart, M. D.; Hung, S. C.; Wong, C. H. Mechanism of human alpha-1,3-fucosyltransferase V: Glycosidic cleavage occurs prior to nucleophilic attack *Biochemistry* **1997**, *36*, 823-831.

(66) Qiao, L.; Murray, B. W.; Shimazaki, M.; Schultz, J.; Wong, C. H. Synergistic inhibition of human alpha-1,3-fucosyltransferase V *J. Am. Chem. Soc.* **1996**, *118*, 7653-7662.

(67) Singh, A. N.; Hester, L. S.; Raushel, F. M. Examination of the Mechanism of Sucrose Synthetase by Positional Isotope Exchange *J. Biol. Chem.* **1987**, *262*, 2554-2557.

(68) Kim, S. C.; Singh, A. N.; Raushel, F. M. The Mechanism of Glycogen-Synthetase as Determined by Deuterium-Isotope Effects and Positional Isotope Exchange Experiments *J. Biol. Chem.* **1988**, *263*, 10151-10154.

(69) Kim, S. C.; Singh. A. N.; Raushel, F. M. Analysis of the Galactosyltransferase Reaction by Positional Isotope Exchange and Secondary Deuterium-Isotope Effects *Archives of Biochemistry and Biophysics* **1988**, *267*, 54-59.

(70) Tvaroska, I.; Andre, I.; Carver, J. P. Ab initio molecular orbital study of the catalytic mechanism of glycosyltransferases: Description of reaction pathways and determination of transition-state structures for inverting N-acetylglucosaminyltransferases *J. Am. Chem. Soc.* **2000**, *122*, 8762-8776.

(71) Withers, S. G.; Wakarchuk, W. W.; Strynadka, N. C. J. One step closer to a sweet conclusion *Chemistry & Biology* **2002**, *9*, 1270-1273.

(72) Sinnott, M. L.; Jencks, W. P. Solvolysis of D-Glucopyranosyl Derivatives in Mixtures of Ethanol and 2,2,2-Trifluoroethanol *J. Am. Chem. Soc.* **1980**, *102*, 2026-2032.

(73) Klein, H. W.; Im, M. J.; Palm, D. Mechanism of the Phosphorylase Reaction - Utilization of D-Gluco-Hept-1-Enitol in the Absence of Primer *Eur. J. Biochem.* **1986**, *157*, 107-114.

(74) Asano, N.; Nash, R. J.; Molyneux, R. J.; Fleet, G. W. J. Sugar-mimic glycosidase inhibitors: natural occurrence, biological activity and prospects for therapeutic application *Tetrahedron Assym.* **2000**, *11*, 1645-1680.

(75) Inoue, S. T., T.; Niida, T. *J. Antibiot.* **1966**, *19*, 288.

(76) Inoue, S. T., T.; Ito, T.; Niida, T. *Tetrahedron* **1968**, *24*, 2125.

(77) Ezure, Y.; Maruo, S.; Miyazaki, K.; Kawamata, M. Moranoline (1-Deoxynojirimycin) Fermentation and Its Improvement *Agricultural and Biological Chemistry* **1985**, *49*, 1119-1125.

(78) Fellows, L. E.; Bell, E. A.; Lynn, D. G.; Pilkiewicz, F.; Miura, I.; Nakanishi, K. Isolation and Structure of an Unusual Cyclic Amino Alditol from a Legume *Journal of the Chemical Society-Chemical Communications* **1979**, 977-978.

(79) Kite, G. C.; Fellows, L. E.; Fleet, G. W. J.; Liu, P. S.; Scofield, A. M.; Smith, N. G. Alpha-Homonojirimycin 2,6-Dideoxy-2,6-Imino-D-Glycero-L-Gulo-Heptitol from Omphalea-Diandra L - Isolation and Glucosidase Inhibition *Tetrahedron Lett.* **1988**, *29*, 6483-6486.

(80) Molyneux, R. J.; Pan, Y. T.; Tropea, J. E.; Elbein, A. D.; Lawyer, C. H.; Hughes, D. J.; Fleet, G. W. J. 2-Hydroxymethyl-3,4-Dihydroxy-6-Methylpyrrolidine (6-Deoxy-Dmdp), an Alkaloid Beta-Mannosidase Inhibitor from Seeds of Angylocalyx-Pynaertii *J. Nat. Prod.* **1993**, *56*, 1356-1364.

(81) Junge, B. M., M.; Stoltefuss, J. *In Handbook of Experimental Pharmacology* New York, 1996; Vol. 119,411-482.

(82) Fleet, G. W. J.; Karpas, A.; Dwek, R. A.; Fellows, L. E.; Tyms, A. S.; Petursson, S.; Namgoong, S. K.; Ramsden, N. G.; Smith, P. W.; Son, J. C.; Wilson, F.; Witty, D. R.; Jacob, G. S.; Rademacher, T. W. Inhibition of Hiv Replication by Amino-Sugar Derivatives *Febs Letters* **1988**, *237*, 128-132.

(83) Karpas, A.; Fleet, G. W. J.; Dwek, R. A.; Petursson, S.; Namgoong, S. K.; Ramsden, N. G.; Jacob, G. S.; Rademacher, T. W. Aminosugar Derivatives as Potential Anti-Human Immunodeficiency Virus Agents *Proc. Natl. Acad. Sci. U. S. A.* **1988**, *85*, 9229-9233.

(84) Schweden, J.; Borgmann, C.; Legler, G.; Bause, E. Characterization of Calf Liver Glucosidase-I and Its Inhibition by Basic Sugar Analogs *Archives of Biochemistry and Biophysics* **1986**, *248*, 335-340.

(85) Vandenbroek, L.; Vermaas, D. J.; Heskamp, B. M.; Vanboeckel, C. A. A.; Tan, M.; Bolscher, J. G. M.; Ploegh, H. L.; Vankemenade, F. J.; Degoede, R. E. Y.; Miedema, F. Chemical Modification of Azasugars, Inhibitors of N-Glycoprotein-Processing Glycosidases and of Hiv-I Infection - Review and Structure-Activity-Relationships *Recueil Des Travaux Chimiques Des Pays-Bas-Journal of the Royal Netherlands Chemical Society* **1993**, *112*, 82-94.

(86) Hohenschutz, L. D.; Bell, E. A.; Jewess, P. J.; Leworthy, D. P.; Pryce, R. J.; Arnold, E.; Clardy, J. Castanospermine, a 1,6,7,8-Tetrahydroxyoctahydroindolizine Alkaloid, from Seeds of Castanospermum-Australe *Phytochemistry* **1981**, *20*, 811-814.

(87) Nash, R. J.; Fellows, L. E.; Dring, J. V.; Stirton, C. H.; Carter, D.; Hegarty, M. P.; Bell, E. A. Castanospermine in Alexa Species *Phytochemistry* **1988**, *27*, 1403-1404.

(88) Colegate, S. M.; Dorling, P. R.; Huxtable, C. R. Spectroscopic Investigation of Swainsonine - Alpha-Mannosidase Inhibitor Isolated from Swainsona-Canescens *Australian Journal of Chemistry* **1979**, *32*, 2257-2264.

(89) Molyneux, R. J.; James, L. F. Loco Intoxication - Indolizidine Alkaloids of Spotted Locoweed (Astragalus-Lentiginosus) *Science* **1982**, *216*, 190-191.

(90) Saul, R.; Ghidoni, J. J.; Molyneux, R. J.; Elbein, A. D. Castanospermine Inhibits Alpha-Glucosidase Activities and Alters Glycogen Distribution in Animals *Proc. Natl. Acad. Sci. U. S. A.* **1985**, *82*, 93-97.

(91) Cenci di Bello, I. M., D.; Nash, R. J.; Winchester, B. *In Lipid Storage Disorders*; Plenum: New York, 1988,635-641.

(92) Saunier, B.; Kilker, R. D.; Tkacz, J. S.; Quaroni, A.; Herscovics, A. Inhibition of N-Linked Complex Oligosaccharide Formation by 1-Deoxynojirimycin, an Inhibitor of Processing Glucosidases *J. Biol. Chem.* **1982**, *257*, 4155-4161.

(93) Zeng, Y. C.; Pan, Y. T.; Asano, N.; Nash, R. J.; Elbein, A. D. Homonojirimycin and N-methyl-homonojirimycin inhibit N-linked oligosaccharide processing *Glycobiology* **1997**, *7*, 297-304.

(94) Szumilo, T.; Kaushal, G. P.; Elbein, A. D. Purification and Properties of Glucosidase-I from Mung Bean Seedlings *Archives of Biochemistry and Biophysics* **1986**, *247*, 261-271.

(95) Humphries, M. J.; Matsumoto, K.; White, S. L.; Olden, K. Inhibition of Experimental Metastasis by Castanospermine in Mice - Blockage of 2 Distinct Stages of

Tumor Colonization by Oligosaccharide Processing Inhibitors *Cancer Research* **1986**, *46*, 5215-5222.

(96) Spearman, M. A.; Ballon, B. C.; Gerrard, J. M.; Greenberg, A. H.; Wright, J. A. The Inhibition of Platelet-Aggregation of Metastatic H-Ras-Transformed 10t1/2 Fibroblasts with Castanospermine, an N-Linked Glycoprotein Processing Inhibitor *Cancer Letters* **1991**, *60*, 185-191.

(97) Hadwiger, A.; Niemann, H.; Kabisch, A.; Bauer, H.; Tamura, T. Appropriate Glycosylation of the Fms Gene-Product Is a Prerequisite for Its Transforming Potency *Embo Journal* **1986**, *5*, 689-694.

(98) Fischer, P.; Collin, M.; Karlsson, G. B.; James, W.; Butters, T. D.; Davis, S. J.; Gordon, S.; Dwek, R. A.; Platt, F. M. The Alpha-Glucosidase Inhibitor N-Butyldeoxynojirimycin Inhibits Human-Immunodeficiency-Virus Entry at the Level of Post-Cd4-Binding *Journal of Virology* **1995**, *69*, 5791-5797.

(99) Platt, F. M.; Neises, G. R.; Dwek, R. A.; Butters, T. D. N-Butyldeoxynojirimycin Is a Novel Inhibitor of Glycolipid Biosynthesis *J. Biol. Chem.* **1994**, *269*, 8362-8365.

(100) Fu, Y. K.; Hart, T. K.; Jonak, Z. L.; Bugelski, P. J. Physicochemical Dissociation of Cd4-Mediated Syncytium Formation and Shedding of Human-Immunodeficiency-Virus Type-1 Gp120 *Journal of Virology* **1993**, *67*, 3818-3825.

(101) Sattentau, Q. J.; Zollapazner, S.; Poignard, P. Epitope Exposure on Functional, Oligomeric Hiv-1 Gp41 Molecules *Virology* **1995**, *206*, 713-717.

(102) Tulsiani, D. R. P.; Harris, T. M.; Touster, O. Swainsonine Inhibits the Biosynthesis of Complex Glycoproteins by Inhibition of Golgi Mannosidase-Ii *J. Biol. Chem.* **1982**, *257*, 7936-7939.

(103) Dorling, P. R.; Huxtable, C. R.; Colegate, S. M. Inhibition of Lysosomal Alpha-Mannosidase by Swainsonine, an Indolizidine Alkaloid Isolated from Swainsona-Canescens *Biochem. J.* **1980**, *191*, 649-651.

(104) Harris, E. M. S.; Aleshin, A. E.; Firsov, L. M.; Honzatko, R. B. Refined Structure for the Complex of 1-Deoxynojirimycin with Glucoamylase from Aspergillus-Awamori Var X100 to 2.4-Angstrom Resolution *Biochemistry* **1993**, *32*, 1618-1626.

(105) Weill, C. E.; Burch, R. J.; Van Dyk, J. W. *Cereal Chem.* **1954**, *31*, 150-158.

(106) Manjunath, P.; Shenoy, B. C.; Raghavendra Rao, M. R. *J. Appl. Biochem* **1983**, *5*, 235-260.

(107) Chambers, R. S. B., M.J.; Cannon, R.D.; Carne, A.; Emerson, G.W.; Sullivan, P.A. An exo-ß-(1,3)-glucanase of Candida albicans: purification of the enzyme and molecular cloning of the gene *J. Gen. Microbiol.* **1993**, *139*, 325-334.

(108) Sue M. Cutfield1, G. J. D., Garib Murshudov2, Bryan F. Anderson3, Peter C. E. Moody2, Patrick A. Sullivan1, 3 and John F. Cutfield The structure of the exo- -(1,3)-glucanase from Candida albicans in native and bound forms: relationship between a pocket and groove in family 5 glycosyl hydrolases1 *J. Mol. Biol.* **1999**, *294*, 771-783.

(109) Hempel, A.; Camerman, N.; Mastropaolo, D.; Camerman, A. Glucosidase Inhibitors - Structures of Deoxynojirimycin and Castanospermine *J. Med. Chem.* **1993**, *36*, 4082-4086.

(110) Wang, Y. F.; Takaoka, Y.; Wong, C. H. Remarkable Stereoselectivity in the Inhibition of Alpha-Galactosidase from Coffee Bean by a New Polyhydroxypyrrolidine Inhibitor *Angew. Chem., Int. Ed. Engl.* **1994**, *33*, 1242-1244.

(111) Liu, K. K. C.; Kajimoto, T.; Chen, L. R.; Zhong, Z. Y.; Ichikawa, Y.; Wong, C. H. Use of Dihydroxyacetone Phosphate Dependent Aldolases in the Synthesis of Deoxyazasugars *J. Org. Chem.* **1991**, *56*, 6280-6289.

(112) Legler, G.; Pohl, S. Synthesis of 5-Amino-5-Deoxy-D-Galactopyranose and 1,5-Dideoxy-1,5-Imino-D-Galactitol, and Their Inhibition of Alpha-and Beta-D-Galactosidases *Carbohydr. Res.* **1986**, *155*, 119-129.

(113) Frankowski, A.; Seliga, C.; Bur, D.; Streith, J. Imidazole-Analogs of 6-Epicastanospermine and of 3,7a-Diepialexine *Helv. Chim. Acta* **1991**, *74*, 934-940.

(114) Frankowski, A.; Deredas, D.; Lenouen, D.; Tschamber, T.; Streith, J. On the Way to Glycoprocessing Inhibitors - Synthesis of an Imidazo-L-Xylo-Piperidinose Derivative *Helv. Chim. Acta* **1995**, *78*, 1837-1842.

(115) Frankowski, A.; Deredas, D.; Streith, J.; Tschamber, T. Synthesis of an imidazolo-L-lyxo-piperidinose derivative *Tetrahedron* **1998**, *54*, 9033-9042.

(116) Streith, J.; Boiron, A.; Frankowski, A.; Lenouen, D.; Rudyk, H.; Tschamber, T. On the Way to Glycoprocessing Inhibitors - a General One-Pot Synthesis of Imidazolosugars *Synthesis-Stuttgart* **1995**, 944-946.

(117) Tschamber, T.; Siendt, H.; Boiron, A.; Gessier, F.; Deredas, D.; Frankowski, A.; Picasso, S.; Steiner, H.; Aubertin, A. M.; Streith, J. Stereoisomeric imidazolo-pentoses - Synthesis, chiroptical properties, and evaluation as glycosidase inhibitors *European J. Org. Chem.* **2001**, 1335-1347.

(118) Granier, T.; Gaiser, F.; Hintermann, L.; Vasella, A. Synthesis via a carbohydrate-derived Munchnone of pyrrolopyridines (indolizines) and imidazopyridines, and their evaluation as inhibitors of B-D-Glucosidases *Helv. Chim. Acta* **1997**, *80*, 1443-1456.

(119) Lillelund, V. H.; Jensen, H. H.; Liang, X. F.; Bols, M. Recent developments of transition-state analogue glycosidase inhibitors of non-natural product origin *Chem. Rev.* **2002**, *102*, 515-553.

(120) Panday, N.; Granier, T.; Vasella, A. Synthesis and evaluation of indolizine-type inhibitors of N-acetyl-beta-D-glucosaminidases *Helv. Chim. Acta* **1998**, *81*, 475-490.

(121) Krulle, T.; delaFuente, C.; Pickering, L.; Aplin, R. T.; Tsitsanou, K. E.; Zographos, S. E.; Oikonomakos, N. G.; Nash, R. J.; Griffiths, R. C.; Fleet, G. W. J. Triazole carboxylic acids as anionic sugar mimics? Inhibition of glycogen phosphorylase by a D-glucotriazole carboxylate *Tetrahedron Assym.* **1997**, *8*, 3807-3820.

(122) Tatsuta, K.; Miura, S.; Ohta, S.; Gunji, H. Total Syntheses of De-Branched Nagstatin and Its Analogs Having Glycosidase Inhibiting Activities *Tetrahedron Lett.* **1995**, *36*, 1085-1088.

(123) Vonhoff, S.; Heightman, T. D.; Vasella, A. Inhibition of glycosidases by lactam oximes: Influence of the aglycon in disaccharide analogues *Helv. Chim. Acta* **1998**, *81*, 1710-1725.

(124) Streith, J.; Rudyk, H.; Tschamber, T.; Tarnus, C.; Strehler, C.; Deredas, D.; Frankowski, A. The synthesis of imidazol sugars which mimic cyclic carboxonium ions formed during the glycosidase-catalysed hydrolysis of oligo- and polysaccharides *European J. Org. Chem.* **1999**, 893-898.

(125) Yuasa, H.; Takada, J.; Hashimoto, H. Synthesis of salacinol *Tetrahedron Lett.* **2000**, *41*, 6615-6618.

(126) Ghavami, A.; Johnston, B. D.; Pinto, B. M. A new class of glycosidase inhibitor: Synthesis of salacinol and its stereoisomers *J. Org. Chem.* **2001**, *66*, 2312-2317.

(127) Yoshikawa, M.; Murakami, T.; Yashiro, K.; Matsuda, H. Kotalanol, a potent alpha-glucosidase inhibitor with thiosugar sulfonium sulfate structure, from antidiabetic ayurvedic medicine Salacia reticulata *Chemical & Pharmaceutical Bulletin* **1998**, *46*, 1339-1340.

(128) Yoshikawa M, M. T., Shimada H, Matsuda H, Yamahara J, Tanabe G, Muraoka O Salacinol, potent antidiabetic principle with unique thiosugar sulfonium sulfate structure from the ayurvedic traditional medicine Salacia reticulata in Sri Lanka and India *Tetrahedron Lett.* **1997**, *38*, 8367-8370.

(129) Jespersen, T. M.; Dong, W. L.; Sierks, M. R.; Skrydstrup, T.; Lundt, I.; Bols, M. Isofagomine, a Potent, New Glycosidase Inhibitor *Angew. Chem., Int. Ed. Engl. in English* **1994**, *33*, 1778-1779.

(130) Jespersen, T. M.; Bols, M.; Sierks, M. R.; Skrydstrup, T. Synthesis of Isofagomine, a Novel Glycosidase Inhibitor *Tetrahedron* **1994**, *50*, 13449-13460.

(131) Paulsen, H. *Liebigs Ann. Chim.* **1965**, *683*, 187-198.

(132) Stutz, A. E. *Iminosugars As Glycosidase Inhibitors: Nojirimycin and Beyond*; Wiley-VCH: Weinheim, 1999.

(133) Ichikawa, Y.; Igarashi, Y.; Ichikawa, M.; Suhara, Y. 1-N-iminosugars: Potent and selective inhibitors of beta-glycosidases *J. Am. Chem. Soc.* **1998**, *120*, 3007-3018.

(134) Bols, M. 1-aza sugars, apparent transition state analogues of equatorial glycoside formation/cleavage *Acc. Chem. Res.* **1998**, *31*, 1-8.

(135) Dong, W. L.; Jespersen, T.; Bols, M.; Skrydstrup, T.; Sierks, M. R. Evaluation of isofagomine and its derivatives as potent glycosidase inhibitors *Biochemistry* **1996**, *35*, 2788-2795.

(136) Heightman, T. D.; Vasella, A. T. Recent insights into inhibition, structure, and mechanism of configuration-retaining glycosidases *Angew. Chem., Int. Ed. Engl.* **1999**, *38*, 750-770.

(137) Bulow, A.; Plesner, I. W.; Bols, M. A large difference in the thermodynamics of binding of isofagomine and 1-deosynojirimycin to beta-glucosidase *J. Am. Chem. Soc.* **2000**, *122*, 8567-8568.

(138) Liu, H. Z.; Liang, X. F.; Sohoel, H.; Bulow, A.; Bols, M. Noeuromycin, a glycosyl cation mimic that strongly inhibits glycosidases *J. Am. Chem. Soc.* **2001**, *123*, 5116-5117.

(139) Williams, S. J.; Hoos, R.; Withers, S. G. Nanomolar versus millimolar inhibition by xylobiose-derived azasugars: Significant differences between two structurally distinct xylanases *J. Am. Chem. Soc.* **2000**, *122*, 2223-2235.

(140) Varrot, A.; Tarling, C. A.; Macdonald, J. M.; Stick, R. V.; Zechel, D. L.; Withers, S. G.; Davies, G. J. Direct observation of the protonation state of an imino sugar glycosidase inhibitor upon binding *J. Am. Chem. Soc.* **2003**, *125*, 7496-7497.

(141) Truscheit, E.; Frommer, W.; Junge, B.; Muller, L.; Schmidt, D. D.; Wingender, W. Chemistry and Biochemistry of Microbial Alpha-Glucosidase Inhibitors *Angew. Chem., Int. Ed. Engl. in English* **1981**, *20*, 744-761.

(142) Legler, G.; Herrchen, M. N-Substituted D-Galactosylamines as Probes for the Active-Site of Beta-D-Galactosidase from Escherichia-Coli *Carbohydr. Res.* **1983**, *116*, 95-103.

(143) Legler, G.; Stutz, A. E.; Immich, H. Synthesis of 1,5-Dideoxy-1,5-Imino-D-Arabinitol (5-nor-L-Fuco-1-Deoxynojirimycin) and Its Application for the Affinity Purification and Characterization of Alpha-L-Fucosidase *Carbohydr. Res.* **1995**, *272*, 17-30.

(144) Guo, W. F.; Hiratake, J.; Ogawa, K.; Yamamoto, M.; Ma, S. J.; Sakata, K. beta-D-glycosylamidines: Potent, selective, and easily accessible beta-glycosidase inhibitors *Bioorg. & Med. Chem. Lett.* **2001**, *11*, 467-470.

(145) Maity, S. K.; Dutta, S. K.; Banerjee, A. K.; Achari, B.; Singh, M. Design and Synthesis of Mannose Analogs as Inhibitors of Alpha-Mannosidase *Tetrahedron* **1994**, *50*, 6965-6974.

(146) Lai, W.; Martin, O. R. Synthesis and Inhibition Studies of C-(D-Glycopyranosyl)Methylamines *Carbohydr. Res.* **1993**, *250*, 185-193.

(147) Bemiller, J. N.; Gilson, R. J.; Myers, R. W.; Santoro, M. M.; Yadav, M. P. N-Substituted (Beta-D-Galactopyranosylmethyl) Amines as Reversible Inhibitors of Beta-D-Galactosidase *Carbohydr. Res.* **1993**, *250*, 93-100.

(148) Bemiller, J. N.; Yadav, M. P.; Kalabokis, V. N.; Myers, R. W. N-Substituted (Beta-D-Galactopyranosylmethyl)Amines, and C-Beta-D-Galactopyranosylformamides, and Related-Compounds *Carbohydr. Res.* **1990**, *200*, 111-126.

(149) Dietrich, H.; Schmidt, R. R. Aminosubstituted Alpha-D-Glucosylmethylbenzenes (Benzyl Alpha-C-Glucosides) and an N-(C-Alpha-D-Glucosylmethy)Aniline (Anilinomethyl Alpha-C-Glucoside) - Novel Alpha-D-Glucosidase Inhibitors *Carbohydr. Res.* **1993**, *250*, 161-176.

(150) Schmidt, R. R.; Dietrich, H. Amino-Substituted Beta-Benzyl-C-Glycosides - Novel Beta-Glycosidase Inhibitors *Angew. Chem., Int. Ed. Engl. in English* **1991**, *30*, 1328-1329.

(151) Berecibar, A.; Grandjean, C.; Siriwardena, A. Synthesis and biological activity of natural aminocyclopentitol glycosidase inhibitors: Mannostatins, trehazolin, allosamidins, and their analogues *Chem. Rev.* **1999**, *99*, 779-844.

(152) Tong, M. K.; Papandreou, G.; Ganem, B. Potent, Broad-Spectrum Inhibition of Glycosidases by an Amidine Derivative of D-Glucose *J. Am. Chem. Soc.* **1990**, *112*, 6137-6139.

(153) Ganem, B. Inhibitors of carbohydrate-processing enzymes: Design and synthesis of sugar-shaped heterocycles *Acc. Chem. Res.* **1996**, *29*, 340-347.

(154) Ganem, B.; Papandreou, G. Mimicking the Glucosidase Transition-State - Shape Charge Considerations *J. Am. Chem. Soc.* **1991**, *113*, 8984-8985.

(155) Pan, Y. T.; Kaushal, G. P.; Papandreou, G.; Ganem, B.; Elbein, A. D. D-Mannonolactam Amidrazone - a New Mannosidase Inhibitor That Also Inhibits the Endoplasmic-Reticulum or Cytoplasmic Alpha-Mannosidase *J. Biol. Chem.* **1992**, *267*, 8313-8318.

(156) Ermert, P.; Vasella, A. Synthesis of a Glucose-Derived Tetrazole as a New Beta-Glucosidase Inhibitor - a New Synthesis of 1-Deoxynojirimycin *Helv. Chim. Acta* **1991**, *74*, 2043-2053.

(157) Aoyagi, T.; Suda, H.; Uotani, K.; Kojima, F.; Aoyama, T.; Horiguchi, K.; Hamada, M.; Takeuchi, T. Nagstatin, a New Inhibitor of N-Acetyl-Beta-D-Glucosaminidase, Produced by Streptomyces-Amakusaensis Mg846-Ff3 - Taxonomy, Production, Isolation, Physicochemical Properties and Biological-Activities *Journal of Antibiotics* **1992**, *45*, 1404-1408.

(158) Aoyama, T.; Naganawa, H.; Suda, H.; Uotani, K.; Aoyagi, T.; Takeuchi, T. The Structure of Nagstatin, a New Inhibitor of N-Acetyl-Beta-D-Glucosaminidase *Journal of Antibiotics* **1992**, *45*, 1557-1558.

(159) Panday, N.; Vasella, A. Synthesis of glucose- and mannose-derived N-acetylamino imidazopyridines and their evaluation as inhibitors of glycosidases *Synthesis-Stuttgart* **1999**, 1459-1468.

(160) Tatsuta, K. Total synthesis and chemical design of useful glycosidase inhibitors *Pure and Applied Chemistry* **1996**, *68*, 1341-1346.

(161) Tatsuta, K.; Miura, S. Total Synthesis of Nagstatin, an N-Acetyl-Beta-D-Glucosaminidase Inhibitor *Tetrahedron Lett.* **1995**, *36*, 6721-6724.

(162) Tatsuta, K.; Miura, S.; Gunji, H. The total synthesis of a glycosidase inhibitor, nagstatin *Bulletin of the Chemical Society of Japan* **1997**, *70*, 427-436.

(163) Tatsuta, K.; Miura, S.; Ohta, S.; Gunji, H. Syntheses and Glycosidase Inhibiting Activities of Nagstatin Analogs *Journal of Antibiotics* **1995**, *48*, 286-288.

(164) Tatsuta, K.; Ikeda, Y.; Miura, S. Synthesis and glycosidase inhibitory activities of nagstatin triazole analogs *Journal of Antibiotics* **1996**, *49*, 836-838.

(165) Panday, N.; Canac, Y.; Vasella, A. Very strong inhibition of glucosidases by C(2)-substituted tetrahydroimidazopyridines *Helv. Chim. Acta* **2000**, *83*, 58-79.

(166) Nishimura, Y.; Adachi, H.; Satoh, T.; Shitara, E.; Nakamura, H.; Kojima, F.; Takeuchi, T. All eight stereoisomeric D-glyconic-delta-lactams: Synthesis, conformational analysis, and evaluation as glycosidase inhibitors *J. Org. Chem.* **2000**, *65*, 4871-4882.

(167) Panday, N.; Meyyappan, M.; Vasella, A. A comparison of glucose- and glucosamine-related inhibitors: Probing the interaction of the 2-hydroxy group with retaining beta-glucosidases *Helv. Chim. Acta* **2000**, *83*, 513-538.

(168) Williams, S. J.; Notenboom, V.; Wicki, J.; Rose, D. R.; Withers, S. G. A new, simple, high-affinity glycosidase inhibitor: Analysis of binding through X-ray crystallography, mutagenesis, and kinetic analysis *Journal of the American Chemical Society* **2000**, *122*, 4229-4230.

(169) Sohoel, H.; Liang, X. F.; Bols, M. Isogalactofagomine lactam. A neutral nanomolar galactosidase inhibitor *J. Chem. Soc., Perkin Trans. 1* **2001**, 1584-1585.

(170) Darrow, J. W.; Drueckhammer, D. G. A cyclic phosphonamidate analogue of glucose as a selective inhibitor of inverting glycosidases *Bioorganic & Medicinal Chemistry* **1996**, *4*, 1341-1348.

(171) LeMerrer, Y.; Fuzier, M.; Dosbaa, I.; Foglietti, M. J.; Depezay, J. C. Synthesis of thiosugars as weak inhibitors of glycosidases *Tetrahedron* **1997**, *53*, 16731-16746.

(172) Turner, G. A.; Goodarzi, M. T.; Thompson, S. Glycosylation of alpha-1-proteinase inhibitor and haptoglobin in ovarian cancer: evidence for two different mechanisms *Glycoconjugate Journal* **1995**, *12*, 211-218.

(173) Couldrey, C.; Green, J. E. Metastases: the glycan connection *Breast Cancer Research* **2000**, *2*, 321-323.

(174) Schumacher, U.; Mohamed, M.; Mitchell, B. S. Differential expression of carbohydrate residues in human breast and colon cancer cell lines grown in vitro and in vivo in SCID mice *Cancer Journal* **1996**, *9*, 247-254.

(175) Touitou, I.; Garcia, M.; Westley, B.; Capony, F.; Rochefort, H. Effect of tunicamycin and endoglycosidase H and F on the estrogen regulated 52000-Mr protein secreted by breast cancer cells *Biochimie* **1985**, *67*, 1257-1266.

(176) Rostenberg, I.; Guizar-Vazquez, J.; Suarez, P.; Rico, R.; Nungaray, L.; Dominguez, C. Distinct glycosylation of serum proteins in patients with cancer *Journal of the National Cancer Institute* **1978**, *60*, 83-87.

(177) McGuckin, M. A.; Devine, P. L.; Ward, B. G. Early steps in the biosynthesis of MUC2 epithelial mucin in colon cancer cells *Biochemistry and Cell Biology* **1996**, *74*, 87-93.

(178) Schumacher, U.; Adam, E.; Flavell, D. J.; Boehm, D.; Brooks, S. A.; Leathem, A. J. Glycosylation patterns of the human colon cancer cell line HT-29 detected by Helix pomatia agglutinin and other lectins in culture, in primary tumors and in metastases in SCID mice *Clinical & Experimental Metastasis* **1994**, *12*, 398-404.

(179) Hakomori, S. Glycosylation defining cancer malignancy: New wine in an old bottle *Proceedings of the National Academy of Sciences of the United States of America* **2002**, *99*, 10231-10233.

(180) Scanlin, T. F.; Glick, M. C. Terminal glycosylation and disease: influence on cancer and cystic fibrosis *Glycoconjugate Journal* **2001**, *17*, 617-626.

(181) Dennis, J. W.; Granovsky, M. Protein glycosylation and cancer *Carbohydrates in Chemistry and Biology* **2000**, *4*, 923-943.

(182) Catterall, J. B.; Jones, L. M. H.; Turner, G. A. Membrane protein glycosylation and CD44 content in the adhesion of human ovarian cancer cells to hyaluronan *Clinical & Experimental Metastasis* **2000**, *17*, 583-591.

(183) Dennis, J. W. G., M.; Warren, C. E. Glycoprotein glycosylation and cancer progression *Biochimica et Biophysica Acta* **1999**, *1473*, 21-34.

(184) Kim, Y. J.; Varki, A. Perspectives on the significance of altered glycosylation of glycoproteins in cancer *Glycoconjugate Journal* **1997**, *14*, 569-576.

(185) Dall'Olio, F. Protein glycosylation in cancer biology: an overview *Clinical Molecular Pathology* **1996**, *49*, M126-M135.

(186) Taylor-Papadimitriou, J.; Epenetos, A. A. Exploiting altered glycosylation patterns in cancer: progress and challenges in diagnosis and therapy *Trends in Biotechnology* **1994**, *12*, 227-233.

(187) Hakomori, S. Aberrant glycosylation in cancer cell membranes as focused on glycolipids: overview and perspectives *Cancer Research* **1985**, *45*, 2405-2414.

(188) Narayanan, S. Sialic acid as a tumor marker *Annals of Clinical and Laboratory Science* **1994**, *24*, 376-384.

(189) Korytnyk, W.; Angelino, N.; Klohs, W.; Bernacki, R. Cmp and Cmp-Sugar Analogs as Inhibitors of Sialic-Acid Incorporation into Glycoconjugates *European J. Med. Chem.* **1980**, *15*, 77-84.

(190) Camarasa, M. J.; Fernandezresa, P.; Garcialopez, M. T.; Delasheras, F. G.; Mendezcastrillon, P. P.; Alarcon, B.; Carrasco, L. Uridine 5'-Diphosphate Glucose Analogs - Inhibitors of Protein Glycosylation That Show Antiviral Activity *J. Med. Chem.* **1985**, *28*, 40-46.

(191) Vaghefi, M. M.; Bernacki, R. J.; Dalley, N. K.; Wilson, B. E.; Robins, R. K. Synthesis of Glycopyranosylphosphonate Analogs of Certain Natural Nucleoside Diphosphate Sugars as Potential Inhibitors of Glycosyltransferases *J. Med. Chem.* **1987**, *30*, 1383-1391.

(192) Cai, S.; Stroud, M. R.; Hakomori, S.; Toyokuni, T. Synthesis of Carbocyclic Analogs of Guanosine 5'-(Beta-L-Fucopyranosyl Diphosphate) (Gdp-Fucose) as Potential Inhibitors of Fucosyltransferases *J. Org. Chem.* **1992**, *57*, 6693-6696.

(193) Endo, T.; Kajihara, Y.; Kodama, H.; Hashimoto, H. Novel aspects of interaction between UDP-Gal and GlcNAc beta-1,4-galactosyltransferase: Transferability and remarkable inhibitory activity of UDP-(mono-O-methylated gal), UDP-Fuc and UDP-Man *Bioorganic & Medicinal Chemistry* **1996**, *4*, 1939-1948.

(194) Wang, R.; Steensma, D. H.; Takaoka, Y.; Yun, J. W.; Kajimoto, T.; Wong, C. H. A search for pyrophosphate mimics for the development of substrates and inhibitors of glycosyltransferases *Bioorganic & Medicinal Chemistry* **1997**, *5*, 661-672.

(195) Muller, B.; Schaub, C.; Schmidt, R. R. Efficient sialyltransferase inhibitors based on transition-state analogues of the sialyl donor *Angew. Chem., Int. Ed. Engl.* **1998**, *37*, 2893-2897.

(196) Hindsgaul, O.; Kaur, K. J.; Srivastava, G.; Blaszczykthurin, M.; Crawley, S. C.; Heerze, L. D.; Palcic, M. M. Evaluation of Deoxygenated Oligosaccharide Acceptor Analogs as Specific Inhibitors of Glycosyltransferases *J. Biol. Chem.* **1991**, *266*, 17858-17862.

(197) Lowary, T. L.; Hindsgaul, O. Recognition of Synthetic Deoxy and Deoxyfluoro Analogs of the Acceptor Alpha-L-Fucp-(1- 2)-Beta-D-Galp-or by the Blood-Group-a and Blood-Group-B Gene-Specified Glycosyltransferases *Carbohydr. Res.* **1993**, *249*, 163-195.

(198) Kajihara, Y.; Kodama, H.; Wakabayashi, T.; Sato, K.; Hashimoto, H. Characterization of Inhibitory Activities and Binding Mode of Synthetic 6'-Modified Methyl N-Acetyl-Beta-Lactosaminide toward Rat-Liver Cmp-Deuterium-Neu5acdeuterium-Galactoside-(2- 6)-Alpha-Deuterium-Sialyltransferase *Carbohydr. Res.* **1993**, *247*, 179-193.

(199) Bause, E. Active-Site-Directed Inhibition of Asparagine N-Glycosyltransferases with Epoxy-Peptide Derivatives *Biochem. J.* **1983**, *209*, 323-330.

(200) Hendrickson, T. L.; Spencer, J. R.; Kato, M.; Imperiali, B. Design and evaluation of potent inhibitors of asparagine-linked protein glycosylation *J. Am. Chem. Soc.* **1996**, *118*, 7636-7637.

(201) Platt, F. M.; Neises, G. R.; Reinkensmeier, G.; Townsend, M. J.; Perry, V. H.; Proia, R. L.; Winchester, B.; Dwek, R. A.; Butters, T. D. Prevention of lysosomal storage in Tay-Sachs mice treated with N-butyldeoxynojirimycin *Science* **1997**, *276*, 428-431.

(202) Inokuchi, J. I.; Radin, N. S. Preparation of the Active Isomer of 1-Phenyl-2-Decanoylamino-3-Morpholino-1-Propanol, Inhibitor of Murine Glucocerebroside Synthetase *Journal of Lipid Research* **1987**, *28*, 565-571.

(203) Palcic, M. M.; Heerze, L. D.; Srivastava, O. P.; Hindsgaul, O. A Bisubstrate Analog Inhibitor for Alpha-(1- 2)-Fucosyltransferase *J. Biol. Chem.* **1989**, *264*, 17174-17181.

(204) Hashimoto, H.; Endo, T.; Kajihara, Y. Synthesis of the first tricomponent bisubstrate analogue that exhibits potent inhibition against GlcNAc:beta-1,4-galactosyltransferase *J. Org. Chem.* **1997**, *62*, 1914-1915.

(205) Kim, Y. J.; Ichikawa, M.; Ichikawa, Y. A rationally designed inhibitor of alpha-1,3-galactosyltransferase *J. Am. Chem. Soc.* **1999**, *121*, 5829-5830.

(206) Schaub, C.; Muller, B.; Schmidt, R. R. Sialyltransferase inhibitors based on CMP-quinic acid *European J. Org. Chem.* **2000**, 1745-1758.

(207) Natsuka, S.; Lowe, J. B. Enzymes Involved in Mammalian Oligosaccharide Biosynthesis *Current Opinion in Structural Biology* **1994**, *4*, 683-691.

(208) Holmes, E. H.; Ostrander, G. K.; Hakomori, S. Biosynthesis of the Sialyl-Lex Determinant Carried by Type-2 Chain Glycosphingolipids (Iv3neuaciii3fucnlc4, Vi3neuacv3fucnlc6, and Vi3neuaciii3v3fuc2nlc6) in Human-Lung Carcinoma Pc9 Cells *J. Biol. Chem.* **1986**, *261*, 3737-3743.

(209) Hanisch, F. G.; Mitsakos, A.; Schroten, H.; Uhlenbruck, G. Biosynthesis of Cancer-Associated Sialyl-X Antigen by a (1- 3)-Alpha-L-Fucosyltransferase of Human Amniotic-Fluid *Carbohydr. Res.* **1988**, *178*, 23-28.

(210) Hakomori, S.; Nudelman, E.; Levery, S. B.; Kannagi, R. Novel Fucolipids Accumulating in Human Adenocarcinoma .2. Glycolipids with Difucosylated or Trifucosylated Type-2 Chain *J. Biol. Chem.* **1984**, *259*, 4672-4680.

(211) Feizi, T. Demonstration by Monoclonal-Antibodies That Carbohydrate Structures of Glycoproteins and Glycolipids Are Onco-Developmental Antigens *Nature* **1985**, *314*, 53-57.

Chapter 2

On the Design, Properties and Applications of Purine Nucleoside Phosphorylase, Nucleoside Hydrolase and Phosphoribosyltransferase Inhibitors

ABSTRACT

Purine nucleoside phosphorylase, nucleoside hydrolase and phosphoribosyltransferase are important enzymes that are involved in the salvage and regulation of purine and pyrimidine pools. They are all basically N-glycanases like glycosidases and glycosyl transferases. Kinetic isotope effect studies support the conclusion that oxocarbenium ions are features of the transition states for all these enzymes. A large amount of work has been devoted to development of effective inhibitors against these enzymes. The potential use of such inhibitors includes the development of antiviral, cancer and autoimmune drugs as well as drugs against certain neurological disorders. In this chapter, the structure-based design of inhibitors and transition state-based analogs of these three enzyme classes and related enzymes are reviewed

2.1. Indroduction

Purine nucleoside phosphorylases (PNP) are the enzymes that catalyze the cleavage (phosphorolysis) of the glycosidic bond (C-1' to N-9) of ribo- and 2'-deoxyribo-nucleoside to form the purine base and α-D-(deoxy)riboside-1-phosphate[1]. The main substrates of PNP are inosine (**figure 2.1**), guanosine and 2'-deoxyguanosine. PNP is an important enzyme in the base salvage pathway. It has been discovered that lack of PNP can result in human T-cell immunodeficiency[2,3]. Because PNP is the only enzyme that degrade 2-deoxyguanosine, if it is inhibited, 2-deoxyguanosine can be transported and phosphorylated by deoxycytidine kinase to deoxyguanosine triphosphate (dGTP)[4-7]. The dGTP can accumulate in the blood because of the high level of deoxycytidine kinase, and low activity of nucleotidases, that degrade dGTP. High levels of dGTP in T-cells can cause inhibition of ribonucleotide reductase, which is responsible for the cellular formation of dCDP and dUDP. This prevents DNA synthesis for T-cell proliferation[8-10].

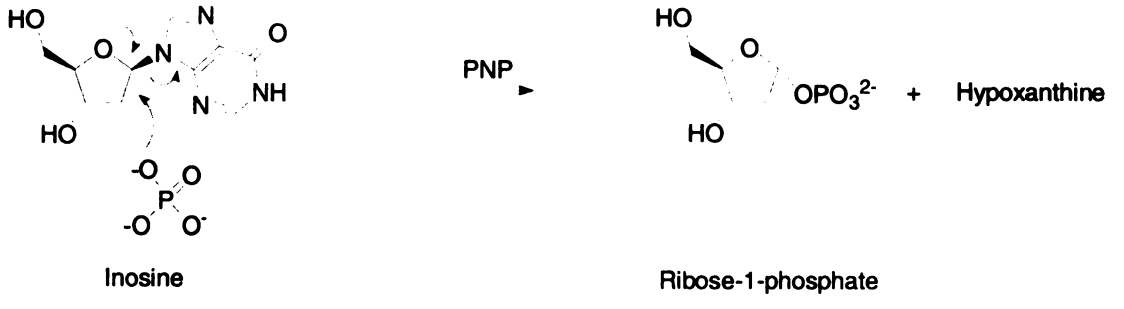

Figure 2.1. PNP catalyzed reaction

Undesirable T-cell activation and proliferation result in psoriasis, rheumatoid arthritis, T-cell leukemias and lymphomas, transplant tissue rejection, and other type IV autoimmune disorders. Consequently PNP inhibition has become a very important target for the development of drugs for a variety of diseases including cancer and autoimmune diseases[11-14].

Nucleoside N-riboside hydrolases (nucleoside hydrolases) are enzymes that catalyze the hydrolysis of the N-ribosidic bond of purine and purimidine nucleoside. **Figure 2.2** shows the hydrolysis of inosine catalyzed by nucleoside hydrolase. Nucleoside hydrolases are found in protozoan parasites and bacteria (*rihA*, *rihB* and *rihC* genes in *E. coli*)[15], but not in mammalian cells[16]. Nucleoside hydrolases play important roles in protozoa because they provide free bases to DNA and RNA synthesis for these organisms[17]. The protozoa have no ability for *de novo* purine biosyntehsis, therefore, the required bases are completely obtained from the host by a base salvage pathway. Nucleoside hydrolases are essential for the base recovery, and they have been found in the purine salvage pathway of the trypanosomes including *Crithidia fasciculate*[18,19]. Their specific role in the protozoa made them an important target for antibiotic design. The role of nucleoside hydrolases in bacteria is not well understood but they could be important during infection because the organisms could use the host nucleosides to make its own genetic material.

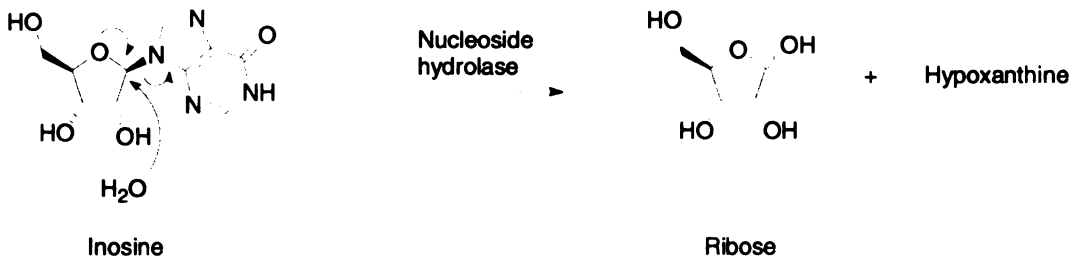

Figure 2.2. Nucleoside N-riboside hydrolases catalyzed reaction

Hypoxanthine-guanine phosphoribosyltransferases (HGPRTases) catalyze the transfer of 5'-phosphoribose from 5'-phosphoribosylpyrophosphate to the purine base hypoxanthine to form a nucleoside 5'-phosphate (inosine monophosphate) and pyrophosphate (**figure 2.3**). HGPRTases are manganese dependent enzymes and they are critical in both the base *de novo* and salvage pathway to obtain hypoxanthine, guanosin, or xanthine for the synthesis of DNA and RNA in protozoa parasites. Human HGPRTase does not use xanthine as substrate. Deficiency of human HGPRTase results in Lesch-Nyhan syndrome. Hyperuricemia and neurological disorders are features of this disease[20]. Because of their key roles in the nucleotide metabolism, they are also targeted as a drug strategy in antimicrobial, antiparasite and anticancer therapeutics.

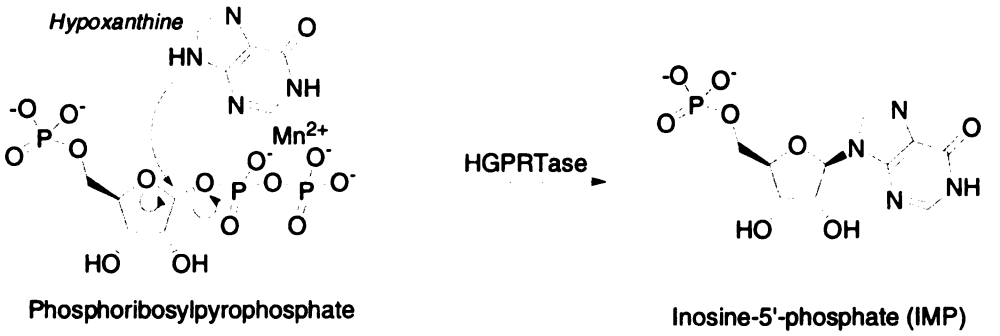

Figure 2.3. Hypoxanthine-guanine phosphoribosyltransferases catalyzed reaction

The three kinds of enzymes are all basically N-glycanases like glycosidases and glycosyltransferases, and they are involved in the salvage and regulation of purine and pyrimidine pools[12]. They also are involved in base excision repair and in the inactivation of ribosomes[21,22]. Therefore, a large amount of work has been devoted to studies of enzyme mechanisms, transition states to seek powerful inhibitors for those enzymes. Vern. L. Schramm etc. have developed methods for the determination of the transition state structures by kinetic isotope effect studies at multiple positions in the substrate molecule[23-26]. The methods include measuring kinetic isotope effects at every position in a substrate molecule that might be perturbed at the transition state, computing a truncated transition state structure with bond lengths and angles matching the isotope effects, and then optimizing the structure for the transition state. The results showed oxocarbenium ions are features for all these enzymes. The difference exists in the degree of the oxocarbenium ion formation and the nucleophilic displacement[27]. PNP and HGPRTase catalyze reactions with inversion of configuration at the anomeric center. According to Schramm[28-31], the transition state of PNP has bond order 0.4 to the leaving group, but

bond order < 0.04 to the incoming nucleophile. In nucleoside hydrolase[16,32,33], the oxocarbenium ion is nearly fully developed, with C-1' rehybridized almost completely to sp^2, and the attack of the water nucleophile is late well behind N-ribosidic bond breaking with approximately 0.03 bond order from the attacking oxygen to C1'. An S_N1 type reaction is more likely. Schramm proposes that for all these enzymes, the nucleophilic displacement occurs relatively late in the reaction coordinate. As we will see later, this conflicts with the finding that placing a nitrogen atom at the anomeric position in transition state inhibitors leads to better binding and better inhibition. According to the Schramm's model: the low bond order to the anionic nucleophile with significant bond order to the leaving group causes the ribosyl group to be electron deficient, with partial oxocarbenium character; the N-7 of the purine ring in these transition states is protonated or hydrogen-bonded to assist the departure of the leaving group; The pK_a of this group is elevated toward 7 or above as the ribosidic bond is broken. **Figure 2.4** illustrates the substrate inosine, PNP transition state, nucleoside hydrolase and HGPRTase transition states according to Schramm. The PNP transition state is reached when the C1'-N9 bond distance is elongated to 1.77Å from 1.44Å in inosine, with 3.0Å from the anomeric carbon, and the phosphate anion is proposed to play an important electrostatic role in the transition state stabilization.

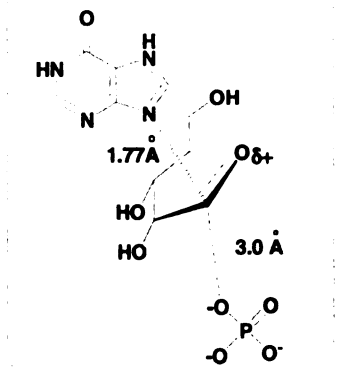

PNP transition state

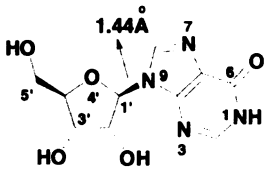

Inosine

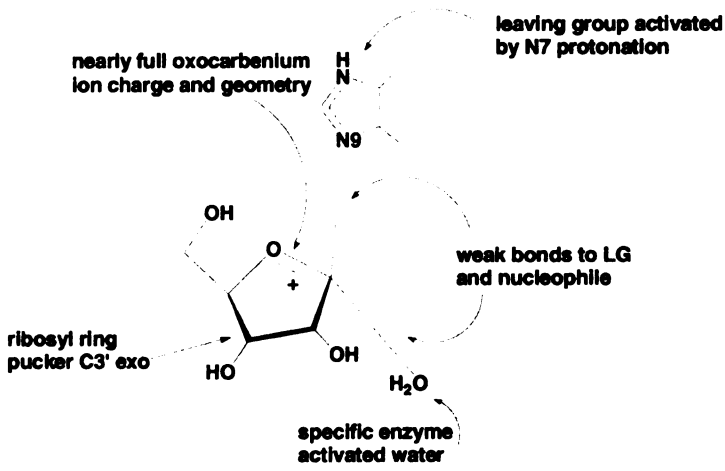

Nucleoside hydrolases trasition state

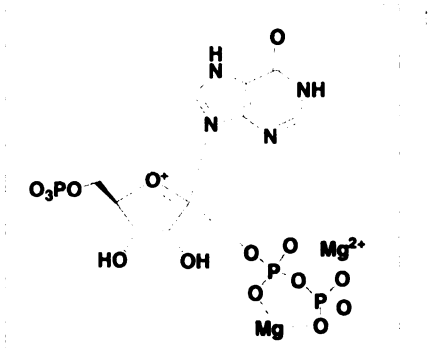

HGPRTase transition state

Figure 2.4. Substrate inosine, PNP transition state, nucleoside hydrolase and HGPRTase transition states.

2.2. Structure-based Design of PNP inhibitors

Structure-based design and structure-activity relationships have been used for the PNP inhibitor design[34-39]. It is based on the three-dimensional structure of the native PNP and computer-assisted molecular modeling. The catalytic site of PNP containing substrates or product analogs or weak inhibitors was sequentially filled with newly designed analogs followed by subsequent structural and kinetic characterization and refinement of catalytic site contacts. A number of 9-substituted deazaguanine derivatives were designed to search for the potent inhibitors with favorable interaction with PNP active site including purine binding site, the hydrophobic pocket and the phosphate binding site. The N-9 was replaced with carbon because no interaction was identified between N-9 and PNP residue, and 9-deazainosine itself binds 15-20 times more tightly than inosine[40]. A linkage to carbon instead of nitrogen is desirable because such a linkage cannot be cleaved by N-glycosidases of any sort. Compounds with substitution at the 9-position by aromatic, alicyclic and heteroalicyclic groups attached through a methylene group were found to be good inhibitors[34] (**Figure 2.5**) even if the substituents bore no similarity to a sugar residue and an equivalent of a positively charged glycosyl ring oxygen or anomeric carbon was not present. Aryl groups such as thienyl, furanyl, pyridyl and phenyl provided potent inhibitors. The 3- and 4-substituted phenyl group gave low IC_{50} values in the nanomolar range, but compounds with 2-chloro and 2-hydroxylphenyl groups are poor inbitors. This is probably due to the displacement of the 9-deazaguanine moiety from its optimal binding position resulting in disturbing of the noncovalent interactions. Cyclopentyl, cyclohexyl, tetrahydrothienyl, dithianyl derivatives which have greater hydrophobicity also showed equal potency when assayed in 1 mM phosphate. They all

have favorable interaction with the purine and hydrophobic binding sites of PNP, and they can penetrate the cells more easily.

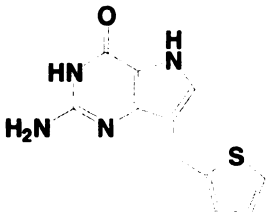

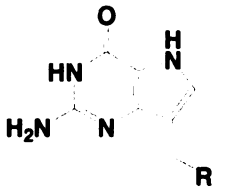

	R	IC_{50} (nM) in 1 mM PO_4
1	3,4-dichlorophenyl	17
2	3-chlorophenyl	20
3	4-iodophenyl	23
4	3-fluorophenyl	24
5	4-chlorophenyl	25
6	phenyl	51
7	3-methylphenyl	57
8	3-methoxylphenyl	82

IC_{50} = 21 nM (1 mM PO_4)

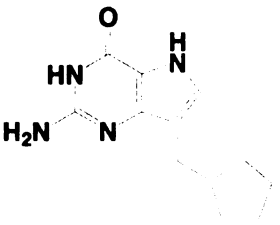

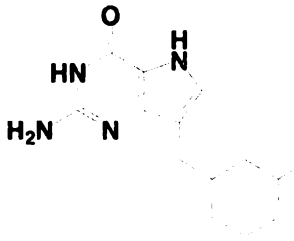

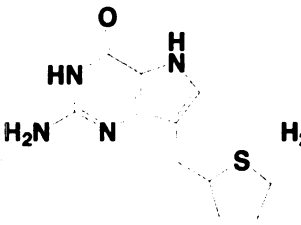

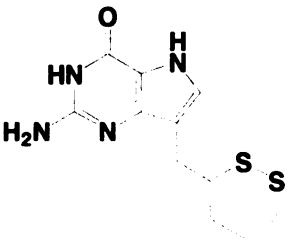

IC_{50} (nM)			
(1 mM PO_4) = 29	25	11	18
9	10	11	12

Figure 2.5. PNP inhibitors

To increase the binding affinity of the inhibitors, functional groups which can interact with the PNP phosphate binding site can be introduced. A potent PNP inhibitor, acyclovir diphosphate[41] (ACVdir) (**Figure 2.6**) was found to be a bisubstrate inhibitor binding in

the purine binding site and in the phosphate binding site with some interaction of the ACV side chain with the hydrophobic pocket[42]. Some 9-substituted guanines were investigated as phosphate mimics with the functional end being sulfonic acid, carboxylic acid, sulfonamide, carboxamide and nitrile[38]. The result showed that the sulfonic acid and the carboxylic acid end groups interact significantly with the phosphate binding site, but both of them bind more weakly than the phosphate (**Figure 2.6**). The sulfonamide, carboxamide, and the nitrile have no interaction with the phosphate binding site. It was suggested that the only phosphate mimics that bind like phosphate are themselves ionic, probably with limited ability to penetrate cell membranes.

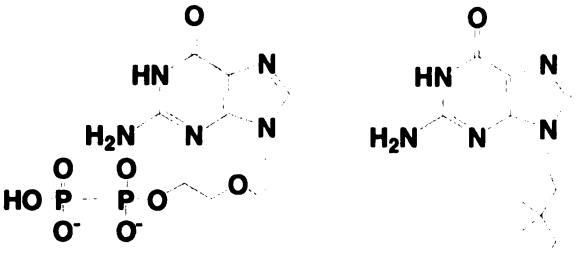

Acyclovir Diphosphate
K_i = 8.7 nM

	X	IC_{50} (μM) 1mM PO_4
13	PO_3H_2	0.044
14	SO_3H	0.18
15	SO_2NH_2	100
16	COOH	8.0
17	$CONH_2$	200

Figure 2.6. Phosphate mimics for PNP inhibitors

More hydrophobic mimics were developed to improve the cell penetration and oral activity (**Figure 2.7**). Compound **18** was found to be a good inhibitor with IC_{50} 35 nM. Derivatives with different substituents were studied and compound (S)-**20** with 3-chlorophenyl and $-CH_2COOH$ group has IC_{50} of 5.9 nM, whereas the corresponding (R)-isomer was 30-fold less potent[36,37].

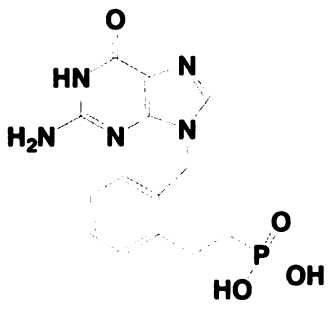

18

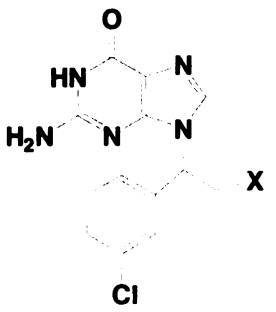

no.	X	IC_{50} (nM) 1mM PO_4
19	H	20
(S)-20	CH_2CO_2H	5.9
(R)-20	CH_2CO_2H	160
21	CH_2CN	11
22	CH_2CH_2O	25
23	CH_2CO_2Me	85

Figure 2.7. More hydrophobic mimics.

2.3. Transition State Inhibitor

The transition state studies have guided the transition state analog inhibitor design. Chemically stable compounds with the same molecular shape and volume, incorporating the key transition state features should provide inhibitors with high affinity to the target enzymes. Because of the oxocarbenium ion feature of the transition state, 1,4-dideoxy-1,4-imino-D-ribitol compounds which can be largely protonated at pH 7 (pK_a = 6.5)[43], should be potent transition state analog inhibitors of both PNP and nucleoside hydrolases. Compounds such as phenyl iminoribitol **24**[33,44-46], amidrazone **25**[47], and nicotinamide-based analog **26**[46] were studied and revealed potent (nM) inhibitors of the *Crithidia fasciculata* nucleoside hydrolase such as p-bromo or p-aminophenyl iminoribitol.

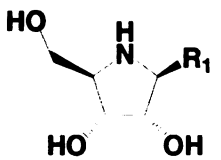

R_1 = substituted phenyl

24

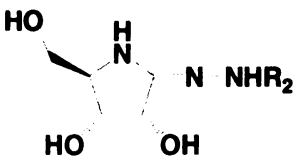

R_2 = H, C_6H_5, p-I-C_5H_4, p-NO_2-C_6H_4

25

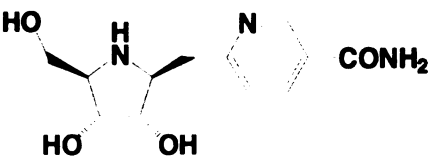

26

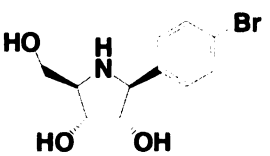

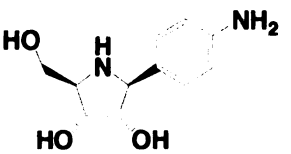

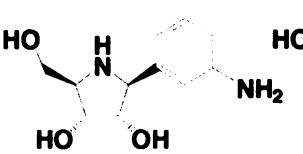

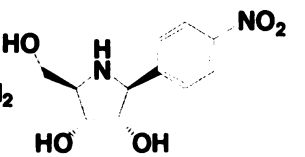

K_i values (nM) for *Crithidia fasciculata* nucleoside hydrolase

28 30 51 1100

27 28 29 30

Further investigation of the substituted iminoribitol led to the conclusion that for more potent inhibition of PNP, hydrolases, and transferaes, the R_1 group needs to better mimic the purine base of the substrate. Therefore, a family of Immucillins (Imm) was designed and synthesized specifically to mimic the transition state structures. ImmH (**31**, (1*S*)-1-(9-deazahypoxanthin-9-yl)-1,4-dideoxy-1,4-imino-D-ribitol) and ImmG (**32**, (1*S*)-1-(9-deazaguanin-9-yl)-1,4-dideoxy-1,4-imino-D-ribitol) were developed first[48-51]. In the structure of ImmH, The ring oxygen is replaced by imino group, the same strategy in the glycosidase inhibitor design. It mimics the partial positive charge of the ribooxocarbenium transition state upon protonation. The C-C ribosidic bond instead of C-N bond would mimic the lengthened C-N linkage in transition state and provide chemical stability against breaking. The N7 of ImmH has greater pK_a (9.8), and can be easily

protonated, similar to inosine at transition state and unlike N7 in the substrate (pK_a=1.2). These features cause immucillins in the picomolar range inhibitors (**Figure 2.8**), and immucillin-H is currently in the phase I/II clinic trials for the treatment of T-cell leukemia.

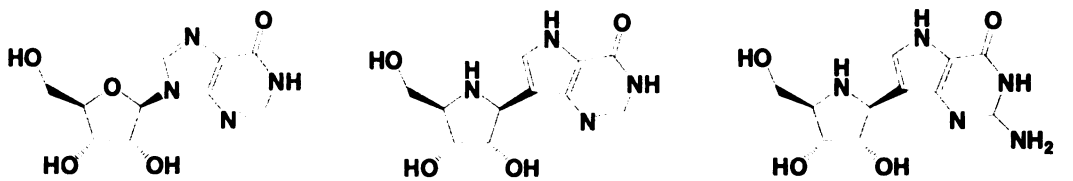

Inosine

ImmH 31
K_i = 23 pM (bovine PNP)
K_i = 72 pM (Human PNP)

ImmG 32
K_i = 30 pM (bovine PNP)
K_i = 29 pM (Human PNP)

Figure 2.8. ImmH family.

The crystal structure of PNP complex with immucillin-H and PO_4 has been solved[31]. Together with the PNP-substrate (Michaelis complex)[52] and PNP-product structures[52], they have provided important information about the structural details of the catalytic mechanism. **Figure 2.9** is the noncovalent interactions in the active sites of bovine PNP complexes. The structure of the PNP·ImmH·PO_4 resembles the structures of PNP·inosine·SO_4 (reactant) and PNP·hypoxanthine·ribose 1-PO_4 (products), but PNP·ImmH·PO_4 complex involves closer contacts between the protein and ImmH (**Figure 2.9**). Five direct hydrogen bonds to the purine base and two additional hydrogen bonds in a proton-transfer bridge characterize the PNP interactions in these complexes. Six of these seven contacts are shortened in the PNP·ImmH·PO_4 complex compared to the

Michaelis complex. The ribose and phosphate moieties also form closer interactions with the enzyme. This results in high affinity of ImmH and decreased protein dynamics. The distance between N9 of inosine or hypoxanthine to O4 of the phosphate group, called reaction coordinate distance, is 4.8Å in PNP·ImmH·PO_4 complex, while they are 5.6 and 5.2Å in the Michaelis and product complex, respectively. This shorter distance indicates tight binding between PNP and the inhibitor. It also ruled out an S_N1 mechanism in which approximately 6Å is required for the formation of a fully developed oxocarbenium ion transition state while the shorter distances are associated with significant bond orders to leaving and/or attacking groups. There is no direct interaction from protein to stabilize the partial positive charge developed at transition state, but neighboring groups play important roles in the transition state stabilization. The distance between O4 of the phosphate and N4' of ribosyl group is 2.8Å in PNP·ImmH·PO_4 complex, which is significantly shorter than the O4-O4' sulfate interaction in the PNP-substrate structure. This stabilization of transition state provided by neighboring group phosphate ion is different from the glycosidases and glycosyltransferases, in which a pair of enzymatic carboxylates stabilizes the oxocarbenium ion transition state.

a) PNP-inosine-SO_4

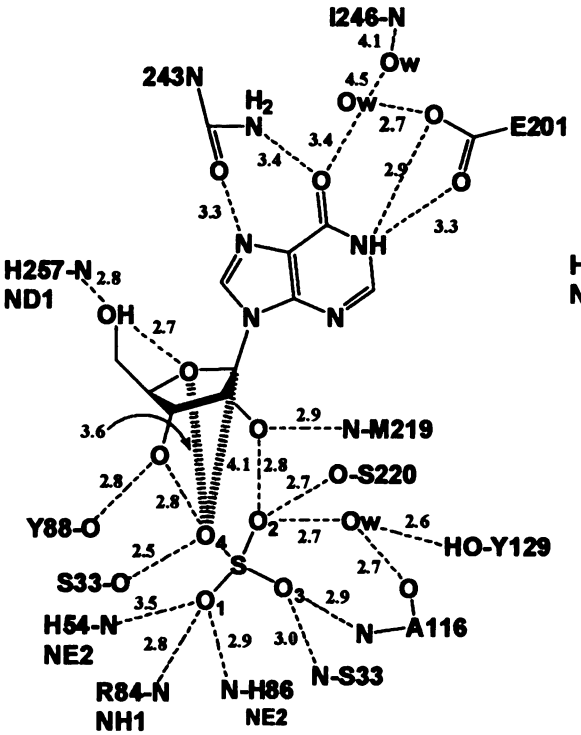

b) PNP-ImmH-PO_4

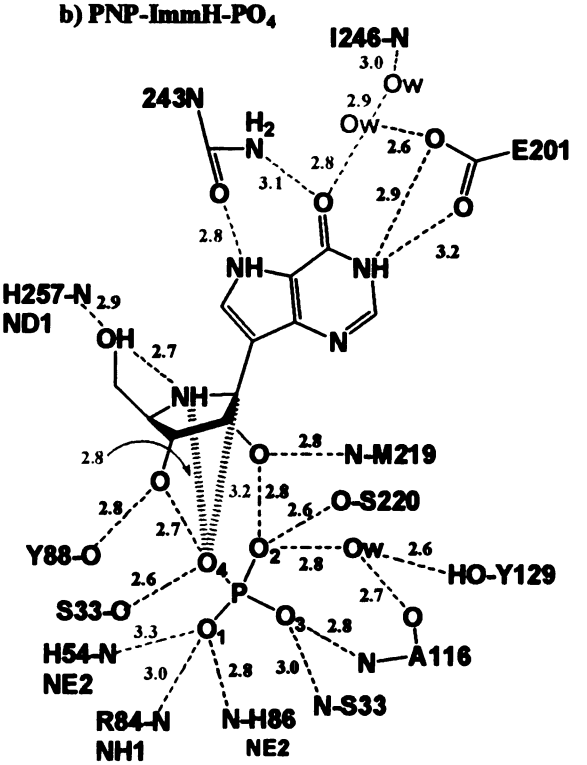

c) PNP-Hx-R-1-PO_4

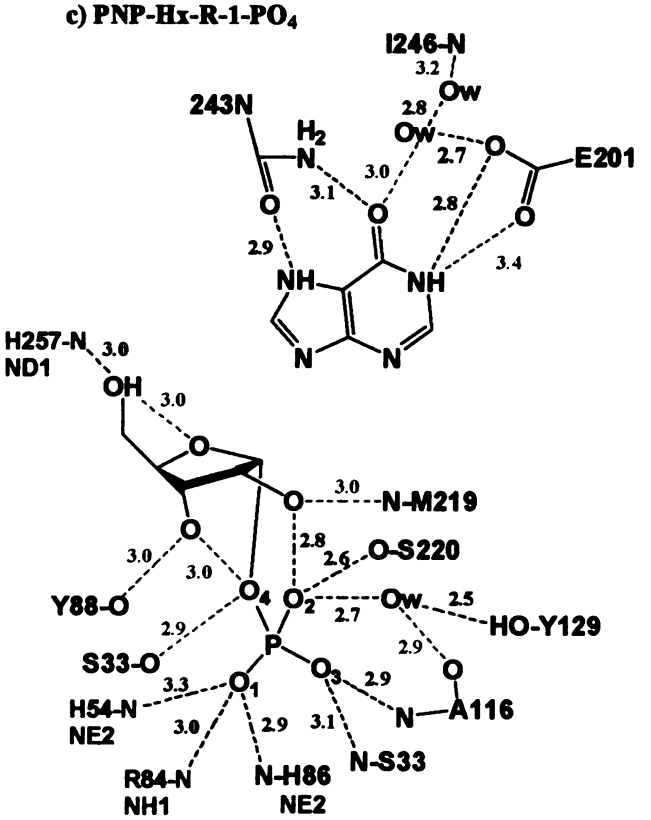

Figure 2.9. The structures of bovine PNP with substrate analogues (inosine+SO_4), transition-state complex (Imm-H+PO_4) and products (hypoxanthine+ribose 1-PO_4) bound at the catalytic sites. Hydrogen bond distances are shown in angstroms. Red indicates bonds that shorten significantly and blue indicates bonds that lengthen significantly in the conversion of (a) to (b), and of (b) to (c).

One important feature of these complexes is the immobilization of the nucleophile phosphate. It forms 10 relatively well positioned H-bonds from main chain atoms, side chain atoms, a water molecule, and the 2'- and 3'-hydroxyl groups of the ribosyl group. Therefore, the nucleophile is 'fixed' in the binding site and the C1' of ribosyl group has to 'migrate' towards the nucleophile oxygen (O4 of phosphate). Comparison of PNP·inosine·SO_4 to PNP·ImmH·PO_4 revealed that the enzyme brings the iminoribitol C1' 0.9 Å nearer to O4 of phosphate in the PNP·ImmH·PO_4 complex (**Figure 2.10a**). Thus, formation of the transition state involves the electrostatically driven migration of the ribooxocarbenium carbon from the purine ring towards the phosphate. The transition state is reached when the C1'-N9 bond has lengthened from 1.44 to 1.77 (**Figure 2.10b**), while the 5'-hydroxyl of the ribosyl group remain immobile. This migration of the anomeric carbon also occurs in the glycosidases and glycosyltrnasferases. It reflects the ability of enzymes to accomplish atomic motion of reactive groups in the protected environment of the catalytic site[31,53].

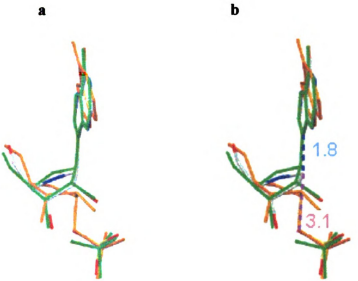

Figure 2.10. Superpositions of the reactants (green), bound transition state analogues (white with blue nitrogens and red oxygens), and products (gold) in the active sites of bovine PNP (a) are compared with the superpositions of reactants, experimentally determined transition states, and products (b). Distances (in angstroms) shown in (b) are deduced from transition state analyses for PNP.

To favor the ribosyl oxocarbenium ion formation, there is a significant distortion of the ImmH geometry (**Figure 2.11**). The conformation of the iminoribitol moiety changes from a C2'-endo to a C4'-endo on formation of the complex. The N9-C1'-C2'-H2' dihedral angle is near 0° in the bound ImmH, which is consistent with the favored transition state conformation with orbital overlap between the breaking N9-C1' bond and C2'-H2' bond of inosine. This angle is 42° in the unbounded ImmH. The 5'-hydroxyl is *anti* to the ribosyl group in the free conformation, but adopts a *syn* conformation when bound to PNP. This conformation place the 5'-oxygen 2.7 Å above O4' or N4', with O4 of phosphate 2.8 Å below the oxocarbenium oxygen. This ribosyl ring oxygen (O4') is sandwiched by two electron-rich oxygens, favoring release of electron from O4', cleavage of the C1'-N9 bond, and formation of the oxocarbenium ion transition state.

bound /free ImmH

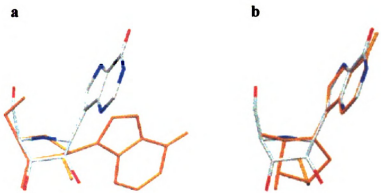

Figure 2.11. Conformations of free and bound immucillins are from the small molecule crystal structure of ImmH (gold) and ImmH in PNP·ImmH·PO_4 (PDB 1B8O, white with blue nitrogens and red oxygens). Molecular overlap in (a) is C3' and C4' and in (b) is the purine rings.

The purine and pyrimidine phosphoribosyltransferases[27,54-56] and ribosyl hydrolases[57,58] adopt the similar migrating oxocarbenium mechanism. The pyrophosphate in phosphoribosyltransferases is immobilized by two bidentate magnesium ions in a scaffold of 12 noncovalent interactions. It is important to note that the scenarios outlined above are rationalizations and inferences based on the X-ray crystal structures which themselves cannot provide direct proof of the pathways leading up to the structures. Detailed molecular dynamics analyses that can support these inferences are still outside of computational reach because of the significant length scales and time scales involved.

Analogs of ImmH have also been developed to seek for powerful inhibitors of PNP, hydrolases, and other ribosyltransferases. ImmH **31** and ImmG **32** are very potent inhibitors of PNP. ImmH **31**, ImmG **32**, and ImmA **33** are inhibitors of nucleoside hydrolase[46,59]. 5'-phosphate ImmH **34** and ImmG **35** are the most potent inhibitors known of several purine phosphoribosyltransferases[60] (**table 2.1**).

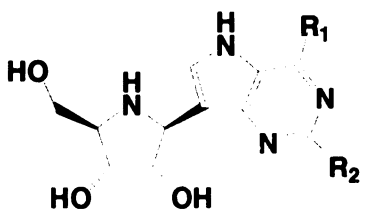

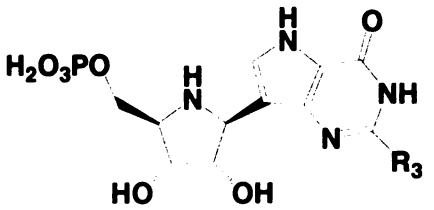

31 ImmH R_1=OH, R_2=H
32 ImmG R_1=OH, R_2=NH_2
33 ImmA R_1=NH_2, R_2=H

34 ImmHP R_3=H
35 ImmGP R_3=NH_2

Table 2.1. Inhibition constants for nucleohydrolase and HGPRT

K_i (nM)	IU[a]	IAG[b]	Human HGPRT	Malarial HGPRT
ImmH	42	24		
ImmG	84	110		
ImmA	7	0.9		
ImmHP			1.8	1.0
ImmGP			4.6	14

[a] IU = inosine-uridine nucleoside hydrolase from *Crithidia fasciculate.* [b] IAG = inosine-adenosine-guanosine nucleoside hydrolase from *Trypanosoma brucei.*

Because early studies on transition state analogs of AMP-N-ribosylhydrolase revealed that formycin 5'-phosphate **36** is a powerful inhibitor[61,62], 8-aza-immucillins **37-39** were synthesized to study the effect of the extra nitrogen on the inhibition by modifying the pK_a of the 7-NH residue[63]. The result showed that 8-aza-immucillins are powerful inhibitors for mammalian PNPs, comparable to the parent immucillins (**table 2.2**). Immucillin **38** was inactive against human and bovine PNP. Perturbation of N-7

interactions with target enzymes by the extra 8-nitrogen has little effect on PNPs but cause weaker inhibition on nucleosides hydrolases.

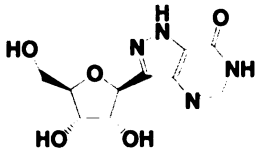

36

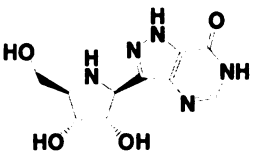

37

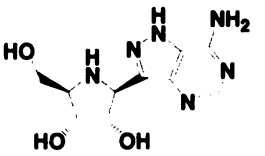

38

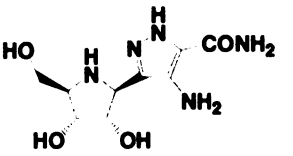

39

Table 2.2. Inhibition constants

K_i (nM)	Human PNP	Bovine PNP	IU	IAG
ImmH	0.072	0.023		
37	0.104	0.042	1600	13900
38			150	14000
39	0.096	0.060	4800	3700

The structure-activity relationship studies of immucillin analogs have been carried out to obtain more potent inhibitors[64]. Modifications at the 2'-, 3'- or 5'-positions of the azasugar moiety or at the 6-, 7-, or 8-positions of the deazapurine, as well as methylene-bridged analogs resulted in poorer inhibitors than the parent immucillins for human PNP. This reflects the close mimic of the transition state features by immucillins.

Immucillins have been established to be the most potent PNP inhibitors reported. ImmH is a 23 pM inhibitor for bovine PNP but a 2-3 fold weaker inhibitor for the human PNP. Because of the different binding affinity of ImmH with human and bovine PNPs[48,65], the transition state structure of human PNP was examined. Despite an 87% amino acid

identity between these two enzymes[48], transition state of human PNP showed the more dissociated nature between the ribosyl group and the leaving purine, with bond length greater than 2.5Å, and the necleophile is also farther for human PNP than for bovine PNP. These led to a further developed oxocarbenium ion transition state with more positive charge character at C1'. **Figure 2.12** is the transition state structures for bovine and human PNP. This has guided the design of the second generation of PNP inhibitors[66-68], which are specifically targeted to human PNP. **Figure 2.13** is the second generation inhibitor DADME (4'-deaza-1'-aza-2'-deoxy-1'-(9-methylene))-immucillin-H, DADME-immucillin-G, and 8-aza-DADME-immucillin-H. In the structure of DADME-immucillin-H, the nitrogen (immino group) is moved from the 4' position to the corresponding C1', which mimics the more positive charged anomeric position in the transition state. The methylene bridge between the deaza purine and ribosyl analogues groups of DADME-immucillin-H separates the two parts with 2.5 Å in distance, which makes the inhibitor similar to the more dissociated transition state. The inhibition studies showed greater binding affinities of DADME-immucillins to the human PNP (**Figure 2.13**), and they are the most powerful PNP inhibitors yet described. Comparing the structures of PNP transition state, ImmH, and DADME-ImmH, we can conclude that closer match to the transition state in both electrostatics and geometry are required to achieve high affinity to the enzyme. Although those chemically stable analogs are imperfect mimics of the enzyme transition state because of their covalent nature, strategies based on the understanding of the transition state nature can be developed to approach the goal of the transition state inhibitors.

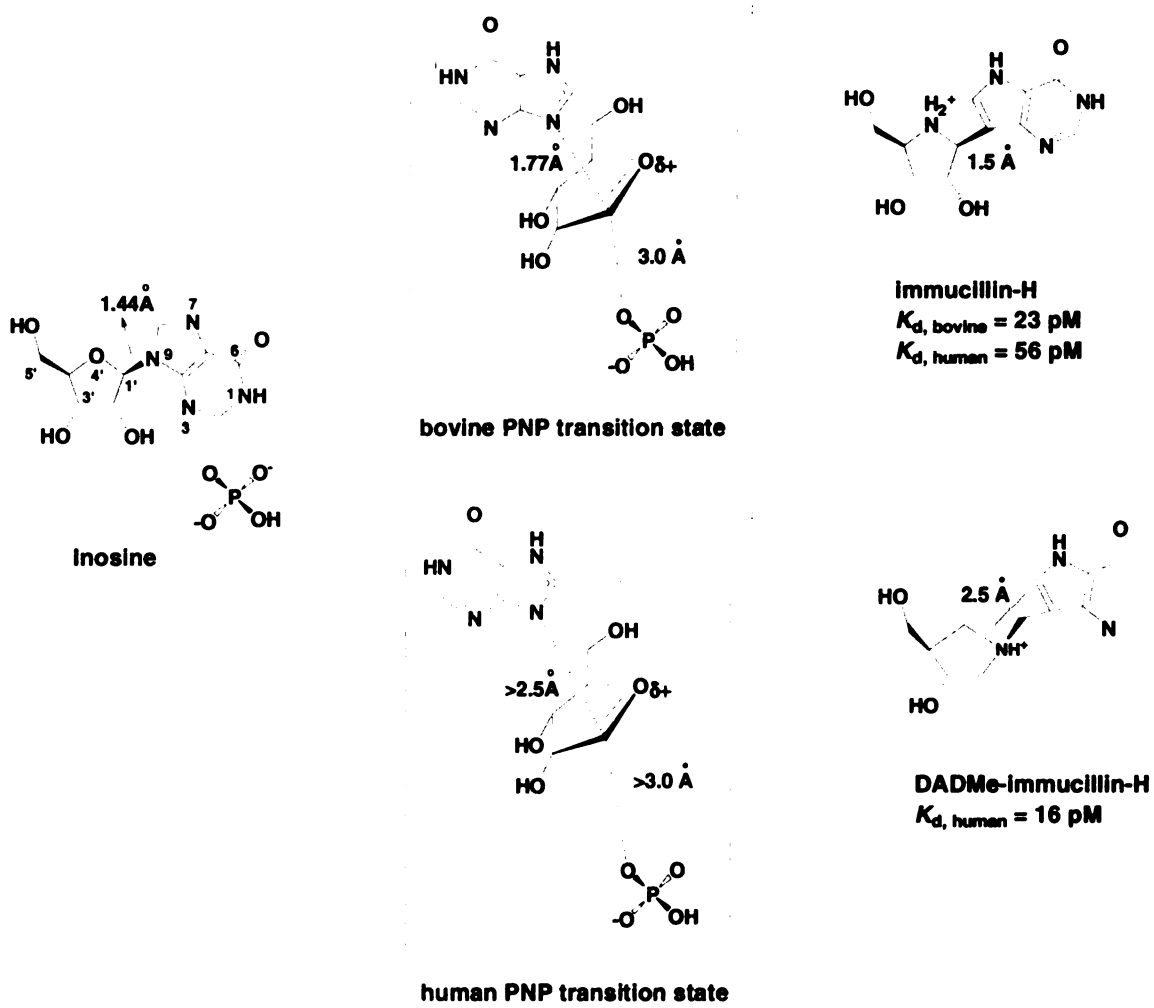

Figure 2.12. Transition state structures for bovine and human PNP. The distances of 1.5 Å for immucillin-H and 2.5 Å for DADMe-immucillin-H refer to the linear distance between the deazapurine ring and C-1' or N-1' of the ribosyl analogues.

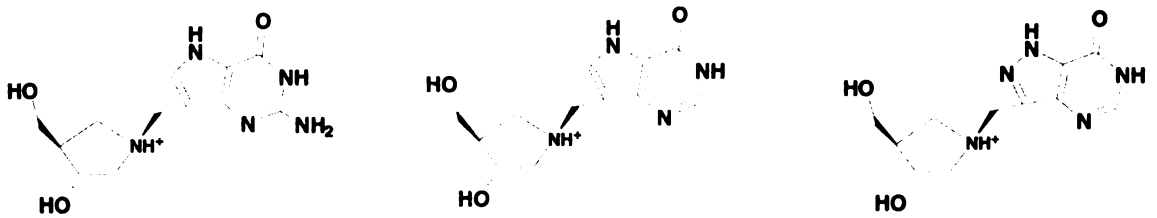

DADMe-immucillin-G
K_d = 7 pM

40

DADMe-immucillin-H
K_d = 16 pM

41

8-aza-DADMe-Imm-H
K_d = 2.0 nM

42

Figure 2.13. Second generation inhibitors for human purine nucleoside phosphorylase

2.4. References

(1) Stoeckler, J. D.; Cambor, C.; Parks, R. E. Human Erythrocytic Purine Nucleoside Phosphorylase - Reaction with Sugar-Modified Nucleoside Substrates *Biochemistry* **1980**, *19*, 102-107.

(2) Hershfield, M. S., Mitchell, B. S. In *The Metabolic Basis of Inherited Disease*; 7th ed.; Scriber, C. R., Beaudet, A. L., Sly, W. S., Valle, D., Ed.; McGraw-Hill: New York, 1995, pp 1725-1768.

(3) Markert, L. M. *Immunodefic. Rev.* **1991**, *3*, 45-81.

(4) Krenitsky, T. A.; Tuttle, J. V.; Koszalka, G. W.; Chen, I. S.; Beacham, L. M.; Rideout, J. L.; Elion, G. B. Deoxycytidine Kinase from Calf Thymus - Substrate and Inhibitor Specificity *Journal of Biological Chemistry* **1976**, *251*, 4055-4061.

(5) Carson, D. A., Kaye, J., Seegmiller, J. E. Lymphospecific toxicity in adenosine deaminase deficiency and purine nucleoside phosphorylase deficiency: possible role of nucleoside kinase(s) *Proc. Natl. Acad. Sci. U. S. A.* **1977**, *74*, 5677-5681.

(6) Mitchell, B. S.; Mejias, E.; Daddona, P. E.; Kelley, W. N. Purinogenic Immunodeficiency Diseases - Selective Toxicity of Deoxyribonucleosides for T-Cells *Proc. Natl. Acad. Sci. U. S. A.* **1978**, *75*, 5011-5014.

(7) Ullman, B.; Gudas, L. J.; Clift, S. M.; Martin, D. W. Isolation and Characterization of Purine-Nucleoside Phosphorylase-Deficient T-Lymphoma Cells and Secondary Mutants with Altered Ribonucleotide Reductase - Genetic Model for Immunodeficiency Disease *Proc. Natl. Acad. Sci. U. S. A.* **1979**, *76*, 1074-1078.

(8) Thelander, L., Reichard, P. Reduction of ribonucleotides *Annu. Rev. Biochem.* **1979**, *48*, 133-158.

(9) Snyder, F. F., Jenuth, J. P., Mably, E. R., Mangat, R. K. Point mutations at the purine nucleoside phosphorylase locus impair thymocyte differentiation in the mouse *Proc. Natl. Acad. Sci. USA* **1997**, *94*, 2522-2527.

(10) Boehncke, W. H.; Gilbertsen, R. B.; Hemmer, J.; Sterry, W. Evidence for a Pathway Independent from 2'-Deoxyguanosine and Reversible by Il-2 by Which Purine Nucleoside Phosphorylase Inhibitors Block T-Cell Proliferation *Scandinavian Journal of Immunology* **1994**, *39*, 327-332.

(11) Montgomery, J. A. Purine Nucleoside Phosphorylase - a Target for Drug Design *Medicinal Research Reviews* **1993**, *13*, 209-228.

(12) Morris, P. E., Montgomery, J. A. Inhibitors of the enzyme purine nucleoside phosphorylase *Exp. Opin. Therapeut. Pats.* **1998**, *8*, 283-299.

(13) Parsons, W. H. In *Annual Reports in Medicinal Chemistry, Vol 29*, 1994; Vol. 29, pp 175-184.

(14) Sircar, J. C.; Gilbertsen, R. B. Purine nucleoside phosphorylase (PNP) inhibitors: Potentially selective immunosuppressive agents *Drugs of the Future* **1988**, *13*, 653-668.

(15) Petersen, C.; Moller, L. B. The RihA, RihB, and RihC ribonucleoside hydrolases of Escherichia coli - Substrate specificity, gene expression and regulation *Journal of Biological Chemistry* **2001**, *276*, 884-894.

(16) Gopaul, D. N.; Meyer, S. L.; Degano, M.; Sacchettini, J. C.; Schramm, V. L. Inosine-uridine nucleoside hydrolase from Crithidia fasciculata. Genetic characterization, crystallization, and identification of histidine 241 as a catalytic site residue *Biochemistry* **1996**, *35*, 5963-5970.

(17) Hammond, D. J.; Gutteridge, W. E. Purine and pyrimidine metabolism in the trypanosomatidae *Mol. Biochem. Parasitol.* **1984**, *13*, 243-261.

(18) Parkin, D. W.; Horenstein, B. A.; Abdulah, D. R.; Estupinan, B.; Schramm, V. L. Nucleoside Hydrolase from Crithidia-Fasciculata - Metabolic Role, Purification, Specificity, and Kinetic Mechanism *J. Biol. Chem.* **1991**, *266*, 20658-20665.

(19) Estupinan, B.; Schramm, V. L. Guanosine-Inosine-Preferring Nucleoside N-Glycohydrolase from Crithidia-Fasciculata *J Biol. Chem.* **1994**, *269*, 23068-23073.

(20) Sculley, D. G.; Dawson, P. A.; Emmerson, B. T.; Gordon, R. B. A Review of the Molecular-Basis of Hypoxanthine-Guanine Phosphoribosyltransferase (Hprt) Deficiency *Human Genetics* **1992**, *90*, 195-207.

(21) Fong, W. P.; Wong, R. N. S.; Go, T. T. M.; Yeung, H. W. Enzymatic-Properties of Ribosome-Inactivating Proteins (Rips) and Related Toxins *Life Sciences* **1991**, *49*, 1859-1869.

(22) Barbieri, L.; Battelli, M. G.; Stirpe, F. Ribosome-Inactivating Proteins from Plants *Biochimica Et Biophysica Acta* **1993**, *1154*, 237-282.

(23) Rodgers, J.; Femec, D. A.; Schowen, R. L. Isotopic Mapping of Transition-State Structural Features Associated with Enzymic Catalylis of Methyl Transfer *J. Am. Chem. Soc.* **1982**, *104*, 3263-3268.

(24) Cleland, W. W. The use of isotope effects to determine transition-state structure for enzymic reactions *Methods Enzymol.* **1982**, *87*, 625-641.

(25) Northrop, D. B. Steady-state analysis of kinetic isotope effects in enzymic reactions *Biochemistry* **1975**, *14*, 2644-2651.

(26) Schramm, V. L. Enzymatic transition states and transition state analog design *Annual Review of Biochemistry* **1998**, *67*, 693-720.

(27) Tao, W.; Grubmeyer, C.; Blanchard, J. S. Transition state structure of Salmonella typhimurium orotate phosphoribosyltransferase *Biochemistry* **1996**, *35*, 14-21.

(28) Kline, P. C.; Schramm, V. L. Purine Nucleoside Phosphorylase - Inosine Hydrolysis, Tight-Binding of the Hypoxanthine Intermediate, and 3rd-the-Sites Reactivity *Biochemistry* **1992**, *31*, 5964-5973.

(29) Kline, P. C.; Schramm, V. L. Purine Nucleoside Phosphorylase - Catalytic Mechanism and Transition-State Analysis of the Arsenolysis Reaction *Biochemistry* **1993**, *32*, 13212-13219.

(30) Kline, P. C.; Schramm, V. L. Pre-Steady-State Transition-State Analysis of the Hydrolytic Reaction Catalyzed by Purine Nucleoside Phosphorylase *Biochemistry* **1995**, *34*, 1153-1162.

(31) Fedorov, A.; Shi, W.; Kicska, G.; Fedorov, E.; Tyler, P. C.; Furneaux, R. H.; Hanson, J. C.; Gainsford, G. J.; Larese, J. Z.; Schramm, V. L.; Almo, S. C. Transition state structure of purine nucleoside phosphorylase and principles of atomic motion in enzymatic catalysis *Biochemistry* **2001**, *40*, 853-860.

(32) Mazzella, L. J.; Parkin, D. W.; Tyler, P. C.; Furneaux, R. H.; Schramm, V. L. Mechanistic diagnoses of N-ribohydrolases and purine nucleoside phosphorylase *J. Am. Chem. Soc.* **1996**, *118*, 2111-2112.

(33) Parkin, D. W.; Limberg, G.; Tyler, P. C.; Furneaux, R. H.; Chen, X. Y.; Schramm, V. L. Isozyme-specific transition state inhibitors for the trypanosomal nucleoside hydrolases *Biochemistry* **1997**, *36*, 3528-3534.

(34) Montgomery, J. A.; Niwas, S.; Rose, J. D.; Secrist, J. A.; Babu, Y. S.; Bugg, C. E.; Erion, M. D.; Guida, W. C.; Ealick, S. E. Structure-Based Design of Inhibitors of Purine Nucleoside Phosphorylase .1. 9-(Arylmethyl) Derivatives of 9-Deazaguanine *J. Med. Chem.* **1993**, *36*, 55-69.

(35) Secrist, J. A.; Niwas, S.; Rose, J. D.; Babu, Y. S.; Bugg, C. E.; Erion, M. D.; Guida, W. C.; Ealick, S. E.; Montgomery, J. A. Structure-Based Design of Inhibitors of Purine Nucleoside Phosphorylase .2. 9-Alicyclic and 9-Heteroalicyclic Derivatives of 9-Deazaguanine *J. Med. Chem.* **1993**, *36*, 1847-1854.

(36) Erion, M. D.; Niwas, S.; Rose, J. D.; Ananthan, S.; Allen, M.; Secrist, J. A.; Babu, Y. S.; Bugg, C. E.; Guida, W. C.; Ealick, S. E.; Montgomery, J. A. Structure-Based

Design of Inhibitors of Purine Nucleoside Phosphorylase .3. 9-Arylmethyl Derivatives of 9-Deazaguanine Substituted on the Methylene Group *J. Med. Chem.* **1993**, *36*, 3771-3783.

(37) Erion, M. D.; Niwas, S.; Rose, J. D.; Ananthan, S.; Allen, M.; Secrist, J. A.; Babu, Y. S.; Bugg, C. E.; Guida, W. C.; Ealick, S. E.; Montgomery, J. A. Structure-Based Design of Inhibitors of Purine Nucleoside Phosphorylase .3. 9-Arylmethyl Derivatives of 9-Deazaguanine Substituted on the Methylene Group (Vol 36, Pg 3773, 1993) *J. Med. Chem.* **1994**, *37*, 1034-1034.

(38) Guida, W. C.; Elliott, R. D.; Thomas, H. J.; Secrist, J. A.; Babu, Y. S.; Bugg, C. E.; Erion, M. D.; Ealick, S. E.; Montgomery, J. A. Structure-Based Design of Inhibitors of Purine Nucleoside Phosphorylase .4. A Study of Phosphate Mimics *J. Med. Chem.* **1994**, *37*, 1109-1114.

(39) Farutin, V.; Masterson, L.; Andricopulo, A. D.; Cheng, J. M.; Riley, B.; Hakimi, R.; Frazer, J. W.; Cordes, E. H. Structure-activity relationships for a class of inhibitors of purine nucleoside phosphorylase *J. Med. Chem.* **1999**, *42*, 2422-2431.

(40) Stoeckler, J. D. R., J. B.; Parks, R. E., Jr.; Chu, M.-Y.; Lim,; M.-L.; Ren, W.-Y. K., R. S., Inhibitors of Purine Nucleoside Phosphorylase: Effecta of 9-Deazapurine Ribonucleorrides and Synthesis of 5'-Deoxy-5'-iodo-s-deazainosine *Cancer Res.* **1986**, *46*, 1774-1778.

(41) Tuttle, J. V. K., T. A. Effects of Acyclovir and Its Metabolites on Purine Nucleoside Phosphorylase *J. Biol. Chem.* **1984**, *269*, 40664069.

(42) Ealick, E. B., Y. S.; Bugg, C. E.; Erion, M. D.; Guida, W. C.;; Montgomery, J. A. S., J. A.; . III. Application of Crystallographic and Modeling Methods in the Design of Purine Nucleoside Phosphorylase Inhibitors *Proc. Natl. Acad. Sei. U.S.A.* **1991**, *88*, 11540-11644.

(43) Horenstein, B. A.; Schramm, V. L. Electronic Nature of the Transition-State for Nucleoside Hydrolase - a Blueprint for Inhibitor Design *Biochemistry* **1993**, *32*, 7089-7097.

(44) Horenstein, B. A.; Zabinski, R. F.; Schramm, V. L. A New Class of C-Nucleoside Analogs - 1-(S)-Aryl-1,4-Dideoxy-1,4-Imino-D-Ribitols, Transition-State Analog Inhibitors of Nucleoside Hydrolase *Tetrahedron Lett.* **1993**, *34*, 7213-7216.

(45) Furneaux, R. H.; Limberg, G.; Tyler, P. C.; Schramm, V. L. Synthesis of transition state inhibitors for N-riboside hydrolases and transferases *Tetrahedron* **1997**, *53*, 2915-2930.

(46) Furneaux, R. H.; Schramm, V. L.; Tyler, P. C. Transition state analogue inhibitors of protozoan nucleoside hydrolases *Bioorganic & Medicinal Chemistry* **1999**, *7*, 2599-2606.

(47) Boutellier, M.; Ganem, B.; Horenstein, B. A.; Schramm, V. L. Design and Synthesis of D-Ribofuranoamidrazones as Inhibitors of Nucleoside Processing Enzymes *Synlett* **1995**, 510-512.

(48) Miles, R. W.; Tyler, P. C.; Furneaux, R. H.; Bagdassarian, C. K.; Schramm, V. L. One-third-the-sites transition-state inhibitors for purine nucleoside phosphorylase *Biochemistry* **1998**, *37*, 8615-8621.

(49) Evans, G. B.; Furneaux, R. H.; Gainsford, G. J.; Schramm, V. L.; Tyler, P. C. Synthesis of transition state analogue inhibitors for purine nucleoside phosphorylase and N-riboside hydrolases *Tetrahedron* **2000**, *56*, 3053-3062.

(50) Schramm, V. L. Development of transition state analogues of purine nucleoside phosphorylase as anti-T-cell agents *Biochimica Et Biophysica Acta-Molecular Basis of Disease* **2002**, *1587*, 107-117.

(51) Schramm, V. L. Enzymatic transition state poise and transition state analogues *Acc. Chem. Res.* **2003**, *36*, 588-596.

(52) Mao, C.; Cook, W. J.; Zhou, M.; Federov, A. A.; Almo, S. C.; Ealick, S. E. Calf spleen purine nucleoside phosphorylase complexed with substrates and substrate analogues *Biochemistry* **1998**, *37*, 7135-7146.

(53) Schramm, V. L.; Shi, W. X. Atomic motion in enzymatic reaction coordinates *Current Opinion in Structural Biology* **2001**, *11*, 657-665.

(54) Shi, W. X.; Li, C. M.; Tyler, P. C.; Furneaux, R. H.; Cahill, S. M.; Girvin, M. E.; Grubmeyer, C.; Schramm, V. L.; Almo, S. C. The 2.0 angstrom structure of malarial purine phosphoribosyltransferase in complex with a transition-state analogue inhibitor *Biochemistry* **1999**, *38*, 9872-9880.

(55) Shi, W. X.; Li, C. M.; Tyler, P. C.; Furneaux, R. H.; Grubmeyer, C.; Schramm, V. L.; Almo, S. C. The 2.0 angstrom structure of human hypoxanthineguanine phosphoribosyltransferase in complex with a transition-state analog inhibitor *Nature Struct. Biol.* **1999**, *6*, 588-593.

(56) Heroux, A.; White, E. L.; Ross, L. J.; Davis, R. L.; Borhani, D. W. Crystal structure of Toxoplasma gondii hypoxanthine-guanine phosphoribosyltransferase with XMP, pyrophosphate, and two Mg2+ ions bound: Insights into the catalytic mechanism *Biochemistry* **1999**, *38*, 14495-14506.

(57) Horenstein, B. A.; Parkin, D. W.; Estupinan, B.; Schramm, V. L. Transition-State Analysis of Nucleoside Hydrolase from Crithidia-Fasciculata *Biochemistry* **1991**, *30*, 10788-10795.

(58) Degano, M.; Almo, S. C.; Sacchettini, J. C.; Schramm, V. L. Trypanosomal nucleoside hydrolase. A novel mechanism from the structure with a transition-state inhibitor *Biochemistry* **1998**, *37*, 6277-6285.

(59) Miles, R. W.; Tyler, P. C.; Evans, G. B.; Furneaux, R. H.; Parkin, D. W.; Schramm, V. L. Iminoribitol transition state analogue inhibitors of protozoan nucleoside hydrolases *Biochemistry* **1999**, *38*, 13147-13154.

(60) Li, C. M.; Tyler, P. C.; Furneaux, R. H.; Kicska, G.; Xu, Y. M.; Grubmeyer, C.; Girvin, M. E.; Schramm, V. L. Transition-state analogs as inhibitors of human and malarial hypoxanthine-guanine phosphoribosyltransferases *Nature Struct. Biol.* **1999**, *6*, 582-587.

(61) Dewolf, W. E.; Fullin, F. A.; Schramm, V. L. Catalytic Site of Amp Nucleosidase - Substrate-Specificity and Ph Effects with Amp and Formycin 5'-Po4 *J. Biol. Chem.* **1979**, *254*, 868-875.

(62) Leung, H. B.; Schramm, V. L. Adenylate Degradation in Escherichia-Coli - the Role of Amp Nucleosidase and Properties of the Purified Enzyme *J. Biol. Chem.* **1980**, *255*, 867-874.

(63) Evans, G. B.; Furneaux, R. H.; Gainsford, G. J.; Hanson, J. C.; Kicska, G. A.; Sauve, A. A.; Schramm, V. L.; Tyler, P. C. 8-aza-immucillins as transition-state analogue inhibitors of purine nucleoside phosphorylase and nucleoside hydrolases *J. Med. Chem.* **2003**, *46*, 155-160.

(64) Evans, G. B.; Furneaux, R. H.; Lewandowicz, A.; Schramm, V. L.; Tyler, P. C. Exploring structure-activity relationships of transition state analogues of human purine nucleoside phosphorylase *J. Med. Chem.* **2003**, *46*, 3412-3423.

(65) Kicska, G. A.; Tyler, P. C.; Evans, G. B.; Furneaux, R. H.; Kim, K.; Schramm, V. L. Transition state analogue inhibitors of purine nucleoside phosphorylase from Plasmodium falciparum *J. Biol. Chem.* **2002**, *277*, 3219-3225.

(66) Lewandowicz, A.; Tyler, P. C.; Evans, G. B.; Furneaux, R. H.; Schramm, V. L. Achieving the ultimate physiological goal in transition state analogue inhibitors for purine nucleoside phosphorylase *J. Biol. Chem.* **2003**, *278*, 31465-31468.

(67) Evans, G. B.; Furneaux, R. H.; Lewandowicz, A.; Schramm, V. L.; Tyler, P. C. Synthesis of second-generation transition state analogues of human purine nucleoside phosphorylase *J. Med. Chem.* **2003**, *46*, 5271-5276.

(68) Evans, G. B.; Furneaux, R. H.; Tyler, P. C.; Schramm, V. L. Synthesis of a transition state analogue inhibitor of purine nucleoside phosphorylase via the Mannich reaction *Org. Lett.* **2003**, *5*, 3639-3640.

Chapter 3

Trihydroxy-2-Thiaquinolizidine Derivatives as a New Class of Bicyclic Glycosidase Inhibitors

ABSTRACT

Trihydroxy-2-thiaquinolizidines, a new class of bicyclic dideoxy-iminohexitol glycosidase inhibitor derivatives with nominally the D-*gluco*, L-*ido*, D-*manno* and L-*gulo* configurations were synthesized. X-ray analyses indicated that the preferred conformation for D-*gluco* and D-*manno* derivatives was a flat *trans*- fused system. Unlike deoxynojirimycin, compound with D-*gluco* configuration was selective for α-glucosidases (yeast and rice) and showed no inhibitory activity towards β-glucosidase (almond), α-galactosidase (green coffee beans), α-galactosidase (*E-coli*) and α-mannosidase (jack bean), while L-*ido* derivative was specific for β-glucosidase (almond). Possible reasons for the specificity will be discussed.

3.1. Introduction

Glycosidase inhibitors such as deoxynojirimycin **1** and castanospermine **2**, generally known as iminoalditols or azasugars and their derivatives have great promise for numerous medical applications[1-3] ranging from diabetes[4-6] and other metabolic disorders through antimicrobials[7-9], cancer[10], autoimmune diseases[11-14], and neurological disorders[15]. Despite this, they have not realized their full clinical potential. This is largely because of a lack of commercially viable syntheses and difficulty in preparing a comprehensive palette of variant structures. Many of the possible drug candidates are available in only small exploratory amounts.

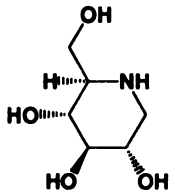

1
deoxynojirimycin

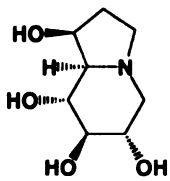

2
castanospermine

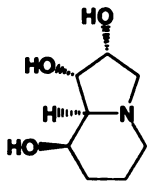

3
Swainsonine

Azasugars are carbohydrate pyranose or furanose analogs in which the ring oxygen atom is replaced with a nitrogen atom. This presents a significant synthetic challenge to organic chemists. Bicyclic systems such as castanospermine **(2)** and swainsonine **(3)** are especially interesting because of their potency as glycosidase inhibitors. Their structural rigidity and the added interaction of the second ring might be contributing factors to this. This second ring increases the difficulty of the synthesis. A number of chemical and enzymatic syntheses of azasugars have been reported in recent years[16-31]. Several strategies have been used to introduce a basic nitrogen atom in the ring of

deoxynojirimycin and its derivatives. These strategies include chemo-enzymatic method, aminomercuration, double-reductive amination, N-alkylation, reductive double-alkylation and triple reductive amination. Some representative methods are described below:

3.1.1. Chemo-enzymatic Synthesis

The chemo-enzymatic approach has been extensively developed by C.-H. Wong[22-25]. It is generally a two-step process involving an enzymatic aldol condensation and a catalytic intramolecular reductive amination. The asymmetric synthesis of **1** and **8** is shown in **figure 3.1**. However, this method of synthesis involving enzymes is not a general method and it is limited by scale-up problems.

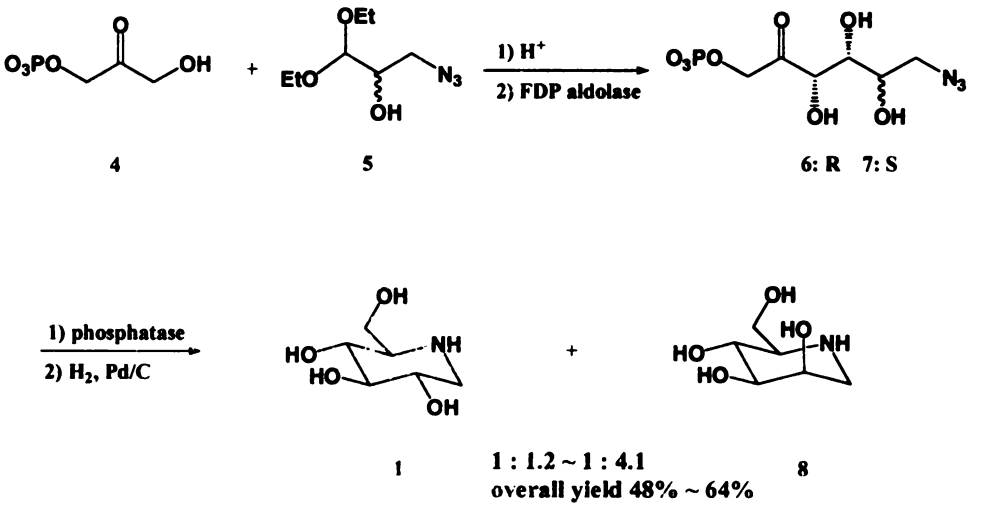

Figure 3.1. Chemo-enzymatic synthesis of **1** and **8**

3.1.2. Aminomercuration[26]

The intramolecular aminomercuration is illustrated in **figure 3.2** for the case of D-glucose. A one-pot, reductive ring opening and reductive amination afforded an aminoalkene. When this key intermediate was reacted with mercuric trifluoroacetate in anhydrous THF, a 3:2 mixture of bromomercurials **11** and **12** was isolated. The major cyclization product **11** could be transformed to 1-deoxynojirimycin **1** by reductive oxygenation ($NaBH_4$-DMF-O_2) and hydrogenolytic deprotection. In this synthesis, only one of the bromomercurials (**11**) can give the desired product, which results in a low yield of deoxynojirimycin **1**. The mercury toxicity is also a problem.

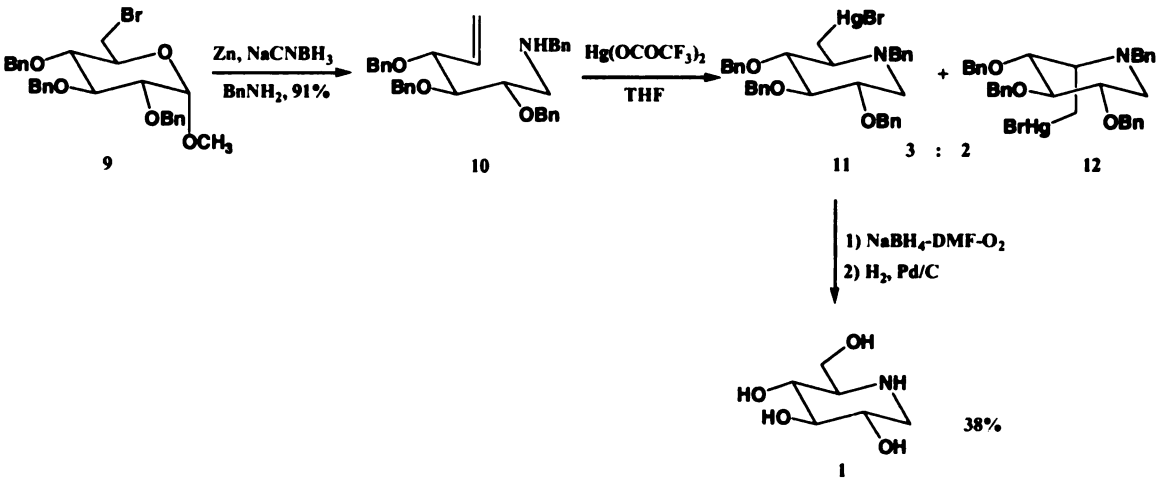

Figure 3.2. Aminomercuration

3.1.3. Double Reductive Amination[27,28]

The double reductive amination of dicarbonyl sugars with primary amines and sodium cyanoborohydride in methanol allowed for the syntheses of 1-deoxynojirimycin, 1-deoxymannojirimycin and N-alkylated derivatives (**figure 3.3**).

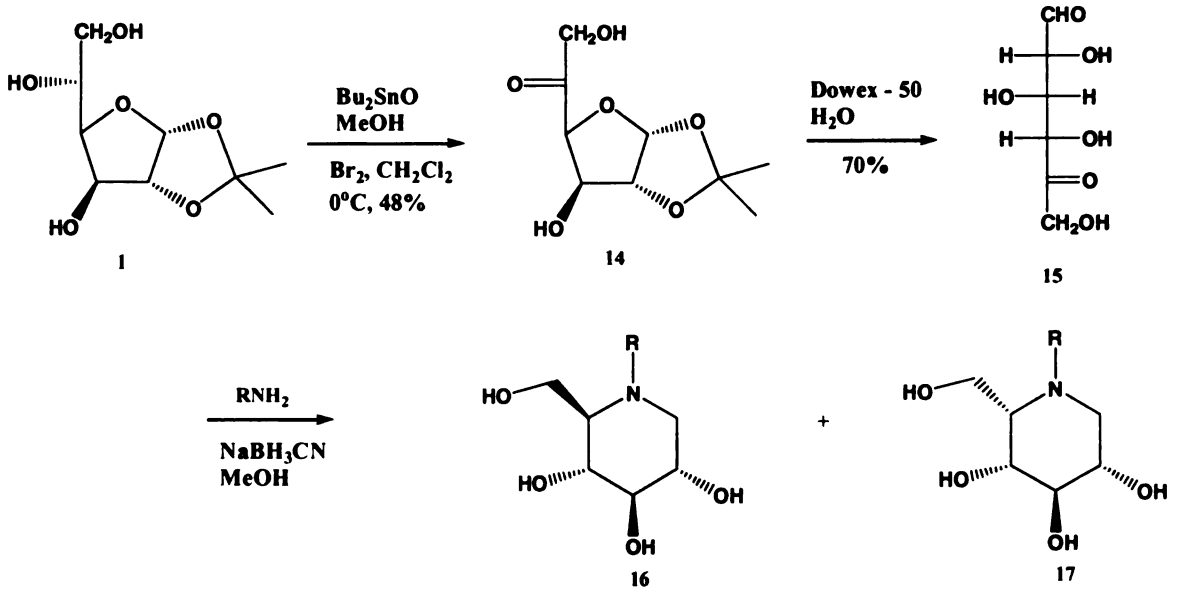

RNH_2	yield	ratio	
Ph_2CHNH_2	70%	95	5
$Ph_2CHCH_2NH_2$	73%	95	5
$C_4H_9NH_2$	55%	95	5
$C_{12}H_{25}NH_2$	27%	95	5

Figure 3.3. Double reductive amination

3.1.4. Intramolecular N-Alkylation[30]

In this approach, the cyclization to furnish the ring nitrogen was achieved by a direct intramolecular N-alkylation of a primary amino group by mesyl displacement in a partially protected hexitol prepared in several steps from diethyl tartrate. This approach for the synthesis of **1** in enantiomerically pure form is illustrated in **figure 3.4.**

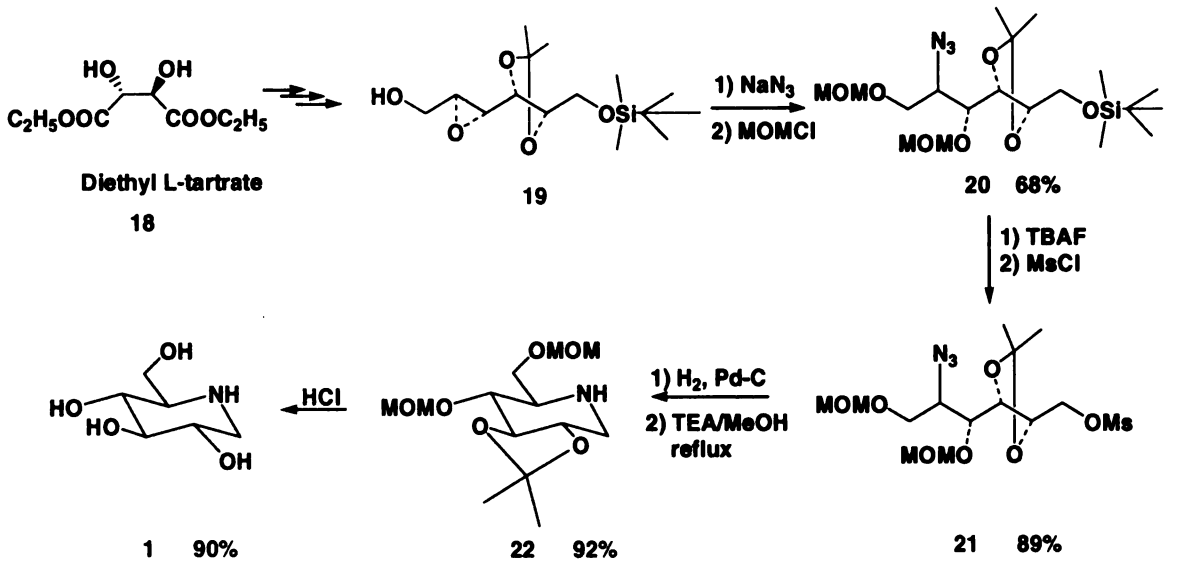

Figure 3.4. N-Intramolecular alkylation

3.1.5. Reductive Double-alkylation[31]

A reductive double-cyclization has been employed in the synthesis of analogs of the mannosidase inhibitor swainsonine (**3**). The synthesis of the ring-expanded derivatives (**30, 31**) of swainsonine started from D-arabinose. Protection of hydroxyl groups, Wittig reaction and Mitsunobu reaction afforded the azide **26**. Epoxidation with mCPBA yielded two diastereomeric epoxides. The epoxide group and a chlorinated carbon were the two nucleophilic centers involved. Upon reduction, primary amines were generated, which were cyclized to give quinolizidines **30** and **31** (**figure 3.5**). This synthesis yields the bicyclic azasugars, however, the diastereoselectivity is not high and it still suffers from the drawback that separation of the diastereoisomers has to be performed (**28** and **29**).

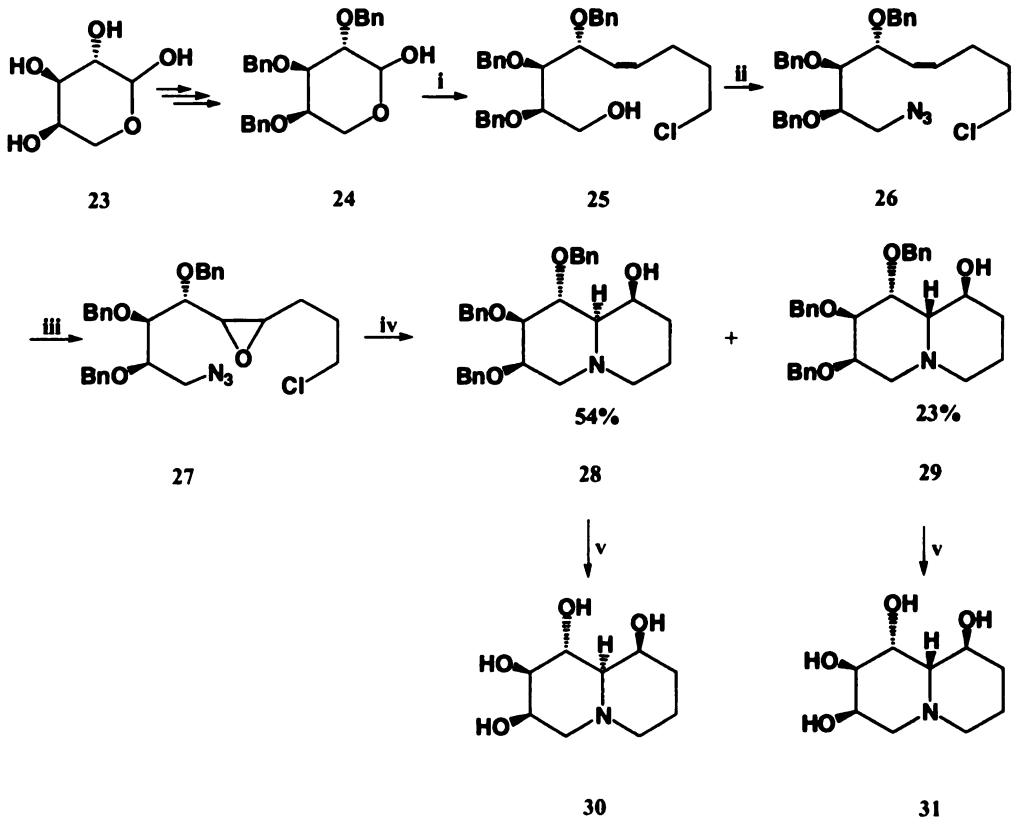

Figure 3.5. Reductive double-alkylation. i, $BrPh_3P(CH_2)_4Cl$, $KN(TMS)_2$, 71%; ii, HN_3, PPh_3, DEAD, 84%; iii, mCPBA, 88%; iv, a, H_2, Pd/C, EtOH; b, K_2CO_3, EtOH, reflux; c, separate diasteromers; v, H_2 (45psl), Pd/C, HCl, MeOH, 99%.

3.1.6. Triple Reductive Amination (TRA)[29]

A triple reductive amination involving three carbonyl groups and an amine was used for the synthesis of the bicyclic aza sugars castanospermine **2** (**figure 3.6**) and swainsonine **3**. It was suggested that initial amination occurred at one of the carbonyl groups, and the resulting carbinolamine underwent sequential intramolecular reactions with the remaining carbonyl groups at a faster rate than competing intermolecular processes. The TRA approach is efficient for the synthesis of compounds with bicyclic indolizidine

framework, but the preparation of the precursor with aldehyde and ketone functionalities is not an easy exercise.

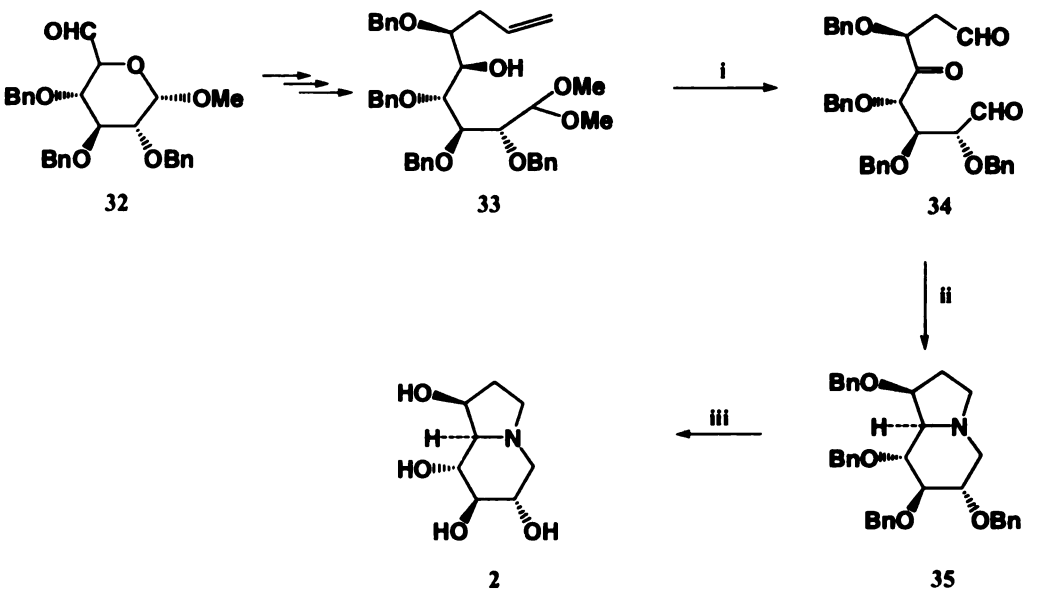

Figure 3.6. Triple reductive amination i, (a) Swern oxidation; (b) O_3, CH_2Cl_2, -78°C then Ph_3P; (c) THF-9M HCl 74% for 3 steps; ii, NH_4HCO_2, $NaCNBH_3$, MeOH, 78%; iii, 10% Pd-C, MeOH-HCOOH, 80%.

3.2. Results and Discussions

3.2.1. Synthesis of Trihydroxy-2-thiaquinolizidine Derivatives

We explored the possibility of synthesizing bicyclic analogs of iminohexitols such as deoxynojirimycin and related compounds in which O-6 were replaced by a sulfur atom. We also envisaged bridging the 6-position to the ring nitrogen with a two-carbon fragment to form a trihydroxy-2-thiaquinolizidine ring system thus increasing rigidity and increasing lipophilicity. Such systems have never been reported before but hold great promise because the formation of a carbon-carbon bond is circumvented as in **2, 3** and **30**. The presence of sulfur (closely related to oxygen) at a position that is normally

oxygenated is also a decided advantage. If such systems could be reached using a general strategy, analogs with differing configurations at the various carbon centers and differing substitution patterns could be made, increasing the chance of obtaining compounds with useful therapeutic potential. A total of four such systems (**36a, 36b, 51a,** and **51b**) were prepared corresponding to the D-*gluco*, L-*ido*, D-*manno*, L-*gulo* configurations.

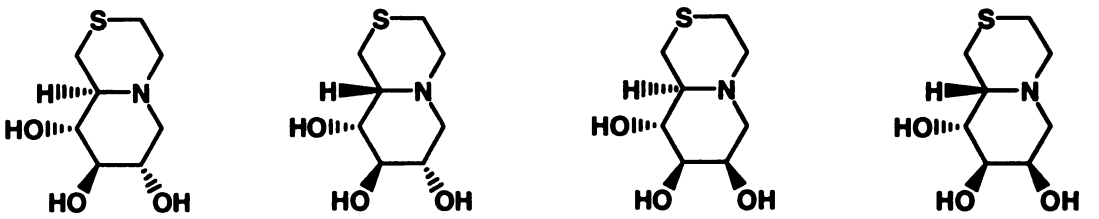

36a **36b** **51a** **51b**

Figure 3.7 shows the synthesis for the "D-*gluco*" and "L-*ido*" compounds. It starts from the β-methyl-D-glucopyranoside. Triphenylphosphine and carbon tetrabromide selectively converted the primary hydroxyl group to a bromo group. The hydroxyl groups at C(2), C(3), C(4) positions were protected by acylation using pivaloyl chloride (trimethylacetyl chloride). The selection of protecting group was based on the tolerance of the chromium oxidation and the subsequent reactions. Normal protecting groups such as acetals, being attacked, methyl ether and benzyl ethers are unsuitable under this condition. Methyl and benzyl ethers have been reported to be attacked by chromium trioxide in acetic acid[32]. Ester groups are stable as the protecting group. Pivaloyl groups were selected over acetyl groups because of the partial deacylation of acetates by aminoethanethiol, resulting in difficulty in purification and low yield. Oxidation of the

peracylated 6-bromo-6-deoxy-glycoside **39** with chromium trioxide in acetic acid afforded a 5-ulosonic acid ester **40**. The oxidation of acetylated β-glycopyranosides by chromium trioxide has been reported by S. J. Angyal and K. James[33] to afford 5-keto esters, independent of the configurations on C2, C3, or C4. The oxidation is specific to β-glycopyranosides, while α-glycopyranosides are not attacked. Treatment of **40** with 2-aminoethanethiol yielded the aminal **41** directly which underwent reduction by $NaBCNH_3$ and cyclization to the desired lactam **42a** and the L-*ido* isomer **42b**. The recyclization to form lactams occurred spontaneously over one day. On adding sodium carbonate, the rate was accelerated of lactam formation. There was some variability in the actual amount formed ranging from traces to 2.5:1 in favor of the D-*gluco* analog. Reduction of the lactams with borane yielded clean amine products, with protecting groups intact. The crude product underwent deacylation by methoxide to afford the *D-gluco* and *L-ido* compounds.

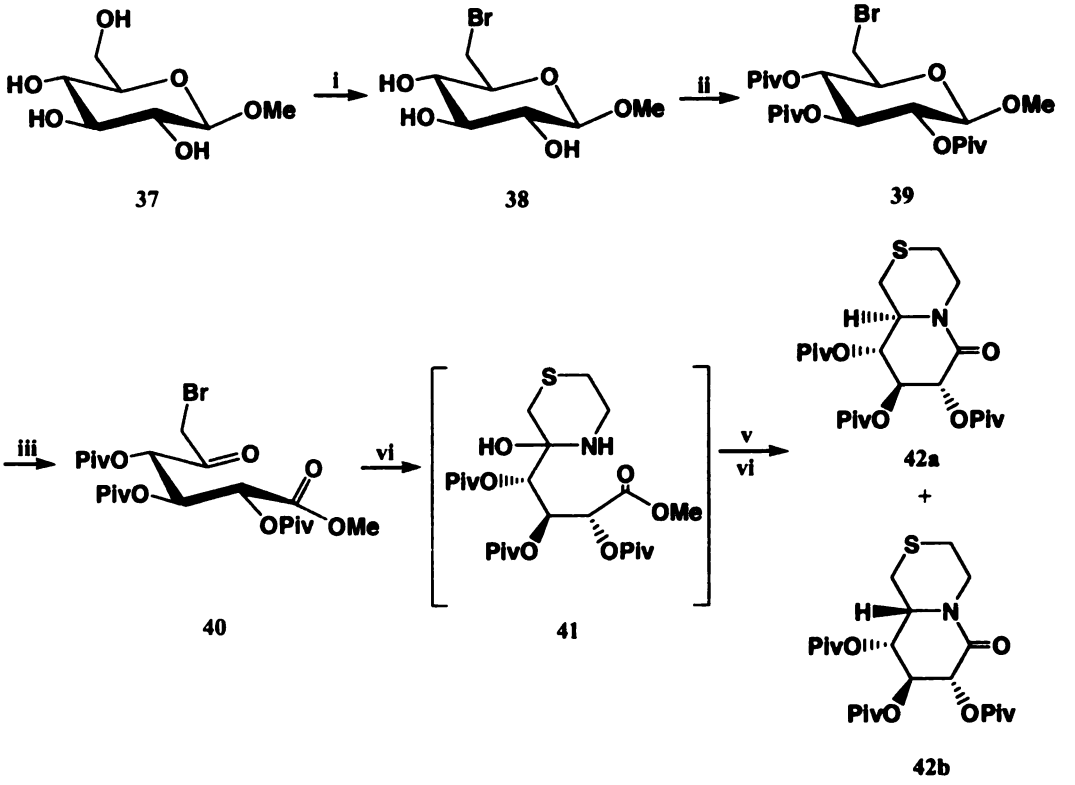
OH
HO
HO
O
OMe
OH
37
i
Br
HO
HO
O
OMe
OH
38
ii
Br
PivO
PivO
O
OMe
OPiv
39
iii
Br
PivO
PivO
O
O
OPiv
OMe
40
vi
S
HO
NH
PivO
O
OMe
PivO
OPiv
41
v
vi
S
H
N
PivO
O
PivO
OPiv
42a
+
S
H
N
PivO
O
PivO
OPiv
42b

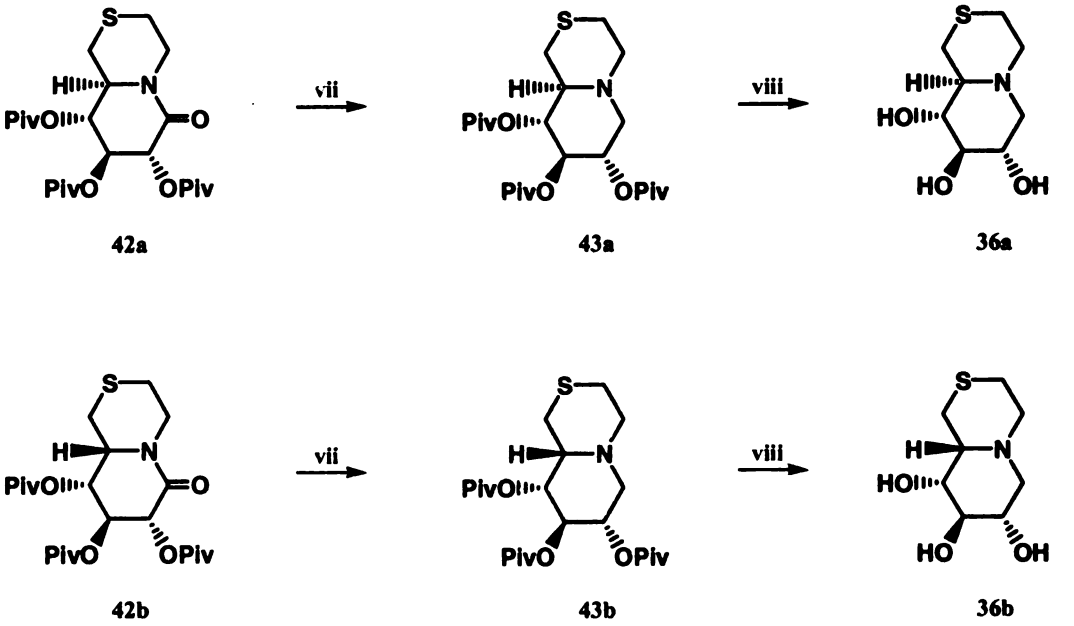
S
H
N
PivO
O
PivO
OPiv
42a
vii
S
H
N
PivO
PivO
OPiv
43a
viii
S
H
N
HO
HO
OH
36a
S
H
N
PivO
O
PivO
OPiv
42b
vii
S
H
N
PivO
PivO
OPiv
43b
viii
S
H
N
HO
HO
OH
36b

Figure 3.7. Synthesis of products with D-*gluco* and L-*ido* configurations. i. Ph_3P, CBr_4, pyridine, 85%; ii. PivCl, pyridine, 84%; iii. CrO_3, Ac_2O, HOAc, 97%; iv. $HS(CH_2)_2NH_2$, CH_3OH; v. $NaCNBH_3$, CH_3OH; vi. Na_2CO_3, $CHCl_3$, 74% for 3 steps; vii. BH_3-THF; viii. $NaOCH_3$, CH_3OH, 71% for **36a** and 75% for **36b** for 2 steps.

Products with the *D-manno* and *L-gulo* configurations (**51a** and **51b**) were also obtained in the same fashion starting from β-methyl-D-mannoside (**figure 3.8**). The *D-manno* lactam **49a** and *L-gulo* lactam **49b** was obtained in 4:1 ratio in favor of the *D-manno* lactam. Reduction of lactams and deprotection yielded products **51a** and **51b** in good yields. Besides the bromo function, the leaving group at the C(6) position can also be mesyl and other groups that are stable under chromiun oxidation conditions. Therefore, this synthetic strategy is a powerful method to synthesize bicyclic azasugars with different configurations starting from methyl β-D-glycopyranosides. The ease of synthesis can lead to the generation of a large family of bicyclic azasugars, with possibilities of identifying active compounds against glycosidases.

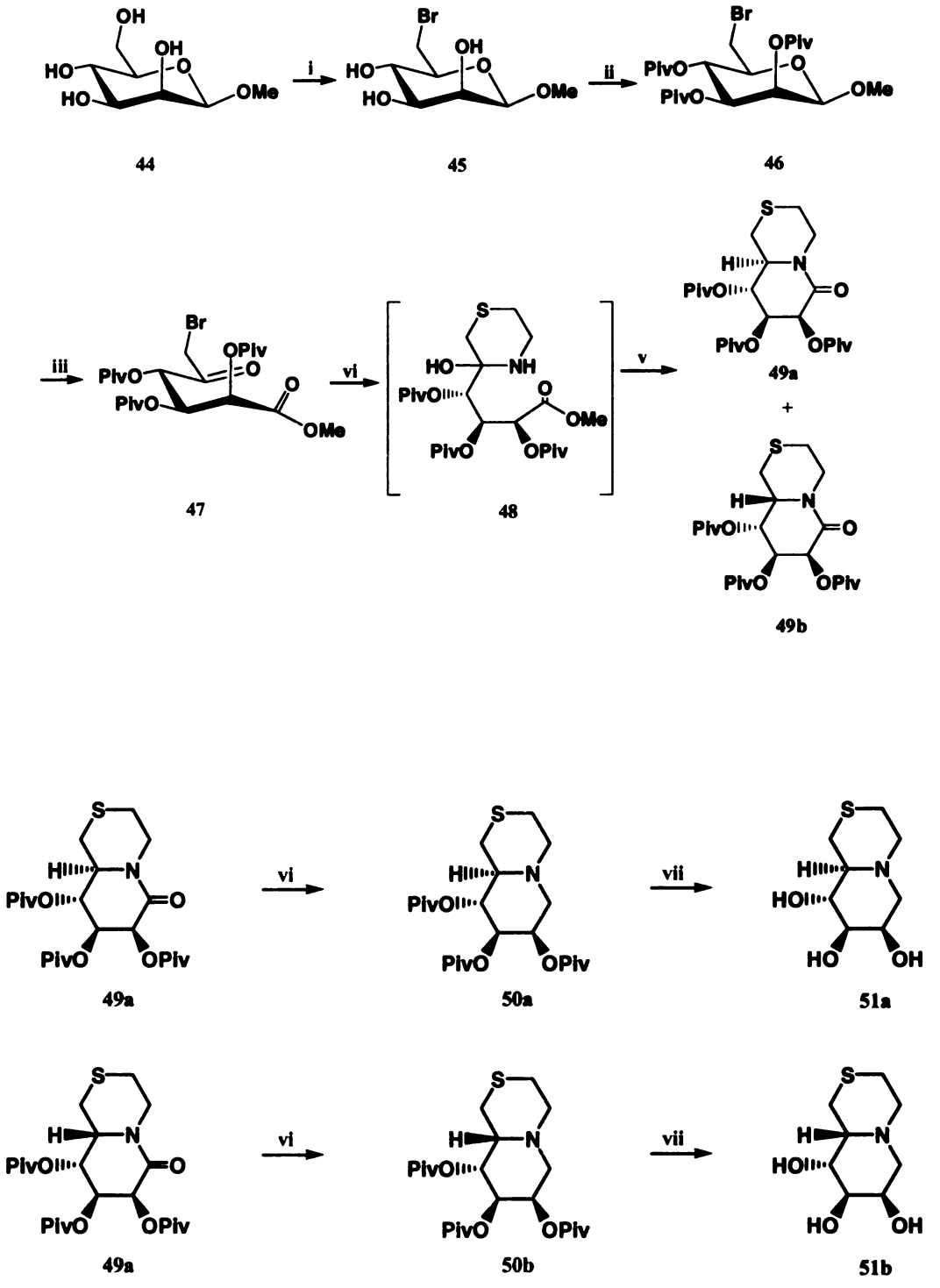

Figure 3.8. Synthesis of products with the *D-manno* and *L-gulo* configurations. i. Ph_3P, CBr_4, pyridine, 84%; ii. PivCl, pyridine, 80%; iii. CrO_3, Ac_2O, HOAc, 91%; iv. $HS(CH_2)_2NH_2$, CH_3OH; v. $NaCNBH_3$, CH_3OH, 81% for 2 steps; vi. BH_3-THF; vii. $NaOCH_3$, CH_3OH, 73% for **51a** and 71% for **51b** for 2 steps.

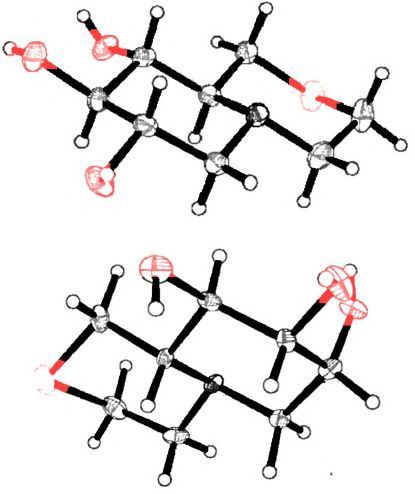

Figure 3.9. X-ray structure of 7(*S*),8(*R*),9(*R*),10(S)-trihydroxy-2-thiaquinolizidine **36a** and 7(*R*),8(*R*),9(*R*),10(S)-trihydroxy-2-thiaquinolizidine **51a** showing the trans-type ring junction and overall flat geometry.

Products **36a** and **51a** were recrystalized in water to give colorless crystals. X-ray crystallography analysis (**figure 3.9**) indicated two six-membered rings with relaxed chair conformation for both D-*gluco* and D-*manno* products. A *trans*-diequatorial type fusion between the rings gives the molecules an overall flat geometry. The expected intermediate oxocarbenium species is very flat because of the double bond character between the ring oxygen and C-1 (**Figure 3.10**).

Figure 3.10. Structure of oxycarbenium intermediate in the hydrolysis of glucosides from an *ab initio* calculation showing equipotential contours.

The sulfur atom at 6-position can be derivatized easily to give the corresponding sulfone or sulfoxide. From lactam **42a**, mCPBA oxidation afforded the clean product **52** and after reduction of the lactam and deprotection, the sulfone can be obtained in 84% yield from the lactam **42a** without purification of the intermediates (**figure 3.11**).

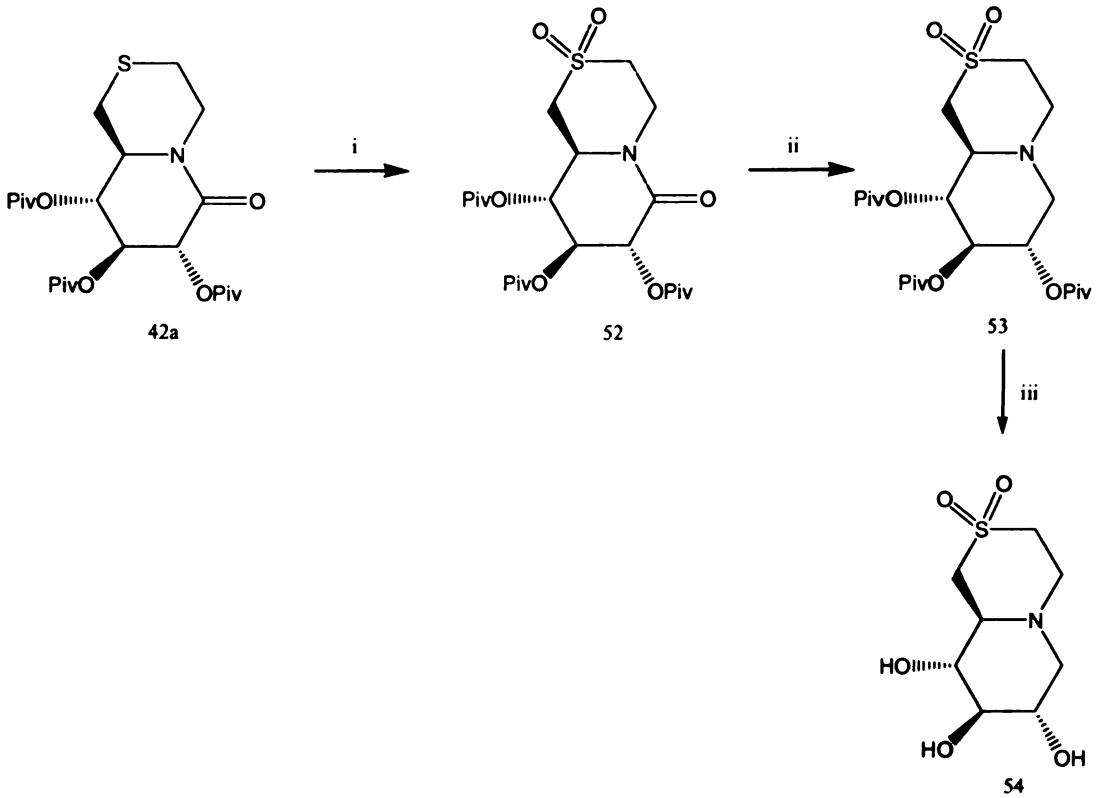

Figure 3.11. Synthesis of 2,2-dioxy-7(*S*),8(*R*),9(*R*),10(*S*)-trihydroxy-2-thiaquinolizidin-2-one. i, mCPBA, CH_2Cl_2; ii, BH_3, THF; iii, NaOMe, MeOH, 84% yield overall.

3.2.2. Inhibitory Activities of Trihydroxy-2-thiaquinolizidine Derivatives against Glycosidases

The inhibitory activity is evaluated by the dissociation constant K_i of the inhibitor. The enzyme inhibition is described by the Michaelis – Menten rate law. The scheme that corresponds to competitive inhibition is **figure 3.12**[34].

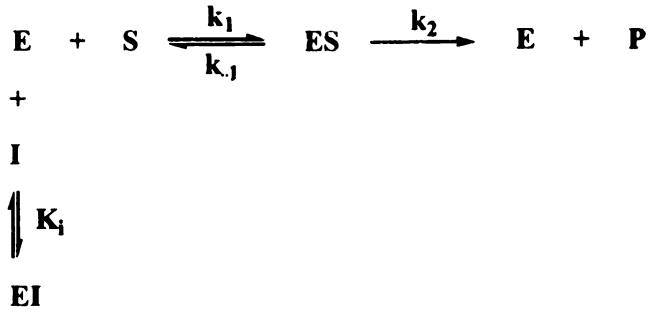

Figure 3.12. Enzyme inhibition scheme.

The dissociation constant for the inhibitor is

$$K_i = \frac{[E]\,[I]}{[EI]} \qquad \textbf{eq. 1}$$

By steady-state assumption, the resulting Michaelis-Menten equation is

$$V = \frac{V_{max}\,[S]}{K_M\left(1 + \frac{[I]}{K_i}\right) + [S]} \qquad \text{where } K_M = \frac{k_{-1} + k_2}{k_1} \qquad \textbf{eq. 2}$$

A lineweaver – Burk plot can be used to determine the inhibition constant K_i. Taking the reciprocal of equation 2, we obtain

$$\frac{1}{V} = \frac{K_M}{V_{max}}\left(1 + \frac{[I]}{K_i}\right)\frac{1}{[S]} + \frac{1}{V_{max}} \qquad \textbf{eq. 3}$$

The slope of the line will be

$$\text{Slope} = \frac{K_M}{V_{max}}\left(1 + \frac{[I]}{K_i}\right) \qquad \textbf{eq. 4}$$

Thus, K_i can be determined by plotting the slope values vs. [I]. The resulting secondary plot will have Y-axis intercept of K_M/V_{max} and a slope of $K_M/V_{max}\,K_i$. The value of K_i is the intercept /slope of this plot.

Enzymes were assayed according to standard procedures[35] by following the hydrolysis of nitrophenyl glycosides spectrophotometrically except α-glucosidase (rice). A series of enzyme assays using α-glucosidase (yeast), α-glucosidase (rice), β-glucosidase (almond), α-galactosidase (green coffee beans), β-galactosidase (*E. Coli*), α-mannosidase (jack beans) were carried out to study the inhibitory activities of compound **36a, 36b, 51a, 51b** and **54**. The corresponding p-nitrophenyl glycopyranosides were used as substrates for α-glucosidase (yeast), β-glucosidase, α-galactosidase, β-galactosidase, α-mannosidase. Each assay was performed in a phosphate or an acetate buffer at the optimal pH for each enzyme. Inhibition studies were performed by adding the inhibitor to a final concentration of 0.05 mM to 11mM to the respective buffer solutions along with enzyme. The solutions were incubated at 37°C before adding substrates to the reactions. The release of product, p-nitrophenyl alcohol was monitored at 400nm. For α-glucosidase (rice), maltose was used as the substrate, and the assay was based on the glucose oxidase/peroxidase enzyme procedure (**figure 3.13**). The glucose released from maltose can be oxidized by glucose oxidase to generate D-gluconic acid and hydrogen peroxide. Under the catalysis of peroxidase, hydrogen peroxide will react with dianisidine to give the oxidized form with brown color. The absorbance of the solution was determined at 500 nm for oxidized o-dianisidine.

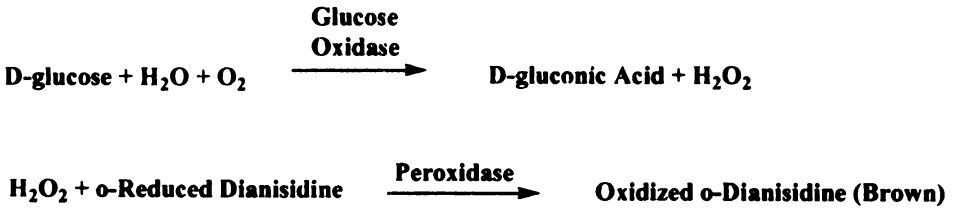

Figure 3.13. glucose oxidase/peroxidase enzyme mechanism

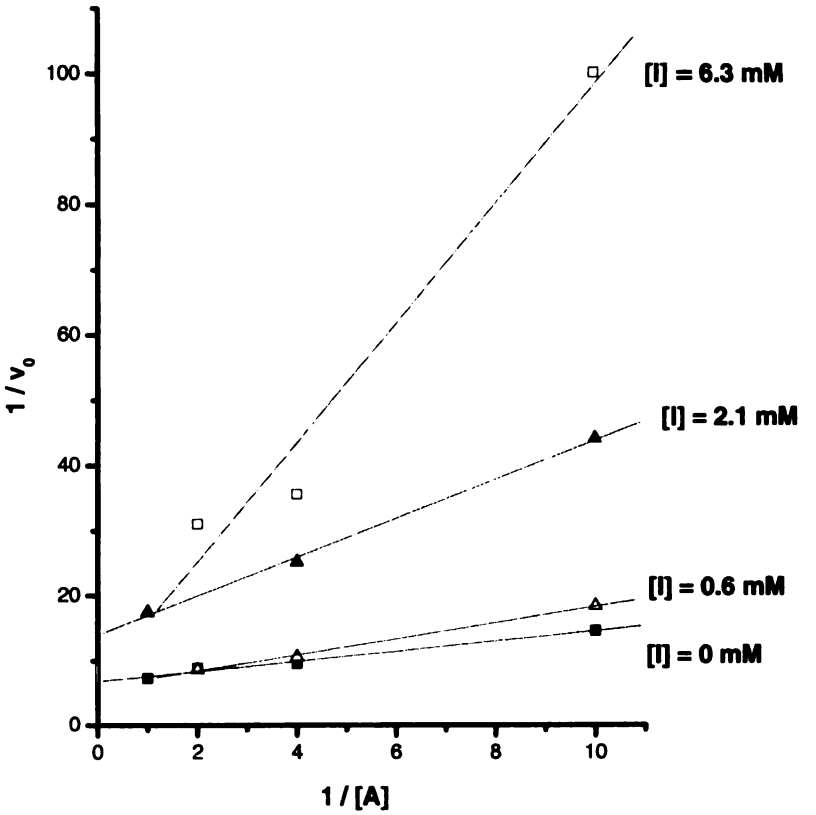

Figure 3.14. Lineweaver-Burk plot for the determination of inhibition constant for **36a**

Figure 3.14 is the double reciprocal plot of initial rates and substrate concentrations ($1/v_o$ *vs* 1/[A]) for inhibitor concentrations of 0 mM, 0.6 mM, 2.1 mM, and 6.3mM for 7(S),8(R),9(R),10(*S*)-trihydroxy-2-thiaquinolizidine (**36a**) using yeast α-glucosidase and *p*-nitrophenylglucoside as substrate. **Figure 3.15** is the plot of slope from **figure 3.14** vs inhibitor concentration [I] (mM).

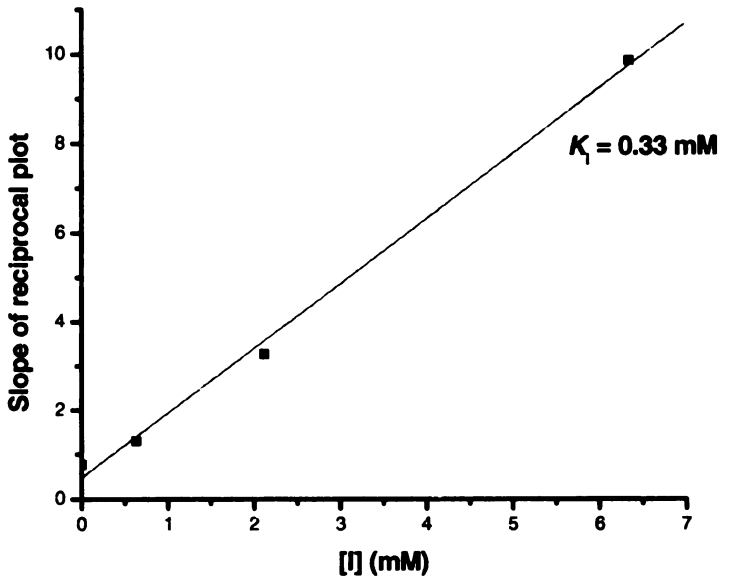

Figure 3.15. Slope from **figure 3.14** vs inhibitor concentration

So the K_i value for α-glucosidase (yeast) is

$$K_i = \text{intercept} / \text{slope} = 0.485 / 1.46 = 0.33 \text{ mM}$$

Figure 3.16 and **3.17** are similar plot for **36a** where the enzyme is rice α-glucosidase and the rate is monitored by a coupled enzyme reaction in which freed glucose from maltose is oxidized to gluconic acid by glucose oxidase. The concentrations of compound **36a** are 0, 0.42 and 8.87 mM, and the inhibition constant is 0.9 mM.

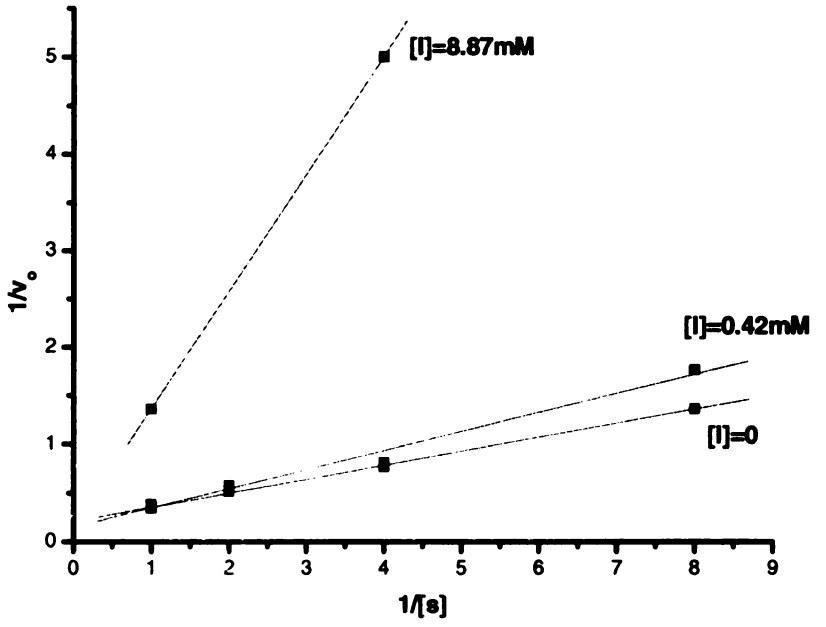

Figure 3.16. Lineweaver-Burk plot for the determination of inhibition constant for **36a**

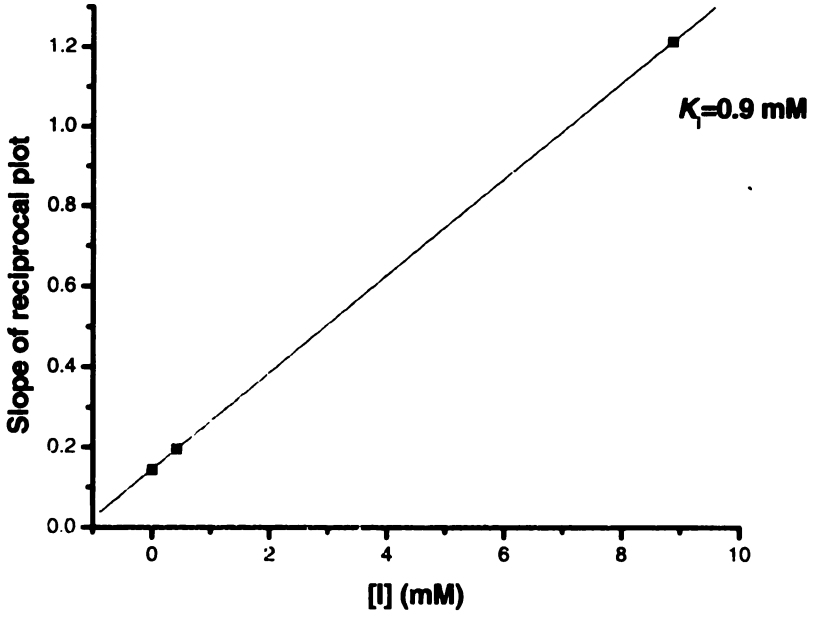

Figure 3.17. slope from **figure 3.15** vs inhibitor concentration

For β-glucosidase, α-galactosidase, β-galactosidase, α-mannosidase, no significant inhibition was observed for **36a** at this inhibitor concentration range. Compound **36b** was tested against α-glucosidase (yeast), β-glucosidase and α-mannosidase. It showed opposite inhibition pattern to compound **36a.** It only inhibits β-glucosidase with K_i value 1 mM without inhibiting α-glucosidase and α-mannosidase. **Figure 3.18** is the double reciprocal plot of initial rates and substrate concentrations using yeast α-glucosidase and *p*-nitrophenylglucoside as substrate.

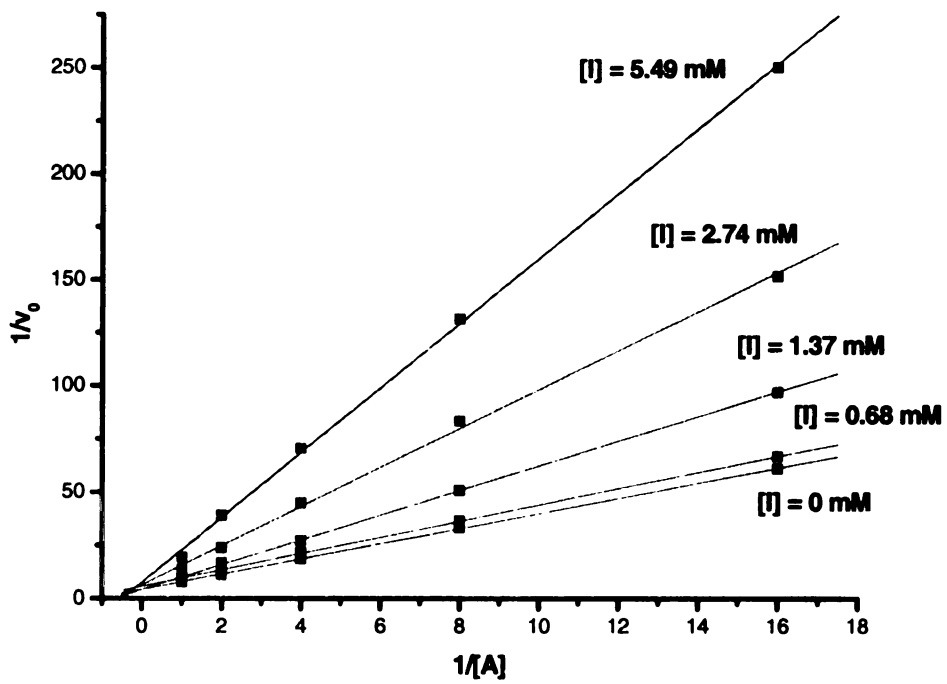

Figure 3.18. Lineweaver-Burk plot for the determination of inhibition constant for **36b**

Compound **51a** and **51b** were also tested for α-mannosidase (jack beans) and no inhibition was observed. Compound **54** was tested against α-glucosidase (yeast) and some inhibition was observed with K_i value 1.32 mM (**Figure 3.19**).

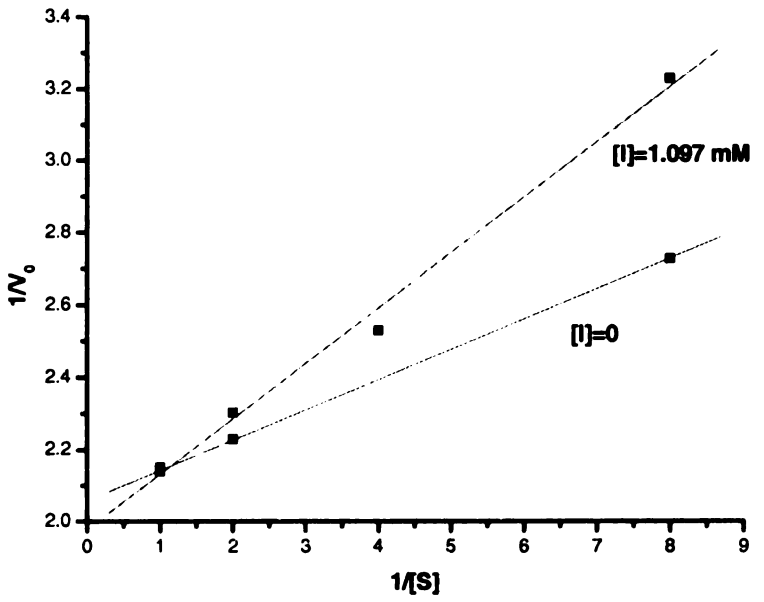

Figure 3.19. Lineweaver-Burk plot for the determination of inhibition constant for **54**

Table 3.1 is the inhibition constants (mM) for compounds **36a, 36b, 51a, 51b** and **54.** The results indicate that compound **36a** is a specific inhibitor of α-glucosidase. This is consistent with the study that deoxynojirimycin type inhibitors with nitrogen atom at the ring oxygen position are more selective for α-glucosidase[26,36-38]. According to the stereoelectronic requirements, in α-glycosidases, the positively charged leaving group and the lone pair of the ring oxygen are positioned antiperiplanar and cooperatively facilitate the glycosidic bond cleavage. Thus, oxocarbonium ion **56** can be formed directly, with the positive charge development at the endocyclic oxygen (**figure 3.20**). Under the assumption that deoxynojirimycin type inhibitors including compound **36a** were protonated in the active site, those results suggest that an oxacarbonium ion **56** is important for enzymes catalyzing axial glycoside cleavage (α-glucosidase). For β-glycosidases, the glycosidic bond cleavage cannot receive aid form the lone pair of the

ring oxygen, so the ring could flip to a boat (**58**) or other conformations (**59**) to facilitate the bond cleavage. Substrate distortion is generally the case for β-glycosidases. Compound **36a** with its rigid bicyclic structure, is locked in its *trans*-fused chair conformation, so it cannot flip or change to other conformations. Therefore, it showed no inhibition against β-glucosidase. In contrast, compound **36b** showed specific inhibition against β-glucosidase while no inhibition for α-glucosidase. This is probably because of the change of the conformation caused by the inverted stereochemistry of the second ring. With the axial position of the second ring, conformation **61** is not stable for compound **36b**. This whole molecule may flip to conformation **62** with the second ring in equatorial position while the hydroxyl groups in axial position. This is the kind of conformation which puts the β-glycosidic bond in axial position to facilitate the cleavage by stereoelectronic control.

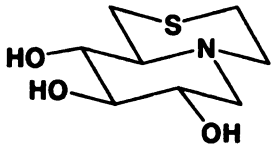

36a

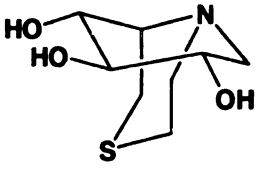

61

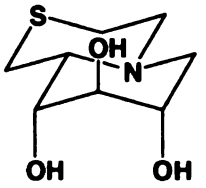

62

Table 3.1. Inhibition constants (mM) for compounds **36a, 36b, 51a, 51b** and **54**

enzymes	**36a**	**36b**	**51a**	**51b**	**54**
α-glucosidase (yeast)	0.33	ni	nd	nd	1.32
α-glucosidase (rice)	0.9	nd	nd	nd	nd

β-glucosidase (almond)	ni	1.0	nd	nd	ni
α-galactosidase	ni	nd	nd	nd	nd
(green coffee beans)					
β-galactosidase (*E. Coli*)	ni	nd	nd	nd	nd
α-mannosidase (jack beans)	ni	nd	ni	ni	nd

ni, no inhibition observed in this concentration range
nd, not determined

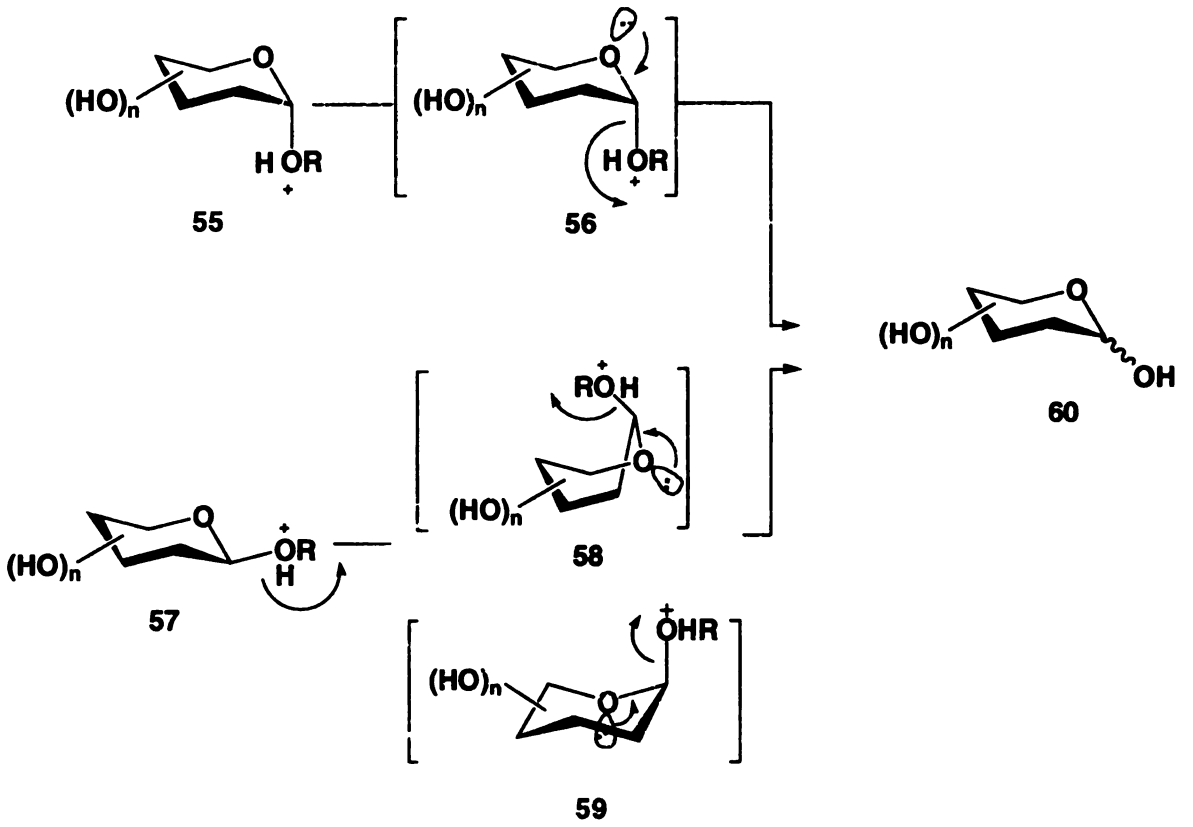

Figure 3.20. Stereoelectronic requirements for cleavage of α- and β-glycosidases.

The activities and specificities of the known aza-bicyclic systems and key monocyclic systems are shown in **table 3.2**. Compared to deoxynojirimycin, compound **36a** is a

relatively weak inhibitor, but it showed specificity for α-glucosidase. No inhibitory activity towards β-glucosidase (almond), α-galactosidase (green coffee beans), α-galactosidase (*E-coli*) and α-mannosidase (jack bean) was observed. Compared to 6-deoxy derivatives **63** and **64**, compound **36a** showed superior activity against α-glucosidase. One of the major problems with the use of iminosugars and their derivatives as inhibitors is the lack of specificity. Hence compound **1** in **table 3.2** has low K_i values but shows poor specificity. Compound **36a** showed very specific activity against α-glucosidase, and **36b** showed specificity against β-glucosidase. The specificity comes from the structural rigidity, which prevents **36a** from distortion to boat or other conformations that are important for β-glucosidase. Compound **36b** could flip to other conformations to put the second ring in equatorial position and favor β-glucosidase binding. Compound **51a** showed no activity against α-mannosidase (jack beans). This is probably because of the rigid structure and the second 6-member ring, which interfere the hydrogen bonding between 2-hydroxyl group and the enzyme.

Castanospermine is one of the most active bicyclic systems. It showed poor activity against yeast α-glucosidase but strongly inhibited the rice enzyme. However, it showed non-selectivity by inhibiting almond β-glucosidase. It has relatively flexible structure compared to **36a** and **36b,** and it presented a twisted boat conformation of the 6-member ring when bounded to Exo-β-(1,3)-gluconase[39]. This distortion can not be made for compound **36a** which has a *trans*-diequatorial type fusion between the rings. Compound **30**, which is the slightly ring-expanded version of the potent α-mannosidase inhibitor swainsonine (**3**) showed complete loss of inhibition of α-mannosidase (**table 3.2**). As a general rule, decalin-type bicyclic systems show much reduced or no inhibitory activity

compared to their acyclic or octahydroindene-type analogs. Therefore, one important conclusion that can be made is that structural flexibility leads to nonspecific inhibitory activity. Monocyclic systems generally showed poor specificity by inhibiting both α- and β-glycosidsaes because of their flexible structures. Castanospermine (**2**) and the thiaquinolizidine described here (**36a**) are the most impressive of the reported bicyclic aza-type iminosugar derivatives with a nitrogen atom at the ring junction. Thiaquinolizidine **36a** was superior against and selective for α-glucosidases compared to Castanospermine. Thiaquinolizidines therefore represent a significant advancement in this area.

Table 3.2. Activities (K_i mM) of the known aza-bicyclic systems and key monocyclic systems

Enzymes	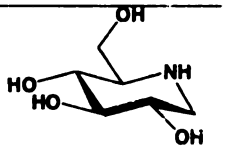			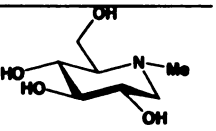
	1[22]	**63**[40]	**64**	**65**[22]
α-glucosidase				
Yeast	$8.67*10^{-6}$	ni 1.56×10^{-3} [22]	ni [41] ni [42]	$3.69*10^{-4}$
Rice		ni		
Rat intestinal maltase		ni		
Rat intestinal isomaltase		ni		
Rat intestinal sucrase		ni		
Type I (calf liver)	$1*10^{-6}$			$7.0*10^{-8}$
β-glucosidase				
Sweet almond	$1.8*10^{-5}$	7.8×10^{-4} [22]	$2.5*10^{-3}$ [41] IC_{50} $1.4*10^{-3}$ [42]	$4.3*10^{-5}$

Human liver			97% inhibition at conc. 1mM with substrate 0.5mM [43]
α-D-mannosidase Jack bean	$4*10^{-4}$		ni [41] ni [42]
α-galactosidase Green coffee bean			ni [41] IC_{50} $4.44*10^{-6}$ [42]
β-D-galactosidase Jack bean	ni		ni [41] IC_{50} $3.6*10^{-6}$ [42]

Table 3.2. continued

Enzymes		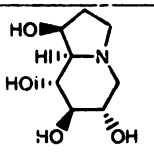	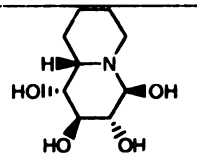	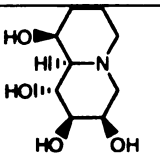
	36a	**2**[44]	**66**[45]	**30**[31]
α-glucosidase Yeast	$3.3*10^{-4}$	>1500μM		IC_{50}>2000
Rice	$9*10^{-4}$	$1.5*10^{-8}$		
Rat intestinal sucrase		$5.5*10^{-10}$		
β-glucosidase Sweet almond Human liver	ni	$1.5*10^{-6}$	ni	IC_{50}>2000
α-D-mannosidase Jack bean	ni			IC_{50}>2000
α-galactosidase Green coffee bean	ni		ni	

ni, no inhibition observed.

3.2.3. Antibacterial Activities of Trihydroxy-2-thiaquinolizidine Derivatives

Compounds **36a, 51a** and **54** were tested against five gram-positives strains *S. aureus 43300, S. aureus 29213, E. faecalis 51299, E. faecalis 29212, B. subtilis PY79* and six gram-negative strains *E.aerogenes 49469, E. coli 25922, E.coli DH5 alpha, E. cloacea 49141, P. aeruginosa 27853, Salmonella sp.35664*. Among the 11 strains tested, three of them showed inhibition of growth by these compounds, and they are all gram-positive strains. All three compounds showed inhibition against *S. aureus 43300* (**figure 3.21**). Compound **51a** and **54** showed inhibitions against *E. faecalis 51299* (**figure 3.22**), while only compound **54** has inhibitory activity against *E. faecalis 2921* (**figure 3.23**). The inhibition pattern all showed the initial drop of the reading, followed by slow decrease. Compound **54** is the most active in the three compounds, and both **54** and **51a** can inhibit *E. faecalis 51299* very well. At concentration 0.49 μg/mL, both compounds have over 50% inhibition of the bacterial growth. The 50% inhibition of the other two strains can be reached at 125 μg/mL or 250 μg/mL. Compared to compound **36a, 54** has a sulfone functional group, which is a very important factor for its antibacterial activity. Further modification should lead to more active compounds against bacteria.

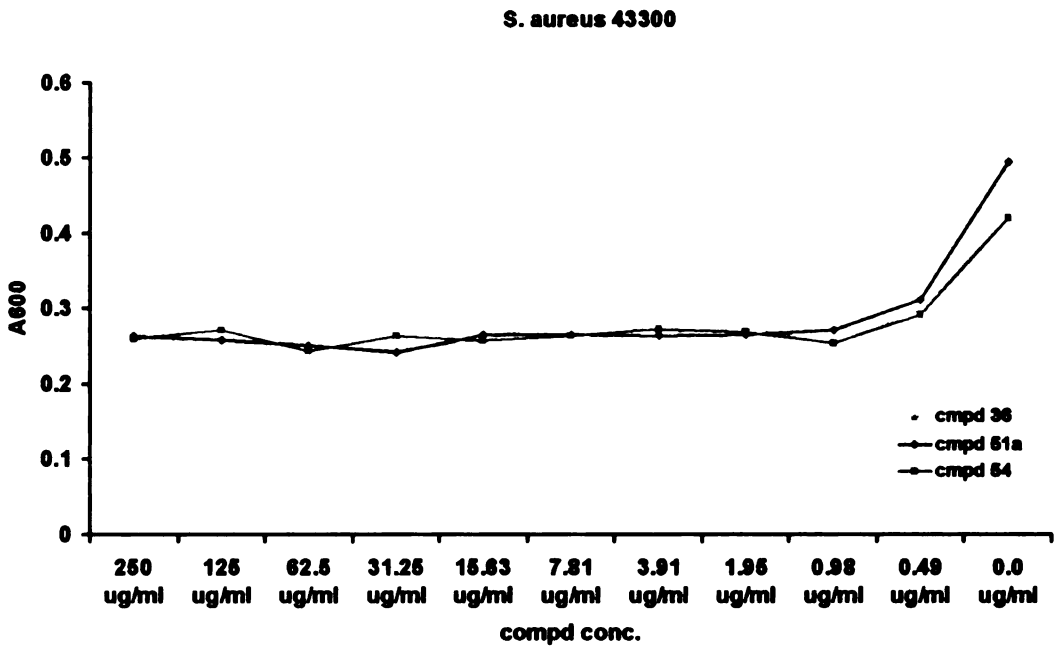

Figure 3.21. Inhibitory activity against *S. aureus 43300*

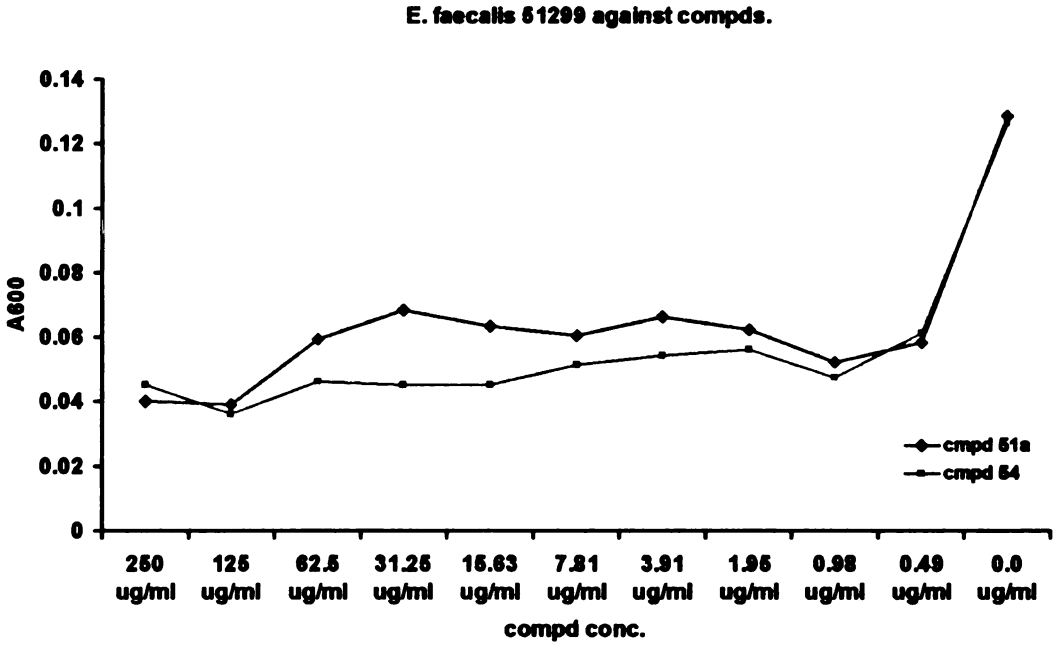

Figure 3.22. Inhibitory activity against *E. faecalis 51299*

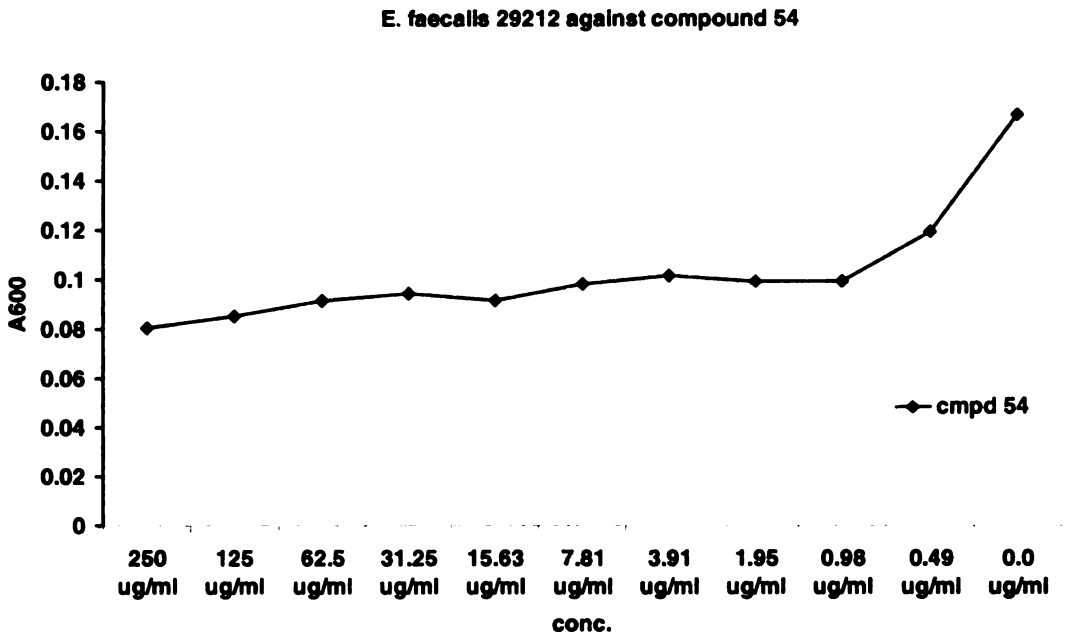

Figure 3.23. Inhibitory activity against *E. faecalis 292129*

3.3. Experimental Section

3.3.1. General Procedures

Melting points were measured on a Ficher-Johns melting point apparatus. Optical rotations were measured (λ = 589 nm) at room temperature using a Jasco P-1010 polarimeter. IR spectra were recorded on a FT-IR instrument. The ^{1}H (and ^{13}C) NMR spectra were recorded at 500 (125.5) MHz on a Varian VXR spectrometer. The HRMS FAB mass spectra were obtained using a Jeol HX-110 double-focusing mass spectrometer operating in positive ion mode.

3.3.2. Inhibition Assay

Inhibitory potency was determined by spectrophotometrically measuring the residual hydrolytic activities of the glycosidases against the corresponding nitrophenyl α- or β-D-

glucopyranoside except α-glucosidase (rice). The glycosidases used were α-glucosidase (yeast), α-glucosidase (rice), β-glucosidase (almond), α-galactosidase (green coffee beans), β-galactosidase (E. *coli*) and α-mannosidase (jack beans). All enzymes were purchased from Sigma. α-Glucosidase, β-glucosidase assays were performed in 50 mM phosphate buffer, pH 6.8 at 37°C. α-Galactosidase assays were performed in 50 mM phosphate buffer, pH 7.3 at 37°C. β-Galactosidase assays were performed in 50 mM phosphate buffer, pH 5.0 at 37°C. α-Mannosidase assay was performed in 50 mM acetate buffer, pH 4.5 at 37°C. Inhibition studies were performed by adding the inhibitor to a final concentration of 0.05 mM to 11 mM to the respective buffer solutions along with enzyme. The solutions were incubated at 37°C before adding substrates to the reactions. The absorbance of the resulting mixture was determined at 400 nm (for *p*-nitrophenol). For α-glucosidase (rice), maltose was used as the substrate, and the assay was based on the glucose oxidase/peroxidase enzyme procedure. The assay was performed in sodium acetate buffer at pH 4.0 at 37°C. The inhibitor was added to a final concentration of 0.4 mM and 8.9 mM to the substrate solution. The enzyme was added to the solution at 37°C, and the reaction was stopped after 10 and 30mins by dilute perchloric acid solution. Pipette the glucose oxidase/peroxidase solution into the reaction mixture, and incubate at 37°C for 30mins. The absorbance of the solution was determined at 500 nm for oxidized o-dianisidine.

3.3.3. MIC Testing Procedure

Compounds were assayed according to the standard MIC testing procedure for antimicrobials. Inhibitory potency was determined by spectrophotometrically measuring

the growth of the bacteria at 600 nm. The organisms used were five gram-positives strains *S. aureus 43300, S. aureus 29213, E. faecalis 51299, E. faecalis 29212, B. subtilis PY79* and six gram-negative strains *E.aerogenes 49469, E. coli 25922, E.coli DH5 alpha, E. cloacea 49141, P. aeruginosa 27853, Salmonella sp.35664*. Serial dilutions are made of the compounds in bacterial growth media M-H media. The concentration range from 250μg/mL, to 0.49μg/mL, 0μg/mL. Bacteria were grown to reach 1.5×10^6 cfu/mL and then added to the dilutions of the compounds. The solutions were incubated at 37°C and the growth of the bacteria was monitored at 2, 5, 14, 18, and 24 hours.

Methyl 6-Bromo-6-deoxy-β-D-glucopyranoside (38) To a stirred solution of methyl β-D-glucopyranoside **37** (10.15g, 50mmol) in anhydrous pyridine (300mL) at 0°C were added triphenylphosphine (26.2g, 100mmol) and carbon tetrabromide (24.87g, 75mmol). The resulting mixture was protected from moisture and stirred at 0 °C for ten minutes, then was allowed to warm to 65 °C and was stirred for 4 hours. Methanol (10mL) was added to decompose any excess of reagent. The solvent was removed by evaporation and the residue was purified by column chromatography (CH_2Cl_2, followed by 20:1 CH_2Cl_2/MeOH). Crystallization from methanol-hexanes afforded white crystalline solid (10.96g, 85%), m.p. 139-140 °C, lit. m.p. 154 °C, $[\alpha]^{20}_D = -27.6°$ (c 0.22, H_2O).

Methyl 6-Bromo-6-deoxy-2,3,4-tri-*O*-pivaloyl-β-D-glucopyranoside (39) Pivaloylation of **38** (6.73g, 26mmol) by trimethylacetyl chloride (28.8mL, 32.4mmol) in pyridine (300mL) at room temperature for 2 days afforded an white solid **8** (11.2g, 84%), m.p. 109-110 °C, $[\alpha]^{20}_D = -2.4°$ (c 0.31, $CHCl_3$). IR (CH_3Cl) ν_{max} 2971.7, 1745.6, 1140.9 cm^{-1}.

^{1}H NMR (500MHz, $CDCl_3$) δ 5.29 (1H, t, *J*=9.5 Hz), 4.99 (2H, t, *J*=9.7 Hz), 4.42 (1H, d, *J*=8.0 Hz), 3.70 (1H, m), 3.50 (3H, s), 3.39-3.12 (2H, m), 1.14 (9H, s), 1.13 (9H, s), 1.08 (9H, s); ^{13}C NMR (125.5MHz, $CDCl_3$) δ 177.14, 176.63, 176.51, 101.36, 73.7, 71.9, 71.2, 70.8, 57.1, 38.8, 38.7, 30.6 ppm; HR-FABMS (M + H^+) Calcd. 509.1750, found 509.1736.

6-Bromo-6-deoxy-2,3,4-tri-O-pivaloyl-D-*xylo*-5-ulosonicacid methylester (40). To a solution of **39** (1g, 1.96mmol) in acetic acid (100mL) and acetic anhydride (10mL), chromium trioxide (1.18g, 11.8mmol) was added and the suspension was stirred at room temperature for 3 hours. The mixture was then poured slowly into cold water (500mL). The water was extracted 5 times with CH_2Cl_2 and the combined organic phase was washed with brine, saturated sodium bicarbonate and dried (Na_2SO_4), concentrated. The resulting residue was passed through a small pad of silica gel to give **9** as a colorless oil (1g, 97%), $[\alpha]^{20}_D$ = +36.5° (c 0.12 $CHCl_3$), IR (CH_2Cl_2) ν_{max} 2975.85, 1743.63, 1132.00 cm^{-1}. ^{1}H NMR (500MHz, $CDCl_3$) δ 5.72, (1H, t, *J*=4.8 Hz), 5.57 (1H, d, *J*=4.5 Hz), 5.23 (1H, d, *J*=5.0 Hz), 4.12 (1H, d, *J*=14.0 Hz), 4.01 (1H, d, *J*=13.5 Hz), 3.72 (3H, s), 1.25 (9H, s), 1.21 (9H, s), 1.18 (9H, s); ^{13}C NMR (125.5MHz, $CDCl_3$) δ 194.5, 177.1, 176.9, 176.8, 167.1, 72.9, 70.2, 69.4, 52.7, 38.9, 38.8, 38.7, 31.6, 27.0, 26.9 ppm; HRFABMS (M + H^+) Calcd. 523.1543, found 523.1530.

7(*S*),8(*R*),9(*R*),10(S)-Trihydroxy-2-thiaquinolizidin-6-one (42a) and 7(*S*),8(*R*),9(*R*),10(R)-Trihydroxy-2-thiaquinolizidin-6-one (42b) A solution of **40** (7g, 13.4mmol) and $HS(CH_2)_2NH_2$ (1.24g, 16.1mmol) in methanol (250 mL) was stirred at

room temperature for one hour, followed by addition of sodium cyanoboron hydride (1.26g, 20mmol). The reaction mixture was stirred overnight and sodium carbonate was added to facilitate the lactam cyclization. After stirred for several hours, the suspension was filtered and acetic acid (2mL) was added and concentrated. The residue was purified by column chromatography (10:1 Hexanes/Acetone) to yield two lactam diastereomers **42a** and **42b** (4.64g, 73.6%), the ratio is 2.5 : 1.

Lactam **42a** (3.31g, 52.6%) was given as a white solid, m.p. 188-190 °C, $[\alpha]^{20}_{D}$ = +12.6° (c 0.1 $CHCl_3$), IR ($CHCl_3$) ν_{max} 1744.54, 1685.34 cm^{-1}. ^1H NMR (500MHz, $CDCl_3$) δ 5.53 (1H, t, *J*=10.5 Hz), 5.30 (1H, d, *J*=11.0 Hz), 5.19 (1H, dd, *J*=10.5, 8 Hz), 4.94 (1H, dt, *J*=13.5, 3 Hz), 3.53 (1H, ddd, *J*=9.8, 8.4, 3.4 Hz), 2.87 (1H, td, *J*=14.3, 2.5 Hz), 2.66 (1H, td, *J*=13.0, 3.0 Hz), 2.61-2.49 (3H, m); 1.21 (9H, s), 1.17 (9H, s), 1.12 (9H, s); ^{13}C NMR (125.5MHz, $CDCl_3$) δ 177.4, 177.1, 176.6, 164.3, 70.4, 69.4, 67.8, 60.2, 44.7, 38.9, 38.7, 31.8, 27.1, 26.6 ppm. HRFABMA ($M + H^+$) calcd. 472.2369, found 472.2379.

Lactam **42b** (1.33g, 21.0%) was given as a white solid, m.p. 179-181°C. IR (CH_2Cl_2) ν_{max} 1741.07, 1679.15, 1137.70 cm^{-1}; ^1H NMR (500MHz, $CDCl_3$) δ 5.76 (1H, t, *J*=10.3 Hz), 5.27 (1H, dd, *J*=11.5, 6.3 Hz), 4.78 (1H, m), 4.02 (1H, ddd, *J*=11.8, 6.3, 2.0 Hz), 3.07 (1H, t, 12.3 Hz), 2.98-2.88 (3H, m), 2.50 (1H, d, *J*=13.0 Hz), 2.35 (1H, m), 1.20 (9H, s), 1.17 (9H, s), 1.14 (9H, s); ^{13}C NMR (125.5MHz, $CDCl_3$) δ 177.42, 176.82, 163.67, 67.66, 67.03, 59.23, 47.05, 38.90, 38.69, 27.74, 27.11, 27.06, 26.96, 26.34 ppm. FABMS ($M + H^+$) calcd. 472.2369, found 472.2.

7(*S*),8(*R*),9(*R*),10(S)-Trihydroxy-2-thiaquinolizidine (36a)

A solution of lactam **42a** (2g, 4.24mmol) and BH_3-THF (20mL, 1.5M) in anhydrous THF (30mL) was refluxed for 4 hours and the TLC and NMR showed the completion of the reduction. The solvent was removed and methanol was added and concentrated for 3 times. The residue was dissolved in methanol (30mL), followed by addition of NaOMe (0.15g, 2.8mmol). The reaction was stirred for 8 hours and concentrated. The residue was applied to an ion exchange column (Dowex 50WX8-400, 30g), which was washed with water (50 mL) and eluted with NH_4OH (50mL). The elution was concentrated and purified by column chromatography (15:1 CH_2Cl_2/MeOH) to afford a white solid (0.62g, 71%), m.p. 235-237 °C; $[\alpha]^{20}_D$ = + 20.2° (c 0.06 H_2O); IR (KBr) ν_{max} 3355.78, 3275.61 cm^{-1}; ^1H NMR (500MHz, $CDCl_3$) δ 3.50 (1H, ddd, *J*=11.0, 9.1, 4.9 Hz), 3.25 (1H, t, *J*=9.3 Hz), 3.12 (1H, dt, *J*=12.5, 3.0 Hz), 3.06 (1H, t, *J*=9.5 Hz), 2.93 (1H, dt, *J*=14.0, 2.5 Hz), 2.84 (1H, dd, *J*=11.5, 5.0 Hz), 2.75 (1H, td, *J*=13.0, 3.0 Hz), 2.52 (1H, m), 2.45 (1H, t, *J*=12.3 Hz), 2.43 (1H, m), 2.19 (1H, t, *J*=11.3 Hz), 2.13 (1H, td, *J*=10.0, 2.5 Hz); ^{13}C NMR (125.5MHz, CDCl3) δ 77.9, 74.1, 68.5, 65.6, 59.4, 55.7, 29.3, 26.3 ppm. HR-FABMS (M + H^+) calcd. 206.0851, found 206.0849.

7(*S*),8(*R*),9(*R*),10(R)-Trihydroxy-2-thiaquinolizidine (36b) was obtained by the same method as **36a from lactam 42B** (75% from 42b). ^1H NMR (500MHz, D_2O) δ 3.51-2.42 (2H, m), 3.06 (2H, d, *J*=10.0 Hz), 2.90 (4H, dd, *J*=26.0, 12.5 Hz), 2.82 (2H, t, *J*=10.5 Hz), 2.60 (2H, dd, *J*=12.0, 4 Hz), 2.20 (2H, d, *J*=14.0 Hz). HR-FABMS (M + H^+) calcd. 206.0851, found 206.0849.

Manno-derivatives were obtained in the same fashion as gluco-derivatives.

Methyl 6-Bromo-6-deoxy-β-D-mannopyranoside (45) was given as white solid (84%). ^{1}H NMR (500MHz, D_2O) δ 3.91 (1H, d, *J*=2 Hz), 3.75 (1H, d, *J*=2.5 Hz), 3.73 (1H, d, *J*=2.5 Hz), 3.571 (2H, dd, *J*=11.8, 5.8 Hz), 3.569 (1H, d, *J*=1.5 Hz), 3.46 (3H, s), 3.43 (1H, m); ^{13}C NMR (125.5MHz, D_2O) δ 101.41, 74.89, 72.83, 70.47, 68.96, 57.24, 32.95 ppm.

Methyl 6-Bromo-6-deoxy-2,3,4-tri-*O*-pivaloyl-β-D-mannopyranoside (46) was obtained as white solid (80%). ^{1}H NMR (500MHz, $CDCl_3$) δ 5.41 (1H, dd, *J*=3, 0.75 Hz), 5.24 (1H, t, *J*=10 Hz), 5.08 (1H, dd, *J*=10, 3 Hz), 4.57 (1H, d, *J*=1 Hz), 3.68 (1H, m), 3.49 (3H, s), 3.47-3.39 (2H, m), 1.24 (9H, s), 1.15 (9H, s), 1.09 (9H, s); ^{13}C NMR (125.5MHz, $CDCl_3$) δ 177.28, 177.22, 176.80, 99.74, 73.82, 70.85, 68.31, 68.21, 57.18, 39.06, 38.84, 38.75, 31.08, 27.16, 27.04, 27.02 ppm. HRFABMA (M + H^+) Calcd. 509.1750, found 509.1748.

Methyl 6-Bromo-2,3,4-tri-*O*-pivaloyl-5-keto-ester (47) was obtained as colorless oil (91%). ^{1}H NMR (500MHz, $CDCl_3$) δ 5.73 (1H, dd, *J*=8.5, 3 Hz), 5.71 (1H, d, *J*=2.5 Hz), 5.01 (1H, d, *J*=9 Hz), 4.13 (1H, d, *J*=14 Hz), 4.00 (1H, d, *J*=13.5 Hz) 3.69 (3H, s), 1.24 (9H, s), 1.21 (9H, s), 1.15 (9H, s); ^{13}C NMR (125.5MHz, $CDCl_3$) δ 194.78, 176.90, 176.85, 176.59, 167.76, 73.16, 68.99, 68.85, 52.75, 38.91, 38.81, 38.69, 38.91, 38.81, 38.69, 31.38, 26.96, 26.86, 26.84 ppm. HRFABMA (M + H^+) Calcd. 523.1543, found 523.1545.

Lactam 49a was obtained as white solid (65%). ^{1}H NMR (500MHz, $CDCl_3$) δ 5.67 (1H, d, *J*=3.5 Hz), 5.39 (1H, m), 5.01 (1H, m), 4.99 (1H, t, *J*=3 Hz), 3.66 (1H, dt, *J*=11.5, 2 Hz), 2.99 (1H, m), 2.85 (1H, td, *J*=13, 2 Hz), 2.74 (1H, td, *J*=13, 2.5 Hz), 2.59 (1H, dt, *J*=13.5, 2 Hz), 2.46 (1H, m), 1.22 (9H, s), 1.21 (9H, s), 1.20 (9H, s); ^{13}C NMR (125.5MHz, $CDCl_3$) δ 176.94, 176.86, 176.36, 163.27, 69.43, 68.18, 66.51, 62.75, 46.54, 38.91, 38.85, 38.81, 31.06, 27.18, 27.08, 26.98, 26.66 ppm. HRFABMA (M + H^+) calcd. 472.2369, found 472.2366.

Lactam 49b was obtained as white solid (16%). ^{1}H NMR (500MHz, $CDCl_3$) δ 5.65 (1H, d, *J*=2.5 Hz), 5.34 (1H, t, *J*=5 Hz), 5.31 (1H, m), 5.04 (1H, dt, *J*=8.5, 3 Hz), 3.77 (1H, m), 2.79 (1H, td, *J*=13.5, 2 Hz), 2.68 (2H, m), 2.53 (1H, m), 2.39 (1H, dt, *J*=13.5, 2 Hz), 1.25 (9H, s), 1.20 (9H, s), 1.18 (9H, s); ^{13}C NMR (125.5MHz, $CDCl_3$) δ 177.12, 176.66, 176.23, 165.11, 67.13, 66.90, 66.34, 58.60, 44.57, 39.14, 38.94, 38.85, 28.78, 27.19, 27.11, 27.04 ppm. HRFABMA (M + H^+) calcd. 472.2369, found 472.2367.

7(*R*),8(*R*),9(*R*),10(S)-Trihydroxy-2-thiaquinolizidine (51a) was obtained as white solid (73% from 49a). ^{1}H NMR (500MHz, D_2O) δ 3.93 (1H, m), 3.43 (1H, dd, *J*=10, 3.5 Hz), 3.35 (1H, t, *J*=9.5 Hz), 3.06 (1H, dt, *J*=12.5, 3 Hz), 2.90 (1H, dt, *J*=8.5, 2.5 Hz), 2.81-2.74 (2H, m), 2.51-2.44 (2H, m), 2.39-2.32 (2H, m), 2.05 (1H, t, *J*=9 Hz); ^{13}C NMR (125.5MHz, D_2O) δ 73.90, 71.15, 67.48, 66.24, 59.37, 55.87, 28.77, 26.02 ppm. HRFABMA (M + H^+) calcd. 206.0851, found 206.0851.

7(*R*),8(*R*),9(*R*),10(R)-Trihydroxy-2-thiaquinolizidine (51b) was obtained by the same way as **51a** (71% from 49b). ^{1}H NMR (500MHz, D_2O) δ 3.97 (1H, m), 3.87 (1H, s), 3.69

(1H, d, J=2.0 Hz), 3.10 (1H, d, J=12.5 Hz), 2.84 (2H, dd, J=13.5, 11.0 Hz), 2.76 (1H, m), 2.61 (2H, m), 2.44 (2H, t, J=11.0 Hz), 2.36 (1H, d, J=14.0 Hz). HRFABMA ($M + H^+$) calcd. 206.0851, found 206.0850.

2,2-dioxy-7(*S*),8(*R*),9(*R*),10(R)-Trihydroxy-2-thiaquinolizidin-2-one (sulfone 52)

Lactam **42a** (0.5g, 1.1mmol) was dissolved in 30mL dichloromethane, and cooled to 0°C. 5mL dichloromethane solution of m-chloroperbenzoic acid (0.65g, 70% w/w) was added to the reaction in several portions. After stirred at room temperature for half an hour, saturated sodium bicarbonate solution was added to neutralize the reaction. The product was extracted by dichloromethane for 3 times and the combined organic phase was washed with saturated sodium bicarbonate, brine and dried (Na_2SO_4). The resulting sulfone 2 was obtained as white solid and was used to the next step without purification. ^{1}H NMR (500MHz, $CDCl_3$) δ 5.59 (1H, t, J=10 Hz), 5.41 (1H, d, J=10.5 Hz), 5.28 (1H, m), 4.99 (1H, dt, J=10.5, 3.5 Hz), 3.89 (1H, m), 3.23-3.01 (5H, m), 1.19 (9H, s), 1.17 (9H, s), 1.10 (9H, s); ^{13}C NMR (125.5MHz, $CDCl_3$) δ 177.54, 177.09, 176.35, 164.22, 69.13, 68.97, 67.53, 57.06, 54.58, 50.03, 40.41, 38.81, 38.79, 38.68, 27.03, 26.97 ppm.

2,2-Dioxy-7(*S*),8(*R*),9(*R*),10(*S*)-Trihydroxy-2-thiaquinolizidin-2-one (sulfone 54)

A solution of sulfone **52** (0.40g, 0.08mmol) and BH_3-THF (5.0mL, 7.5mmol) in anhydrous THF (10mL) was refluxed for 8 hours and NMR showed the completion of the reduction. The solvent was removed and methanol was added and concentrated for 3 times. The residue was dissolved in methanol (15mL), followed by addition of NaOMe (0.10g, 1.8mmol). The reaction was stirred for overnight and concentrated. The residue

was applied to an ion exchange column (Dowex 50WX8-400, 2g), which was washed with water (30 mL) and eluted with 2N NH_4OH (30mL). The elution was concentrated to afford a white solid (0.15g, 84%). ^1H NMR (500MHz, D_2O) δ 3.56 (1H, m), 3.53 (1H, m), 3.30-3.23 (4H, m), 3.14 (1H, t, *J*=9.5 Hz), 3.01 (2H, m), 2.85 (1H, m), 2.58 (1H, m), 2.27 (1H, t, *J*=11.5 Hz); ^{13}C NMR (125.5MHz, D_2O) δ 76.88, 73.11, 68.50, 63.03, 57.99, 52.25, 52.06, 49.98 ppm. HRFABMA ($M + H^+$) calcd. 238.0748, found 238.0748.

3.4. References

(1) Vandenbroek, L.; Vermaas, D. J.; Heskamp, B. M.; Vanboeckel, C. A. A.; Tan, M.; Bolscher, J. G. M.; Ploegh, H. L.; Vankemenade, F. J.; Degoede, R. E. Y.; Miedema, F. Chemical Modification of Azasugars, Inhibitors of N-Glycoprotein-Processing Glycosidases and of Hiv-I Infection - Review and Structure-Activity-Relationships *Recueil Des Travaux Chimiques Des Pays-Bas-Journal of the Royal Netherlands Chemical Society* **1993**, *112*, 82-94.

(2) Scheen, A. J. Drug treatment of non-insulin-dependent diabetes mellitus in the 1990s - Achievements and future developments *Drugs* **1997**, *54*, 355-368.

(3) Witczak, Z. J. In *Carbohydrates as New and Old Targets for Future Drug Design in Carbohydrates in Drug Design*; Witczak, Z. J., Ed.; Marcel Dekker Inc.: New York, 1997, p 1.

(4) Anzeveno, P. B.; Creemer, L. J.; Daniel, J. K.; King, C. H. R.; Liu, P. S. A Facile, Practical Synthesis of 2,6-Dideoxy-2,6-Imino-7-O-Beta-D-Glucopyranosyl-D-Glycero-L-Gulo-Heptitol (Mdl 25,637) *J. Org. Chem.* **1989**, *54*, 2539-2542.

(5) Platt, F. M.; Neises, G. R.; Reinkensmeier, G.; Townsend, M. J.; Perry, V. H.; Proia, R. L.; Winchester, B.; Dwek, R. A.; Butters, T. D. Prevention of lysosomal storage in Tay-Sachs mice treated with N-butyldeoxynojirimycin *Science* **1997**, *276*, 428-431.

(6) Truscheit, E.; Frommer, W.; Junge, B.; Muller, L.; Schmidt, D. D.; Wingender, W. Chemistry and Biochemistry of Microbial Alpha-Glucosidase Inhibitors *Angew. Chem., Int. Ed. Engl. in English* **1981**, *20*, 744-761.

(7) Karpas, A.; Fleet, G. W. J.; Dwek, R. A.; Petursson, S.; Namgoong, S. K.; Ramsden, N. G.; Jacob, G. S.; Rademacher, T. W. Aminosugar Derivatives as Potential Anti-Human Immunodeficiency Virus Agents *Proc. Natl. Acad. Sci. U. S. A.* **1988**, *85*, 9229-9233.

(8) Taylor, D. L.; Sunkara, P. S.; Liu, P. S.; Kang, M. S.; Bowlin, T. L.; Tyms, A. S. 6-0-Butanoylcastanospermine (Mdl 28,574) Inhibits Glycoprotein Processing and the Growth of Hiv *Aids* **1991**, *5*, 693-698.

(9) Fleet, G. W. J.; Karpas, A.; Dwek, R. A.; Fellows, L. E.; Tyms, A. S.; Petursson, S.; Namgoong, S. K.; Ramsden, N. G.; Smith, P. W.; Son, J. C.; Wilson, F.; Witty, D. R.; Jacob, G. S.; Rademacher, T. W. Inhibition of Hiv Replication by Amino-Sugar Derivatives *Febs Letters* **1988**, *237*, 128-132.

(10) Goss, P. E.; Baker, M. A.; Carver, J. P.; Dennis, J. W. Inhibitors of carbohydrate processing: A new class of anticancer agents *Clinical Cancer Research* **1995**, *1*, 935-944.

(11) Kino, T.; Inamura, N.; Nakahara, K.; Kiyoto, S.; Goto, T.; Terano, H.; Kohsaka, M.; Aoki, H.; Imanaka, H. Studies of an Immunomodulator, Swainsonine .2. Effect of Swainsonine on Mouse Immunodeficient System and Experimental Murine Tumor *Journal of Antibiotics* **1985**, *38*, 936-940.

(12) Elbein, A. D. Glycosidase Inhibitors - Inhibitors of N-Linked Oligosaccharide Processing *Faseb J.* **1991**, *5*, 3055-3063.

(13) Das, P. C.; Roberts, J. D.; White, S. L.; Olden, K. Activation of Resident Tissue-Specific Macrophages by Swainsonine *Oncology Research* **1995**, *7*, 425-433.

(14) Elbein, A. D. M., R. J. In *Iminosugars as Glycosidase Inhibitors*; Stutz, A. E., Ed.; Wiley-VCH: Weinheim, 1999, pp 216-251 and references therein.

(15) Molyneux, R. J.; McKenzie, R. A.; Osullivan, B. M.; Elbein, A. D. Identification of the Glycosidase Inhibitors Swainsonine and Calystegine B-2 in Weir Vine (Ipomoea Sp Q6 Aff Calobra) and Correlation with Toxicity *J. Nat. Prod.-Lloydia* **1995**, *58*, 878-886.

(16) Ermert, P.; Vasella, A. Synthesis of a Glucose-Derived Tetrazole as a New Beta-Glucosidase Inhibitor - a New Synthesis of 1-Deoxynojirimycin *Helv. Chim. Acta* **1991**, *74*, 2043-2053.

(17) Brandstetter, T. W.; Davis, B.; Hyett, D.; Smith, C.; Hackett, L.; Winchester, B. G.; Fleet, G. W. J. Tetrazoles of Manno-Pyranoses and Rhamno-Pyranoses - Inhibition of Glycosidases by Tetrazoles and Other Mannose Mimics *Tetrahedron Lett.* **1995**, *36*, 7511-7514.

(18) Igarashi, Y. I., M.; Ichikawa, Y. Synthesis of a new inhibitor of -fucosidase *Bioorg. Med. Chem. Lett.* **1996**, *6*, 553-558.

(19) Legler, G.; Stutz, A. E.; Immich, H. Synthesis of 1,5-Dideoxy-1,5-Imino-D-Arabinitol (5-nor-L-Fuco-1-Deoxynojirimycin) and Its Application for the Affinity Purification and Characterization of Alpha-L-Fucosidase *Carbohydr. Res.* **1995**, *272*, 17-30.

(20) Takahashi, S. K., H. Syntheses of L-fucopyranose and its homologs with ring heteroatoms other than oxygen. Stereocontrolled conversion of a common D-arabinofuranoside intermediate *Chem. Lett* **1992**, 21-24.

(21) Defoin, A. S., H.; Streith, J. Synthesis of 1,6-dideoxynojirimycin, 1,6-dideoxy-D-allo-nojirimycin, and 1,6-dideoxy-D-gulo-nojirimycin via asymmetric hetero-Diels-Alder reactions *Helv. Chim. Acta.* **1996**, *79*, 560-567.

(22) Kajimoto, T.; Liu, K. K. C.; Pederson, R. L.; Zhong, Z. Y.; Ichikawa, Y.; Porco, J. A.; Wong, C. H. Enzyme-Catalyzed Aldol Condensation for Asymmetric-Synthesis of

Azasugars - Synthesis, Evaluation, and Modeling of Glycosidase Inhibitors *J. Am. Chem. Soc.* **1991**, *113*, 6187-6196.

(23) Kajimoto, T.; Chen, L. R.; Liu, K. K. C.; Wong, C. H. Palladium-Mediated Stereocontrolled Reductive Amination of Azido Sugars Prepared from Enzymatic Aldol Condensation - a General-Approach to the Synthesis of Deoxy Aza Sugars *J. Am. Chem. Soc.* **1991**, *113*, 6678-6680.

(24) Wong, C. H.; Ichikawa, Y.; Krach, T.; Gautheronlenarvor, C.; Dumas, D. P.; Look, G. C. Probing the Acceptor Specificity of Beta-1,4-Galactosyltransferase for the Development of Enzymatic-Synthesis of Novel Oligosaccharides *J. Am. Chem. Soc.* **1991**, *113*, 8137-8145.

(25) Liu, K. K. C.; Kajimoto, T.; Chen, L. R.; Zhong, Z. Y.; Ichikawa, Y.; Wong, C. H. Use of Dihydroxyacetone Phosphate Dependent Aldolases in the Synthesis of Deoxyazasugars *J. Org. Chem.* **1991**, *56*, 6280-6289.

(26) Ganem, B. Inhibitors of carbohydrate-processing enzymes: Design and synthesis of sugar-shaped heterocycles *Acc. Chem. Res.* **1996**, *29*, 340-347.

(27) Baxter, E. W.; Reitz, A. B. Expeditious Synthesis of Azasugars by the Double Reductive Amination of Dicarbonyl Sugars *J. Org. Chem.* **1994**, *59*, 3175-3185.

(28) Dhavale, D. D.; Saha, N. N.; Desai, V. N. A stereoselective synthesis of 1,6-dideoxynojirimycin by double-reductive amination of dicarbonyl sugar *J. Org. Chem.* **1997**, *62*, 7482-7484.

(29) Zhao, H.; Hans, S.; Cheng, X. H.; Mootoo, D. R. Allylated monosaccharides as precursors in triple reductive amination strategies: Synthesis of castanospermine and swainsonine *J. Org. Chem.* **2001**, *66*, 1761-1767.

(30) Iida, H.; Yamazaki, N.; Kibayashi, C. Total Synthesis of (+)-Nojirimycin and (+)-1-Deoxynojirimycin *J. Org. Chem.* **1987**, *52*, 3337-3342.

(31) Pearson, W. H.; Hembre, E. J. Synthesis of tetrahydroxyquinolizidines: Ring-expanded analogs of the mannosidase inhibitor swainsonine *J. Org. Chem.* **1996**, *61*, 5537-5545.

(32) Angyal, S. J. J., K. Oxidative demethylation with chromium trioxide in acetic acid *Carbohydr. Res.* **1970**, *12*, 147-149.

(33) Angyal, S. J.; James, K. Oxidation of Carbohydrates with Chromium Trioxide in Acetic Acid .1. Glycosides *Australian Journal of Chemistry* **1970**, *23*, 1209-&.

(34) Mathews, C. K., Van Holde K.E. In *Biochemistry*; Benjamin/Cummings Pub. Co., Inc.: Menlo Park, Calif., 1996., pp 375-388.

(35) Halvorson, H. O. *Methods Enzymol.* **1966**, *8*, 55.

(36) Gijsen, H. J. M.; Qiao, L.; Fitz, W.; Wong, C. H. Recent advances in the chemoenzymatic synthesis of carbohydrates and carbohydrate mimetics *Chem. Rev.* **1996**, *96*, 443-473.

(37) Wong, C. H.; Halcomb, R. L.; Ichikawa, Y.; Kajimoto, T. Enzymes in Organic-Synthesis - Application to the Problems of Carbohydrate-Recognition .1 *Angew. Chem., Int. Ed. Engl.* **1995**, *34*, 412-432.

(38) Wong, C. H.; Halcomb, R. L.; Ichikawa, Y.; Kajimoto, T. Enzymes in Organic-Synthesis - Application to the Problems of Carbohydrate-Recognition .2 *Angew. Chem., Int. Ed. Engl.* **1995**, *34*, 521-546.

(39) Cutfield, S. M.; Davies, G. J.; Murshudov, G.; Anderson, B. F.; Moody, P. C. E.; Sullivan, P. A.; Cutfield, J. F. The structure of the exo- -(1,3)-glucanase from Candida albicans in native and bound forms: relationship between a pocket and groove in family 5 glycosyl hydrolases1 *J. Mol. Biol.* **1999**, *294*, 771-783.

(40) Yasuda, K. K., H.; Yamashita, T.; Kameda, Y.; Kato, A.; Nash, R. J.; Fleet, G. W. J.; Molyneux, R. J.; Asano, N. New Sugar-Mimic Alkaloids from the Pods of Angylocalyx pynaertii *J. Nat. Prod.* **2002**, *65*, 198-202.

(41) Bernotas, R. C. P., G.; Urbach, J.; Oanem, B. A new family of five-carbon iminoalditols which are potent glycosidase inhibitors *Tetrahedron Lett.* **1991**, *31*, 3393-3396.

(42) Patil, N. T. J., S.; Sabharwal, S. G.; Dhavale, D. D. 1-Aza-sugars from -glucose. Preparation of 1-deoxy-5-dehydroxymethyl-nojirimycin, its analogues and evaluation of glycosidase inhibitory activity *Bioorg. Med. Chem.* **2002**, *10*, 2155-2160.

(43) Godskesen, M. L., I.; Madsen, R.; Winchester, B. Deoxyiminoalditols from aldonolactones — V. Preparation of the four stereoisomers of 1,5-dideoxy-1,5-iminopentitols. Evaluation of these iminopentitols and three 1,5-dideoxy-1,5-iminoheptitols as glycosidase inhibitors *Bioorg. Med. Chem.* **1996**, *6*, 1857-1865.

(44) Legler, G. Glycoside hydrolases: Mechanistic information from studies with reversible and irreversible inhibitors *Adv. Carbohydr. Chem. Biochem.* **1990**, *48*, 319-385.

(45) van Hooft, P. A. V. L., R. E. J. N.; van der Marel, G. A.; van Boeckel, C. A. A.; van Boom, J. H. Stereoselective Transformations on D-Glucose-Derived Eight-Membered Ring Carbocycles *Org. Lett.* **2001**, *3*, 731-733.

Chapter 4

Design and Synthesis of Iminopentitol Scaffolds for the Preparation of Riboside Hydrolase, Phosphorylase and Transferase Inhibitors

ABSTRACT

Two bicyclic molecular scaffolds containing the structural essence of a ribosyl cation in the form of a 1,4-dideoxy-1,4-iminopentitol (or pentose "aza-sugar") have been prepared. These molecules, with a carboxymethyl substituted dihydroxyhexahydro-pyrrolothiazine or pyrrolobenzothiazine contain provision to facilitate the attachment of analogs of departing and incoming groups at the anomeric position with the correct orientation. This would allow the facile preparation of glycosyl transferase and glycosidase inhibitors covering several families of enzymes that are important drug targets for a variety of disease treatment applications.

4.1. Introduction

Iminopentitols, especially those with the D-*ribo* configuration, are extremely valuable for the development of glycosidase and glycosyltransferase inhibitors across the entire spectrum of possible applications. They are literal mimetics of furanosidic oxocarbenium ion species and they closely mimic the transition states of pyranosidic species. Glycosidic linkages in nucleosides and nucleotides are involved in all kinds of important processes. The ribooxocarbenium species are key features for N-glycanases including nucleoside hydrolases[1-3], hypoxanthine-guanine phosphoribosyltransferases[4] (HGPRTases) and purine nucleoside phosphorylases[5-8] (PNP). Examples of *ribo* iminopentitols that have been successfully used as inhibitors are immucillin-H (**1**)[9,10] and its derivatives.

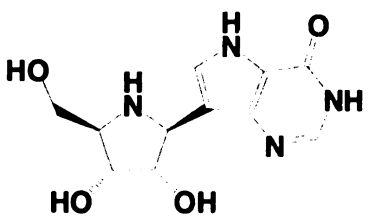

ImmH 1

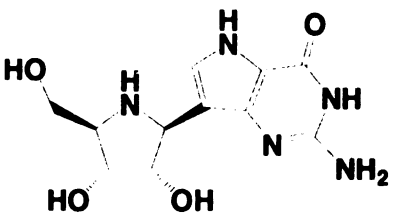

ImmG 2

Naturally occurring iminopentitols that have the D-*ribo* (**3**) as well as L and D-*arabino* configurations (**4** and **5** respectively) have been isolated from several sources[11-14].

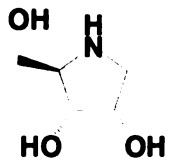

3

D-*ribo*-1,4-dideoxy-1,4-iminopentitol

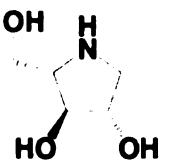

4

L-*arabino*-1,4-dideoxy-1,4-iminopentitol

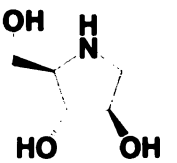

5

D-*arabino*-1,4-dideoxy-1,4-iminopentitol

Some synthetic schemes have been developed for the preparation of the D-*ribo* iminopentitols. Examples are described below:

George W.J. Fleet[15] first reported the synthesis of 1,4-imino-D-ribitol **3** from sugar lactone **6**. D-gulonolactone was converted to pyrrolidine by reduction of the lactone to diol, followed by recyclization with benzylamine. Periodate oxidation of the diol **10** and reduction of the resulting aldehyde afforded the imino-D-ribitol (**figure 4.1**).

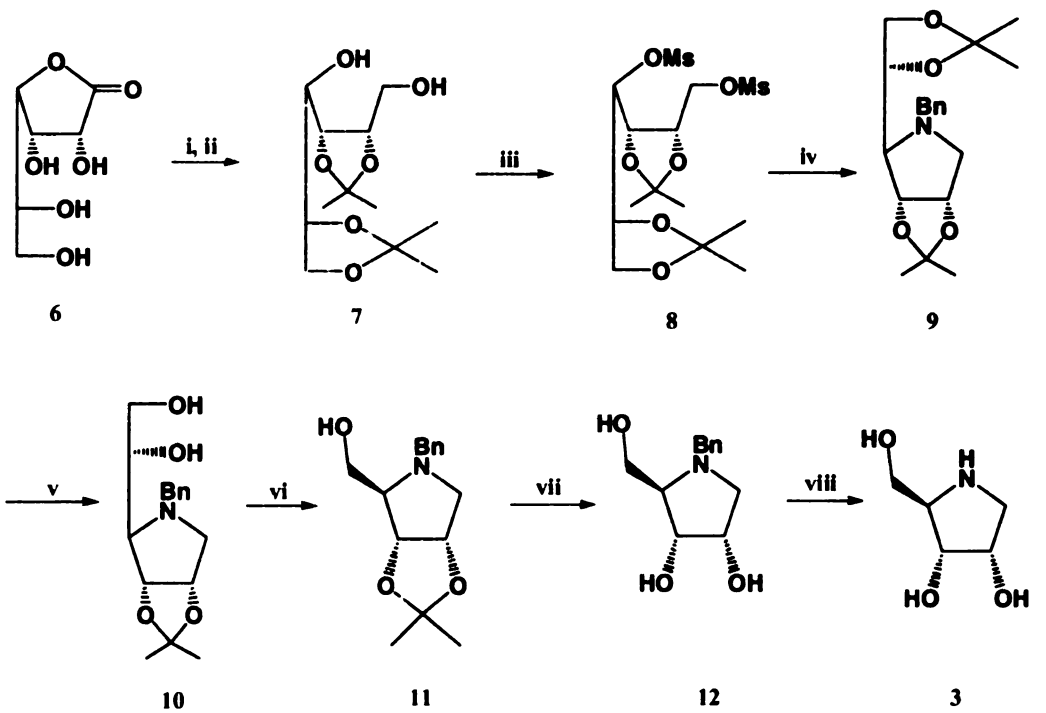

Figure 4.1. Synthesis of 1,4-imino-D-ribitol **3**. i, acetone, dimethoxypropane, 85%; ii,

LAH, 87%; iii, Methanesulphonyl chloride; iv, $BnNH_2$, 77%; v, 80% acetic acid, 93%; vi, a, HIO_4; b, $NaBH_4$, 71%; vii, H^+, 86%; viii, H_2, 78%.

In the synthesis of 1,4-dideoxy-1,4-imino-L-lyxitol (**figure 4.2**) and 1,5-dideoxy-1,5-imino-D-ribitol (**figure 4.3**) reported by K. H. Park[16], a partially protected chiral 3,4,5-trihydroxy-1-pentene (**13**) was used as the starting material. The diastereoselective epoxidation of this chiral synthon afforded the key intermediate (**15**). Conversion of the epoxide to an amino alcohol via an azide, hydroxyl activation and cyclization yielded the desired products.

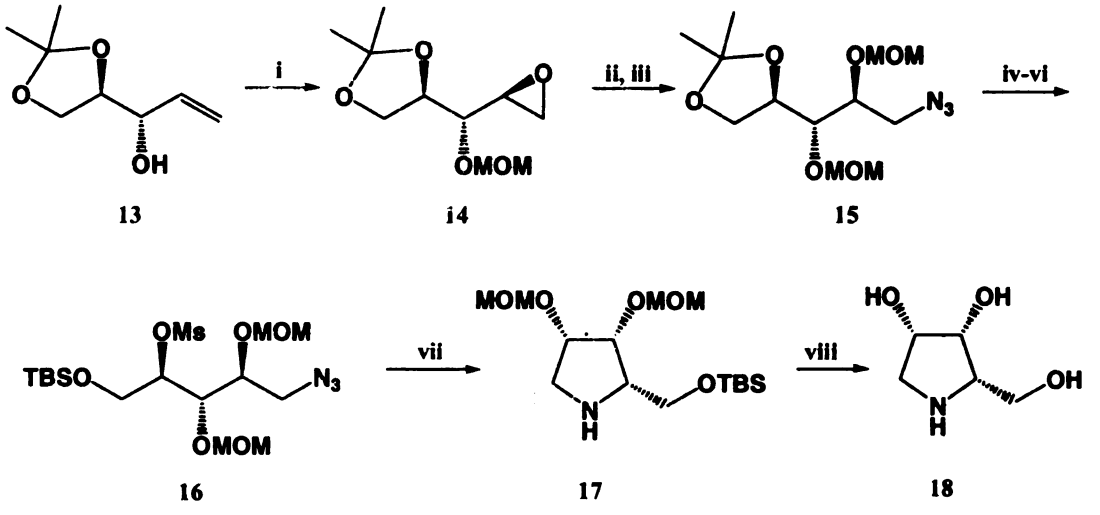

Figure 4.2. Synthesis of 1,4-dideoxy-1,4-imino-L-lyxitol. i, mCPBA, CH_2Cl_2; ii, NaN_3, NH_4Cl, $MeOH/H_2O$ (8/1), reflux, 12 h; iii, MOMCl, *N*-ethyldiisopropylamine, CH_2Cl_2, 0 °C - rt, 12 h; iv, 70% AcOH, rt, 8 h; v, TBDMSCl, Imidazole, DMF, rt, 10 min; vi, MsCl, Et_3N, THF, 0 °C, 10 min; vii, H_2, 10% Pd/C, MeOH, 0.5 N NaOH, rt, 10 h; viii, Dowex 50W-X8, MeOH, reflux, 12 h.

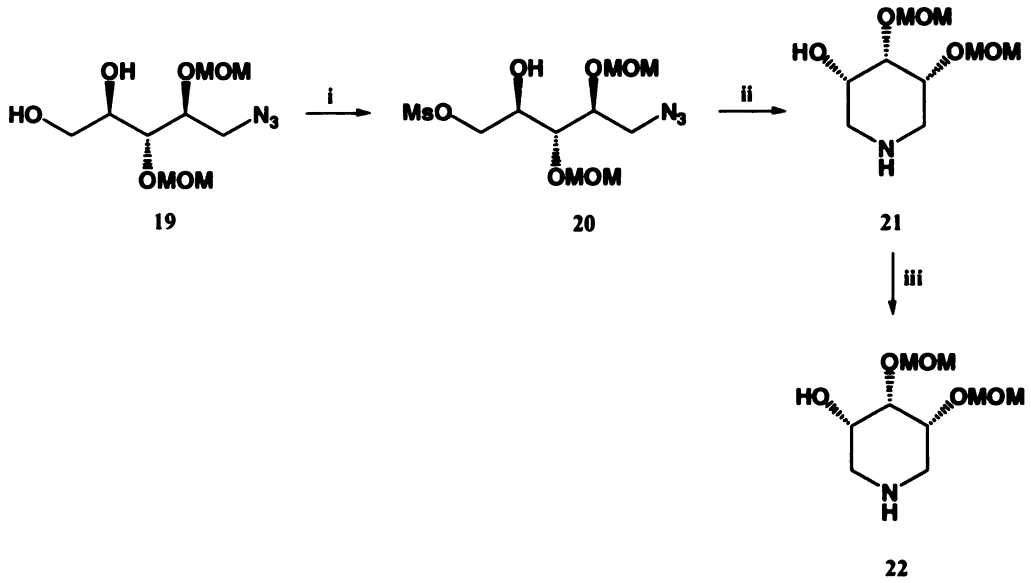

Figure 4.3. Synthesis of 1,5-dideoxy-1,5-imino-D-ribitol. i, MsCl, Et_3N, CH_2Cl_2, -40 °C, 20 min; vii, H_2, Pd/C, MeOH, 0.5 N NaOH, rt, 9 h; viii, Dowex 50W-X8, MeOH, reflux, 12 h.

In the synthesis reported by Hassner, The asymmetric synthesis of 1,4-dideoxy-1,4-imino-D-ribitol was achieved utilizing the stereoselective addition of allylphenylsulfone to a chiral N-sulfinyl-2-furfuryl imine and ring-closing metathesis[17] (**figure 4.4**).

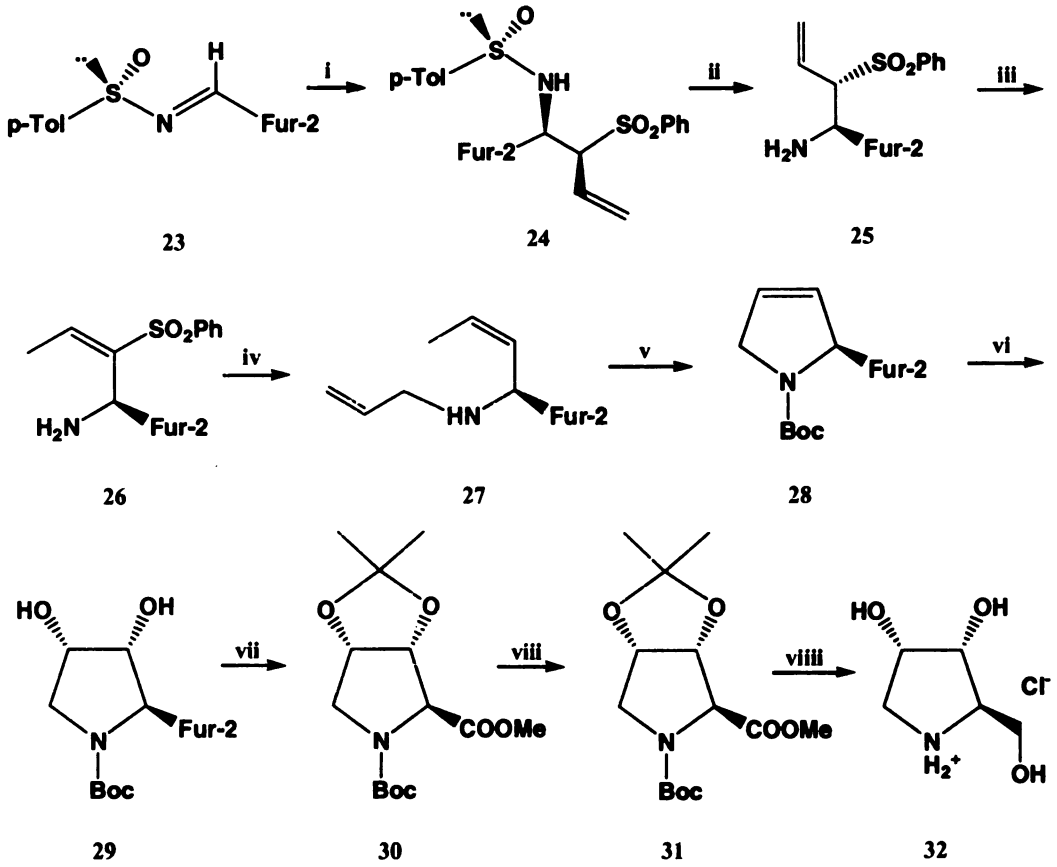

Figure 4.4. Synthesis of 1,4-dideoxy-1,4-imino-D-ribitol. i, allylphenylsulfone, LDA, THF, -100 °C; ii, TFA, MeOH, 0°C; iii, t-BuOH, THF, 0°C; iv, (a) allylbromide, K_2CO_3; (b) SmI_2-THF, HMPA, -20°C; v, (a) N-TBCBT; (b) $[Cl_2(Pcy_3)_2Ru{=}CHPh]$; vi, Cat. OsO_4, NMO, t-BuOH; vii, (a) 2,2-DMP, Cat.p-TSA; (b) Cat. RuO_2, $NaIO_4$; (c) CH_2N_2; viii, DIBAL-H, -78°C; viiii, (a) 80% TFA, (b) aq HCl.

The synthesis of ImmH and its derivatives started from imine **33**[10], derived from 1,4-dideoxy-1,4-imino-D-ribitol. Assembling of the 9-deazapurine on the preformed aza-C-glycoside afforded the desired product (**figure 4.5**).

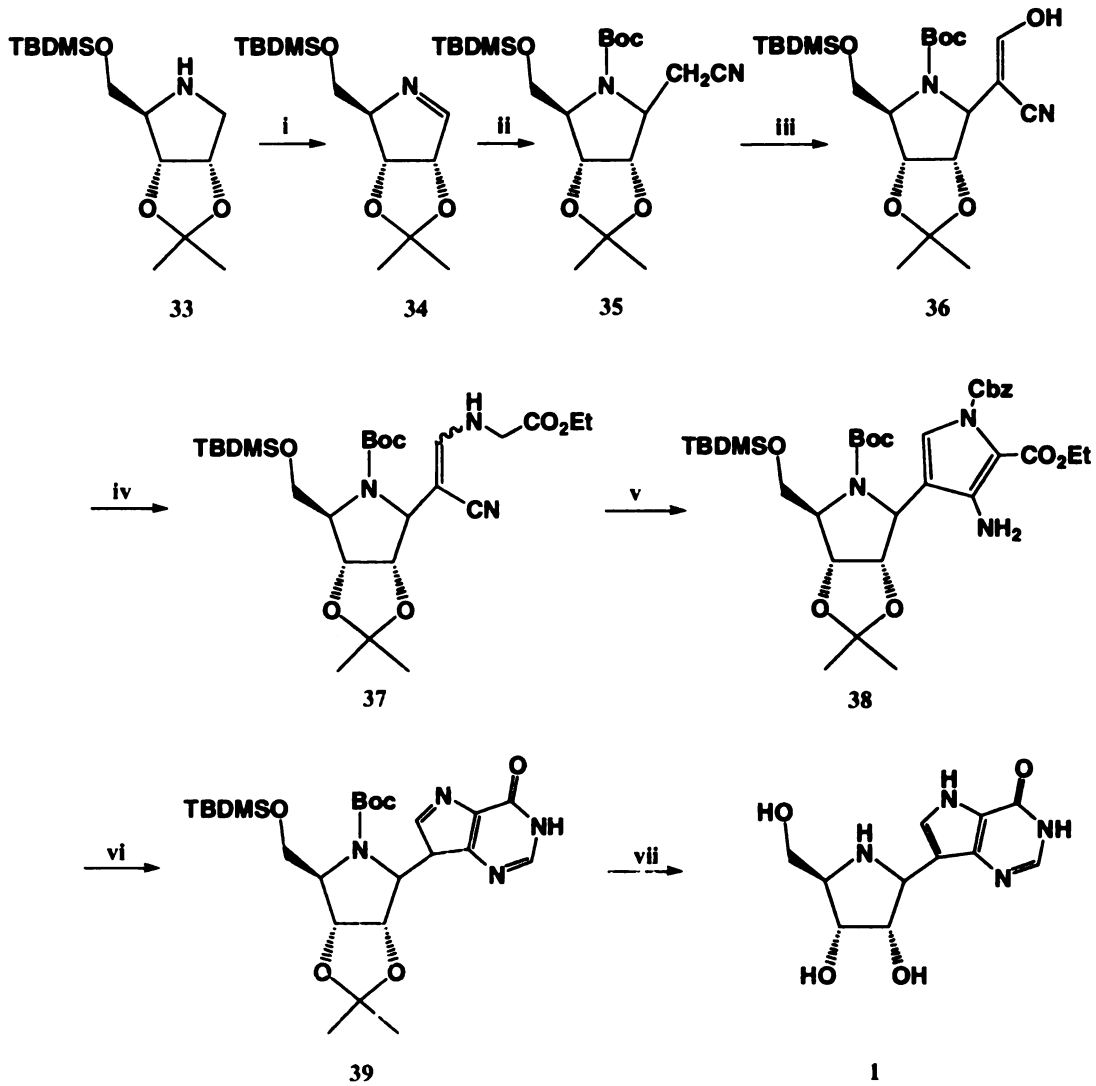

Figure 4.5. Synthesis of JmmH. i, a, NCS, pentane; b, LiTMP, -78°C; ii, a, $CNCH_2MgX$ or $CNCH_2Li$; b, $(Boc)_2O$; iii, a, t-$BuOCH(NMe_2)_2$, DMF, 70°C; b, THF, HOAc, H_2O; iv, $H_2NCH_2COOEt.HCl$, NaOAc, MeOH; v, $ClCO_2Bn$, DBU, CH_2Cl_2, reflux; vi, a, H_2, Pc/C, EtOH; b, $H_2NCH{=}NH.HOAc$, EtOH, reflux; vii, TFA.

Imino sugars hold tremendous promise as well as tremendous challenges for drug development targeting glycosyl transferases and glycosidases. Unfortunately, none of the ones obtainable from natural sources are readily functionalizable in ways that can augment their activity or enhance or alter their specificity. There is therefore a great need

for scaffolds and the synthetic methodology that allow the development of drugs that target these enzymes. There is no general strategy for the preparation of imino-sugar based transition state nucleoside sugar mimetics. Aromatic groups, carboxylic acid, alcohol or amino groups strategically placed at the anomeric position are not present in the naturally occurring or synthetic compounds that have been described in the literature. Those functional groups allow modifications and functionalizations that alter binding or specificity. None of the naturally occurring or synthetic candidates contain ring systems in positions that allow the modification of the solubility, polarity, dipole moment, polarizability or general steric bulk or shape of candidates without affecting the recognition role of the hydroxyl groups. These considerations are all important in tuning the biological properties of drugs. Therefore, our strategy for developing inhibitors to enzymes that process ribosides through the formation of an oxocarbenium intermediate is to tether the aglycon analogue structures to the iminoalditol moiety so that the two are in a relative orientation reflecting bond making and breaking at the transition state (**figure 4.1**). Structures that integrate the key structural features of the ribosyl cation and have provision for the easy integration of the glycosidically linked components were therefore developed. To this end, synthetic strategies aimed at preparing the hexahydro-pyrrolothiazines **40** and **41a** were designed. The ester function can be readily transformed to a free acid making the coupling to a variety of aglycon analogues via ester, amide or other linkages possible. Alternatively the carboxylate group can be converted to an alcohol function thus expanding the number of linkage possibilities. The phenyl ring can be easily modified to tether aglycon analogs, the length and type of tether can be adjusted to provide the flexibility. The aromatic moiety also provides aspect of the environment of

purine base in PNP and related enzymes. A related compound with the targeted structure **42a** was prepared to facilitate conformational studies through crystallography and to allow evaluation of the ring fusion on the biological activity of the iminopentitol component.

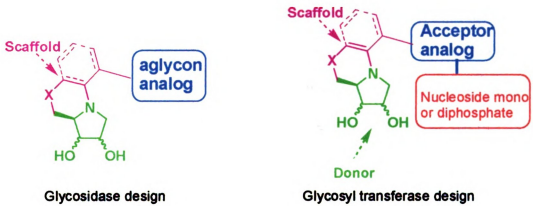

Figure 4.6. Architecture of glycosidase and transferase inhibitors based on dihydroxyhexahydropyrrolothiazine scaffold.

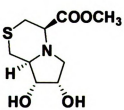

40

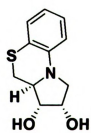

41a

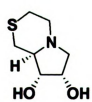

42a

4.2. Results and Discussions

4.2.1. Synthesis of Iminopentitol Derivatives

The synthesis of compound **40** starting from D-ribose **43** is illustrated in **figure 4.7**. Treatment of D-ribose with methanol and an acid catalyst yielded the methyl glycoside **44** which was converted to the 5-bromo-5-deoxy riboside **45** by treatment with carbon tetrabromide and triphenylphosphine. Compound **45** was transformed to its 2, 3-dipivaloyl derivative **46** oxidation of which with chromium trioxide yielded the 5-bromo-5-deoxy-4-ulosonic acid methyl ester **47**. Chromium trioxide can oxidize both α- and β-protected ribosides to keto esters[18]. Therefore, both isomers can be used as the starting materials unlike the case with the pyranosides where only the β-isomer can be oxidized. Reaction of **47** with L-cysteine methyl ester hydrochloride in mild base followed by reduction with cyanoborohydride yielded the lactam **48** and uncyclized product **49**. The lactam **48** was readily reduced with borane and deacylated to the desired compound **40**.

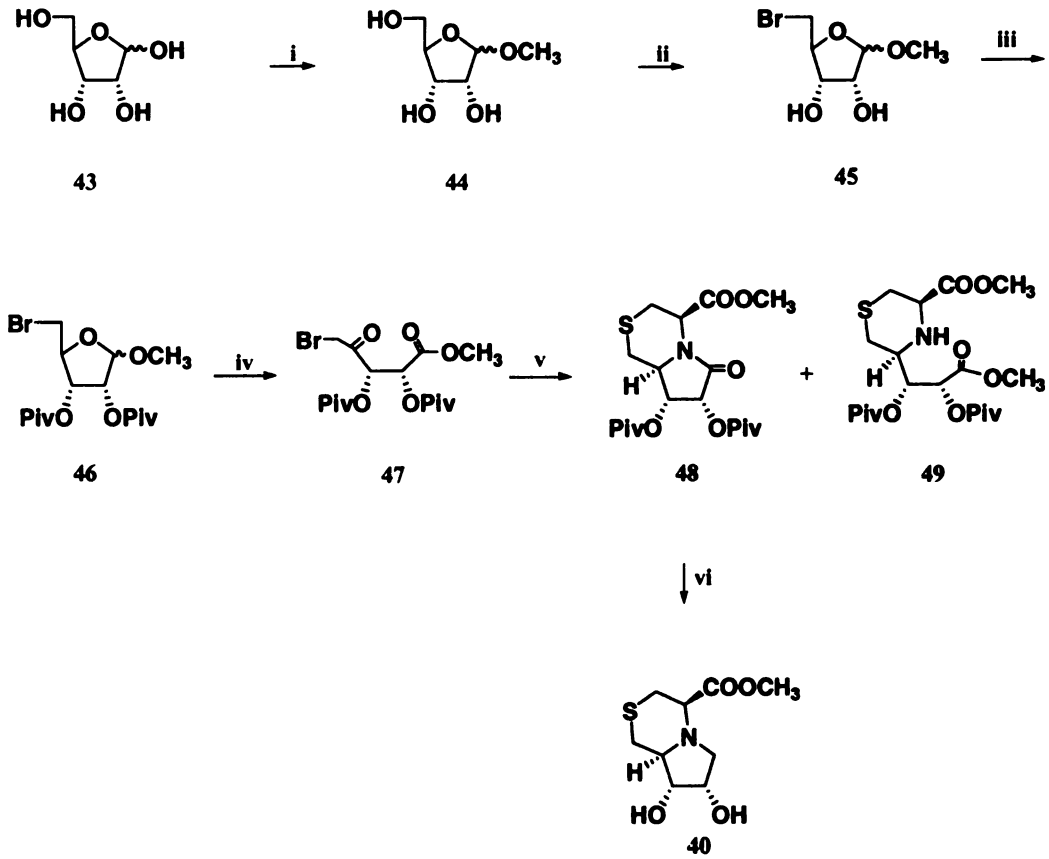

Figure 4.7. Synthesis of compound **40**. i. HCl/MeOH; ii. Ph_3P, CBr_4, pyridine, 86.7% for 2 steps; iii PivCl, pyridine, 91.1%; iv. CrO_3, Ac_2O, HOAc, 96.6%; v. (1) cysteinmethyl ester hydrochloride, $NaHCO_3$, CH_3OH, (2) $NaCNBH_3$, CH_3OH; (3) Na_2CO_3, CH_2Cl_2, 32% for 3 steps; vi. (1) BH_3-THF; (2) $NaOCH_3$, CH_3OH, 81% for 2 steps.

The synthesis of product **41a** was attempted by treating the 5-bromo-5-deoxy-4-ulosonic acid methyl ester **47** with aminothiophenol followed by the reduction, cyclization and deprotection. Lactams **50a** and **50b** and some uncyclized product were formed with the L-*lyxo* configuration lactam **50b** as the major product (**figure 4.8**). This was indicated by a small ~3Hz coupling constant of the three protons of the aza-ribo moiety.

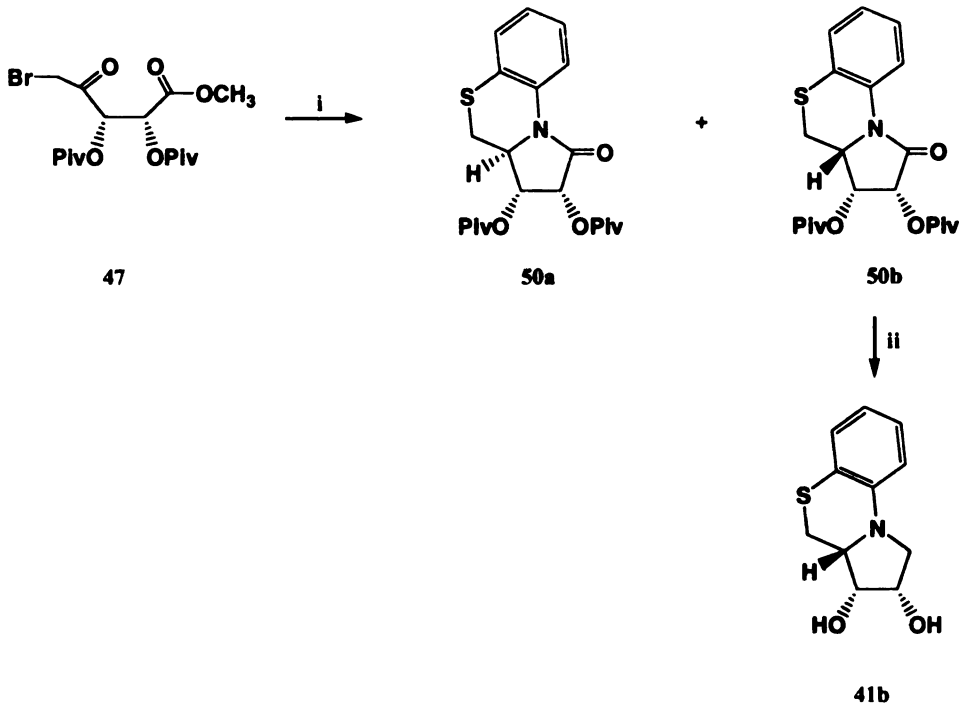

Figure 4.8. Synthesis of compound **41b.** i. (1) 2-aminothiophenol, CH_3OH; (2) $NaCNBH_3$, CH_3OH; (3) Na_2CO_3, CH_2Cl_2, 67% for 2 steps; ii. (1) BH_3-THF; (2) $NaOCH_3$, CH_3OH, 90.9% for 2 steps.

A similar scheme (**figure 4.9**) was used in an attempt to prepare compound **42a** except that aminoethanethiol was used instead of cysteinemethyl ester. In this case two other products were obtained namely the compound with the alternative configuration of the carbon at the ring junction (**52b**) and an elimination product **53**. Conditions under which the elimination product was not formed were developed. Basic conditions were avoided by adding sodium cyanoborohydride / trifloroacetic acid at the same time as the aminoethanethiol. Only lactam **52a** and **52b** were formed with the desired compound being the minor component (20% yield for lactam **52a**) based on the coupling constants of the three protons of the azasugar ring. The formation of the elimination product was

suppressed the sooner sodium cyanoborohydride was added after mixing compound **47** and the aminoethanethiol.

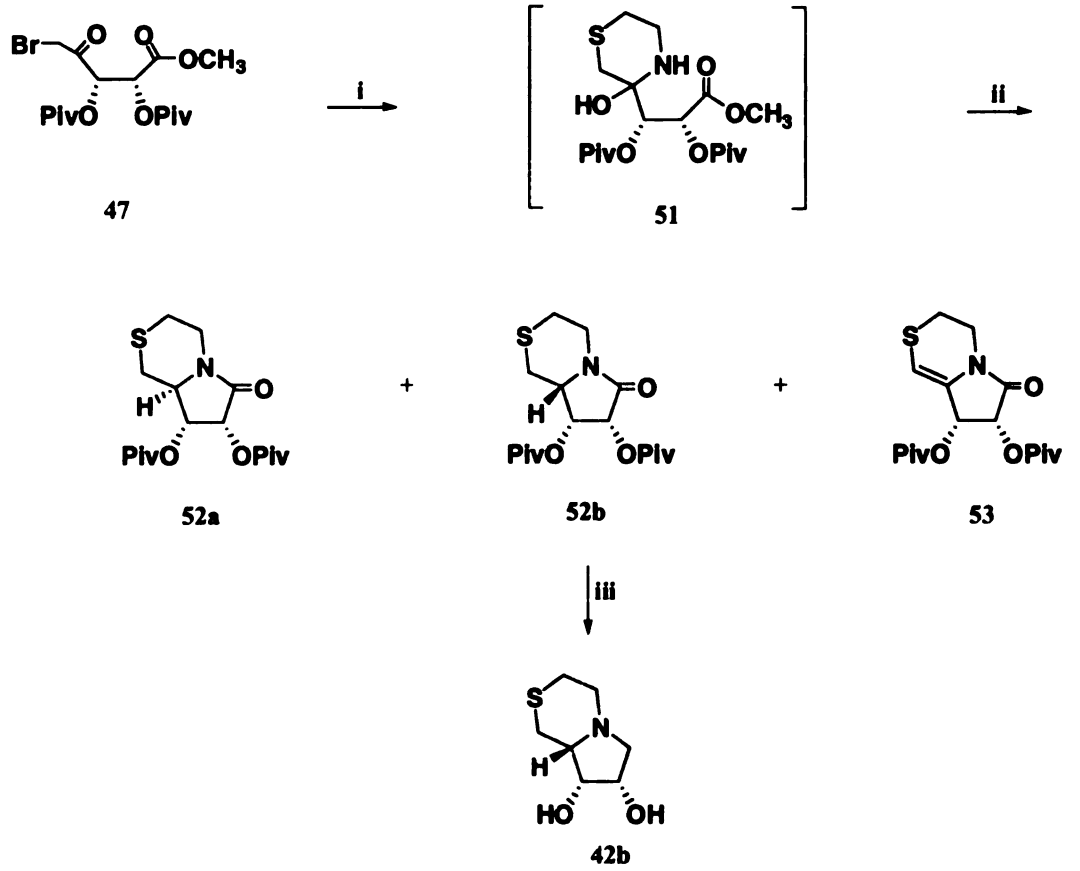

Figure 4.9. Synthesis of compound **42b.** i. $HS(CH_2)_2NH_2$, CH_3OH; ii. $NaCNBH_3$, CF_3COOH, 57% for 2 steps; iii. (1) BH_3-THF; (2) $NaOCH_3$, CH_3OH, 85% for 2 steps.

The crystal structures of compounds **41b, 42b** and **53** were obtained (**figures 4.10a, b, and c**). This allowed the definitive identification of the correct stereochemistry of the intermediate lactams. The X-ray structure of compound **53** confirmed the presence of a double bond. It also indicated that the ethylene fragment bridging the two heteroatoms in **53** could take either of two possible orientations. These structures are invaluable from a computation and modeling perspective. They provided information on the geometry

about the ring junction, and allowed more than one geometrical perspective on how attaching an aglycon analogue to **40** and **41** (**a** or **b**) would satisfy the geometric constraints of an actual substrate. They also served as benchmarks in the evaluation how reliably semi-empirical methods and molecular mechanics methods described the geometry and conformational preferences of this class of molecules. Although in one case the desired D-*ribo* analog was not obtained as the major product, the evaluation of geometric constraints on the placement of the aglycon moiety was still favorable based on the x-ray analysis and computational studies.

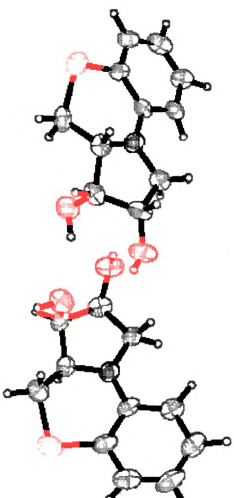

a

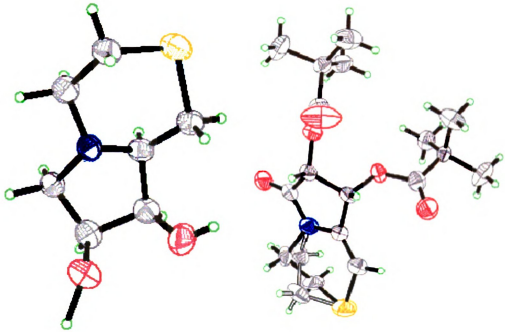

b c

Figure 4.10 (a) Ortep drawing of X-ray structure of **41b.** (b) Ortep drawing of X-ray structure of **42b.** (c) Ortep drawing of X-ray structure of **53.**

As reported earlier, the structures of the PNP imino-sugar inhibitor Imm-H (1,4-dideoxy-1,4-imino-1-(S)-(9-deazahypoxanthin-9-Yl)-D-ribitol)[8] and a formycin-A derivative (1-C-(7-amino-1H-pyrazolo[4,3-d]pyrimidin-3-yl)-1,4-anhydro-D-ribitol)[19] bound to the active site of the enzyme have been determined by X-ray crystallography. These structures were used as starting points for determining the proper orientation of the aglycon and deciding the structural and geometric requirements of the tether and the aglycon analogue. **Figures 4.11a** shows the crystal structure of ImmH and **figure 4.11b** shows the superimposition of the crystal structures of **42b** and ImmH. The asterisk indicates the hydrogen atom that is replaced by a carboxymethyl group in compound **40** or a phenyl group in **41** (**a** or **b**). Molecular mechanics models based on these X-ray

structures indicate that the choice of cysteine isomer (L or D) could be used to position the aglycon analog at the appropriate position above (as is the case with PNP inhibitors) or below the plane of the iminopentitol ring respectively. The phenyl group of **41** (**a** or **b**) can also be attached to a variety of aglycons at the proper orientation. The sulfur atom in **42b** is at the same position as the 5-OH of the inhibitors shown in **figures 4.11**. This provides another possibility for modifying this structure at a strategic point by oxidizing the sulfur to a sulfoxide or a sulfone. The negative charge of the sulfone oxygen can stabilize some transition states where the 5-position of the sugar ring might be phosphorylated.

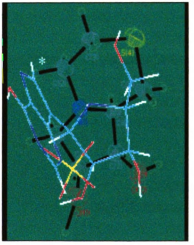

Figure 4.11. (a) X-ray derived structure of 1,4-dideoxy-1,4-imino-1-(S)-(9-deazahypoxanthin-9-Yl)-D- ribitol (b) Comparison of X-ray structure **42b** and 1,4-dideoxy-1,4-imino-1-(S)-(9-deazahypoxanthin-9-Yl)-D- ribitol.

4.2.2. Inhibitory Activity of Iminopentitol Derivatives

Compounds **40**, **41b** and **42b** were tested against bacterial produced β-ribosidase. The mechanism of action of β-ribosidase also features the ribooxocarbenium ion transition state, similar to riboside hydrolase, phosphorylase and related enzymes. In this assay,

3',4'-dihydroxyflavone-4'-β-D-ribofuranoside **54** (DHF-riboside) was used as the substrate[20]. This chromogenic substrate can be hydrolyzed by β-ribosidase-producing bacteria to release 3',4'-dihydroxyflavone, which forms a chelate with iron (**55**). The assay was performed in phosphate buffered saline (PBS) at pH 7.0. *P. aeruginosa 27853* and *Salmonella sp.35664* strains were used to produce β-ribosidase. Both whole cell and lysed strain were tested. Inhibition studies were performed by adding the inhibitor to a final concentration of 0.2μg/μL to 15μg/μL to the respective buffer solutions along with DHF-riboside and ferric ammonium citrate. Each strain was grown and added to each buffer solution containing substrate and inhibitor. The solutions were incubated at 37°C and the absorbance of this complex **55** was determined at 387 nm.

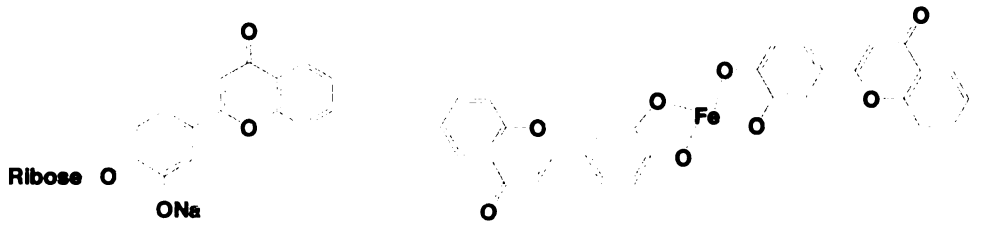

55

Figure 4.12. (a) Structure of 3',4'-dihydroxyflavone-4'-β-D-ribofuranoside sodium salt **54** and (b) the putative chelate **55** formed with iron after enzymatic hydrolysis.

Figure 4.13 is the absorbance of the chelate **55** produced in the lysate assay with inhibitor **41b** concentration from 0 ~ 15 μg/μL and **figure 4.14** is the similar plot for the whole cell assay. The results showed compound **41b** has good inhibitory activity against β-ribosidase produced from strain. About 70% inhibition at concentration 15 μg/μL

(67mM) at 24 hours for both whole cell and lysate was observed. At concentration 7.5 μg/μL, about 50% inhibition was observed. Compound **40** and **42b** have no significant inhibition for the same strain. These results suggest that phenyl group in compound **41b** represents an important factor for the activity. The phenyl ring increases the hydrophobicity of the inhibitor, which enhance the affinity towards enzyme. The increased hydrophobicity also makes it easy to penetrate the cell membrane. The same inhibition observed for compound **41b** in the lystate and whole cell experiments demonstrates the easy uptake through the cell envelope. It is also important to note that with increasing concentration of the inhibitor, lysate experiment showed inhibition gradually, while the whole cell experiment showed inhibition only after certain inhibitor concentration. It suggests that the inhibitor needs to reach some concentration in the cell to start inhibition.

The activity of compound **41b** against ribosidase demonstrated that these iminopentitol scaffolds can provide key features of the ribosyl cation, which represents an important state of a variety of nucleoside related enzymes. These scaffolds are also easy to couple with all kinds of aglycon analogs, such as bases and phosphate groups. It opens up possibilities to the preparation of a wide range of biological important compounds.

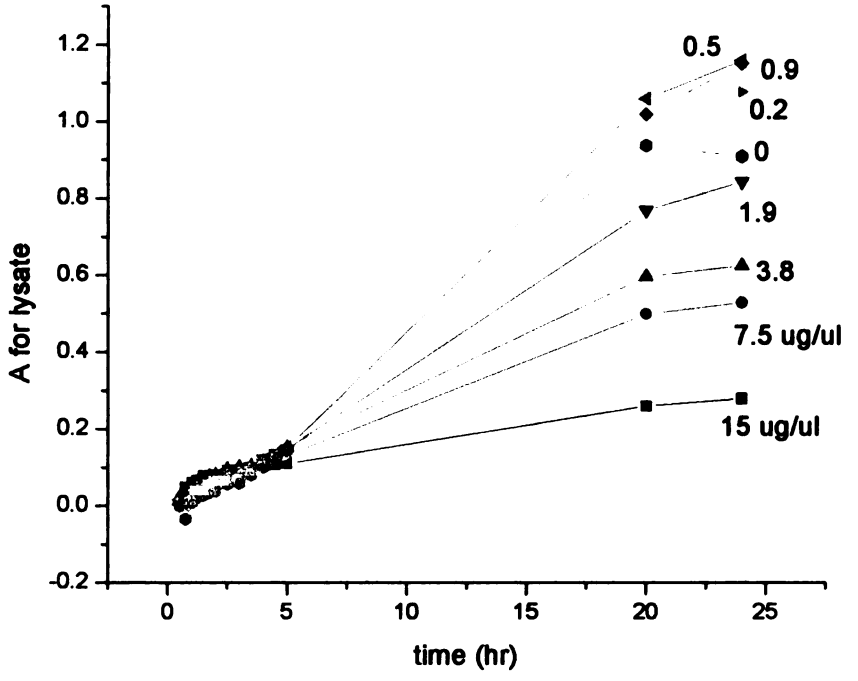

Figure 4.13. Aabsorbance of the chelate **55** produced in the lysate assay with inhibitor **41b** concentration from 0 ~ 15 μg/μL

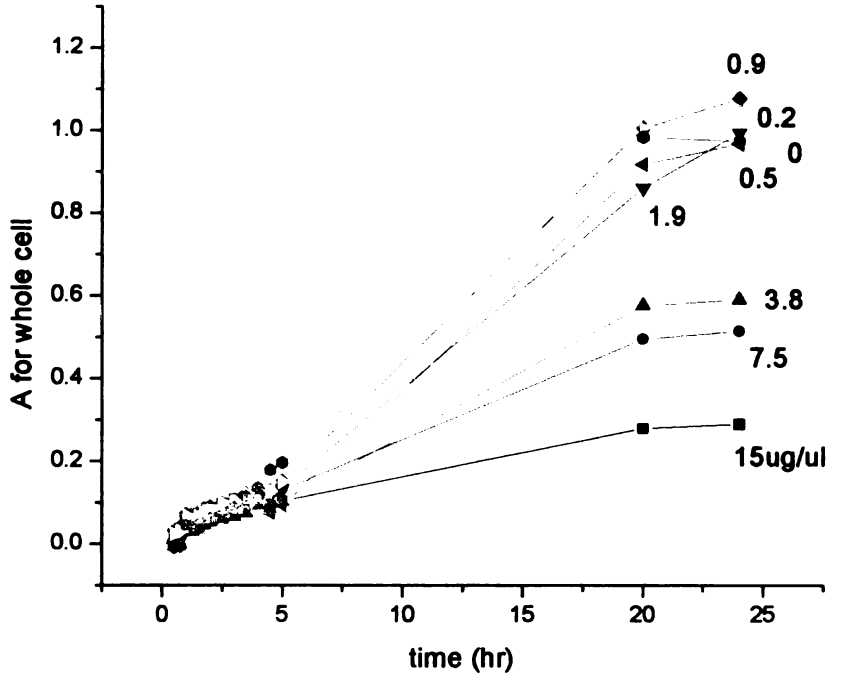

Figure 4.14. Absorbance of the chelate **55** produced in the whole cell assay with inhibitor **41b** concentration from 0 ~ 15 μg/μL

In conclusion, novel hetero bicyclic aza-sugars **40** and **41b** have been designed and synthesized. The relatively easy synthesis constitutes a general approach to bicyclic structures with either natural or unnatural stereochemistry. This strategy provides an easy access to preparation of iminopentitol scaffolds for ribosidase, phosphorylase and related enzyme inhibitors. With an iminopentitol moiety, an ester function or phenyl group and a heteroatom, sulfur, a variety of aza-sugar with different aglycon and their analogues can be synthesized. Those functional groups make the preparation of compound libraries with different aglycon analogues possible.

Based on computational and modeling studies, the conformation of the iminopentitol ring in these bicyclic systems and the general presentation of the hydroxyl groups and the additional ring residue match closely the structures of the known inhibitors. The inhibition studies show the activity of this kind of compounds against β-ribosidase, and indicate the importance of the ribooxocarbenium ion mimicry and hydrophobicity for the inhibition. These iminopentitol scaffolds therefore provide key features of the ribosyl cation and easy integration of an aglycon component. The possibility of obtaining the L-*lyxo* conformation and the fact that such derivative is still active against ribosidase really expand the scope of this approach.

4.3. Experimental Section

4.3.1. General Procedures

IR spectra were recorded on a Nicolet 710 FT-IR instrument. The ^{1}H (and ^{13}C) NMR spectra were recorded at 500 MHz (125.5 MHz for 13-C) on a Varian VXR spectrometer. The HRMS FAB mass spectra were obtained using a Jeol HX-110 double-focusing mass spectrometer operating in positive ion mode.

4.3.2. Inhibition Assay

Inhibitory potency of **40**, **41b** and **42b** were determined by spectrophotometrically measuring the residual hydrolytic activities of the bacterial produced β-ribosidase. The bacteria used to produce β-ribosidase were *P. aeruginosa 27853* and *Salmonella sp.35664,* both whole cell and lysed strains. 3',4'-Dihydroxyflavone-4'-β-D-ribofuranoside **54** (DHF-riboside) was used as substrate[20]. The assay was performed in a PBS buffer at pH 7.0, 37°C. Serial dilutions were made of the inhibitors to a final concentration of 0.2μg/μL to 15μg/μL in each assay solution. Each strain was grown to mid exponential phase and removed from the media and rediluted in PBS buffer. Inhibition studies were performed by adding each strain to the respective buffer solutions along with DHF-riboside, ferric ammonium citrate and inhibitors. For compound **41b**, 10% DMSO solution was used to increase the solubility. The solutions were incubated at 37°C and the absorbance of the complex formed between released 3',4'-dihydroxyflavone and iron was determined at 387 nm at time 15min, 30min, 45min, 60min, 75min, 90min, 105min, 2hours, 2.5hours, 3.0hours, 4.0hours, 4.5hours, 5hours, 20hours, and 24hours.

Methyl 5-Bromo-5-deoxy-D-ribofuranoside (45) A solution of D-ribose **43** (15g, 0.1mol) and hydrochloric acid (15mL) in methanol (1500mL) was stirred at room

temperature for 20 hours, followed by addition of sodium carbonate (5g, 0.06mol). The reaction mixture was stirred for 2 hours and two thirds of the solvent was removed at a temperature of less than 30°C. The mixture was filtered and concentrated. The resulting methyl D-riboside **44** was obtained as yellow oil and was used without further purification. To a stirred solution of **44** (5g, 30mmol) in anhydrous pyridine (300mL) at 0°C were added triphenylphosphine (16.0g, 60mmol) and carbon tetrabromide (18.0g, 50mmol). The resulting mixture was protected from moisture and stirred at 0°C for ten minutes. The mixture was then allowed to warm to 65°C and was stirred for 6 hours. Methanol (10mL) was added to decompose any excess reagent. The solvent was removed by evaporation and the residue was dissolved in dichloromethane and was then passed though a pad of silica gel. Dichloromethane was removed by evaporation and the resulting residue was dissolved in toluene and the product was extracted with water for several times. Removal of water afforded the expected mixture of methyl 5-Bromo-5-deoxy-α- and β-D-ribofuranoside **45** (6.0g, 86.7%, α:β = 3:1). IR ($CHCl_3$) ν_{max} 3387.18, 2933.49, 1121.60, 1088.32, 1025.91 cm^{-1}. The mixture was used in the next step without separating the anomer: **Methyl 5-Bromo-5-deoxy-α-D-ribofuranoside** ^1H NMR (500MHz, D_2O) δ 4.86, (1H, s), 4.19-4.13 (2H, m), 4.02 (1H, d, *J*=5 Hz), 3.64 (1H, dd, *J*=11, 4.3 Hz), 3.53 (1H, dd, *J*=11.5, 6.3 Hz), 3.35 (3H, s); ^{13}C NMR (125.5MHz, D_2O) 108.14, 81.73, 74.62, 73.12, 55.44, 34.22 ppm. **Methyl 5-Bromo-5-deoxy-β-D-ribofuranoside** ^1H NMR (500MHz, D_2O) δ 4.97, (1H, d, *J*=4.5 Hz), 4.22 (1H, m), 3.93 (1H, m), 4.15-4.11 (1H, m), 4.01 (1H, m), 3.57 (2H, m), 3.38 (3H, s); ^{13}C NMR (125.5MHz, D_2O) 103.68, 82.98, 71.68, 70.98, 55.77, 33.45 ppm.

Methyl 5-Bromo-5-deoxy-2,3-di-*O*-trimethylacetyl-D-ribofuranoside (46) Pivaloylation of **45** (2.0g, 8.8mmol) by trimethylacetyl chloride (4.34mL, 35.0mmol) in pyridine (150mL) at room temperature for 2 days afforded a white solid **46** (3.2g, 91.1%), IR ($CHCl_3$) ν_{max} 2972.45, 1739.35, 1162.70, 1139.15 cm^{-1}. The mixture was used in the oxidation step without separating the anomer: **Methyl 5-Bromo-5-deoxy-2,3-di-*O*-trimethylacetyl-α-D-ribofuranoside** ^1H NMR (500MHz, $CDCl_3$) δ 5.25, (1H, m), 5.20 (1H, d, *J*=4.5 Hz), 4.82 (1H, s), 4.28, (1H, m), 3.47 (2H, t, *J*=6.5 Hz), 3.37 (3H, s), 1.19 (9H, s), 1.16 (9H, s); ^{13}C NMR (125.5MHz, $CDCl_3$) 177.12, 176.93, 106.24, 80.04, 74.90, 74.05, 55.21, 38.82, 38.67, 33.52, 27.05 ppm. **Methyl 5-Bromo-5-deoxy-2,3-di-*O*-trimethylacetyl-β-D-ribofuranoside** ^1H NMR (500MHz, $CDCl_3$) δ 5.17, (1H, d, *J*=4 Hz), 5.04 (1H, m), 4.90 (1H, m), 4.22 (1H, m), 3.64 (1H, dd, *J*=11, 4 Hz), 3.55 (1H, dd, *J*=11, 4.5 Hz), 3.35 (3H, s), 1.19 (9H, s), 1.18 (9H, s); ^{13}C NMR (125.5MHz, $CDCl_3$) 177.76, 177.47, 101.02, 80.46, 74.05, 71.96, 55.59, 38.82, 38.66, 33.06, 27.05 ppm.

Methyl 5-Bromo-5-deoxy-2,3-di-*O*-trimethylacetyl-D-*erythro*-4-pentulosonic acid methyl ester (47) Chromium trioxide (2.43g, 24.3mmol) was added to a solution of **46** (3.2g, 8.1mmol) in acetic acid (100mL) and acetic anhydride (10mL). The suspension was stirred at room temperature for 2 hours. The mixture was then poured slowly into cold water (500mL). The water was extracted 5 times with CH_2Cl_2 and the combined organic phase was washed with brine, saturated sodium bicarbonate and dried (Na_2SO_4). The solution was passed through a small pad of silica gel to remove coloration due to chromium salts and dried to give **47** as a colorless oil (3.2g, 96.6%). IR ($CHCl_3$) ν_{max} 2975.59, 1745.62, 1125.06 cm^{-1}. ^1H NMR (500MHz, $CDCl_3$) δ 5.86, (1H, d, *J*=3.0 Hz),

5.70 (1H, d, J=2.5 Hz), 4.08 (1H, d, J=13 Hz), 4.01 (1H, d, J=12.5Hz), 3.76 (3H, s), 1.24 (9H, s), 1.20 (9H, s); ^{13}C NMR (125.5MHz, $CDCl_3$) δ 195.60, 176.62, 176.36, 166.72, 74.88, 71.54, 52.86, 38.83, 38.71, 31.28, 26.87 ppm; HRFABMA (M + H^+) Calcd. 409.0862, found 409.0863.

7(S),8(R),9(S)-bis(trimethylacetoxy)-6-oxo-hexahydro-pyrrolo-[1,4]-thiazine-4-carboxylic acid methyl ester (48) A solution of **47** (1.0g, 2.4mmol), sodium bicarbonate (0.25g, 2.4mmol) and cysteinmethyl ester hydrochloride (0.5g, 2.9mmol) in methanol (100 mL) was stirred at room temperature for one hour, followed by addition of sodium cyanoboronhydride (0.23g, 3.7mmol). The reaction mixture was stirred overnight and concentrated. The resulting residue was dissolved in dichloromethane and sodium carbonate was added to facilitate the lactam cyclization. After stirred for overnight, the suspension was filtered and the dichloromethane solution was washed by brine and dried (Na_2SO_4), concentrated. The residue was purified by column chromatography (6:1 Hexanes/Ethyl acetate) to yield lactam **48** (0.3g, 32.0%) and the uncyclized product **49** (0.5g, 53.0%).

Lactam **48** was given as a white solid. IR ($CHCl_3$) ν_{max} 1745.80, 1728.75, 1161.29 cm^{-1}. ^1H NMR (500MHz, $CDCl_3$) δ 5.61 (1H, m), 5.58 (1H, d, J=5.5 Hz), 4.13 (1H, dt, J=11.5, 3.5 Hz), 3.78 (3H, s), 3.13 (1H, dt, J=14, 2.3 Hz), 2.88 (1H, dd, J=13.8, 4.3 Hz), 2.69 (1H, dd, J=13.5, 11.5 Hz), 2.43 (1H, dt, J=13.5, 2.3 Hz), 1.23 (9H, s), 1.23 (9H, s); ^{13}C NMR (125.5MHz, $CDCl_3$) δ 176.94, 176.89, 169.25, 168.55, 69.05, 68.07, 55.07, 52.88, 52.33, 39.11, 38.82, 28.59, 27.21, 27.07, 26.63 ppm; HRFABMA (M + H^+) Calcd. 416.1743, found 416.1742.

Compound **49** was given as a white solid. IR ($CHCl_3$) ν_{max} 1740.01, 1736.18, 1155.51 cm^{-1}. ^1H NMR (500MHz, $CDCl_3$) δ 5.38 (1H, d, *J*=7.5 Hz), 5.16 (1H, dd, *J*=9, 3 Hz), 3.71 (3H, s), 3.70 (3H, s), 3.36 (1H, m), 2.64 (1H, m), 2.51-2.31 (4H, m), 1.22 (9H, s), 1.15 (9H, s); ^{13}C NMR (125.5MHz, $CDCl_3$) δ 177.14, 176.93, 171.43, 167.36, 73.79, 70.30, 59.34, 56.00, 52.32, 52.18, 38.86, 38.75, 29.40, 28.42, 27.00, 26.97 ppm;

7(S),8(R),9(S)-dihydroxy-hexahydro-pyrrolo-[1,4]-thiazine-4-carboxylic acid methyl ester (40) A solution of lactam **48** (0.16g, 0.42mmol) and BH_3-THF (3.5mL, 5.3mmol) in anhydrous THF (10mL) was refluxed for 8 hours and NMR showed the completion of the reduction. The solvent was removed and methanol was added and concentrated for 3 times. The residue was dissolved in methanol (20mL), followed by addition of NaOMe (0.06g, 1.1mmol). The reaction was stirred for overnight and concentrated. The residue was applied to an ion exchange column (Dowex 50WX8-400, 2g), which was washed with water (30 mL) and eluted with 2N NH_4OH (30mL). The elution was concentrated and purified by column chromatography (15:1 CH_2Cl_2/MeOH) to afford a white solid (0.08g, 81%); ^1H NMR (500MHz, $CDCl_3$) δ 4.34-4.30 (1H, m), 3.98 (1H, m), 3.69 (3H, s), 3.43 (1H, d, *J*=11 Hz), 3.23 (1H, d, *J*=9.3 Hz), 2.98 (1H, dd, *J*=14, 4 Hz), 2.84 (1H, dd, *J*=13.8, 3.3 Hz), 2.79-2.74 (1H, m), 2.71 (1H, d, *J*=13 Hz), 2.43 (1H, d, *J*=13 Hz); ^{13}C NMR (125.5MHz, $CDCl_3$) δ 173.53, 72.50, 68.62, 59.11, 58.60, 55.42, 52.29, 28.46, 26.47; HRFABMA ($M + H^+$) Calcd. 234.0800, found 234.0799.

Lactam 50a and **50b** A solution of **47** (2.0g, 4.9mmol) and 2-aminothiophenol (0.73g, 5.9mmol) in methanol (150 mL) was stirred at room temperature for one hour, followed

by addition of sodium cyanoboronhydride (0.56g, 7.3mmol). The reaction mixture was stirred overnight and concentrated. The resulting residue was dissolved in dichloromethane and sodium carbonate was added to facilitate the lactam cyclization. After stirred for overnight, the suspension was filtered and the dichloromethane solution was washed by brine and dried (Na_2SO_4), concentrated. The residue was purified by column chromatography (10:1 Hexanes/Ethyl acetate) to yield two lactam diastereomers

Product **50a** (0.13g, 9.6%) was given as a white solid. IR ($CHCl_3$) ν_{max} 2973.71, 1738.05, 1145.55 cm^{-1}. ^1H NMR (500MHz, $CDCl_3$) δ 8.06 (1H, d, *J*=8 Hz), 7.15-7.06 (3H, m), 5.63 (1H, t, *J*=7.5 Hz), 5.51 (1H, d, *J*=7 Hz), 4.34 (1H, m), 3.17 (1H, t, *J*=12 Hz), 2.96 (1H, dd, *J*=13, 2.5 Hz), 1.27 (9H, s), 1.25 (9H, s); ^{13}C NMR (125.5MHz, $CDCl_3$) δ 177.42, 177.22, 165.28, 132.20, 126.11, 125.75, 124.76, 123.42, 72.97, 71.27, 54.66, 38.87, 38.74, 27.10, 26.95 ppm; HRFABMA (M + H^+) Calcd. 406.1689, found 406.1689.

Product **50b** (0.71g, 57.4%) was given as a white solid. IR ($CHCl_3$) ν_{max} 2972.76, 1742.61, 1155.27 cm^{-1}.; ^1H NMR (500MHz, $CDCl_3$) δ 8.72 (1H, dd, *J*=8.5, 1 Hz), 7.14 (1H, dd, *J*=8, 1.5 Hz), 7.10 (1H, td, *J*=8, 1.5 Hz), 6.99 (1H, td, *J*=7.5, 1.5 Hz), 5.72 (1H, t, *J*=4.8 Hz), 5.65 (1H, d, *J*=5.5 Hz), 4.32 (1H, m), 3.14 (1H, dd, *J*=13, 10.5 Hz), 2.88 (1H, dd, *J*=13, 2.5 Hz), 1.24 (9H, s), 1.21 (9H, s); ^{13}C NMR (125.5MHz, $CDCl_3$) δ 177.14, 176.94, 166.79, 133.69, 127.32, 125.76, 124.51, 121.12, 120.41, 68.96, 67.89, 57.38, 39.18, 38.87, 27.16, 27.08, 25.01; HRFABMA (M + H^+) Calcd. 406.1689, found 406.1691.

1(S) 2(R), 3(S)-dihydroxy-2,3,3a,4-tetrahydro-1H-pyrrolo-[2,1-c][1,4]benzothiazine (41b) A solution of lactam **50b** (0.40g, 1.0mmol) and BH_3-THF (3.3mL, 5.0mmol) in anhydrous THF (10mL) was refluxed for 4 hours and the TLC and NMR showed the completion of the reduction. The solvent was removed and methanol was added and concentrated for 3 times. The residue was dissolved in methanol (20mL), followed by addition of NaOMe (0.20g, 3.8mmol). The reaction was stirred for 8 hours and concentrated. The residue was purified by column chromatography (15:1 CH_2Cl_2/MeOH) to afford a white solid (0.2g, 90.9%). IR ($CHCl_3$) ν_{max} 3113.94, 1124.86 cm^{-1}. ^1H NMR (500MHz, CD_3OD) δ 6.93 (2H, d, *J*=7.5 Hz), 6.48 (1H, td, *J*=7.5, 1 Hz), 6.41 (1H, d, *J*=8 Hz), 4.37 (1H, m), 4.11 (1H, t, *J*=3.8 Hz), 3.80 (1H, dt, *J*=10.5, 3 Hz), 3.51 (1H, t, *J*=8.5 Hz), 3.15 (1H, t, *J*=8.5 Hz), 2.96 (1H, m), 2.85 (1H, dd, *J*=12.5, 3 Hz); ^{13}C NMR (125.5MHz, CD_3OD) δ 146.55, 130.93, 129.84, 119.67, 119.18, 115.14, 77.05, 74.25, 65.67, 55.75, 27.99 ppm; HRFABMA ($M + H^+$) Calcd. 224.0745, found 224.0745.

7(S),8(R),9(S)-hexahydro-bis-trimethylacetoxy-1H-pyrrolo-[1,4]-thiazin-6-one (52a) and 7(S),8(R),9(R)-hexahydro-bis-trimethylacetoxy-1H-pyrrolo-[1,4]-thiazin-6-one (52b): A solution of **47** (0.8g, 2.0mmol), $HS(CH_2)_2NH_2$ (0.18g, 2.3mmol) and $NaCNBH_3$ (0.18g, 2.9mmol) in methanol (50 mL) was stirred at room temperature for 24 hours and then concentrated. The resulting residue was dissolved in dichloromethane and washed by brine, dried (Na_2SO_4) and concentrated. Compound **52a** and **52b** were isolated by column chromatography (4:1 Hexanes/Ethyl acetate).

Product **52a** (0.12g, 20%) was obtained as a white solid. IR ($CHCl_3$) ν_{max} 1739.70, 1717.38, 1160.52, 1136.98 cm^{-1}. ^1H NMR (500MHz, $CDCl_3$) δ 5.34 (1H, d, *J*=7 Hz),

5.09 (1H, dd, J=7, 2.3 Hz), 4.44 (1H, dt, J=13.5, 2.8 Hz), 3.60 (1H, dt, J=11, 2.5 Hz), 3.02 (1H, m), 2.75 (1H, d, J=13 Hz), 2.62-2.51 (2H, m), 2.42 (1H, m), 1.20 (9H, s), 1.16 (9H, s); ^{13}C NMR (125.5MHz, $CDCl_3$) δ 177.41, 177.06, 166.64, 70.12, 68.15, 62.27, 42.24, 38.83, 38.76, 30.10, 27.11, 26.97, 26.41 ppm; HRFABMA (M + H^+) Calcd. 358.1689, found 358.1688. Product **52b** (0.40g, 57%) was obtained as a white solid. IR ($CHCl_3$) ν_{max} 1739.61, 1705.31, 1141.03 cm^{-1}. ^1H NMR (500MHz, $CDCl_3$) δ 5.50 (1H, t, J=5 Hz), 5.43 (1H, dd, J=6, 1.5 Hz), 4.43 (1H, dt, J=13.5, 2.8 Hz), 3.88 (1H, m), 2.97 (1H, m), 2.72-2.64 (2H, m), 2.52 (1H, m), 2.40 (1H, dt, J=13.5, 2.5 Hz), 1.21 (9H, s), 1.20 (9H, s); ^{13}C NMR (125.5MHz, $CDCl_3$) δ 177.03, 176.89, 167.72, 68.78, 67.47, 57.69, 42.23, 39.08, 38.82, 27.31, 27.20, 27.12, 26.97 ppm; HRFABMA (M + H^+) Calcd. 358.1689, found 358.1685. The formation of the elimination product **53** was favored by delaying the addition of sodium cyanoboronhydride. A solution of **47** (1.9g, 4.6mmol) and $HS(CH_2)_2NH_2$ (0.43g, 5.6mmol) in methanol (150 mL) was stirred at room temperature for one hour, followed by addition of sodium cyanoboronhydride (0.44g, 7.0mmol). The reaction mixture was stirred overnight and concentrated. The resulting residue was dissolved in dichloromethane and sodium carbonate was added to facilitate the lactam cyclization. After stirred for several hours, the suspension was filtered and the dichloromethane solution was washed by brine and dried (Na_2SO_4), concentrated. Three products (19, 24.1%; 20, 8.4%; 21, 26.5%) were isolated by column chromatography (4:1 Hexanes/Ethyl acetate). Product **53** (0.44g, 26.5%) was obtained as a yellow solid. IR ($CHCl_3$) ν_{max} 1741.94, 1153.58 cm^{-1}. ^1H NMR (500MHz, $CDCl_3$) δ 5.83 (1H, d, J=6.5 Hz), 5.72 (1H, s), 5.47 (1H, d, J=6.5 Hz), 4.20 (1H, m), 3.67 (1H, m), 2.94-2.89 (2H, m), 1.26 (9H, s), 1.18 (9H, s); ^{13}C NMR (125.5MHz, $CDCl_3$) δ 177.37, 177.08, 167.65,

130.16, 100.02, 67.98, 67.26, 39.91, 38.91, 38.90, 27.14, 26.98, 24.07 ppm; HRFABMA (M^+) Calcd. 355.1454, found 355.1451.

7(S),8(R),9(S)-dihydroxy-hexahydro-1H-pyrrolo-[1,4]-thiazine (42b) A solution of lactam **52b** (0.24g, 0.67mmol) and BH_3-THF (2.2mL, 3.4mmol) in anhydrous THF (10mL) was refluxed for 3 hours and the TLC and NMR showed the completion of the reduction. The solvent was removed and methanol was added and concentrated for 3 times. The residue was dissolved in methanol (20mL), followed by addition of NaOMe (0.10g, 1.9mmol). The reaction was stirred for 8 hours and concentrated. The residue was applied to an ion exchange column (Dowex 50WX8-400, 5g), which was washed with water (30 mL) and eluted with 2N NH_4OH (30mL). The elution was concentrated to afford a white solid (0.1g, 85.0%). ^{1}H NMR (500MHz, D_2O) δ 4.23 (1H, m), 4.07 (1H, m), 3.22 (1H, dt, *J*=12, 2.5 Hz), 2.86-2.74 (3H, m), 2.52 (1H, dt, *J*=13.5, 3 Hz), 2.49 (1H, m), 2.44 (1H, m), 2.33-2.25 (2H, m); ^{13}C NMR (125.5MHz, D_2O) δ 71.92, 67.35, 67.02, 60.90, 53.86, 26.41, 26.28 ppm; HRFABMA ($M + H^+$) Calcd. 176.0745, found 176.0745.

4.4. References

(1) Gopaul, D. N.; Meyer, S. L.; Degano, M.; Sacchettini, J. C.; Schramm, V. L. Inosine-uridine nucleoside hydrolase from Crithidia fasciculata. Genetic characterization, crystallization, and identification of histidine 241 as a catalytic site residue *Biochemistry* **1996**, *35*, 5963-5970.

(2) Mazzella, L. J.; Parkin, D. W.; Tyler, P. C.; Furneaux, R. H.; Schramm, V. L. Mechanistic diagnoses of N-ribohydrolases and purine nucleoside phosphorylase *J. Am. Chem. Soc.* **1996**, *118*, 2111-2112.

(3) Parkin, D. W.; Limberg, G.; Tyler, P. C.; Furneaux, R. H.; Chen, X. Y.; Schramm, V. L. Isozyme-specific transition state inhibitors for the trypanosomal nucleoside hydrolases *Biochemistry* **1997**, *36*, 3528-3534.

(4) Tao, W., Grubmeyer, C., Blanchard, J. S. Transition State Structure of Salmonella typhimurium Orotate Phosphoribosyltransferase *Biochemistry* **1996**, *35*, 14-21.

(5) Kline, P. C.; Schramm, V. L. Purine Nucleoside Phosphorylase - Inosine Hydrolysis, Tight-Binding of the Hypoxanthine Intermediate, and 3rd-the-Sites Reactivity *Biochemistry* **1992**, *31*, 5964-5973.

(6) Kline, P. C.; Schramm, V. L. Purine Nucleoside Phosphorylase - Catalytic Mechanism and Transition-State Analysis of the Arsenolysis Reaction *Biochemistry* **1993**, *32*, 13212-13219.

(7) Kline, P. C.; Schramm, V. L. Pre-Steady-State Transition-State Analysis of the Hydrolytic Reaction Catalyzed by Purine Nucleoside Phosphorylase *Biochemistry* **1995**, *34*, 1153-1162.

(8) Fedorov, A.; Shi, W.; Kicska, G., Fedorov, E.; Tyler, P. C.; Furneaux, R. H.; Hanson, J. C.; Gainsford, G. J.; Larese, J. Z.; Schramm, V. L.; Almo, S. C. Transition state structure of purine nucleoside phosphorylase and principles of atomic motion in enzymatic catalysis *Biochemistry* **2001**, *40*, 853-860.

(9) Miles, R. W.; Tyler, P. C.; Furneaux, R. H.; Bagdassarian, C. K.; Schramm, V. L. One-third-the-sites transition-state inhibitors for purine nucleoside phosphorylase *Biochemistry* **1998**, *37*, 8615-8621.

(10) Evans, G. B.; Furneaux, R. H.; Gainsford, G. J.; Schramm, V. L.; Tyler, P. C. Synthesis of transition state analogue inhibitors for purine nucleoside phosphorylase and N-riboside hydrolases *Tetrahedron* **2000**, *56*, 3053-3062.

(11) Yasuda, K.; Kizu, H.; Yamashita, T.; Kameda, Y.; Kato, A.; Nash, R. J.; Fleet, G. W. J.; Molyneux, R. J.; Asano, N. New sugar-mimic alkaloids from the pods of Angylocalyx pynaertii *J. Nat. Prod.* **2002**, *65*, 198-202.

(12) Asano, N.; Yamashita, T.; Yasuda, K.; Ikeda, K.; Kizu, H.; Kameda, Y.; Kato, A.; Nash, R. J.; Lee, H. S.; Ryu, K. S. Polyhydroxylated alkaloids isolated from mulberry trees (Morus alba L.) and silkworms (Bombyx mori L.) *Journal of Agricultural and Food Chemistry* **2001**, *49*, 4208-4213.

(13) Asano, N.; Yasuda, K.; Kizu, H.; Kato, A.; Fan, J. Q.; Nash, R. J.; Fleet, G. W. J.; Molyneux, R. J. Novel alpha-L-fucosidase inhibitors from the bark of Angylocalyx pynaertii (Leguminosae) *Eur. J. Biochem.* **2001**, *268*, 35-41.

(14) Fleet, G. W. J.; Nicholas, S. J.; Smith, P. W.; Evans, S. V.; Fellows, L. E.; Nash, R. J. Potent Competitive-Inhibition of Alpha-Galactosidase and Alpha-Glucosidase Activity by 1,4-Dideoxy-1,4-Iminopentitols - Syntheses of 1,4-Dideoxy-1,4-Imino-D-Lyxitol and of Both Enantiomers of 1,4-Dideoxy-1,4-Iminoarabinitol *Tetrahedron Lett.* **1985**, *26*, 3127-3130.

(15) Fleet, G. W. J.; Son, J. C. Polyhydroxylated Pyrrolidines from Sugar Lactones - Synthesis of 1,4-Dideoxy-1,4-Imino-D-Glucitol from D-Galactonolactone and Syntheses of 1,4-Dideoxy-1,4-Imino-D-Allitol, 1,4-Dideoxy-1,4-Imino-D-Ribitol, and (2s,3r,4s)-3,4-Dihydroxyproline from D-Gulonolactone *Tetrahedron* **1988**, *44*, 2637-2647.

(16) Jang, K. C.; Jeong, I. Y.; Yang, M. S.; Choi, S. U.; Park, K. H. Stereoselective synthesis of 1,4-dideoxy-1,4-imino-L-lyxitol and 1,5-dideoxy-1,5-imino-D-ribitol *Heterocycles* **2000**, *53*, 887-896.

(17) Kumareswaran, R.; Hassner, A. Stereochemistry 93. Asymmetric synthesis of 1,4-dideoxy-1,4-imino-D-ribitol via stereoselective addition of allylphenylsulfone to an aryl N-sulfinylimine *Tetrahedron Assym.* **2002**, *12*, 3409-3415.

(18) Angyal, S. J.; James, K. Oxidation of Carbohydrates with Chromium Trioxide in Acetic Acid .1. Glycosides *Australian Journal of Chemistry* **1970**, *23*, 1209-&.

(19) Koellner, G. B., A.; Wielgus-Kutrowska, B.; Luic, M.; Steiner, T.; Saenger, W.; Stepinski, J. , 351 Open and closed conformation of the E. coli purine nucleoside phosphorylase active center and implications for the catalytic mechanism *J. Mol. Biol.* **2002**, *315*, 351-371.

(20) Butterworth, L. A., J. D.; Davies, G.; Burton, M.; Reed, R. H.; Gould, F. K. Evaluation of novel ß-ribosidase substrates for the differentiation of Gram-negative bacteria *Journal of Applied Microbiology* **2004**, *96*, 170-176.

Chapter 5

A Facile Approach to Chiral 2,5-Di-Substituted Pyrrolidines

ABSTRACT

Chiral 2,5-di-substituted pyrrolidines, so called homoazasugars or aza-C-glycosides, are an important class of molecules because of their inhibitory activity against glycosidases and their stability towards chemical and enzymatic degradation. Synthesis of this type of molecules is normally difficult because of the multiple chiral centers and the nitrogen atom in the ring. Here we describe a new strategy for the synthesis of 2,5-dihydroxymethyl-3,4-dihydroxypyrrolidines from different methyl 2-acetamido-3,4,6-tri-O-acetyl-2-deoxy-β-D-pyranosides. It is the most efficient route demonstrated to date and provides an easy access to more complicated homoazasugars.

5.1. Introduction

Iminopentitols (five membered ring azasugars) have become an important class of molecules as glycosidase inhibitors. They display envelope conformations which are more flexible conformations than those shown by their six membered ring counterparts, so they can mimic the proposed half chair and related transition states more closely. Of the azasugars developed, those having a hydroxymethyl group or a polyhydroxylated carbon chain linked to the anomeric carbon, so called homoazasugars or aza-C-glycosides (2,5-disubstituted pyrrolidines) are especially interesting because they retain the same or higher biological activity of the parent azasugars. They present the possibility of preparing glycoside analogs which are not suscepitible to cleavage because a carbon to carbon bond now replaces the O-glycoside linkage. Natural homoazasugars have been isolated and synthesized. Typical examples are 2,5-dideoxy-2,5-imino-D-mannitol **1** (DMDP), australine **2**, alexine **3** and hyacinthacine C_1 **4**. They have either *cis* or *trans* hydroxymethyl substituents at C-2 and C-5, combined with either *cis* or *trans* hydroxyl groups at C-3 and C-4, and they all have potent activity against glycosidases.

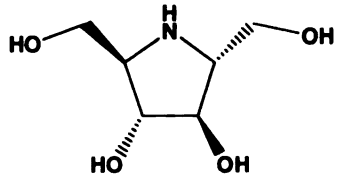

1

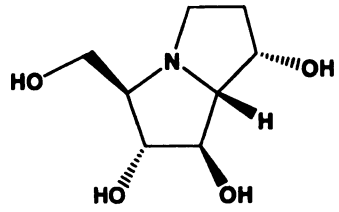

2

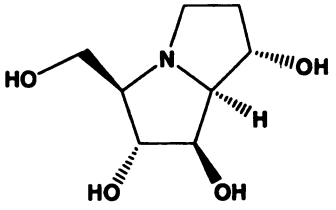

3

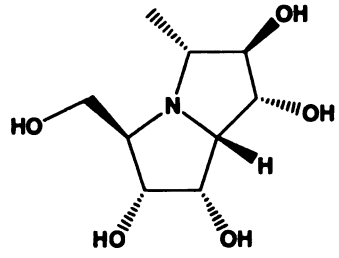

4

Because of its biological importance, several synthetic approaches have been developed for DMDP **1**[1-7]. The first synthesis was reported by Fleet in 1985[1,8] who employed D-glucose as the starting material (**figure 5.1**). Protection with acetone followed by O-benzylation at the 3-position gave the protected sugar **5**. The 5,6-O-isopropylidene group was replaced with a carbonate residue to yield **6**. Acidic cleavage of the 1,2-O-isopropylidene acetal in methanol furnished the α,β-methyl-glucosides. The primary hydroxyl group of the α-isomer was protected and the 2-position was triflated. Subsequent displacement of the triflate group at C-2 with azide gave the key intermediate **7**. Compound **7** was reduced to a primary amine which underwent cyclization to C-5 via a double displacement at that center in which an intermediate epoxide was formed. There was overall retention of configuration at C-5. Subsequent deprotection converted **10** into DMDP **1.** This synthesis is relatively long and only the α-isomer from the mixture after methanolysis of the 1,2-acetal can be used for the subsequent reactions.

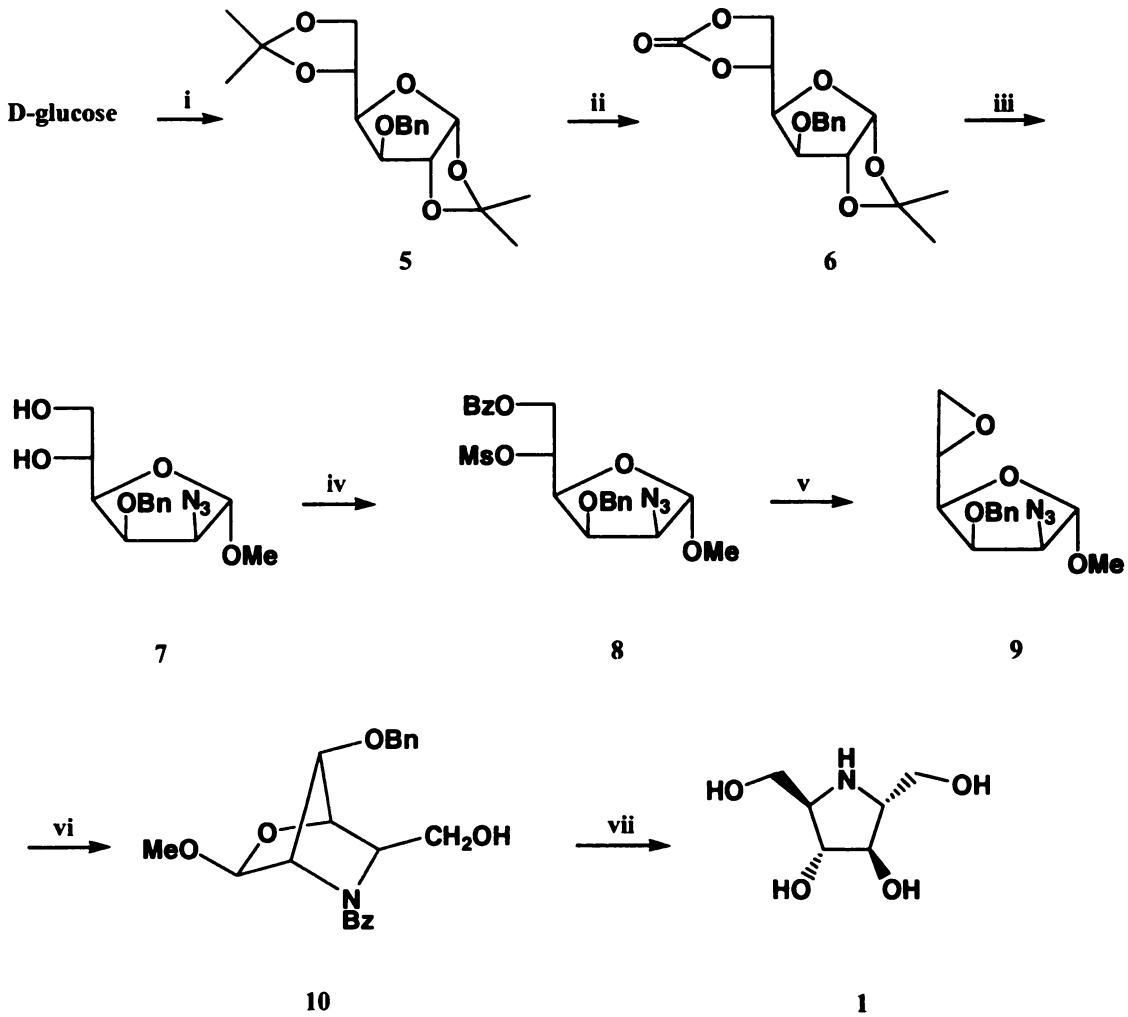

Figure 5.1. Synthesis of DMDP. i, (a) acetone, H^+; (b) BnCl, NaH; ii, (a) 0.5% HCl in MeOH. room temp, 12 h; then $(MeO)_2CO$, NaOMe, reflux; iii, (a) Dowex 50W-X8, MeOH; (b) Tf_2O (1.1 eq) in CH_2Cl_2, -20°C, 20 min, then NaN_3, (3 equiv) dimethyl formamide, 50 °C, 2 d; (c) MeOH with a trace of NaOMe. room temp; iv, (a) BzCl; (b) MsCl; v, NaOMe (2 equiv), DMF, 50°C, 5 h; vi, palladium black, H_2, EtOH; remove catalyst, then 50 °C overnight; $PhCH_2OCOCl$, ether, H_2O containing $NaHCO_3$; vii, CF_3COOH - H_2O (1:1), room temp, 1 h; then $NaBH_4$ in EtOH - H_2O; ix, palladium hydroxide, H_2, EtOH.

Derivatives of DMDP have been synthesized and tested. Wong[9,10] reported the synthesis of 2(R),5(S)-bis(hydroxymethyl)-3(R),4(R)-dihydroxypyrrolidine **17**, the 5-epimer of DMDP **1** (**figure 5.2**). This compound was synthesized via a thermodynamically

controlled fructose-1,6-diphosphate (FDP) aldolase reaction with racemic 2-azido-3-hydroxypropanal and dihydroxyacetone phosphate (DHAP). The azido group was then reduced and the ketone group underwent an intramolecular reductive amination. In the aldol reaction two diasteriomeric products are formed but they can be interconverted through enolization and only one product (the thermodynamically favorable one) is eventually formed. This compound exhibits a broad spectrum of inhibition against glycosidases with K_i in the micromolar range. However, this method of synthesis involving enzymes is not a general method and it is limited by scale-up problems.

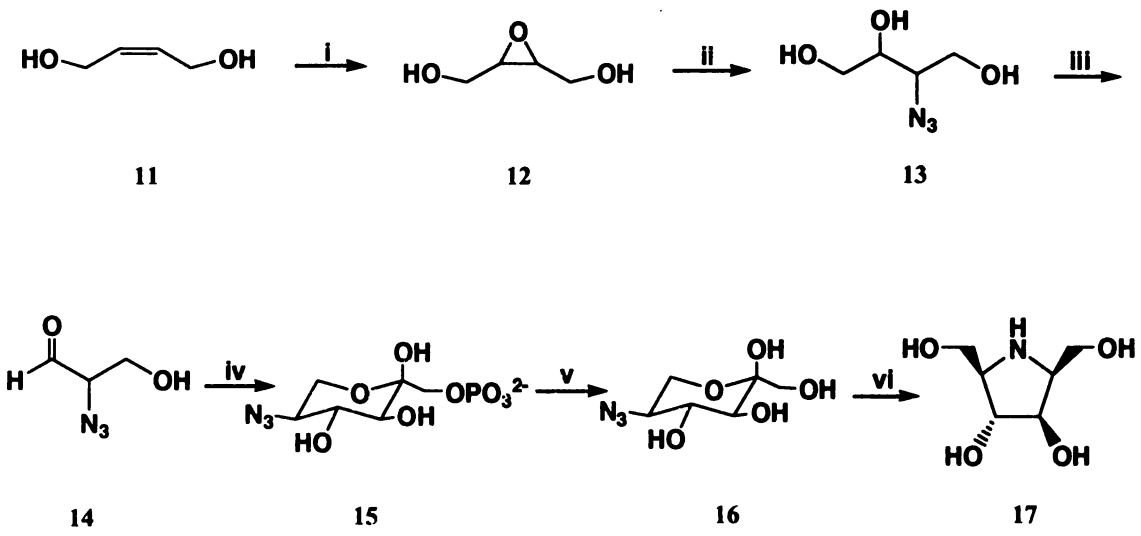

Figure 5.2. Synthesis of 2(R),5(S)-bis(hydroxymethyl)-3(R),4(R)-dihydroxypyrrolidine. i, MCPBA, CH_3CN, 92%; ii, NaN_3, NH_4Cl, $MeOH/H_2O$, reflux, 90%; iii, $NaIO_4$, 0°C, 5min; iv, DHAP/FDP aldolase; v, acid phosphatase, pH 4.7, 37 °C, 78% from **11**; vi, H_2/Pd, 50psi, 97%.

Another synthetic approach[11] **(figure 5.3)** to compound **17** starts from 2-O-triflate **18**, derived from L-gulono-1,4-lactone[12]. The nitrogen was introduced to the molecule via azide displacement of a triflate. A protected lactone intermediate **22** bearing a suitably

located triflate group and in which the azido group has been reduced to an amino group was eventually formed after several steps. Ring opening of the lactone with base allowed the intramolecular displacement of the triflate group by the amino group to form the nitrogen heterocycle. Subsequent reduction and deprotection afforded the desired product **17**.

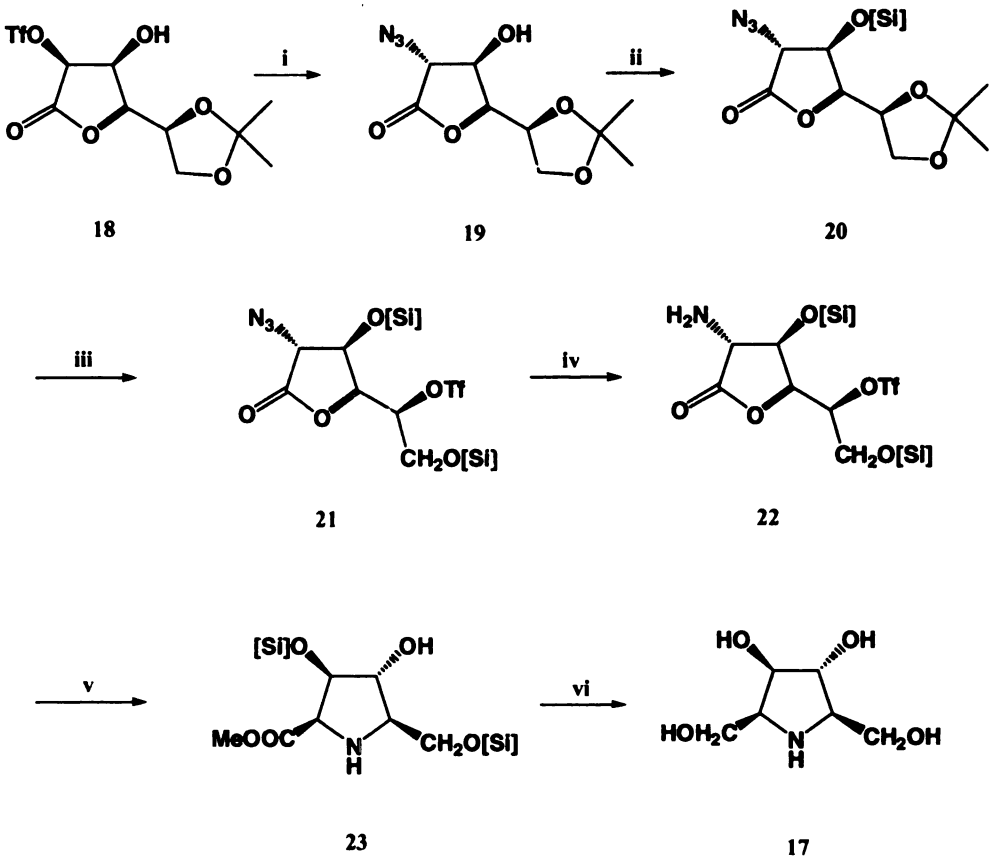

Figure 5.3. Synthesis from L-gulono-1,4-lactone. i, 0.97 eq. NaN_3, DMF, 2.5 h, 75%; ii, TBDMSOTf, pyridine, CH_2Cl_2, 85%; iii, (a) AcOH / H_2O (4:1), 99% (b) TBDMSCl, imidazole, DMF, 76% (c)Tf_2O, pyridine, CH_2Cl_2, 95%; iv, H_2, Pd-black, EtOAc, 99%; v, NaOAc, MeOH, 74%; vi, (a) $LiHBEt_3$, THF; (b) 1% HCl in MeOH, 90%.

A more general strategy for the synthesis of 2,5-dihydroxymethyl-3,4-dihydroxypyrrolidines using a thiazole-based aminohomologation protocol of furanoses

was reported by Dondoni's group[13-15]. This method (**figure 5.4**) starts from 2,3,5-tri-O-benzyl-furanose **24**. The hydroxylamine **25** was obtained as a single α-isomer by treating the furanose with *N*-benzylhydroxylamine. The open-chain form (**26**) of the hydroxylamine was reacted at -70°C with 2-lithiothiazole to afford the product as a mixture of diastereoisomers. Subsequent reductive dehydroxylation using a Zn-Cu couple[16] and cyclization yielded the product **31**. Reduction and deprotection can afford the final homoazasugar **33**. Other 2,5-Dihydroxymethyl-3,4-dihydroxypyrrolidines with different configurations (**1**, **34**, and **35**) were also obtained by the same fashion starting from different furanoses. This strategy is more general than other methods, however, it still suffers from the drawback of the separation of the diastereoisomers, such as **29** and **30**, and the use of lithium reagent is not desirable.

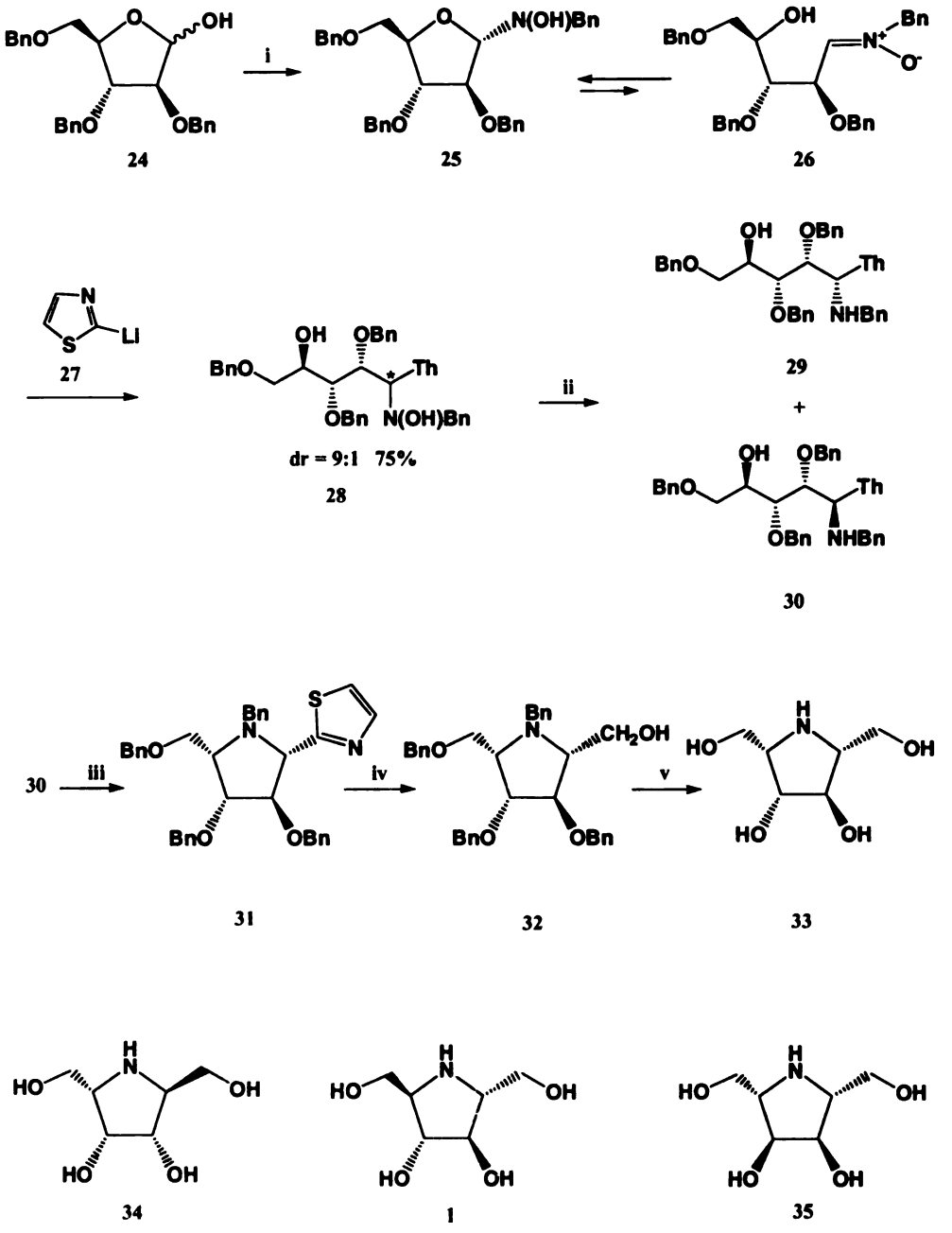

Figure 5.4. Synthesis of 2,5-dihydroxymethyl-3,4-dihydroxypyrrolidines. Th = 2-thiazolyl. Reagents: i, BnNHOH, 88%; ii, $(AcO)_2Cu$, Zn, 8% for **29**, 78% for **30**; iii, Tf_2O, pyridine, 65%; iv, TfOMe; then $NaBH_4$; then $AgNO_3$ in MeCN-H_2O, 54%; v, H_2, 20% $Pd(OH)_2/C$; then Dowex (OH^-), 86%.

The 2,5-Dihydroxymethyl-3,4-dihydroxypyrrolidines are not only potent glycosidase inhibitors, they are also important precursors for the synthesis of more complicated aza-

C-glycosides, such as inhibitors of nucleoside hydrolases[17-19], hypoxanthine-guanine phosphoribosyltransferases[20] (HGPRTases) and Purine nucleoside phosphorylases[21-24] (PNP). In the synthesis of PNP inhibitor immucillin-H (**42**)[25,26] and its derivatives, 1,4-imino-D-ribitol was synthesized first following Fleet's method[27], and the extra carbon was installed later by addition of $CNCH_2Li$ to the imine. Assembling of the 9-deazapurine on the preformed aza-C-glycoside afforded the desired product (**figure 5.5**).

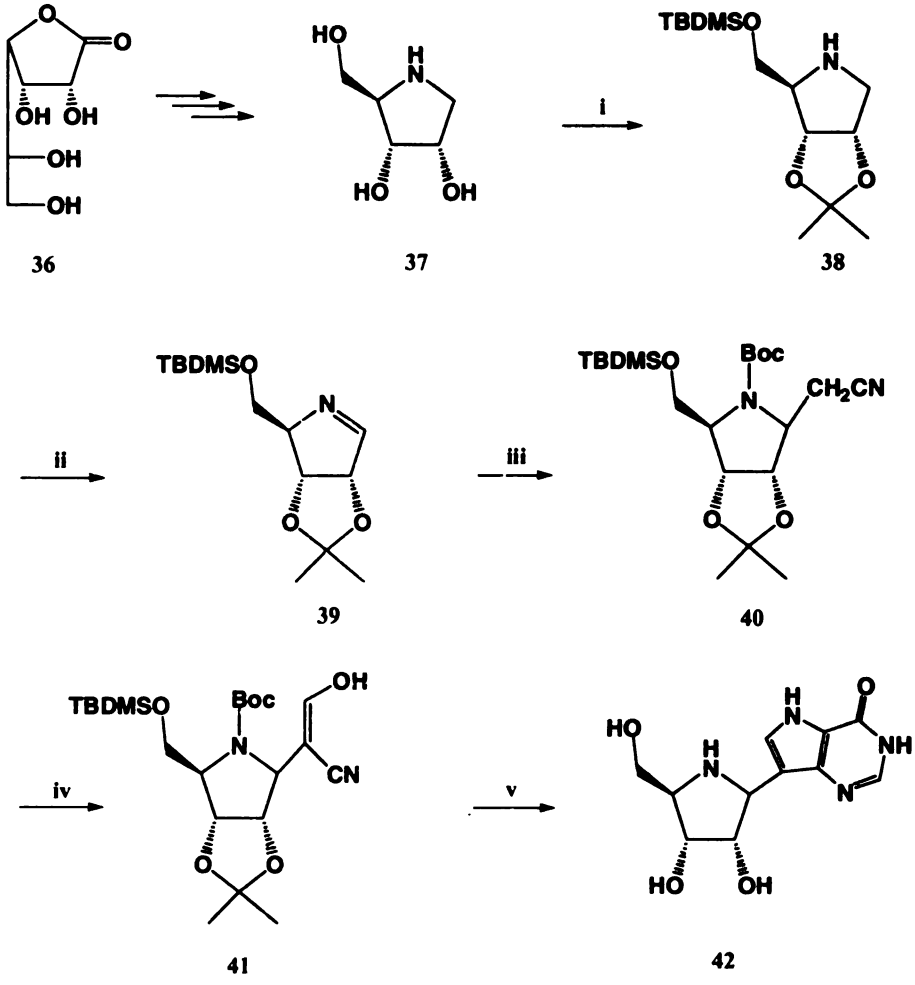

Figure 5.5. Synthesis of ImmH. i, (a) TBDMSCl; (b) Acetone, H^+; ii, (a) NCS, pentane; (b) LiTMP, -78°C; iii, (a) $CNCH_2MgX$ or $CNCH_2Li$; (b) $(Boc)_2O$; iv, (a) t-$BuOCH(NMe_2)_2$, DMF, 70°C; (b) THF, HOAc, H_2O; v, (a) $H_2NCH_2COOEt.HCl$, NaOAc,

MeOH; (b) $ClCO_2Bn$, DBU, CH_2Cl_2, reflux; (c) H_2, Pc/C, EtOH; (d) $H_2NCH{=}NH.HOAc$, EtOH, reflux; (e) TFA.

5.2. Results and Discussions

Our research goal is to develop a simple and general strategy to synthesize homoazasuagrs, especially the 2,5-dihydroxymethyl-3,4-dihydroxypyrrolidines. The desired approach is to use natural carbohydrates as the starting material. Natural glycosamines were chosen because of their intrinsic chirality and the available acetamido group which could provide an amino group that is normally obtained by displacement of a leaving group with azide and reduction. Starting from protected glycosamines, a chromium oxidation-borane reduction strategy was developed and dihydroxypyrrolidines **17** and **34** and **43** were synthesized quickly and efficiently.

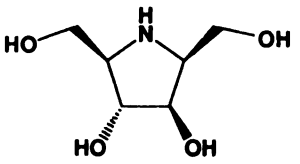

17

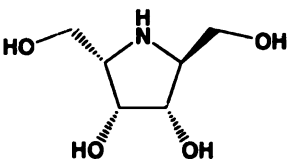

34

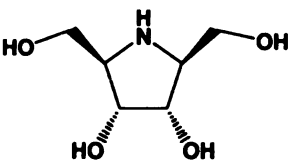

43

The syntheses of the 2,5-dihydroxymethyl-3,4-dihydroxypyrrolidines start from methyl 2-acetamido-3,4,6-tri-*O*-acetyl-2-deoxy-β-D-pyranosides. The D-*gluco* derivatives are readily available from a variety of highly abundant sources such as chitin. The commercially available methyl 2-acetamido-3,4,6-tri-*O*-acetyl-2-deoxy-β-D-glucopyranoside **44** was converted to pyrrolidine **17** in just two steps (**figure 5.6**). Chromium oxidation of glucopyranoside **44** followed by borane reduction yielded a single isomer **17**. The oxidation of acetylated β-glycopyranosides by chromium trioxide

has been reported by S. J. Angyal and K. James[28] to afford 5-keto esters, independent of the configurations on C-2, C-3, or C-4 and we have used this method in previous syntheses. In the present synthesis, the oxidation gave the 5-keto ester **46** as an intermediate. Deacylation of the 2-acetamido group to form a free amino group proceeded oxidation. Some of the N-deacetylated intermediate **45** was actually isolated and the proton NMR spectrum showed signals for three *O*-acetyl groups. After it is formed, the 5-keto function can cyclize to the 2-amino group to form a hemiaminal. The hemiaminal can be acetylated to give the product **47**. This product was obtained as a mixture of diasteroisomers with 3:2 ratio. Both diasteroisomers can be reduced by borane to yield the final 2,5-dihydroxymethyl-3,4-dihydroxypyrrolidines **17** with overall 78% yield.

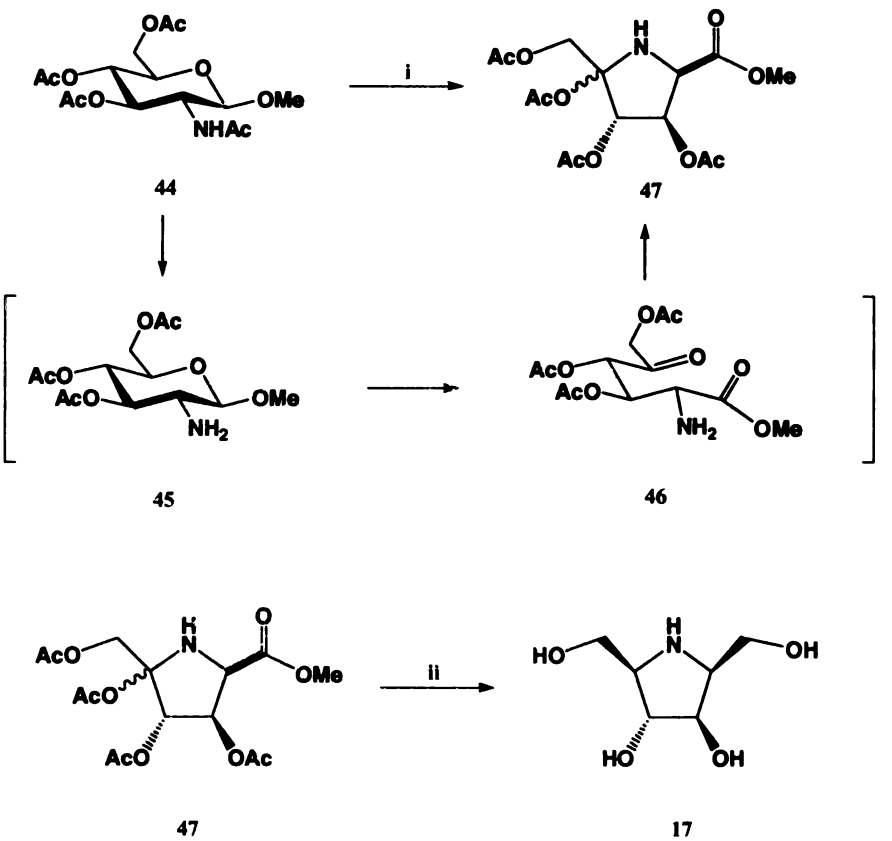

Figure 5.6. Synthesis of compound **17**. i, CrO_3, HOAc, Ac_2O; ii, BH_3, THF, 78% for two steps.

Compounds **34** and **43** were obtained from methyl 2-acetamido-3,4,6-tri-*O*-acetyl-2-deoxy-β-D-allopyranoside. This starting material was synthesized from its gluco-isomer (**figure 5.7**) through an oxidation-reduction sequence to invert the stereochemistry at the C-3 position. The starting glucopyranoside **44** was deacetylated first. Treatment of the triol with benzaldehyde dimethyl acetal gave the 4,6-acetal **49** with the 3-OH free. This hydroxyl group can be oxidized to ketone by chromium trioxide-pyridine system[29] or dimethyl sulfoxide (DMSO)-acetic anhydride (Ac_2O). Both oxidations worked well in this synthesis, but the chromium oxidation was more efficient. In less than 10 minutes, the reaction was done and the yield was over 90%. The DMSO-Ac_2O oxidation took longer time and some competing reactions to give small amounts of byproducts were observed. Reductions of the ketone to give 3-axial hydroxyl group of **51** were tried under different conditions. Products with axial and equatorial products are possible. The desired product has the axial orientation. **Table 5.1** shows the ratio of products with equatorial versus axial hydroxyl group. Sodium borohydride and lithium borohydride gave the equatorial hydroxyl as the major product, while cyanoborohydride gave the opposite result. The reason for this is that for a smaller borohydride, it tends to attack from the axial position, while cyanoborohydride tends to attack from the equatorial position. Another possible reason for cyanoborohydride is it can form some complex with oxygen at 3-position and nitrogen at 2-position to form a five membered ring, so it locks the oxygen at axial position. The reduction result also showed that at lower temperature,

more equatorial product **49** can be obtained, and solvent has little effect on the ratio of the products. This is probably because lower temperature favors the equatorial attack and the formation of the complex is not favored.

Table 5.1. Product ratios under different conditions.

Conditions	equatorial : axial (**49** : **51**)
$NaBH_4$/MeOH, room temp.	3 : 1
$NaBH_4$/MeOH, -10°C ~ 0°C	4 : 1
$NaBH_4$/20%$[CH_3(CH_2)_3]NHSO_4$ MeOH/Propanol, room temp.	3 : 1
$NaBH_4$/20%$[CH_3(CH_2)_3]NHSO_4$ MeOH/Propanol, -10°C ~ 0°C	2.5 : 1
$NaBH_4$/ $[CH_3(CH_2)_3]NHSO_4$ Propanol, -78°C	7 : 1
$LiBH_4$/MeOH, room temp.	5 : 1
$NaBCNH_3$/MeOH, room temp.	1 : 4
$NaBCNH_3$/MeOH, -10°C ~ 0°C	1 : 2
$NaBCNH_3$/Propanol, room temp.	1 : 3.5

With compound **51** in hand, methyl 2-acetamido-3,4,6-tri-*O*-acetyl-2-deoxy-β-D-allopyranoside was obtained by acid deprotection and acetylation. Subsequent chromium oxidation afforded the desired five membered ring product **54** as an imine form instead of the hemiaminal. Borane reduction of this imine yielded two isomers with hydroxymethyl group up (**43**) or down (**34**) at 5-position. Acetylation of the mixture and separation by chromatography yielded products **55** and **56**.

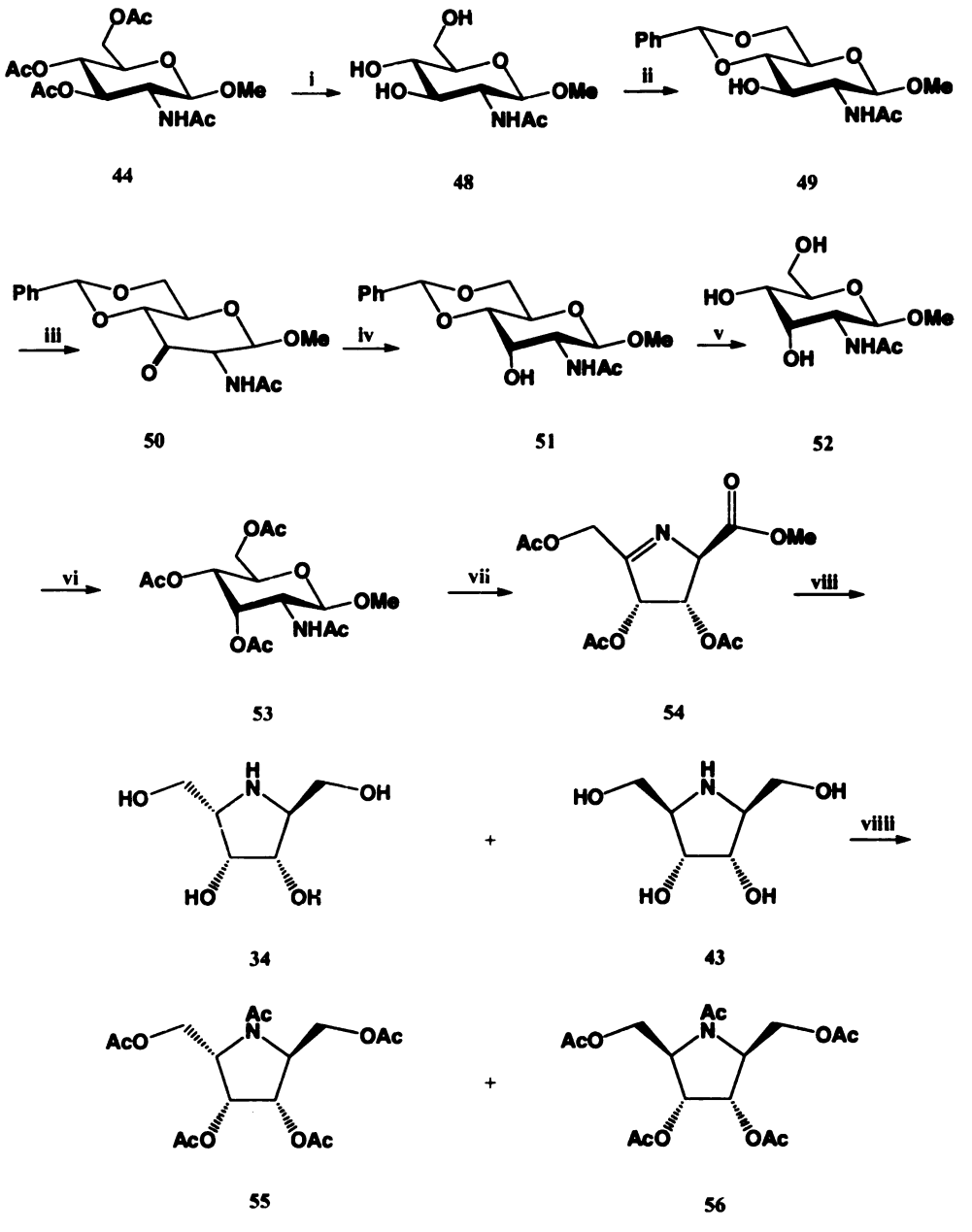

Figure 5.7. Synthesis of products **55** and **56.** i, K_2CO_3, MeOH; ii, Benzaldehyde dimethyl acetal, H_2SO_4, DMF, 74% for two steps; iii, CrO_3-pyridine, CH_2Cl_2, 91% or DMSO-Ac_2O, 82%; iv, $NaCNBH_3$, MeOH, 76%; v, 5% HCl, MeOH; vi, Ac_2O, pyridine, 75% for two steps; vii, CrO_3, HOAc, Ac_2O; viii, BH_3-THF; viiii, Ac_2O, pyridine, 69% for 3 steps.

This synthetic approach we describe here is a quick and easy way to get 2,5-dihydroxymethyl-3,4-dihydroxypyrrolidines from different methyl 2-acetamido-3,4,6-tri-

O-acetyl-2-deoxy-β-D-pyranosides. It is the most efficient route demonstrated to date. Here we take advantages of the multiple chiral centers of carbohydrate and the amino group of the glycosamines to form homoazasugars which are normally difficult to synthesize. More complicated homoazasugars should be synthesized through this strategy and more glycosidase inhibitors should be obtained. In this approach, different oxidations and reductions have been applied at different stages. Chromium oxidation showed its efficiency in the ketone and ketoester formations. Different borohydrides are useful in reducing the 3-ulose to invert the stereochemistry of the hydroxyl group to yield the desired product.

5.3. Experimental Section

General Procedures: Melting points were measured on a Ficher-Johns melting point apparatus. Optical rotations were measured (λ = 589 nm) at room temperature using a Jasco P-1010 polarimeter. The ^{1}H (and ^{13}C) NMR spectra were recorded at 500 (125.5) MHz on a Varian VXR spectrometer. The HRMS FAB mass spectra were obtained using a Jeol HX-110 double-focusing mass spectrometer operating in positive ion mode.

2(R),5(S)-Bis(hydroxymethyl)-3(R),4(R)-dihydroxypyrrolidine (17) To a solution of methyl 2-acetomido-3,4,6-tri-*O*-acetyl-2-deoxy-β-D-glucopyranoside **44** (0.5g, 1.38mmol) in acetic acid (50mL) and acetic anhydride (5mL), chromium trioxide (0.42g, 4.2mmol) was added and the suspension was stirred at room temperature for 5 hours. The mixture was then poured slowly into cold water (300mL). The water was extracted 5 times with CH_2Cl_2 and the combined organic phase was washed with brine, saturated sodium

bicarbonate and dried (Na_2SO_4), concentrated. The resulting residue was passed through a small pad of silica gel to give **47** as a colorless oil (0.44g, 95%). The mixture was used in the next step without separating the diasteroeoisomers.

A solution of **47** (0.1g, 0.3mmol) and BH_3-THF (10mL, 1.5M) in anhydrous THF (10mL) was refluxed for 4 hours and the TLC and NMR showed the completion of the reduction. The solvent was removed and methanol was added and concentrated for 3 times. The residue was purified by column chromatography (6:1 CH_2Cl_2/MeOH) to afford a colorless oil (0.04g, 82%). ^{1}H NMR (500MHz, CD_3OD) δ 3.98 (1H, dd, *J*=6.0, 4.0 Hz), 3.95 (1H, t, *J*=4.0 Hz), 3.76-3.59 (4H, m), 3.06 (1H, dd, *J*=10.0, 4.5 Hz), 2.72 (1H, dd, *J*=7.5, 4.0 Hz); ^{13}C NMR (125.5MHz, CD_3OD) δ 77.07, 76.71, 69.84, 65.12, 61.09, 60.16ppm.

Methyl 2-acetamido-4,6-benzylidine-2-deoxy-β-D-glucopyranoside (49) To a solution of methyl 2-acetamido-3,4,6-tri-*O*-acetyl-2-deoxy-β-D-glucopyranoside **44** (1g, 2.77mmol) in 20mL methanol and 0.5mL water was added potassium carbonate (2.5g, 18mmol), and the suspension was stirred at room temperature for 12 hours. The mixture was then diluted with 50mL methanol and 25mL water and was passed through a mixed bed column (Dowex MR-3). The elution was concentrated and dissolved in 200mL anhydrous DMF. Benzaldehyde dimethyl acetal (0.15g, 1.0mmol) and 30 μL of sulfuric acid were added and the solution was stirred at room temperature for 16 hours. The mixture was then poured into ice containing 2.5g of potassium carbonate and stirred until all the ice melted. The mixture was filtered, washed with water and dried to yield white solid (0.66g, 74%). ^{1}H NMR (500MHz, DMSO) δ 7.79 (1H, d, *J*=9.0 Hz), 7.45-7.43 (2H,

m), 7.37-7.36 (3H, m), 5.59 (1H, s), 5.24 (1H, d, J=5.5 Hz), 4.38 (1H, d, J=8.5 Hz), 4.20 (1H, q, J=5.0 Hz), 3.72 (1H, t, J=10.0 Hz), 3.57 (1H, m), 3.73 (1H, m), 3.53 (1H, t, J=9.0 Hz), 3.41 (1H, t, J=9.0 Hz), 3.33 (3H, s), 1.81 (3H, s); ^{13}C NMR (125.5MHz, DMSO) δ 169.13, 137.74, 128.77, 127.95, 126.30, 102.36, 100.64, 81.27, 70.52, 67.86, 65.95, 55.93, 23.04 ppm. HR-FABMS ($M+H^+$) Calcd. 324.1446, found 324.1447.

Ketone 50: Chromium oxidation: Chromium trioxide (1.24g, 12.4mmol) was added to a stirred solution of pyridine (1.96g, 24.8mmol) in 20mL dry dichloromethane. The mixture was stirred for 15 min and **49** (1g, 3.1mmol) in 10mL dichloromethane was added with stirring at room temperature. Acetic anhydride (1.26g, 12.4mmol) wad added immediately and the reaction was stirred for another 10 min. The reaction mixture was diluted with ethyl acetate and passed through a short column of silica gel. The product was eluted with ethyl acetate and acetone, concentrated to yield a white solid (0.9g, 91%). ^{1}H NMR (500MHz, DMSO) δ 7.44-7.39 (5H, m), 5.68 (1H, s), 4.68 (2H, m), 4.47 (1H, t, J=8.0 Hz), 4.38 (1H, q, J=5.0 Hz), 3.89 (1H, t, J=10.0 Hz), 3.64 (1H, m), 3.43 (3H, s), 1.89 (3H, s); ^{13}C NMR (125.5MHz, DMSO) δ 169.29, 137.05, 129.08, 128.13, 126.25, 103.46, 100.39, 80.91, 68.18, 65.65, 60.71, 56.41, 22.46 ppm. HR-FABMS ($M+H^+$) Calcd. 322.1291, found 322.1292.

MDSO-Ac_2O oxidation: To a solution of **49** (0.5g, 1.6mmol) in 10mL DMSO was added acetic anhydride (0.95g, 9.6mmol) and the solution was stirred at room temperature for 12 hours. The solution was then poured into ice water containing 3g potassium carbonate. The mixture was filtered, washed with water and dried to give a white solid (0.41g, 82%).

Methyl 2-acetamido-4,6-benzylidine-2-deoxy-β-D-allopyranoside (51) Sodium cyanoborohydride (0.39g, 6.2mmol) was added to a mixture of **50** (1g, 3.1mmol) in 300mL methanol. The reaction was stirred at room temperature for 2 hours and concentrated. The two diastereoisomers were separated by flash chromatography (1:1 ethyl acetate/hexanes) and **51** was obtained as white solid (0.76g, 76%). ^{1}H NMR (500MHz, DMSO) δ 7.44-7.40 (5H, m), 5.62 (1H, s), 5.40 (1H, d, *J*=4.0 Hz), 4.55 (1H, d, *J*=8.5 Hz), 4.23 (1H, q, *J*=5.0 Hz), 3.94 (1H, m), 3.85 (1H, m), 3.73 (1H, m), 3.68 (1H, t, *J*=10.0 Hz), 3.28 (3H, s), 1.82 (3H, s); ^{13}C NMR (125.5MHz, DMSO) δ 169.29, 28.76, 127.94, 126.34, 124.88, 100.61, 100.26, 78.53, 68.30, 67.21, 62.79, 56.10, 22.68 ppm. HR-FABMS (M+H$^+$) Calcd. 324.1446, found 324.1445.

Methyl 2-acetamido-3,4,6-tri-*O*-acetyl-2-deoxy-β-D-allopyranoside (53) To a solution of **51** (0.5g, 1.6mmol) in 100mL methanol was added 5mL hydrochloric acid and solution was stirred at 5°C for 1 hour. Potassium carbonated (5g) was added and stirred for 10min, and the mixture was filtered and the solution was concentrated. The residue was dissolved in 20mL pyridine and 15mL acetic anhydride. The solution was stirred at room temperature for 2 hours and concentrated. The residue was purified by flash chromatography (4:1 ethyl acetate/hexanes) to give a colorless oil (0.42g, 75%). ^{1}H NMR (500MHz, $CDCl_3$) δ 5.58 (1H, t, *J*=3.0 Hz), 4.99 (1H, dd, *J*=9.5, 3.0 Hz), 4.60 (1H, d, *J*=8.0 Hz), 4.29 (1H, m), 4.23 (2H, d, *J*=4.0 Hz), 4.03 (1H, m), 3.49 (3H, s), 2.16 (3H, s), 2.09 (3H, s), 1.994 (3H, s), 1.991 (3H, s); ^{13}C NMR (125.5MHz, $CDCl_3$) δ 170.76, 169.66, 169.65, 169.06, 100.32, 70.50, 69.22, 66.83, 62.45, 56.35, 50.19, 23.28, 20.79, 20.74, 20.54 ppm. HR-FABMS (M+H$^+$) Calcd. 362.1451, found 362.1450.

54, 34 and **43** were synthesized following the same method as **47** and **17**.

2(S),5(S)-Bis(acetoxymethyl)-3(R),4(S)-diacetoxypyrrolidine (55) and ***meso*-bis(acetoxymethyl)-3,4-diacetoxypyrrolidine (56)** The mixture of **34** and **43** were acetylated and separated by flash chromatography (2:1 ethyl acetate/hexanes) to give **55** (0.05g, 47%) and **56** (0.02g, 22%).

55: ^{1}H NMR (500MHz, $CDCl_3$) δ 5.43 (1H, m), 5.39 (1H, m), 4.49 (1H, dd, *J*=11.5, 4.5 Hz), 4.43 (1H, m), 4.38 (1H, m), 4.30 (1H, dd, *J*=11.0, 4.0 Hz), 4.26 (1H, m), 4.21 (1H, dd, *J*=10.0, 3.0 Hz), 2.16 (3H, s), 2.12 (3H, s), 2.09 (3H, s), 2.07 (3H, s), 2.04 (3H, s); ^{13}C NMR (125.5MHz, $CDCl_3$) δ 170.62, 170.13, 169.70, 169.47, 73.15, 69.87, 63.36, 61.10, 61.08, 56.86, 20.80. 20.76, 20.63, 20.44 ppm. HR-FABMS ($M+H^+$) Calcd. 374.1451, found 374.1450.

56: ^{1}H NMR (500MHz, $CDCl_3$) δ 5.18 (1H, d, *J*=4.0 Hz), 4.05 (1H, d, *J*=2.5 Hz), 4.04 (1H, d, *J*=1.5 Hz), 3.16 (1H, m), 2.08 (3H, s), 2.07 (3H, s); ^{13}C NMR (125.5MHz, $CDCl_3$) δ 171.05, 170.86, 72.60, 63.84, 63.38, 20.84, 20.72 ppm.

5.4. References

(1) Fleet, G. W. J.; Smith, P. W. Enantiospecific Syntheses of Deoxymannojirimycin, Fagomine and 2r,5r-Dihydroxymethyl-3r,4r-Dihydroxypyrrolidine from D-Glucose *Tetrahedron Lett.* **1985**, *26*, 1469-1472.

(2) Card, P. J.; Hitz, W. D. Synthesis of 2(R),5(R)-Bis(Hydroxymethyl)-3(R),4(R)-Dihydroxypyrrolidine - a Novel Glycosidase Inhibitor *Journal of Organic Chemistry* **1985**, *50*, 891-893.

(3) Reitz, A. B.; Baxter, E. W. Pyrrolidine and Piperidine Aminosugars from Dicarbonyl Sugars in One-Step - Concise Synthesis of 1-Deoxynojirimycin *Tetrahedron Letters* **1990**, *31*, 6777-6780.

(4) Dureault, A.; Portal, M.; Depezay, J. C. Enantiospecific Syntheses of 2,5-Dideoxy-2,5-Imino-D-Mannitol and 2,5-Dideoxy-2,5-Imino-L-Iditol from D-Mannitol *Synlett* **1991**, 225-226.

(5) Hung, R. R.; Straub, J. A.; Whitesides, G. M. Alpha-Amino Aldehyde Equivalents as Substrates for Rabbit Muscle Aldolase - Synthesis of 1,4-Dideoxy-D-Arabinitol and 2(R),5(R)-Bis(Hydroxymethyl)-3(R),4(R)-Dihydroxypyrrolidine *Journal of Organic Chemistry* **1991**, *56*, 3849-3855.

(6) Legler, G.; Korth, A.; Berger, A.; Ekhart, C.; Gradnig, G.; Stutz, A. E. 2,5-Dideoxy-2,5-Imino-D-Mannitol and -D-Glucitol - 2-Step Bioorganic Syntheses from 5-Azido-5-Deoxy-D-Glucofuranose and -L-Idofuranose - Evaluation as Glucosidase Inhibitors and Application in Affinity Purification and Characterization of Invertase from Yeast *Carbohydrate Research* **1993**, *250*, 67-77.

(7) Baxter, E. W.; Reitz, A. B. Expeditious Synthesis of Azasugars by the Double Reductive Amination of Dicarbonyl Sugars *Journal of Organic Chemistry* **1994**, *59*, 3175-3185.

(8) Fleet, G. W. J.; Smith, P. W. Methyl 2-Azido-3-O-Benzyl-2-Deoxy-Alpha-D-Mannofuranoside as a Divergent Intermediate for the Synthesis of Polyhydroxylated Piperidines and Pyrrolidines - Synthesis of 2,5-Dideoxy-2,5-Imino-D-Mannitol 2r,5r-Dihydroxymethyl-3r,4r-Dihydroxypyrrolidine *Tetrahedron* **1987**, *43*, 971-978.

(9) Liu, K. K. C.; Kajimoto, T.; Chen, L. R.; Zhong, Z. Y.; Ichikawa, Y.; Wong, C. H. Use of Dihydroxyacetone Phosphate Dependent Aldolases in the Synthesis of Deoxyazasugars *J. Org. Chem.* **1991**, *56*, 6280-6289.

(10) Wang, Y. F.; Takaoka, Y.; Wong, C. H. Remarkable Stereoselectivity in the Inhibition of Alpha-Galactosidase from Coffee Bean by a New Polyhydroxypyrrolidine Inhibitor *Angew. Chem., Int. Ed. Engl.* **1994**, *33*, 1242-1244.

(11) Long, D. D.; Frederiksen, S. M.; Marquess, D. G.; Lane, A. L.; Watkin, D. J.; Winkler, D. A.; Fleet, G. W. J. Potential intermediates for incorporation of polyhydroxylated prolines into combinatorial libraries *Tetrahedron Lett.* **1998**, *39*, 6091-6094.

(12) Hubschwerlen, C. A Convenient Synthesis of L-(S)-Glyceraldehyde Acetonide from L-Ascorbic-Acid *Synthesis-Stuttgart* **1986**, 962-964.

(13) Dondoni, A.; Giovannini, P. P.; Perrone, D. New synthesis of pyrrolidine homoazasugars via aminohomologation of furanoses and their use for the stereoselective synthesis of aza-C-disaccharides *Journal of Organic Chemistry* **2002**, *67*, 7203-7214.

(14) Dondoni, A.; Giovannini, P. P.; Marra, A. Convergent synthesis of pyrrolidine-based (1 -> 6)- and (1 -> 5)-aza-C-disaccharides *Tetrahedron Letters* **2000**, *41*, 6195-6199.

(15) Dondoni, A.; Perrone, D. New entry to pyrrolidine homoazasugars: conversion of D-arabinose into 2,5-anhydro-2,5-imino-D-glucitol via aminohomologation *Tetrahedron Letters* **1999**, *40*, 9375-9378.

(16) Dondoni, A.; Perrone, D.; Rinaldi, M. Grignard addition to aldonitrones. Stereochemical aspects and application to the synthesis of C-2-symmetric diamino alcohols and diamino diols *Journal of Organic Chemistry* **1998**, *63*, 9252-9264.

(17) Gopaul, D. N.; Meyer, S. L.; Degano, M.; Sacchettini, J. C.; Schramm, V. L. Inosine-uridine nucleoside hydrolase from Crithidia fasciculata. Genetic characterization, crystallization, and identification of histidine 241 as a catalytic site residue *Biochemistry* **1996**, *35*, 5963-5970.

(18) Mazzella, L. J.; Parkin, D. W.; Tyler, P. C.; Furneaux, R. H.; Schramm, V. L. Mechanistic diagnoses of N-ribohydrolases and purine nucleoside phosphorylase *J. Am. Chem. Soc.* **1996**, *118*, 2111-2112.

(19) Parkin, D. W.; Limberg, G.; Tyler, P. C.; Furneaux, R. H.; Chen, X. Y.; Schramm, V. L. Isozyme-specific transition state inhibitors for the trypanosomal nucleoside hydrolases *Biochemistry* **1997**, *36*, 3528-3534.

(20) Tao, W., Grubmeyer, C., Blanchard, J. S. Transition State Structure of Salmonella typhimurium Orotate Phosphoribosyltransferase *Biochemistry* **1996**, *35*, 14-21.

(21) Kline, P. C.; Schramm, V. L. Purine Nucleoside Phosphorylase - Inosine Hydrolysis, Tight-Binding of the Hypoxanthine Intermediate, and 3rd-the-Sites Reactivity *Biochemistry* **1992**, *31*, 5964-5973.

(22) Kline, P. C.; Schramm, V. L. Purine Nucleoside Phosphorylase - Catalytic Mechanism and Transition-State Analysis of the Arsenolysis Reaction *Biochemistry* **1993**, *32*, 13212-13219.

(23) Kline, P. C.; Schramm, V. L. Pre-Steady-State Transition-State Analysis of the Hydrolytic Reaction Catalyzed by Purine Nucleoside Phosphorylase *Biochemistry* **1995**, *34*, 1153-1162.

(24) Fedorov, A.; Shi, W.; Kicska, G.; Fedorov, E.; Tyler, P. C.; Furneaux, R. H.; Hanson, J. C.; Gainsford, G. J.; Larese, J. Z.; Schramm, V. L.; Almo, S. C. Transition state structure of purine nucleoside phosphorylase and principles of atomic motion in enzymatic catalysis *Biochemistry* **2001**, *40*, 853-860.

(25) Miles, R. W.; Tyler, P. C.; Furneaux, R. H.; Bagdassarian, C. K.; Schramm, V. L. One-third-the-sites transition-state inhibitors for purine nucleoside phosphorylase *Biochemistry* **1998**, *37*, 8615-8621.

(26) Evans, G. B.; Furneaux, R. H.; Gainsford, G. J.; Schramm, V. L.; Tyler, P. C. Synthesis of transition state analogue inhibitors for purine nucleoside phosphorylase and N-riboside hydrolases *Tetrahedron* **2000**, *56*, 3053-3062.

(27) Fleet, G. W. J.; Son, J. C. Polyhydroxylated Pyrrolidines from Sugar Lactones - Synthesis of 1,4-Dideoxy-1,4-Imino-D-Glucitol from D-Galactonolactone and Syntheses of 1,4-Dideoxy-1,4-Imino-D-Allitol, 1,4-Dideoxy-1,4-Imino-D-Ribitol, and (2s,3r,4s)-3,4-Dihydroxyproline from D-Gulonolactone *Tetrahedron* **1988**, *44*, 2637-2647.

(28) Angyal, S. J.; James, K. Oxidation of Carbohydrates with Chromium Trioxide in Acetic Acid .1. Glycosides *Australian Journal of Chemistry* **1970**, *23*, 1209-&.

(29) Garegg, P. J.; Samuelsson, B. Oxidation of Primary and Secondary Alcohols in Partially Protected Sugars with Chromium Trioxide-Pyridine Complex in Presence of Acetic-Anhydride *Carbohydrate Research* **1978**, *67*, 267-270.

Chapter 6

5-Substituted Thiomorpholine Carboxylic Acids: A Compound Class with Promising Antibacterial Activity

ABSTRACT

Because of the development of bacterial resistance, new classes of antibacterial agents are in great need. Nitrogen heterocyclic systems with aromatic substituents are typical features of the known antibiotics.The oxazolidinones and the quinolones are two examples of such drugs. The oxazolidinones, with their novel structures and unique mechanism, have been developed as a newest type of antibiotics based on structure-activity relationship studies. A series of enantiopure arylsubstituted 5-phenyl-thiomorpholine-3-carboxylic acid derivatives were synthesized from L- and D-cysteine in just one step. These molecules have key structural features of known antibacterial drugs. Biological testing was performed on these compounds and the results showed promising antibacterial activities. Compounds with electron-withdrawing 2-NO_2 substituent are the most active among the series. These compounds can be a good starting point for development of a new class of antibacterial agents and provide the opportunity for a completely new drug class.

6.1. Introduction

The growing incidence of bacterial resistance to antibiotics has been a serious problem in recent years. Drug resistance, especially multiple drug resistance, has become a primary health concern[1]. There is a great need for new class of antibiotics that are more potent and less prone to resistance development. Heterocyclic systems with nitrogens in rings and aromatic substituents are often good antibiotics. Two common such types of antibiotics are quinolones and oxazolidinones. Typical examples of quinolones are Nalidixic acid, Ciprofloxacin **1** and Levofloxacin. Ciprofloxacin, which has nitrogen heterocyles, fluoro substituent and other functionalities, is the best known drug in this class. The mechanism of action of quinolone antibiotics is tied to the activity of two enzymes, DNA gyrase and DNA topoisomerase IV[2]. Both enzymes are essential enzymes for bacterial growth. Ciprofloxacin targets these two enzymes and eliminates their functions. It also actively poisons cells by trapping these two enzymes on DNA as drug/enzyme/DNA complexes in which double-strand DNA breaks. Ciprofloxacin has been used as an antibiotic for a long time, but its effectiveness has been compromised by bacterial resistance.

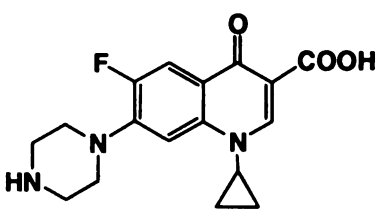

Ciprofloxacin 1

The oxazolidinones are a new class of antibacterial agents. They represent a new development in the effective treatment of Gram-positive bacterial infections including those caused by strains resistant to other antibiotics. Linezolid (Zyvox, Pharmacia Corporation, Peapack, NJ), the first marketed member of this class, is the first antibacterial drug in the last 30 years. It showed good efficacy with an impressive antibacterial spectrum. This includes activity against gram-positive organisms *Staphylococcus aureus, Streptococcus pneumoniae*, and *Enterococcus spp,* which pose a considerable threat to health. They also showed activity against vancomycin-resistant *Enterococcus faecium*, and *E. faecium* related bacteremia[3]. This is related to their unique mechanism of action. It has been generally accepted that oxazolidinones are protein synthesis inhibitors[4], and they interact with ribosomes. However, there are still some debates as to their mode of action. Different results have been reported about more detailed mechanism. In one study, oxazolidinones were found to bind to the 50S ribosomal subunit[5], and to inhibit N-formylmethionyl-tRNA binding in a cell-free system using purified ribosomes from *E. Coli*[6]. It was then determined that linezolid inhibits protein synthesis at the initiation step by preventing binding of the N-formylmethionyl-tRNA to the 70S ribosome[7]. This is different from other antibiotics such as the macrolides and streptogramins that act on the elongation step of protein synthesis. However, another study revealed that oxazolidinones do not interfere with translation initiation during mRNA binding or during formation of 30S pre-initiation complexes[8]. Its mode of action targets at a late step during initiation. It inhibits the puromycin-mediated release of 35S-formylmethionine from 70S initiation complexes in a dose-dependent manner. A more recent study suggested that oxazolidinones inhibit bacterial protein

biosynthesis by interfering with the binding of initiator fMet-tRNA$_i^{Met}$ to the ribosomal peptidyltransferase P-site[9].

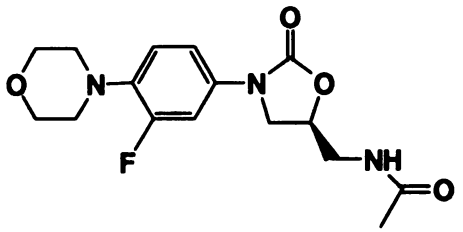

Linezolid 2

Oxazolidinones have been developed through structure-activity relationship. The core structure of oxazolidinones is a simple heterocyclic system that is not found frequently in drug structures. The 3-, 4-, 5-substitutions can lead to all kinds of derivatives of oxazolidinones. The structural simplicity and possible variations allow the performance of comprehensive structure-activity relationship studies. Such structure–activity relationship studies[10] led to the development of the first commercial drug of this kind, linezolid, and will guide additional oxazolidinones marketed in the future.

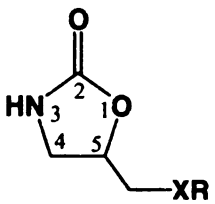

X = a heteroatom (often O or N)
R = alkyl or aryl

Studies from a group at Du Pont were the first in recent times to highlight the potential importance of oxazolidinone compounds. There were two main candidates, Dup-721 and Dup-105[11,12], which originated from a series of racemic 5-halomethyl-3-phenyl-2-

oxazolidinones. Compound **3** is one example of this class[13]. Further modifications led to the enantio pure analog **4**, which showed some in vitro and in vivo activity[14]. From a study of a series of compounds, some structure–activity rules began to appear. Activity was determined to be a function of the size and nature of the 5-substituent, the nature of the 3-substituent, and the configuration at the 5-position.

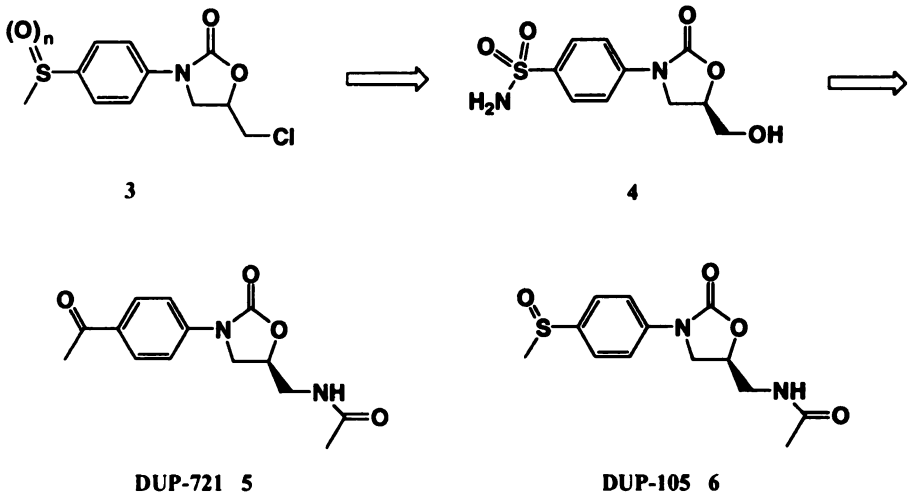

This finding is illustrated in **Figure 6.1**. If the molecule is oriented with the oxazolidinone group to the left and the carbonyl group pointing up then the active molecule is the isomer in which the substituent at the 5-position is coming forward (proximal) and not the one in which it is receding (distal)[15]. In the case of linezolid this corresponds to the (*S*)-isomer. It is important to note that if the acetamido group in linezolid were changed to an acetoxy or thioacetamido group, the Cahn–Ingold–Prelog designation would be (*R*), hence the distal and proximal orientations are used here. The 4-substitution on the ring has no significant effect to the antibacterial activity, and usually it has deleterious or indifferent effect. Another structure-activity feature of oxazolidinones

was that the 3-substituent was invariably a phenyl group. It was observed that molecules containing 3-aryl substituents with 2,4 and 2,5 disubstituents had weak or no antibacterial activity. 3,4-Disubstituted or 4-monosubstituted compounds had good activity provided the 3-substituent was small[16]. It was also observed that conjugated electron-withdrawing substituents in the 4-position of the phenyl group also had increased activity compared to nonconjugated analog of similar lipophilicity.

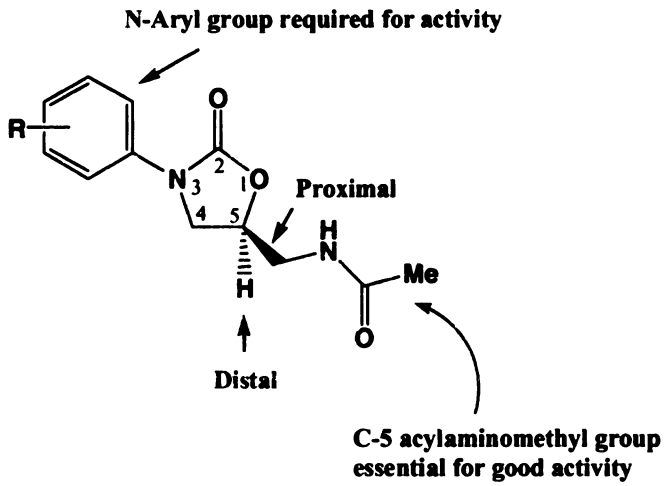

Figure 6.1. Typical features for oxazolidinone antibacterial activity.

Therefore, further modifications are focused on the 3-substututed N-aryl group. Three subclasses of oxazolidinone analogs have been developed by Pharmacia: piperazinylphenyloxazolidinones (for example, PNU-97665)[17], indolinyloxazolidinones (for example, PNU-97456)[18] and the troponylphenyloxazolidinones (for example, PNU-97786)[19,20]. Piperazine derivatives were selected as the candidates because of the excellent *in vitro* and *in vivo* activity, as well as ease of synthesis. It was found that electron withdrawing fluorine atom at the meta position of the phenyl ring enhanced the

antibacterial activity and other desirable properties. These results led to the monoflurophenyl congener PNU-100592 (eperazolid)[21,22], thiomorpholine derivative PNU-100489[23] and morpholine analog PNU-100766, which became known as linezolid[21,22].

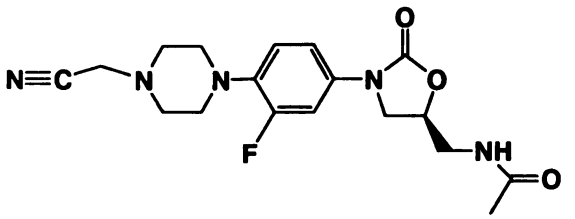

PUN-97665

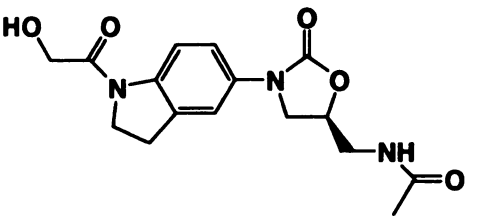

PUN-97456

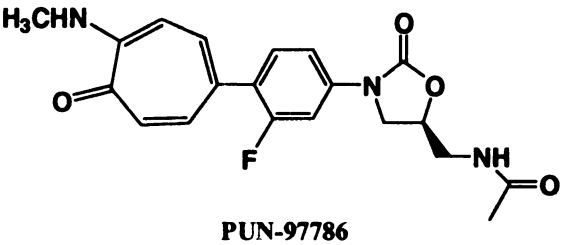

PUN-97786

Synthetic access to oxazolidinones has become a matter of high priority. Synthetic strategies including asymmetric catalysis[24-26] (transition metal and enzymatic), biotransformation[27], and chiral pool approaches[28,29] have been reported. The introduction of the chiral center at 5-position of the ring is an important and general feature for the development of the synthetic strategies. Methods in which a chiral 3-carbon fragment or synthon is coupled to an ativated nitrogen compound dominate the literature on oxazolidinone synthesis.

In the large-scale preparation of Linezolid (**figure 6.2**), a 3-carbon synthon 1-chloro-2,3-dihydroxypropane was reacted with a carbamate **9** to form a 3-aryl-5-hydroxymethyl-2-

oxazolidinone **10**. The primary hydroxyl group is then transformed to an acetamido group by reacting with meta-nitrophenylsulphonyl chloride, and amonia, followed by acetylation to form the 5-acetamidomethyl group[30].

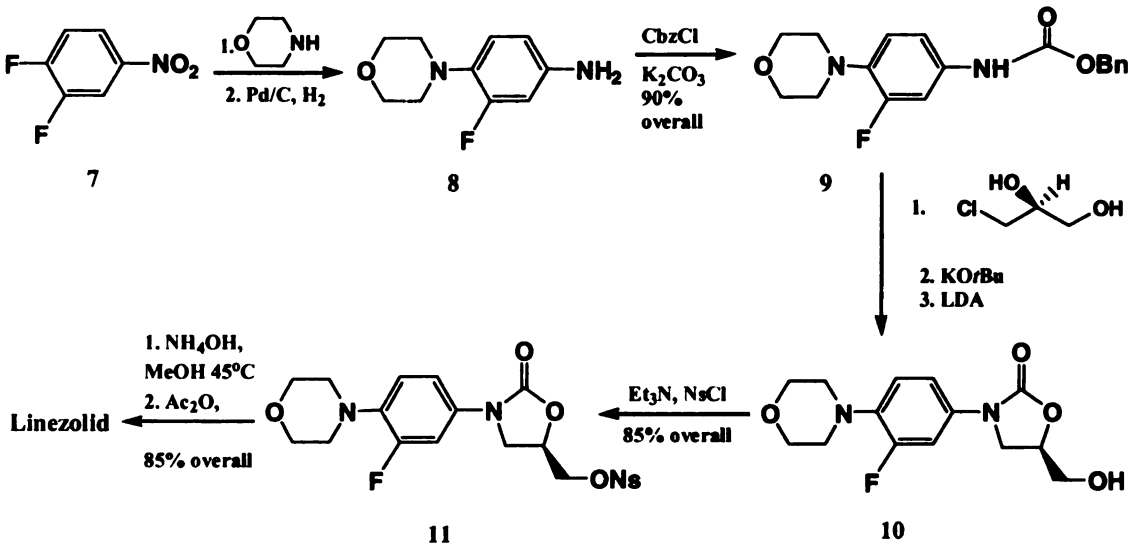

Figure 6.2. Large-scale preparation of Linezolid

A different approach was used in the preparation of DUP-721 (**figure 6.3**). In this synthesis, an isocyanate **12** was reacted with glycidyl butyrate **13** in the presence of tri-*n*-butylphosphine oxide to yield the N-arylated oxazolidinone nucleus directly. The hydroxymethyl group is then deacylated and transformed to the acetamidomethyl group by the same process involving mesylation, displacement by azide, reduction, and acylation described earlier.

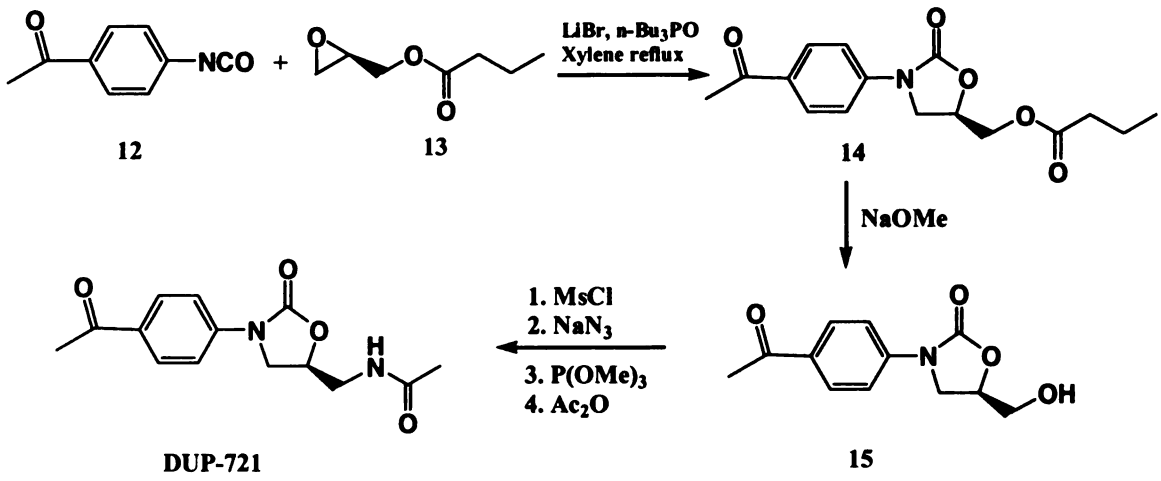

Figure 6.3. Synthesis of DUP-721

The introduction of commercially important methods for preparing optically pure 3,4-dihydroxybutyric acids and various 3- and 4-carbon derivatives[31-33] has opened up the way to the preparation of optically pure oxazolidinones. The 3-hydroxy-γ-butyrolactone **16** can be easily converted to enantiopure 3,4-dihydroxybutyramides **17**. In one method[34], the 4-trityloxy derivative of this butyramide was subject to Hoffmann rearrangement to form 5-trityloxymethyl-2-oxazolidinone **19** (**figure 6.4**). In another method[35], protection of enantiopure 3,4-dihydroxybutyramides with alkyl or arylboronic acids followed by Hoffmann rearrangement yielded the free 5-hydroxymethyloxazolidinones **22** directly (**figure 6.5**). These are new intermediates that can be used for the quick and efficient synthesis of oxazolidinone families. This is an important new development since enantiopure 3,4-dihydroxybutyramides are available in only two steps from starch, lactose, maltose, and hemicelluloses.

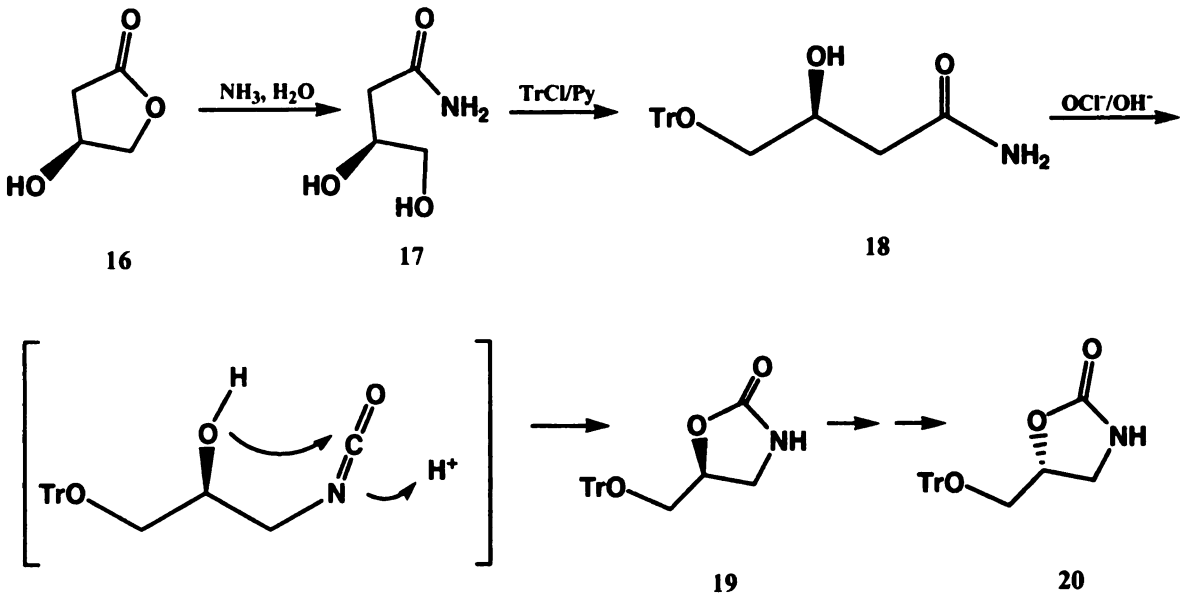

Figure 6.4. Synthesis of 5-trityloxymethyl-2-oxazolidinone

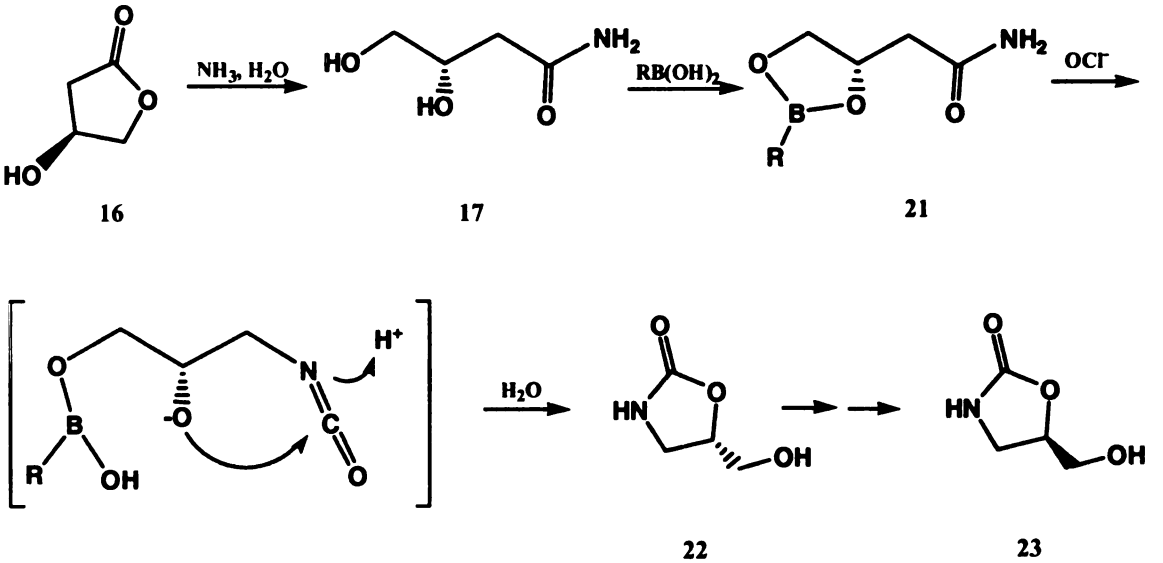

Figure 6.5. Synthesis of 5-hydroxymethyloxazolidinones

Oxazolidinones have showed promising potential to bacterial resistance with their novel structure and unique mechanism. However, incidences of resistance to linezolid have been observed in clinical isolates of *Staphylococcus aureus* and *Enterococcus sp*[36]. A promising approach to developing new antibiotics is to combine two pharmacophores of two different classes of antibiotics in one molecule. This offers the possibility to overcome the current resistance by targeting two different active sites. A series of oxazolidinone-quinolone hybrids has been synthesized and studied[37,38]. These hybrids that combine features of linezolid and ciprofloxacin may act on DNA replication and protein synthesis simultaneously, and offer the opportunity to achieve a broader spectrum towards resistance development. These two systems were connected through a variety of spacers and the structure-activity relationships were studied with variations of spacer, oxazolidinone substructures and quinolone substructures.

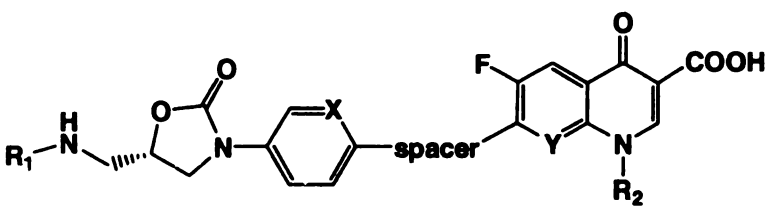

oxazolidinone-quinolone hybrids

The strategy for the synthesis of these hybrids was first to link the oxazolidinone to the central spacer, followed by coupling to the quinolone intermediates. A typical example is illustrated in **figure 6.6** for the synthesis of MCB 3570. The synthesis of oxazolidinones followed the general scheme of linezolid synthesis.

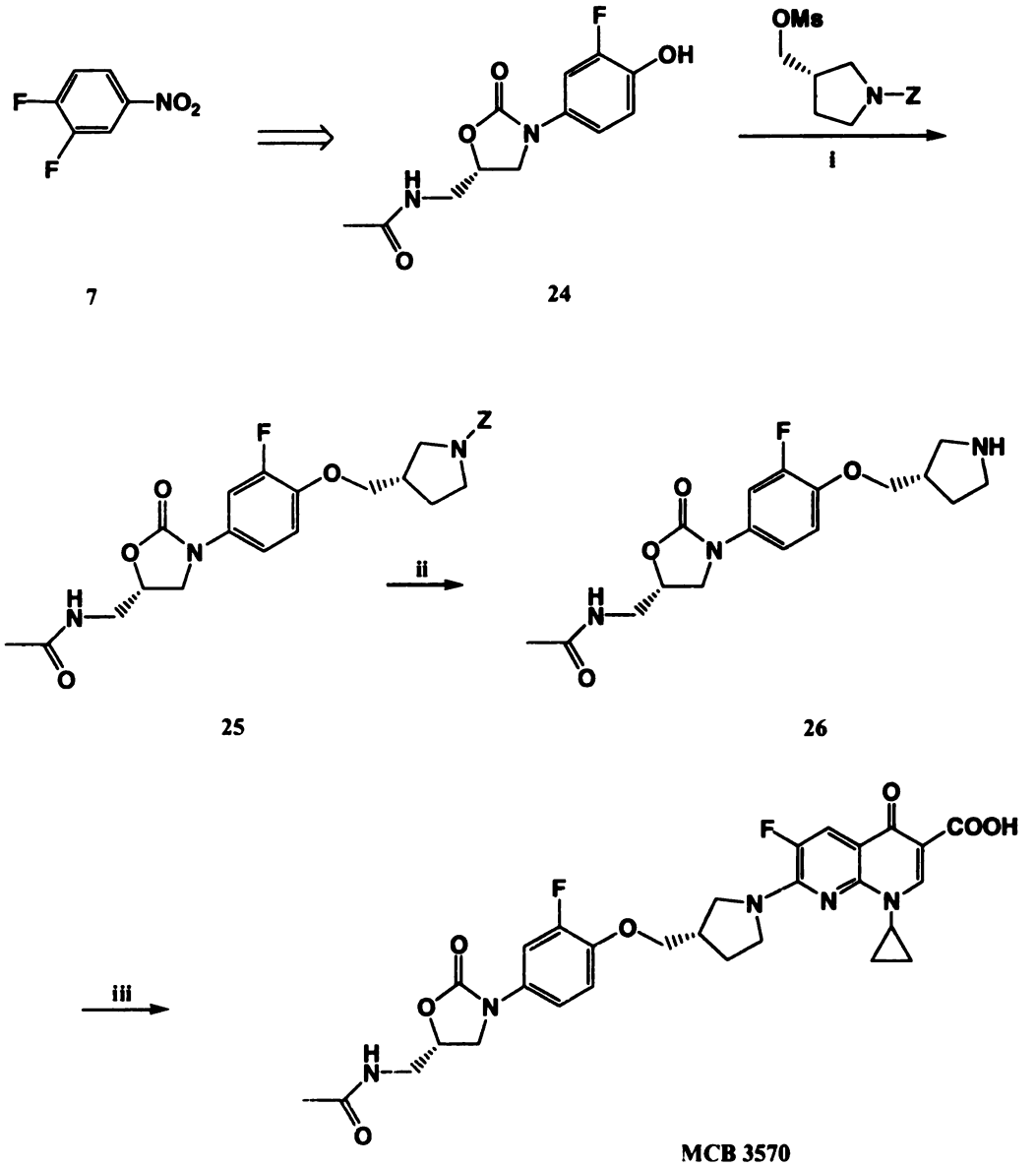

Figure 6.6. Synthesis of MCB 3570. i, spacer as O-mesylate, DMF, 70°C, 12h, 75%; ii, H_2, Pd/C MeOH, EtOAc, 2h, RT, 100%; iii, N-methylpyrrolidinone, 1-cyclopropyl-7-chloro-6-fluoro-1,4-dihydro-4-oxo-1,8-naphthyridine carboxylic acid (commercial), iPr_2EtN, 80°C, 3h, 80%.

The biological testing results showed that substituent variations on the quinolone and oxazolidinone moieties had moderate effect on the antibacterial activity. However, different spacers have dramatic effect on the activity as to acting primarily as a quinolone

or as an oxazolidinone, or retaining both activities. Hybrids containing 6-membered ring spacers normally have weaker activity than 4- or 5-membered ring spacers, and 5-membered ring spacers give the most potent antibacterial activity. Compounds with 3-hydroxymethylpyrrolidinyl spacers displayed the most potent and balanced dual mode of action. MCB 2936 and MCB 2900 which contain the two diastereomeric 3-hydroxypyrrolidinyl spacers showed different antibacterial activity: The quinolone character dominates in the *(S)*-diastereoisomer (MCB 2900) while the oxazolidinone character dominates in the *(R)*-diastereoisomer (MCB 2936). MCB 3570, MCB 3650, MCB 2900 and MCB 3355 were highly active against linezolide as well as ciprofloxacin resistant Gram-positive strains (MICs ≤0.25 μg/ml).

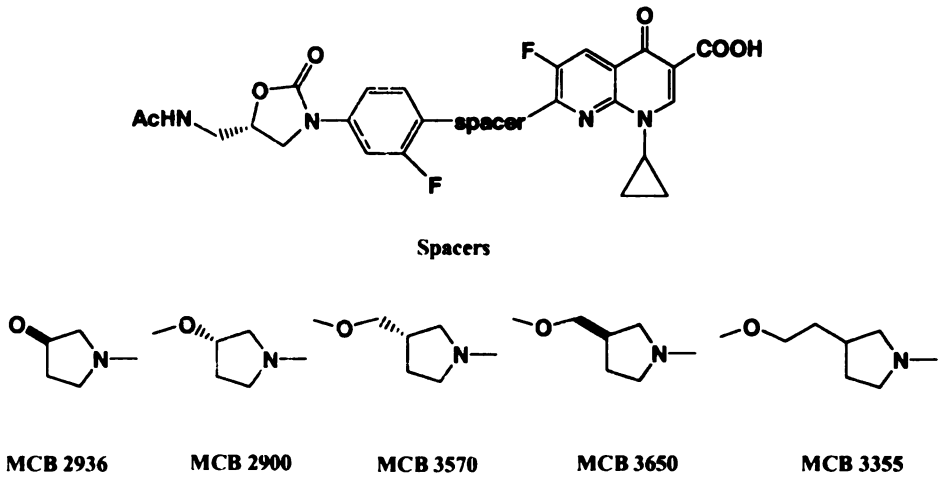

6.2. Results and Discussions

6.2.1. Synthesis of 5-Substituted thiomorpholine carboxylic acid derivatives

Our goal is to synthesize heterocyclic compounds incorporating features of known antibiotics, especially oxazolidinones and ciprofloxacin, by a simple synthetic strategy that readily allows preparation of compound libraries. Biological testing of those

compounds should provide information for the development of structure-activity relationships and provide a starting point for further modification of the structures to develop compounds with good antibacterial activity. Therefore, compounds with substituted phenyl group and nitrogen, sulfur heterocyclic structure are designed and synthesized (**figure 6.7**). They have some features of the known antibiotics linezolid and ciprofloxacin. With amino, sulfur, and carboxylate functional groups, these compounds can be further modified to generate a large number of library molecules for structure-activity relationship study. One important advantage of these structures is their easy synthesis with stereospecific character. All those compounds were synthesized in one step and were obtained as single isomers in very high yields.

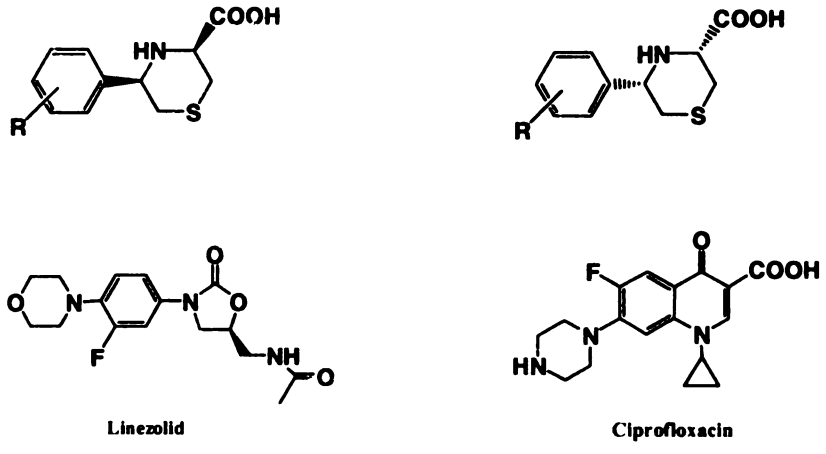

Figure 6.7. General structures of synthetic targets and known antibiotics

Figure 6.8 shows the general procedure for the preparation of arylsubstituted 5-phenyl-thiomorpholine-3-carboxylic acids from L-cysteine and a phenacyl bromide. The enantiomers of these compounds can also be synthesized from D-cysteine (**figure 6.9**). In

this synthesis, the active α-bromo group is easily displaced with sulfur, and the intramolecular reductive amination leads to the heterocyclic ring. The stereoselectivity is induced by the chiral cycteine moiety. Because of this, the reduction by sodium cyanoborohydride proceeds stereoselectively with hydride addition from the less hindered side.

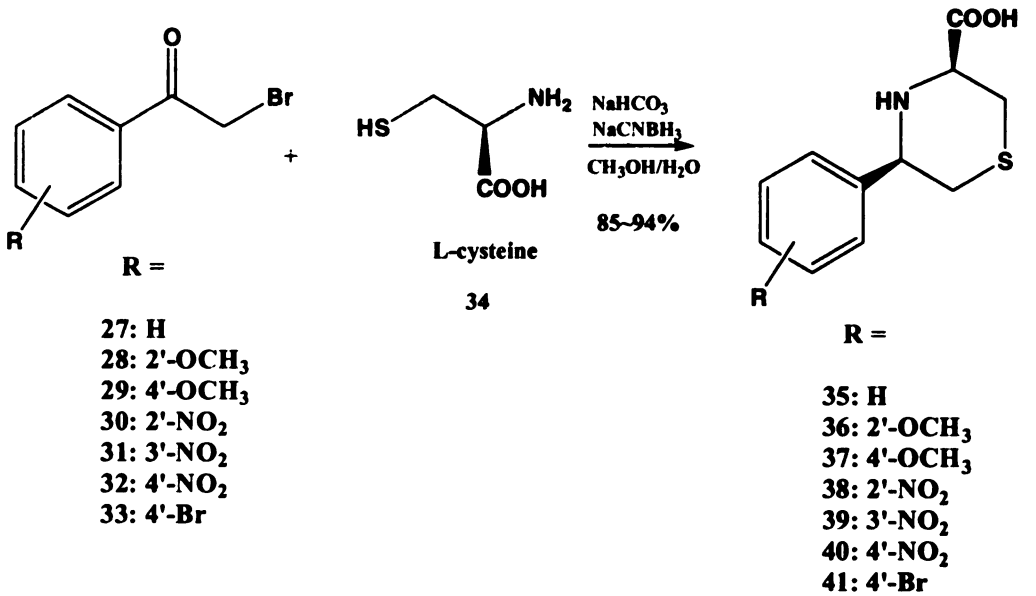

Figure 6.8. Synthesis of arylsubstituted 5-phenyl-thiomorpholine-3-carboxylic acids from L-cysteine.

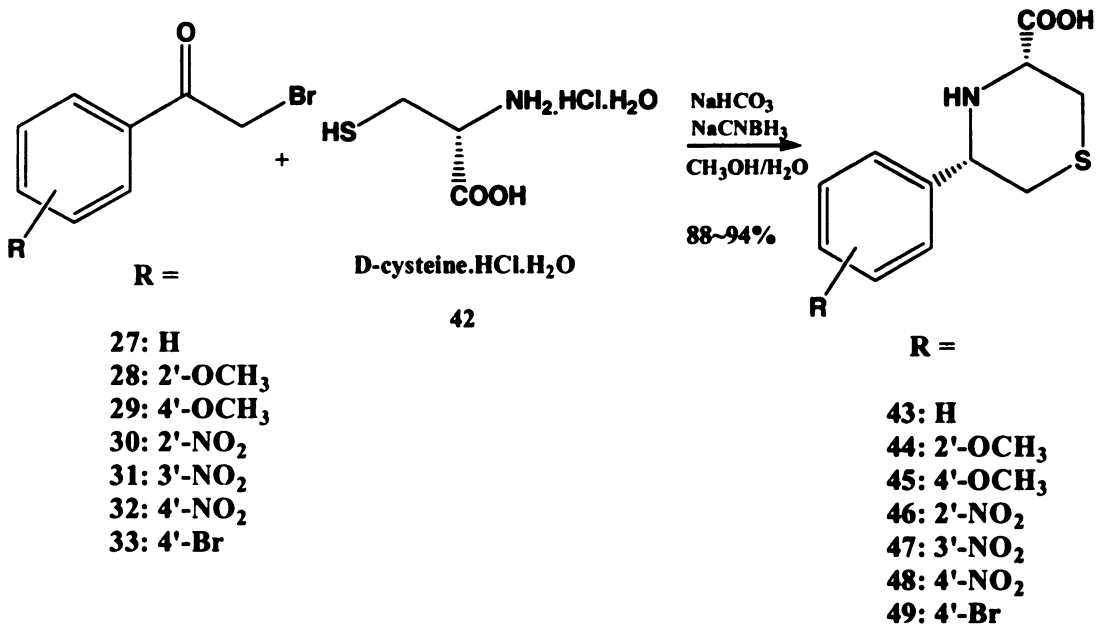

Figure 6.9. Synthesis from D-cysteine

6.2.2. Antibacterial Activities of the Arylsubstituted 5-Phenyl-thiomorpholine-3-carboxylic Acids

The arylsubstituted 5-phenyl-thiomorpholine-3-carboxylic acids were tested for their antibacterial activity against five gram-positive bacterial strains *S. aureus 43300, S. aureus 29213, E. faecalis 51299, E. faecalis 29212, B. subtilis PY79* and six gram-negative strains *E.aerogenes 49469, E. coli 25922, E.coli DH5 alpha, E. cloacea 49141, P. aeruginosa 27853, Salmonella sp.35664*. These compounds were assayed according to the standard MIC testing procedure for antimicrobials. The minimum inhibitory concentration (MIC) of an antibacterial is defined as the maximum dilution of the product that will still inhibit the growth of a test microorganism. Serial dilutions were made of the inhibitors in bacterial growth media. The test organisms are then added to the dilutions of the products, incubated, and scored for growth. The gram-negative strains only showed

weak inhibition by these compounds, but they inhibited gram-positive strains very well. Among the five gram-positive strains, *S. aureus 43300, S. aureus 29213, E. faecalis 51299* and *E. faecalis 29212* were inhibited (**Figure 6.10-6.13**). All seven compounds derived from L-cysteine showed inhibition against *E. faecalis 51299* and *E. faecalis 29212* at the initial dilute concentration, and remain the same kind of inhibition even with the increasing concentrations of the inhibitors. Compound **38** which has the electron-withdrawing 2-nitro substituent showed good activity against *S. aureus 43300* and *S. aureus 29213*. It reached 77% inhibition at the concentration of 250 μg/mL against *S. aureus 43300*, and 57% inhibition against *S. aureus 29213* at this concentration.

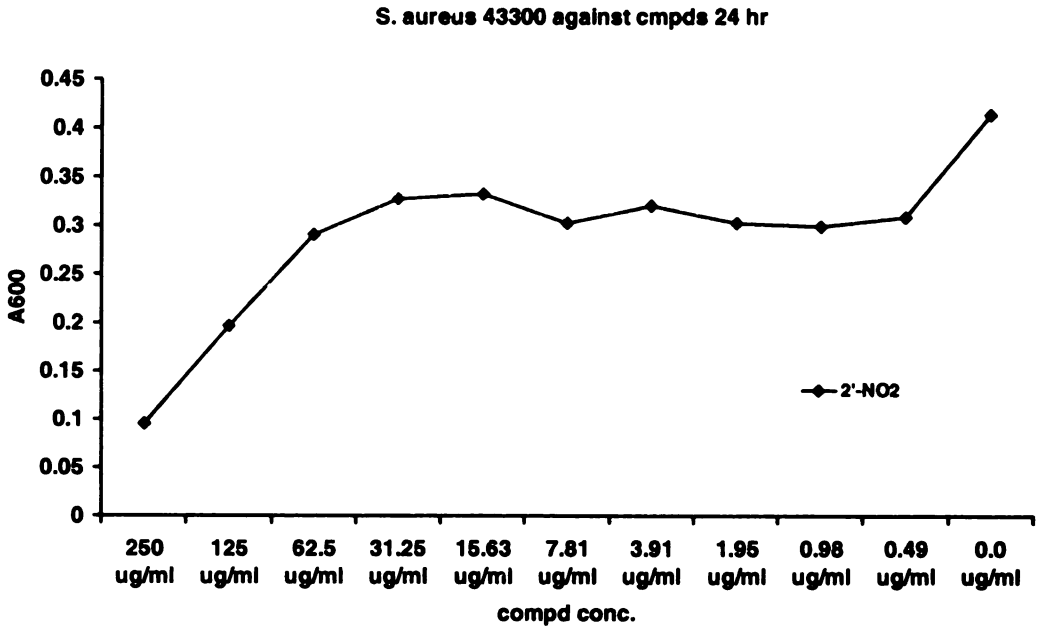

Figure 6.10. Inhibitory activity against *S.aureus 43300*

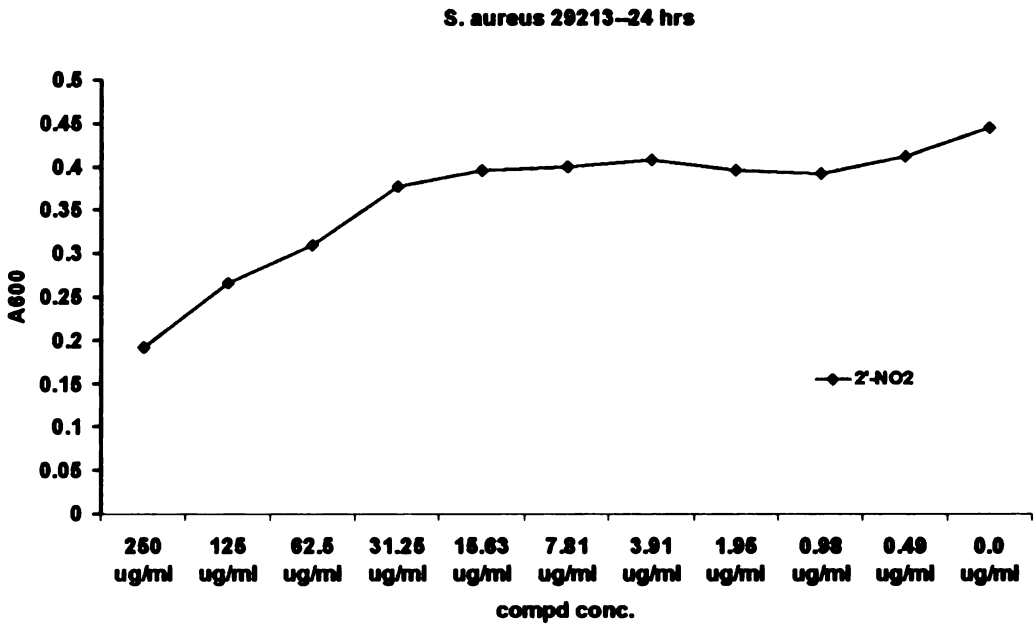

Figure 6.11. Inhibitory activity against *S.aureus 29213*

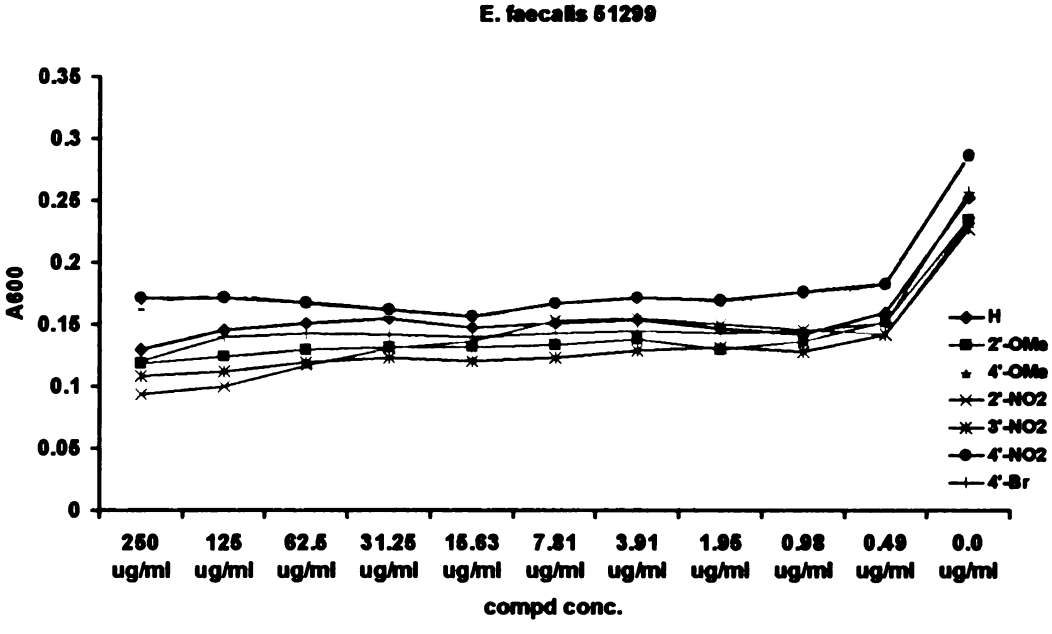

Figure 6.12. Inhibitory activity against *E. faecalis 51299* for compound **35-41**

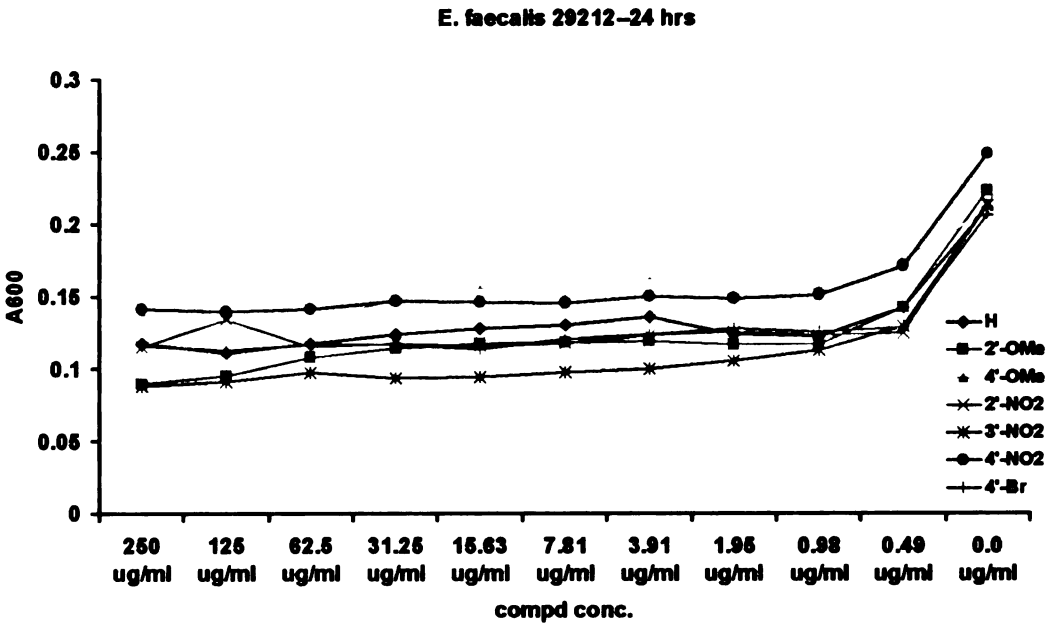

Figure 6.13. Inhibitory activity against *E. faecalis 29212*for compound **35-41**

Figure 6.14 and **figure 6.15** show the inhibition activity of compounds **43-49**. Compared to compounds derived from L-cysteine, **43-49** are less active. They only showed moderate inhibition against *E. faecalis 51299* and *E. faecalis 29212*. Compound **46** with 2-NO_2 is still the most active derivative, with 58% inhibition at concentration 250μg/mL and 72% inhibition at this concentration.

In conclusion, arylsubstituted 5-phenyl-thiomorpholine-3-carboxylic acids can be easily synthesized in a stereoselective manner and provide easy access to compounds for the library screen approach. The preliminary biological testing of the fourteen compounds has showed antibacterial activity against some gram-positive strains and compounds which are derived from L-cysteine generally have better antibacterial activity than their enantiomers. Compounds with electron-withdrawing 2-NO_2 substituent are the most active among the series. It can also been easily modified to many different types of

groups including fluoro group. These compounds can be a good starting point for development of a new class of antibacterial agents and provides the opportunity for a completely new drug class.

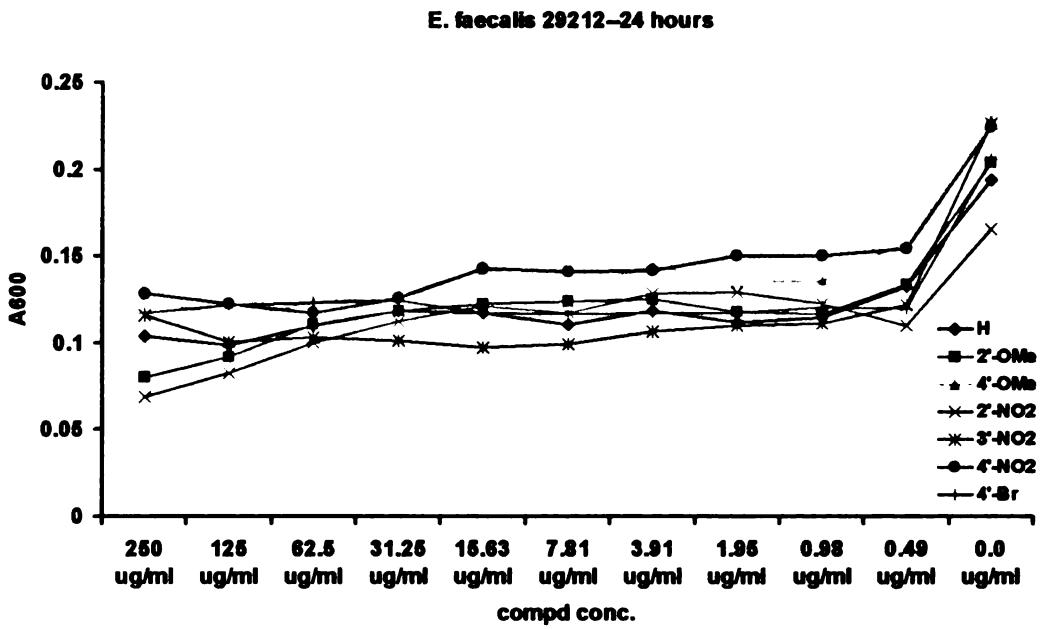

Figure 6.14. Inhibitory activity against *E. faecalis 29212* for compound **43-49**

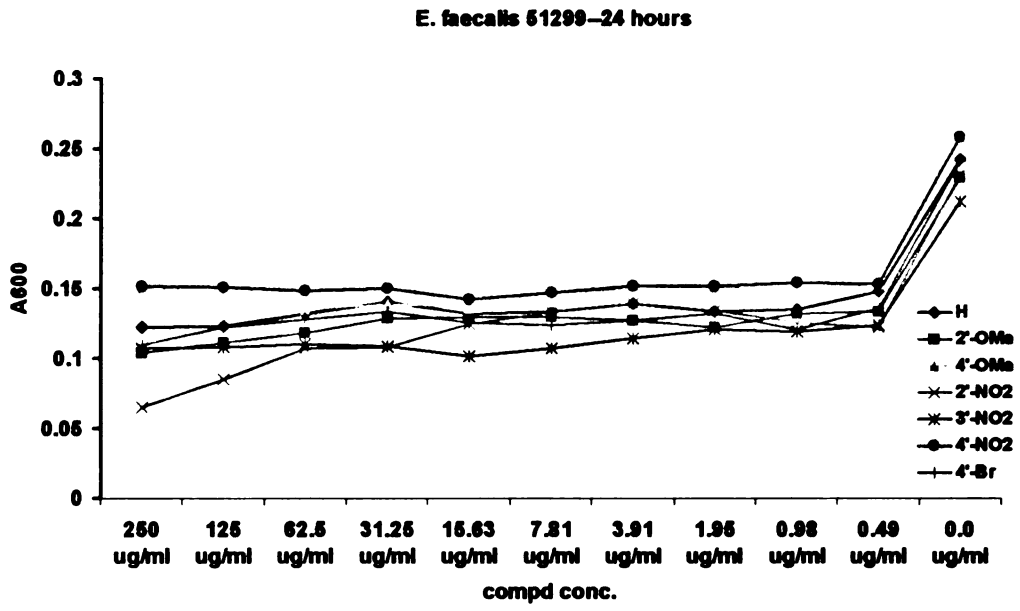

Figure 6.15. Inhibitory activity against *E. faecalis 51299* for compound **43-49**

6.3. Experimental Section

6.3.1. General Procedures

Optical rotations were measured (λ = 589 nm) at room temperature using a Jasco P-1010 polarimeter. IR spectra were recorded on a FT-IR instrument. The ^{1}H (and ^{13}C) NMR spectra were recorded at 500 (125.5) MHz on a Varian VXR spectrometer. The HRMS FAB mass spectra were obtained using a Jeol HX-110 double-focusing mass spectrometer operating in positive ion mode.

6.3.2. MIC Testing Procedure

Compounds were assayed according to the standard MIC testing procedure for antimicrobials. Inhibitory potency was determined by spectrophotometrically measuring

the growth of the bacteria at 600 nm. The organisms used were five gram-positives strains *S. aureus 43300, S. aureus 29213, E. faecalis 51299, E. faecalis 29212, B. subtilis PY79* and six gram-negative strains *E.aerogenes 49469, E. coli 25922, E.coli DH5 alpha, E. cloacea 49141, P. aeruginosa 27853, Salmonella sp.35664*. Serial dilutions are made of the compounds in bacterial growth media M-H media. The concentration range from 250μg/mL, to 0.49μg/mL, 0μg/mL. Bacteria were grown to reach 1.5×10^6 cfu/mL and then added to the dilutions of the compounds. The solutions were incubated at 37°C and the growth of the bacteria was monitored at 2, 5, 14, 18, and 24 hours.

6.3.3. Synthesis from L-cysteine

To a stirred solution of sodium bicarbonate (0.84 g, 10mmol) in 2:1 methanol/water (60 mL) was added L-Cysteine **34** (0.61g, 5mmol) at room temperature. To the mixture, was added the substituted phenacyl bromide followed by addition of sodium cyanoborohydride (0.47g, 7.5mmol). The reaction mixture was stirred for 2 hours after which NMR spectroscopy indicated the completion of the reaction. The solvent was removed by evaporation and the residue was applied to an ion exchange column (Dowex 50WX8-400, 10g), which was washed with water (100 mL) and eluted with ammonium hydroxide (100mL). The eluate was concentrated to yield a crystalline residue of arylsubstituted 5-phenyl-thiomorpholine-3-carboxylic acids.

-H (**35**): was obtained as white solid (1.05g, 94%). ^{1}H NMR (500MHz, CD_3OD) δ 7.50 (2H, d, *J*=7.0 Hz), 7.42-7.36 (3H, m), 4.29 (1H, dd, *J*=11.5, 2.5 Hz), 3.75 (1H, dd, *J*=11.0, 3.0 Hz), 3.13-2.96 (3H, m), 2 64 (1H, d, *J*=14.0 Hz); ^{13}C NMR (125.5MHz, CD_3OD) δ

173.84, 140.61, 130.09, 129.91, 128.13, 64.32, 64.00, 32.42, 28.86 ppm. HR-EIMS (M^+) Calcd. 223.0667, found 223.0664. $[\alpha]^{20}_D$ = -32.5 ° (c 0.1 1*N* HCl).

2-OMe (**36**): was obtained as white solid (1.19g, 94%). ^{1}H NMR (500MHz, D_2O) δ 7.32 (1H, t, *J*=8.0 Hz), 7.26 (1H, d, *J*=7.5 Hz), 6.99 (1H, d, *J*=8.5 Hz), 6.96 (1H, t, *J*=8.0 Hz), 4.45 (1H, dd, *J*=11.0, 2.0 Hz), 3.78 (3H, s), 3.72 (1H, dd, *J*=11.5, 3.0 Hz), 3.02-2.84 (3H, m), 2.56 (1H, d, *J*=14.0 Hz); ^{13}C NMR (125.5MHz, CD_3OD) δ 174.17, 156.54, 130.70, 127.45, 125.95, 121.47, 112.08, 62.30, 57.99, 55.86, 29.21, 27.60 ppm. HR-EIMS (M^+) Calcd. 253.0773, found 253.0775. $[\alpha]^{20}_D$ = -23.0 ° (c 0.2 1*N* HCl).

4-OMe (**37**): was obtained as light yellow solid (1.1g, 87%). ^{1}H NMR (500MHz, CD_3OD) δ 7.40 (2H, d, *J*=8.5 Hz), 6.95 (2H, d, *J*=9.0 Hz), 4.23 (1H, dd, *J*=11.5, 2.5 Hz), 3.79 (1H, s), 3.72 (1H, dd, *J*=11.5, 3.0 Hz), 3.10-3.03 (2H, m), 2.95 (1H, m), 2.63 (1H, dt, *J*=14.0, 2.0 Hz); ^{13}C NMR (125.5MHz, CD_3OD) δ 177.86, 158.74, 135.18, 128.23, 114.54, 63.04, 62.07, 55.75, 32.36, 28.77 ppm. HR-EIMS (M^+) Calcd. 253.0773, found 253.0770. $[\alpha]^{20}_D$ = -26.3 ° (c 0.1 1*N* HCl).

2-NO_2 (**38**): was obtained as yellow solid (1.15g, 86%). ^{1}H NMR (500MHz, D_2O) δ 7.93 (1H, d, *J*=8.5 Hz), 7.70 (2H, m), 7.51 (1H, m), 4.54 (1H, dd, *J*=11.0, 2.0 Hz), 3.65 (1H, dd, *J*=11.0, 3.0 Hz), 2.96-2.80 (3H, m), 2.71 (1H, d, *J*=14.0 Hz); ^{13}C NMR (125.5MHz, CD_3OD) δ 176.08, 148.42, 134.66, 129.73, 128.00, 125.35, 63.01, 57.99, 30.96, 28.23 ppm. HR-FABMS ($M+H^+$) Calcd. 269.0596, found 269.0595. $[\alpha]^{20}_D$ = -66.7 ° (c 0.1 1*N* HCl).

3-NO_2 (**39**): was obtained as light yellow solid (1.2g, 90%). ^{1}H NMR (500MHz, CD_3OD) δ 8.40 (1H, s), 8.19 (1H, dd, *J*=8.0, 2.0 Hz), 7.89 (1H, d, *J*=7.5 Hz), 7.64 (1H, t, *J*=8.0 Hz), 4.34 (1H, dd, *J*=11.0, 2.0 Hz), 3.68 (1H, dd, *J*=11.0, 2.0 Hz), 2.99-2.86 (3H, m), 2.62 (1H, d, *J*=13.5 Hz); ^{13}C NMR (125.5MHz, CD_3OD) δ 175.54, 149.84, 144.60, 134.64, 131.17, 128.18, 122.95, 64.11, 63.57, 33.21, 29.55 ppm. HR-EIMS (M^+) Calcd. 268.0518, found 268.0513. $[\alpha]^{20}_D$ = -17.7 ° (c 0.15 1*N* HCl).

4-NO_2 (**40**): was obtained as light yellow solid (1.24g, 93%). ^{1}H NMR (500MHz, D_2O) δ 7.99 (2H, d, *J*=8.5 Hz), 7.44 (2H, d, *J*=8.5 Hz), 3.97 (1H, d, *J*=11.0 Hz), 3.46 (1H, dd, *J*=11.0, 2.5 Hz), 2.78 (1H, d, *J*=13.5 Hz), 2.67-2.56 (2H, m), 2.37 (1H, d, *J*=13.0 Hz); ^{13}C NMR (125.5MHz, D_2O) δ 178.06, 150.34, 147.01, 127.81, 124.21, 62.70, 62.03, 32.33, 28.82 ppm. HR-FABMS ($M+H^+$) Calcd. 269.0596, found 269.0595. $[\alpha]^{20}_D$ = -18.4° (c 0.1 1*N* HCl).

4-Br (**41**): was obtained as light red solid (1.28g, 85%). ^{1}H NMR (500MHz, CD_3OD) δ 7.57 (2H, d, *J*=8.5 Hz), 7.43 (2H, d, *J*=8.5 Hz), 4.33 (1H, dd, *J*=11.5, 2.0 Hz), 3.77 (1H, dd, *J*=11.5, 2.5 Hz), 3.10-2.95 (3H, m), 2.69 (1H, d, *J*=14.0, Hz); ^{13}C NMR (125.5MHz, CD_3OD) δ 174.06, 138.08, 132.36, 129.00, 122.83, 62.44, 62.08, 31.05, 27.64 ppm. HR-EIMS (M^+) Calcd. 300.9772, found 300.9777. $[\alpha]^{20}_D$ = -23.4 ° (c 0.1 1*N* HCl).

6.3.4. Synthesis from D-cysteine

To a stirred solution of sodium bicarbonate (0.084 g, 1mmol) in 2:1 methanol/water (15 mL) was added D-Cysteine **42** (0.08g, 0.5mmol) at room temperature. To the mixture,

was added the substituted phenacyl bromide (0.5 mmol) followed by addition of sodium cyanoborohydride (0.047g, 0.75mmol). The reaction mixture was stirred for 2 hours after which time NMR spectroscopy indicated the completion of the reaction. The solvent was removed by evaporation and the residue was applied to an ion exchange column (Dowex 50WX8-400, 10g), which was washed with water (20 mL) and eluted with ammonium hydroxide (20mL). The elute was concentrated to yield a crystalline residue of arylsubstituted 5-phenyl-thiomorpholine-3-carboxylic acids.

-H (**43**): was obtained as white solid (0.10g, 91%). ^{1}H NMR (500MHz, CD_3OD) δ 7.50 (2H, dd, *J*=8.0, 1.5 Hz), 7.45-7.39 (3H, m), 4.37 (1H, dd, *J*=11.5, 2.5 Hz), 3.80 (1H, dd, *J*=11.5, 3.0 Hz), 3.13-3.00 (3H, m), 2.73 (1H, dd, *J*=14.5, 2.0 Hz); ^{13}C NMR (125.5MHz, D_2O) δ 173.82, 138.18, 129.44, 129.41, 127.36, 127.00, 62.49, 62.27, 30.43, 27.27 ppm. HR-FABMS ($M+H^+$) Calcd. 224.0745, found 224.0744. $[\alpha]^{20}_D$ = + 32.9 ° (c 0.1 1*N* HCl).

2-OMe (**44**): was obtained as white solid (0.118g, 93%). ^{1}H NMR (500MHz, D_2O) δ 7.29 (1H, t, *J*=8.0 Hz), 7.23 (1H, d, *J*=7.5 Hz), 6.97 (1H, d, *J*=8.5 Hz), 6.93 (1H, t, *J*=7.5 Hz), 4.47 (1H, d, *J*=11.0 Hz), 3.75 (3H, s), 3.73 (1H, dd, *J*=11.0, 3.0 Hz), 3.02-2.82 (3H, m), 2.58 (1H, d, *J*=14.5 Hz); ^{13}C NMR (125.5MHz, D_2O) δ 173.88, 156.47, 130.73, 127.39, 125.56, 121.39, 112.00, 62.19, 57.99, 55.75, 29.04, 27.43 ppm. HR-FABMS ($M+H^+$) Calcd. 254.0851, found 254.0851. $[\alpha]^{20}_D$ = +23.7 ° (c 0.1 1*N* HCl).

4-OMe (**45**): was obtained as white solid (0.119g, 94%). ^{1}H NMR (500MHz, D_2O) δ 7.26 (2H, d, *J*=8.5 Hz), 6.88 (2H, d, *J*=8.0 Hz), 4.21 (1H, d, *J*=11.0 Hz), 3.75 (1H, dd, *J*=12.0,

3.0 Hz), 3.67 (1H, s), 3.03-2.84 (3H, m), 2.52 (1H, d, *J*=14.0 Hz); ^{13}C NMR (125.5MHz, D_2O) δ 173.03, 159.62, 129.93, 128.70, 114.76, 62.22, 61.98, 55.56, 29.97, 27.00 ppm. HR-FABMS ($M+H^+$) Calcd. 254.0851, found 254.0850. $[\alpha]^{20}_D$ = +27.8 ° (c 0.1 1*N* HCl).

2-NO_2 (**46**): was obtained as yellow oil (0.118g, 88%). ^1H NMR (500MHz, D_2O) δ 7.89 (1H, d, *J*=8.5 Hz), 7.65 (2H, m), 7.46 (1H, m), 4.54 (1H, d, *J*=10.5 Hz), 3.64 (1H, dd, *J*=11.5, 3.0 Hz), 2.93-2.77 (3H, m), 2.67 (1H, dd, *J*=13.5, 2.0 Hz); ^{13}C NMR (125.5MHz, CD_3OD) δ 177.96, 150.38, 138.18, 134.43, 129.77, 129.44, 125.06, 64.72, 59.47, 33.75, 30.42 ppm. HR-FABMS ($M+H^+$) Calcd. 269.0596, found 269.0595. $[\alpha]^{20}_D$ = +68.4 ° (c 0.1 1*N* HCl).

3-NO_2 (**47**): was obtained as white solid (0.12g, 90%). ^1H NMR (500MHz, D_2O) δ 8.16 (1H, s), 8.04 (1H, d, *J*=8.0 Hz), 7.69 (1H, d, *J*=7.0 Hz), 7.49 (1H, t, *J*=8.0 Hz), 4.19 (1H, d, *J*=11.5 Hz), 3.59 (1H, d, *J*=11.0 Hz), 2.84-2.71 (3H, m), 2.55 (1H, d, *J*=13.5 Hz); ^{13}C NMR (125.5MHz, CD_3OD) δ 175.85, 148.19, 142.15, 133.72, 130.39, 123.63, 121.96, 62.53, 61.66, 31.17, 27.99 ppm. HR-FABMS ($M+H^+$) Calcd. 269.0596, found 269.0597. $[\alpha]^{20}_D$ = +19.5 ° (c 0.15 1*N* HCl).

4-NO_2 (**48**): was obtained as light yellow solid (0.119g, 89%). ^1H NMR (500MHz, D_2O) δ 8.13 (2H, d, *J*=8.5 Hz), 7.54 (2H, d, *J*=8.5 Hz), 4.33 (1H, d, *J*=11.0 Hz), 3.69 (1H, dd, *J*=11.5, 2.5 Hz), 2.93-2.79 (3H, m), 2.64 (1H, d, *J*=13.5 Hz); ^{13}C NMR (125.5MHz, D_2O) δ 174.68, 147.77, 146.32, 128.12, 124.42, 62.29, 61.79, 30.72, 27.60 ppm. HR-FABMS ($M+H^+$) Calcd. 269.0596, found 269.0595. $[\alpha]^{20}_D$ = + 19.4° (c 0.1 1*N* HCl).

4-Br (**49**): was obtained as white solid (0.137g, 91%). ^{1}H NMR (500MHz, D_2O) δ 7.29 (2H, d, *J*=8.0 Hz), 7.10 (2H, d, *J*=7.5 Hz), 3.99 (1H, d, *J*=11.0 Hz), 3.51 (1H, d, *J*=10.5 Hz), 2.83-2.71 (3H, m), 2.77 (1H, d, *J*=13.5, Hz); ^{13}C NMR (125.5MHz, D_2O) δ 174.51, 138.44, 132.25, 128.88, 122.57, 62.37, 61.99, 31.06, 27.66 ppm. HR-FABMS ($M+H^+$) Calcd. 301.9850, found 301.9849. $[\alpha]^{20}_{D}$ = +23.9 ° (c 0.1 1*N* HCl).

6.4. References

(1) Ford, C. W.; Hamel, J. C.; Stapert, D.; Moerman, J. K.; Hutchinson, D. K.; Barbachyn, M. R.; Zurenko, G. E. Oxazolidinones: New antibacterial agents *Trends in Microbiology* **1997**, *5*, 196-200.

(2) Pfaller, M. A.; Jones, R. N.; Doern, G. V.; Kugler, G. Bacterial pathogens isolated from patients with bloodstream infection: Frequencies of occurrence and antimicrobial susceptibility patterns from the SENTRY antimicrobial surveillance program (United States and Canada, 1997) *Antimicrobial Agents and Chemotherapy* **1998**, *42*, 1762-1770.

(3) Rybak, M. J.; Cappelletty, D. M.; Moldovan, T.; Aeschlimann, J. R.; Kaatz, G. W. Comparative in vitro activities and postantibiotic effects of the oxazolidinone compounds eperezolid (PNU-100592) and linezolid (PNU-100766) versus vancomycin against Staphylococcus aureus, coagulase-negative staphylococci, Enterococcus faecalis, and Enterococcus faecium *Antimicrobial Agents and Chemotherapy* **1998**, *42*, 721-724.

(4) Shinabarger D., M. K., Murray R., Lin A., Melchior E., Swaney S., Dunyak D., Demyan W. and Buysse J. Mechanism of action of oxazolidinones: effects of linezolid and eperezolid on translation reactions. *Antimicrob Agents Chemother* **1997**, *41*, 2132-2136.

(5) Lin A., M. R., Vidmar T. and Marotti K. The oxazolidinone eperezolid binds to the 50S ribosomal subunit and competes with binding of chloramphenicol and lincomycin *Antimicrob Agents Chemother* **1997**, *41*, 2127-2131.

(6) Swaney S., A. H., Ganoza M. and Shinabarger D. The oxazolidinone linezolid inhibits initiation of protein synthesis in bacteria. *Antimicrob Agents Chemother* **1998**, *42*, 3251-3255.

(7) Zurenko, G. E. G., J. K.; Shinabarger, D. L.; Aristoff, P. A.; Ford, C. W.; Tarpley, W.G. Oxazolidinones: a new class of antibacterials *Current Opinion in Pharmacology* **2001**, *1*, 470-476.

(8) Burghardt, H.; Schimz, K. L.; Muller, M. On the target of a novel class of antibiotics, oxazolidinones, active against multidrug-resistant Gram-positive bacteria *Febs Letters* **1998**, *425*, 40-44.

(9) Patel, U.; Yan, Y. P.; Hobbs, F. W.; Kaczmarczyk, J.; Slee, A. M.; Pompliano, D. L.; Kurilla, M. G.; Bobkova, E. V. Oxazolidinones mechanism of action: Inhibition of the first peptide bond formation *J. Biol. Chem.* **2001**, *276*, 37199-37205.

(10) Barbachyn, M. R.; Ford, C. W. Oxazolidinone structure-activity relationships leading to linezolid *Angew. Chem., Int. Ed. Engl.* **2003**, *42*, 2010-2023.

(11) Gregory, W. A.; Brittelli, D. R.; Wang, C. L. J.; Wuonola, M. A.; McRipley, R. J.; Eustice, D. C.; Eberly, V. S.; Bartholomew, P. T.; Slee, A. M.; Forbes, M. Antibacterials - Synthesis and Structure Activity Studies of 3-Aryl-2-Oxooxazolidines .1. The B-Group *J. Med. Chem.* **1989**, *32*, 1673-1681.

(12) Riedl, B.; Endermann, R. Recent developments with oxazolidinone antibiotics *Expert Opinion on Therapeutic Patents* **1999**, *9*, 625-633.

(13) R. B. Fugitt, R. W. L. D. US 4128654 **1978**.

(14) (DuPont), W. A. G. US 4461773 **1984**.

(15) Eustice, D. C.; Brittelli, D. R.; Feldman, P. A.; Brown, L. J.; Borkowski, J. J.; Slee, A. M. An Automated Pulse Labeling Method for Structure Activity Relationship Studies with Antibacterial Oxazolidinones *Drugs under Experimental and Clinical Research* **1990**, *16*, 149-155.

(16) Park, C. H.; Brittelli, D. R.; Wang, C. L. J.; Marsh, F. D.; Gregory, W. A.; Wuonola, M. A.; McRipley, R. J.; Eberly, V. S.; Slee, A. M.; Forbes, M. Antibacterials - Synthesis and Structure Activity Studies of 3-Aryl-2-Oxooxazolidines .4. Multiply-Substituted Aryl Derivatives *J. Med. Chem.* **1992**, *35*, 1156-1165.

(17) D. K. Hutchinson, M. R. B., S. J. Brickner, R. B. Gammill, M. V. Patel (Upjohn) US 5547950 **1996**.

(18) (Upjohn), S. J. B. US 5164510 **1992**.

(19) Barbachyn, M. R.; Toops, D. S.; Ulanowicz, D. A.; Grega, K. C.; Brickner, S. J.; Ford, C. W.; Zurenko, G. E.; Hamel, J. C.; Schaadt, R. D.; Stapert, D.; Yagi, B. H.; Buysse, J. M.; Demyan, W. F.; Kilburn, J. O.; Glickman, S. E. Synthesis and antibacterial activity of new tropone-substituted phenyloxazolidinone antibacterial agents .1. Identification of leads and importance of the tropone substitution pattern *Bioorg. & Med. Chem. Lett.* **1996**, *6*, 1003-1008.

(20) Barbachyn, M. R.; Toops, D. S.; Grega, K. C.; Hendges, S. K.; Ford, C. W.; Zurenko, G. E.; Hamel, J. C.; Schaadt, R. D.; Stapert, D.; Yagi, B. H.; Buysse, J. M.; Demyan, W. F.; Kilburn, J. O.; Glickman, S. E. Synthesis and antibacterial activity of new tropone-substituted phenyloxazolidinone antibacterial agents .2. Modification of the phenyl ring - The potentiating effect of fluorine substitution on in vivo activity *Bioorg. & Med. Chem. Lett.* **1996**, *6*, 1009-1014.

(21) M. R. Barbachyn, S. J. B., D. K. Hutchinson (Upjohn) US 5688792 **1997**.

(22) Brickner, S. J.; Hutchinson, D. K.; Barbachyn, M. R.; Manninen, P. R.; Ulanowicz, D. A.; Garmon, S. A.; Grega, K. C.; Hendges, S. K.; Toops, D. S.; Ford, C. W.; Zurenko, G. E. Synthesis and antibacterial activity of U-100592 and U-100766, two oxazolidinone

antibacterial agents for the potential treatment of multidrug-resistant Gram-positive bacterial infections *J. Med. Chem.* **1996**, *39*, 673-679.

(23) Barbachyn, M. R.; Hutchinson, D. K.; Brickner, S. J.; Cynamon, M. H.; Kilburn, J. O.; Klemens, S. P.; Glickman, S. E.; Grega, K. C.; Hendges, S. K.; Toops, D. S.; Ford, C. W.; Zurenko, G. E. Identification of a novel oxazolidinone (U-100480) with potent antimycobacterial activity *J. Med. Chem.* **1996**, *39*, 680-685.

(24) Schaus, S. E.; Jacobsen, E. N. Dynamic kinetic resolution of epichlorohydrin via enantioselective catalytic ring opening with TMSN(3). Practical synthesis of aryl oxazolidinone antibacterial agents *Tetrahedron Lett.* **1996**, *37*, 7937-7940.

(25) Cardillo, G.; Orena, M.; Sandri, S.; Tomasini, C. An Efficient Synthesis of (R)-(+)-Propranolol and (S)-(-)-Propranolol from Resolved 5-Iodomethyloxazolidin-2-Ones *Tetrahedron* **1987**, *43*, 2505-2512.

(26) Sugiyama, S.; Morishita, K.; Ishii, K. A three-step synthesis of optically active 5-halomethyl-2-oxazolidinones; Asymmetric desymmetrization of prochiral 1,3-dihalo-2-propyl carbamates *Heterocycles* **2001**, *55*, 353-364.

(27) Garcia-Urdiales, E.; Rebolledo, F.; Gotor, V. Enzymatic ammonolysis of ethyl (+/-)-4-chloro-3-hydroxybutanoate. Chemoenzymatic syntheses of both enantiomers of pyrrolidin-3-ol and 5-(chloromethyl)-1,3-oxazolidin-2-one *Tetrahedron Assym.* **1999**, *10*, 721-726.

(28) Lohray, B. B.; Baskaran, S.; Rao, B. S.; Reddy, B. Y.; Rao, I. N. A short synthesis of oxazolidinone derivatives linezolid and eperezolid : A new class of antibacterials *Tetrahedron Lett.* **1999**, *40*, 4855-4856.

(29) Danielmeier, K.; Steckhan, E. Efficient Pathways to (R)-5-Hydroxymethyl-2-Oxazolidinone and (S)-5-Hydroxymethyl-2-Oxazolidinone and Some Derivatives *Tetrahedron Assym.* **1995**, *6*, 1181-1190.

(30) Pearlman, B. A. P., W. R.; Barbachyn, M. R.; Manninen, P.R.; Toops, D. S.; Houser, D. J.; Fleck, T. J. (Upjohn) US5837870 **1998**.

(31) Wang, G. J.; Hollingsworth, R. I. Synthetic routes to L-carnitine and L-gamma-amino-beta-hydroxybutyric acid from (S)-3-hydroxybutyrolactone by functional group priority switching *Tetrahedron Assym.* **1999**, *10*, 1895-1901.

(32) Hollingsworth, R. I. Taming carbohydrate complexity: A facile, high-yield route to chiral 2,3-dihydroxybutanoic acids and 4-hydroxytetrahydrofuran-2-ones with very high optical purity from pentose sugars *J. Org. Chem.* **1999**, *64*, 7633-7634.

(33) Wang, G. J.; Hollingsworth, R. I. Direct conversion of (S)-3-hydroxy-gamma-butyrolactone to chiral three-carbon building blocks *J. Org. Chem.* **1999**, *64*, 1036-1038.

(34) Wang, G. J.; Hollingsworth, R. I. A simple three-step method for preparing homochiral 5-trityloxymethyl-2-oxazolidinones from optically active 3-hydroxy-gamma-butyrolactones *Tetrahedron Assym.* **2000**, *11*, 4429-4432.

(35) Hollingsworth, R. I. W., G. US Pat. 6,288,238 **2001**.

(36) Tsiodras, S.; Gold, H. S.; Sakoulas, G.; Eliopoulos, G. M.; Wennersten, C.; Venkataraman, L.; Moellering, R. C.; Ferraro, M. J. Linezolid resistance in a clinical isolate of Staphylococcus aureus *Lancet* **2001**, *358*, 207-208.

(37) Hubschwerlen, C.; Specklin, J. L.; Sigwalt, C.; Schroeder, S.; Locher, H. H. Design, synthesis and biological evaluation of oxazolidinone-quinolone hybrids *Bioorganic & Medicinal Chemistry* **2003**, *11*, 2313-2319.

(38) Hubschwerlen, C.; Specklin, J. L.; Baeschlin, D. K.; Borer, Y.; Haefeli, S.; Sigwalt, C.; Schroeder, S.; Locher, H. H. Structure-activity relationship in the oxazolidinone-quinolone hybrid series: Influence of the central spacer on the antibacterial activity and the mode of action *Bioorganic & Medicinal Chemistry Letters* **2003**, *13*, 4229-4233.